CGMS

REPORT OF THE TWENTY-THIRD MEETING OF THE COORDINATION GROUP FOR METEOROLOGICAL SATELLITES

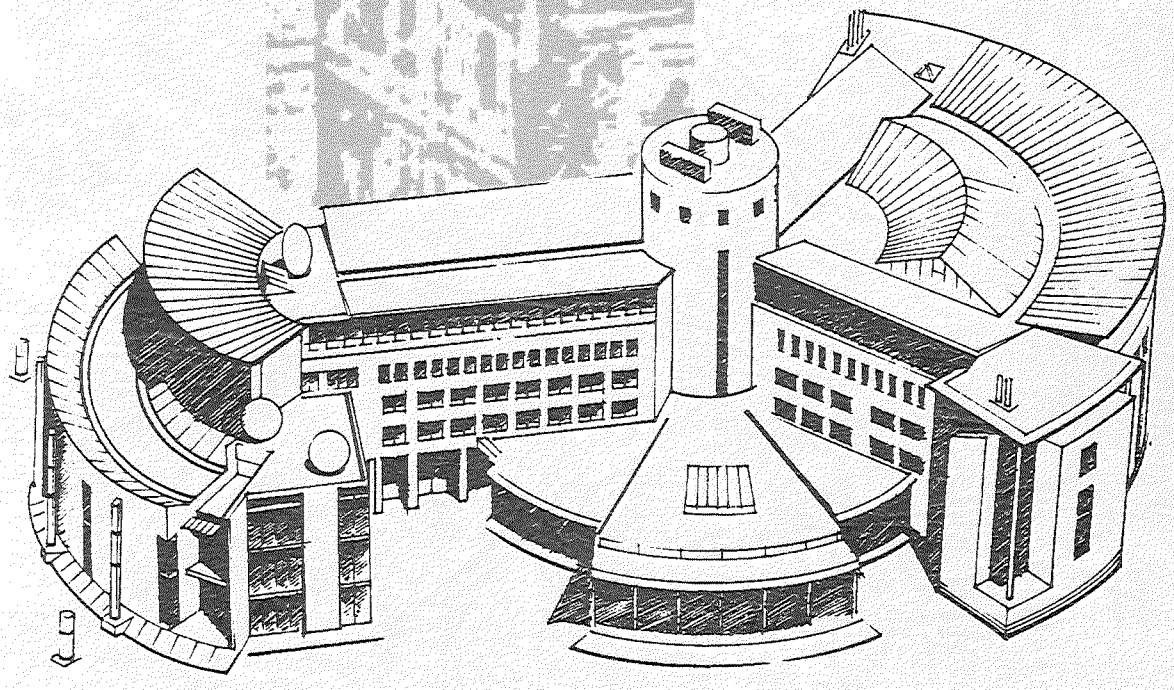

CGMS XXIII

Darmstadt, Germany

15 -19 ~~April~~ May 1995

REPORT OF THE TWENTY THIRD MEETING OF THE CO-ORDINATION GROUP FOR METEOROLOGICAL SATELLITES

CGMS XXIII

Darmstadt, Germany, 15 - 19 May 1995

Cover graphics:
Artist's view of Burg Guttenberg and
the new EUMETSAT Headquarters

Report edited on behalf of CGMS by:
CGMS Secretariat
EUMETSAT
Am Kavalleriesand 31
64295 Darmstadt
Germany

TABLE OF CONTENTS

TWENTY THIRD MEETING OF THE CGMS

FINAL REPORT OF THE PLENARY SESSION

A. PRELIMINARIES

A.1 Introduction

CGMS-XXIII was convened at 9:00 a.m. on 15 May 1995 at EUMETSAT headquarters in Darmstadt, Germany. Mr. John Morgan, Director of EUMETSAT, welcomed representatives from ESA, Japan, the People's Republic of China (PRC), the Russian Federation, the United States and WMO.

A.2 Election of Chairman

Upon a proposal of the USA, supported by WMO, Mr. Morgan was unanimously elected Chairman of CGMS XXIII.

A.3 Adoption of Agenda and Work plan of W/G Sessions

The Agenda (See Annex 1) was adopted. It was agreed that Working Groups I and IV, dealing with telecommunications and wind vectors respectively, would work in parallel on Wednesday morning, followed on Wednesday afternoon by Working Groups II and III, dealing with satellite products and global contingency planning respectively.

The Secretariat provided the consolidated list of 101 working papers submitted to CGMS XXIII, as well as a provisional order of business which was used as a basis for the subsequent discussions.

A.4 Arrangements for the Drafting Committee

The Drafting Committee was appointed, comprising Mr. Tim Stryker, Mr. Carl Staton, Dr. Don Hinsman, Mr. Alexander Uspensky, Mr. Gordon Bridge and Mr. Jérôme Lafeuille. All CGMS Members were invited to provide inputs to this drafting committee for the final report.

A.5 Review of Action Items from Previous Meetings

The Secretariat reminded the participants of the outstanding actions from previous meetings, taking into account the input provided in EUM-WP-01, JAPAN-WP-01, USA-WP-01 and WMO-WP-04.

i) OUTSTANDING ACTIONS FROM PREVIOUS MEETINGS

ACTION 18.3 The Russian Federation to provide Meteor-3 temperature sounding data over the GTS as soon as practical.

Closed, noting that the sounding instrument is no longer operational on Meteor 3-7.

ACTION 18.5 India to provide information on INSAT satellite image transmission schemes.

Closed, noting that India does not attend CGMS meetings.

ACTION 18.11 The People's Republic of China and the Russian Federation to inform the Secretariat when IDCS channels will be implemented.

Closed. PRC confirmed to CGMS XXII its intention to implement IDCS on FY-II, subject to confirmation of technical suitability. The Russian Federation informed CGMS-XXIII that GOMS has a capacity of 33 IDCS channels.

ACTION 21.17 All CGMS Members are requested to indicate planned introduction dates of LRIT.

Continuing. PRC responded on 30 July 1993, and USA indicated that LRIT will be introduced no sooner than 1996 for GOES. Japan is investigating the issue. This was addressed in CGMS-XXIII WG I.

ACTION 21.24 CGMS Members to consider the possible technical measures for the reorganization of the IDCS to include the PRC and any other changes necessary to meet currently foreseen uses of the IDCS.

Continuing. This was addressed within CGMS XXIII WG I.

ACTION 21.32 All satellite operators and WMO to establish lists of products and services needed on national, regional and global scales to serve as a check list when establishing contingency arrangements and to distribute them to other members before the next meeting of CGMS.

Closed. This issue should be addressed within a regular agenda item of future CGMS meetings.

ii) OUTSTANDING ACTIONS FROM CGMS XXII

ACTION 22.01 WMO to distribute to all WMO Members a copy of the LRIT specification document to be provided by EUMETSAT.

Closed. Copy of the LRIT was distributed to all WMO Members and to vendors registered in the WMO database of manufacturers.

ACTION 22.02 Russian Federation to forward for distribution by WMO, to appropriate WMO Members, the data dissemination schemes, frequency plan and transmission characteristics of the GOMS/Elektro Satellite, after its launch and in-orbit commissioning.

Closed. Preliminary information was sent to WMO and distributed through WWW Operational Newsletter. Further details will be provided after commissioning of Elektro, launched on 1 November 1994.

ACTION 22.03 The Secretariat to update as necessary, and forward to WMO a list of current and planned geostationary and polar satellites for distribution in the WWW Monthly Newsletter.

Closed. This was forwarded on 21 June 1994 to WMO, and placed in WWW Operational Newsletter Volume 1994 N°7. Further updates were made by the Secretariat in November 1994 and in March 1995.

It is agreed to review these tables as a permanent action, and to consider appropriate modalities for regular distribution of this updated information within the WWW Operational Newsletter or via Electronic Bulletin Board.

ACTION 22.04 CGMS Members to review the comprehensive description of the space-based portion of the global observing system, as given in Annex I of the Final Report of the Executive Council Panel of Experts on Satellites. CGMS Members to comment by 14 July 1994 if it formed a necessary and sufficient description of WMO contingency requirements.

Closed. Comments were expressed by NOAA, by EUMETSAT and by Japan before CGMS XXIII. These will be brought to the attention of the CBS WG/SAT.

ACTION 22.05 EUMETSAT to consider the possibility of moving a "spare" Meteosat satellite if necessary, in order to provide coverage over the Indian Ocean.

Open. EUMETSAT has not yet been in a position to consider this option, but will review the situation in 1996 if needed, in the light of the result of GOMS commissioning.

ACTION 22.06 NOAA and WMO to investigate the possibility of making Special Sensor Microwave Imager (SSM/I) data and products available on the GTS, so that they could be received by all NWP centres, tropical cyclone RSMCs and regional forecast offices.

Continuing. WMO and NOAA exchanged correspondence on this subject. NOAA to give this issue further consideration and report in advance of CGMS XXIV.

ACTION 22.07 WMO to investigate mechanisms for having WMO Members place satellite image interpretation messages for all polar-orbiting satellites on the GTS.

Closed. Such mechanisms are addressed in WMO WP-06.

ACTION 22-08 CGMS Members to provide WMO, by September 1994, with comments on Appendix A of WMO-WP-07, related to the Requirements for Small Ground Stations.

Closed. Comments were received from several CGMS Members and the updated version of Appendix A was published as WMO/TD N°660.

ACTION 22-09 WMO to be included in the list of addressees informed of non-conformant operations.

Closed. Status on DCP operations are regularly received in WMO.

ACTION 22-10 USA/NOAA to distribute by 1 July [1994] the definition of the LRPT format.

Closed. Final LRPT format specifications are currently undergoing internal concept studies as part of the NPOESS, in consultation with EUMETSAT, and therefore could not be distributed in July 1994.

It is agreed to consider within Working Group I (Telecommunications) which level of minimum specifications is most urgently needed, taking into account both users constraints and programme development schedule. Action 22-10 is provisionally reworded as follows :

ACTION 23-01 USA/NOAA to distribute by 1 November 1995 the definition of the LRPT format.

ACTION 22-11 CGMS Members are requested to notify the Secretariat of their agreement on the proposed LRPT format by 1 December 1994.

Closed. This issue was addressed by CGMS XXIII/WG I. Action 22-1 is reworded as follows:

ACTION 23-02 CGMS Members are requested to notify the Secretariat of their agreement on the proposed LRPT format by CGMS XXIV.

ACTION 22-12 WMO to articulate its operational requirements for the global exchange of satellite image data, to consider how best to achieve such exchange and to make recommendations as appropriate to CGMS.

Closed. This issue is addressed in WMO WP-11 under item G3. Draft operational requirements have been formulated and submitted for discussion.

ACTION 22-13 USA to provide the Russian Federation with existing application notes on the use of soil wetness index derived from SSM/I.

Closed. A package was sent in December 1994 to Roshydromet which expressed its high appreciation.

ACTION 22-14 WMO and NOAA to collaborate on the development of a plan concerning volcano ash satellite monitoring, for submission to WMO/CBS for review and eventual implementation.

Closed. NOAA addressed this issue with ICAO which is primarily interested as a user, and informed CGMS of a possible workshop to be held on this matter. It is noted that there is no direct requirement for a CGMS plan, but CGMS would continue to identify new approaches and techniques that may be of use in extending/improving the usefulness of satellite data for volcanic ash reporting.

ACTION 22.15 All CGMS Members to forward to EUMETSAT a list of topics to be included in a CGMS Directory of Meteorological Applications, by 1 July 1994.

Closed. Input received from several members. The matter will be further discussed under item H4.

ACTION 22.16 EUMETSAT to collect the suggestions of all Members, to draw up on this basis a global outline of a CGMS Directory referring to a target audience and to propose a procedure to implement this project.

Closed. EUMETSAT WP-10 refers, to be discussed under item H4.

ACTION 22.17 CGMS Members to review the updated list of experts in satellite applications and provide to WMO the names of additional experts.

Closed. Correspondence was sent by NOAA and Japan to WMO.

ACTION 22.18 CGMS Members to investigate possibilities to co-sponsor Specialized Satellite Training Centres and report to CGMS-XXIII.

Closed. EUMETSAT WP-11 and WMO WP-08 refer to this matter. Japan and the USA are also considering a contribution in this area.

ACTION 22.19 Satellite operators to provide to the WMO information on users, ground stations, and frequency use, preferably in a database format, by 30 May 1994.

Closed. NOAA/NESDIS, EUMETSAT, Japan and Russia provided an input.

ACTION 22.20 CGMS Participants to provide to the WMO by 15 May 1994 the names

and Omnet or Internet addresses of staff interested in a CGMS. FREQUENCY message forwarding capability.

Closed. NOAA, EUMETSAT and Japan have already responded. Other members may indicate names and Internet addresses at a later stage. It is noted that Omnet is no longer available.

ACTION 22.21 WMO to develop a CGMS.FREQUENCY message forwarding capability for interested CGMS participants prior to 30 May 1994.

Closed. Three List-servers have been implemented by WMO: CGMS-plenary, CGMS-frequency and CGMS-winds.

It is agreed that CGMS should review under item J4 the points of contacts of CGMS members for the various activities.

ACTION 22.22 EUMETSAT and NOAA to consider the operational implementation of periodic Meteosat and GOES cross calibrations in real time, and report to CGMS XXIII.

Closed. Preliminary information was presented by P.Menzel (NOAA) and J.Schmetz (ESA) at the 10th Meteosat Scientific Users' Conference in September 1994. Further information is provided in USA WP-25 for discussion within WG II.

ACTION 22.23 EUMETSAT and NOAA to investigate the use of polar orbiters to normalize geostationary satellite calibration and report to CGMS XXIII.

Closed. This is also addressed by USA WP-25.

ACTION 22.24 CGMS Members to forward to Japan and to the Secretariat their comments on GMS visible reflectance monitoring.

Closed. NOAA/NESDIS expressed much interest about this approach which could be applied for GOES-8.

ACTION 22.25 NOAA/EUMETSAT to respond, to the extent possible to PRC's requests for calibration assistance.

Closed. ESA/ESOC provided the available information on behalf of EUMETSAT. NOAA provided information to the PRC in 1994.

ACTION 22.26 CGMS Members to identify Core Representatives to the Winds Working Group by October 1, 1994.

Closed. Hiroyuki Uchida (Japan), Paul Menzel (USA), Don Hinsman (WMO), Alexander Uspensky (Russia) and Gérard Szejwach

(EUMETSAT) have been designated. PRC is expected to nominate a representative at a later stage.

ACTION 22.27 NOAA will provide documentation to interested parties on the 3-channel technique of precipitable water derivation, following establishment of GOES-I useful performance.

Closed. This technique is described within USA WP-27.

ACTION 22.28 CGMS Members to provide comments on the proposed NOAA K,L,M 1b format direct to NOAA by August 1, 1994.

Closed. No formal comments have been expressed.

ACTION 22.29 EUMETSAT to make available the relevant requirement documentation used to develop the Meteosat Archive and Retrieval Facility.

Closed. Additional copies were available during CGMS XXIII.

ACTION 22.30 EUMETSAT to continue to coordinate the dialogue with Japan and the USA in order to develop an approach for a medium- and long- term global contingency strategy compatible with the plans and constraints of all satellite operators. The first draft of this strategy will be completed and forwarded to CGMS participants for comments by 30 October 1994.

Closed. This matter was addressed within CGMS XXIII/ WG IV.

ACTION 22.31 CGMS Members to review and comment on this draft global contingency strategy in advance of CGMS XXIII.

Closed. This matter was addressed within CGMS XXIII/ WG IV.

iii) PERMANENT ACTIONS BY ALL PARTIES

CGMS Secretariat recalled the following permanent actions:

1. Circulation of Satellite Operational Quarterly Reports and Image Photography.

   CGMS members confirmed that such reports were received and appreciated. However, the following rewording was agreed: ***"Circulation of monthly or quarterly satellite operational reports."***

2. All satellite operators to provide NOAA/NESDIS with information on unexplained anomalies for study, and NOAA to provide solar event information to the satellite operators on request and a status report on the correlation study at each meeting.

   Action to be reviewed within WG II.

3. USA to issue quarterly to all other admitting authorities the consolidated DCP assignments.

Action to be reviewed under agenda item F4.

4. All CGMS Members to inform users to register user stations within their area of responsibility. *(This is normally done.)*

5. CGMS Members generating cloud motion winds to check that monthly statistics are sent and received on a quarterly basis.

Status of action to be reviewed within WG IV.

6. CGMS Members to consider a way to estimate the number of lost messages, and forward to the WMO, on a quarterly basis, statistics of the loss of DCP messages which are normally distributed on the GTS.

It is noted that this is regarding the monitoring of the GTS transmission of DCP messages, rather than the DCP transmission itself. Action to be reviewed in WG I.

7. Each CGMS operator to monitor the unused IDCS channels for interference according to his own scheme, and prepare a report on results for CGMS. If practical, dates of test and channels to be tested will be coordinated (perhaps via the CGMS EBB) in order to obtain information on possible world-wide phenomena.

CGMS noted that NOAA will implement by the end of 1995 a monitoring system for IDCS interference events, providing relevant channel and spectrum information. Japan provides regular reports, and EUMETSAT did not notice significant interference problems. Action to be reviewed by WG I.

8. USA to distribute to CGMS Members updated files on solar activity when the compiled data becomes available.

Such files are not distributed on a regular basis. This action should be reviewed with Action N°2 within the WG II.

9. CGMS Members to provide each other with information on their progress in the further development of archiving and retrieving systems.

This action is deleted, noting that the matter is addressed under item WG II/7 .

10. All CGMS Members to monitor the IDCS allocation list and report any discrepancies to the Secretariat.

This again shall be reviewed within WG I.

As a conclusion of this review of permanent actions, it is agreed that during CGMS XXIII the relevant Working Groups should address the various issues raised by these actions and should make proposals to reformulate or delete any of these actions whenever appropriate.

B. REPORT ON THE STATUS OF CURRENT SATELLITE SYSTEMS

B.1 Polar Orbiting Meteorological Satellites

Russia informed CGMS on the status of the four current Meteor Satellites. As described in RUS-WP-01, Meteor 3-5 is currently the main operational satellite providing both imagery and IR sounding.

In USA-WP-02 NOAA presented a status report on its current polar orbiting satellites NOAA-9, -10, -11, -12, and -14. NOAA-12 is the current operational satellite in the morning orbit, and it is expected that NOAA-14 will become the operational satellite in the afternoon orbit by June 1. NOAA-13 suffered an in-orbit failure soon after its launch in 1993. The other satellites are being employed in a semi-operational or stand-by status, depending on their respective capabilities.

B.2 Geostationary Meteorological Satellites

EUMETSAT reported in EUM-WP-02 about the status of Meteosat Satellites. Meteosat-3 reaching the end of the X-ADC mission would be de-orbited end November 1995. Meteosat-4 in stand-by at 10°E would be used for validation of the new ground-segment and Meteosat-5 was currently the operational satellite. Real time dissemination of high quality images is possible from this satellite thanks to on-ground correction of the radiometer lens anomaly. Meteosat-5 has a fuel reserve until mid-1997. Meteosat-6 is expected to become operational as soon as the current anomaly will be corrected by on-ground image data processing.

Japan presented in JAPAN-WP-02 and JAPAN-WP-03 the status of the Japanese Geostationary Meteorological Satellites (GMS). The GMS-4 is the operational satellite at 140° East since December 4, 1989. The GMS-3 is kept at 120° East as the back-up satellite.

Russia reported about the status of the ELEKTRO Satellite, expected to become "GOMS" when operational. ELEKTRO was launched on 1 November 1994 and is maintained in proper position and attitude in spite of a position sensor failure. Infrared (10.5-12.5 μm) and water vapour channels seem to perform successfully while some degradation is observed on the visible channel. Detailed characteristics were given within RUS-WP-02 and it was noted that the water vapor channel would remain experimental. The CGMS congratulated the Russian Federation for this very important development which is a significant step forward and hoped that the further steps of the commissioning can be successfully completed. The user community will highly appreciate the WEFAX dissemination expected to start by end June. WMO pointed out the value of the infrared images from GOMS over the Indian ocean for use in tropical cyclone monitoring.

USA-WP-03 provided a status report on NOAA geostationary satellite systems. GOES-8, successfully launched in April 1994, is in an operational demonstration phase at 75°W where high quality imagery is operationally provided. Wind vector products and some sounding products are still under operational evaluation. GOES-7 has been relocated to 135°W as the

operational GOES-West satellite. GOES-2 and GOES-3 are still providing telecommunications support.

ESA provided in ESA-WP-01 detailed information on the Extended Atlantic Data Coverage Mission (X-ADC) which will have been successfully completed by 1 June 1995, enabling the USA to bridge the gap until full commissioning of GOES-8. NOAA renewed its thanks to EUMETSAT and ESA for this support of four years of data. ESA-WP-02 and ESA-WP-03 described the various anomalies affecting the performances of Meteosat-4, Meteosat-5 and Meteosat-6, and the various correction schemes developed which allowed those satellites to continue to be used operationally.

In EUM-WP-03 EUMETSAT briefly informed CGMS about the status of the Meteosat Transition Programme, whereby the Meteosat-7 satellite, under construction, is planned for launch mid-1997. The new EUMETSAT ground segment will take over the operations of Meteosat-4, -5 and -6 by mid November 1995.

C. REPORT ON FUTURE SATELLITE SYSTEMS

C.1 Future Polar Orbiting Meteorological Satellite Systems

EUMETSAT, in its EUM-WP-04, reported on the progress being made with the preparation of the EUMETSAT Polar System (EPS) programme which would be submitted to the EUMETSAT Council for approval in June 1995.

People's Republic of China presented PRC-WP-01, noting that FY-1 C would be launched in 1997 or 1998, and its MVISR imager would include 10 channels enabling to extend its mission objectives to Ocean Colour monitoring. CGMS expressed a high interest to these developments and suggested that CGMS-XXIII WG-I gives due consideration to the channel frequencies and formats planned to be used.

RUS-WP-03 described future Russian polar satellites: METEOR 3-8 for launch in 1996, then METEOR 3-M in 1998 and 2000. However, an alternative solution for 1996 would be to launch a RESURS satellite. The meteorological payload for such a RESURS Satellite is under discussion.

In USA-WP-04, NOAA provided a status report on the development of the NOAA-K, -L,-M, -N, -N' satellite series. These satellites will provide enhanced imaging and sounding capabilities through AMSU-A, AMSU-B and a six-channel AVHRR. These satellites will also continue to include HIRS, SBUV, SEM and a communication system to support environmental data collection and Search and Rescue.

In USA-WP-28, NOAA presented information on its plans to establish, in cooperation with EUMETSAT, an Initial Joint Polar-orbiting Meteorological Satellite (IJPS) system. This system would consist of the NOAA-N and -N' satellites, and the EUMETSAT METOP-1 and METOP-2 satellites. This system would precede the longer-term cooperation envisaged by NOAA and EUMETSAT after U.S. establishment of the National Polar Orbiting Environmental Satellite System (NPOESS). USA-WP-29 provided an outline on the NPOESS, which will

be managed by NOAA in cooperation with the U.S. Department of Defense and the National Aeronautics and Space Administration. EUMETSAT has been invited to participate in a joint polar system beginning with METOP-3 and the first NPOESS satellite. This cooperation would complement longstanding plans to provide U.S. instruments for flight on European satellites and European instruments for flight on U.S. satellites.

C.2 Future Geostationary Satellite Systems

EUMETSAT referring to EUM-WP-05, recalled the status of the Meteosat Second Generation (MSG) programme and informed CGMS that the space segment had now reached the end of phase B.

Japan reported on the successful launch of GMS-5, and provided in JAPAN-WP-04 detailed characteristics of data and products available from this satellite. CGMS highly congratulated Japan for this new success and noted the high quality of the sample images (VIS, IR, WV) provided by Japan to each delegation. The plans were given in JAPAN-WP-05 for the successor of GMS-5, the Multi-functional Transport Satellite" (MTSAT), a communication satellite for Japan's aviation authority which will also serve as Japan's meteorological platform. Satellites of this series are expected to be launched every 5 years.

P.R.C. informed CGMS, in PRC-WP-02, of the continuing preparation of the second FY-2 geostationary satellite. CGMS expressed its sympathy with regard to the difficulties encountered on FY-2-A and encouraged P.R.C. to continue its efforts in the development of meteorological satellites.

The Russian Federation presented RUS-WP-04 reporting on the GOMS (Elektro) N2 satellite, similar to GOMS (Elektro) N1, with a nominal lifetime of 3 years, and expected to be launched in 1997 from Baïkonour. The water vapor channel of GOMS-N2 is planned to be operational. In the course of the meeting, Dr. Trifonov, Chief designer of the Elektro satellite, made a detailed presentation on the characteristics of this satellite, the ground segments used to support the METEOR, RESURS and GOMS satellites, and on future plans for the long term, including a possible geosynchronous satellite at 60° inclination.

In USA-WP-05 and USA-WP-06 the USA informed CGMS that GOES-J was ready for launch on 19 May 1995 and that GOES-K, -L and -M were planned for April 1999, 2000 and 2004 respectively. GOES-M, the last in the current series, is planned to have a solar X-Ray imager. The plans beyond GOES-M were presented in USA-WP-07. The 4 satellites constituting the GOES-N, -O, -P, -Q series will include gradual improvements in terms of spatial, spectral and temporal resolution, enabling an efficient and smooth transition to the GOES-R series of the next generation.

D. OPERATIONAL CONTINUITY AND RELIABILITY

D.1 Global Planning, Including Orbital Positions

WMO introduced WMO-WP-14 and described the GCOS-Space Plan version 1.0 that was a result of the most recent meeting of the GCOS Space Panel. The Space Plan is expected to

be finalized soon and it was noted that much of the data provided by operational meteorology instruments are of direct relevance to GCOS. Commenting on this presentation, NOAA informed CGMS of its plans for making decisions on ground and space observing systems. An approach is under discussion which involves the test and evaluation of a variety of observing systems in order to arrive at the "best" mix of systems, including satellites, radiosondes, aircraft measurements, and ground-based remote sensing in support of weather forecasting or climate services. This program will be developed in the coming year in order to set in place a program directed at the definition of a more cost effective observing system.

ACTION 23-03 **WMO to provide CGMS Members with a copy of the GCOS Space Plan version 1.0.**

ACTION 23-04 **CGMS Members to review and comment on the GCOS Space Plan version 1.0, with respect to achievability and proposed priority of implementation into their own plans.**

D.2 Interregional Contingency Measures

No papers submitted on this item.

E. METEOROLOGICAL SATELLITES AS PART OF WMO PROGRAMMES

E.1 World Weather Watch

WMO presented in WMO-WP-01 the outcome of a feasibility study on transmissions of the RSMC Tokyo-Typhoon Centre's data and products via satellites. CGMS noted that such information could be made available in the short-term on Internet or ISDN, while an alternative operational solution of distribution via GMS (or possibly MTSAT) could be considered in 4-5 years, if corresponding resources were available.

In response to CGMS Action 22.07, WMO-WP-06 listed the countries interested in satellite interpretation messages. CGMS noted that there is no detailed requirement yet for such messages.

In WMO-WP-12, WMO informed CGMS of the status of the WMO Satellite Data Requirements, which have been analyzed in the context of the CEOS Task Force for Long-Term Planning. The Chairman suggested that gap analyses be addressed for each of the geostationary locations and for each of the two or three required orbits for polar orbiting satellites. CGMS noted with appreciation the availability of the relational database with information concerning their instruments and mission plans.

E.2 Other Programs

CGMS took note of WMO-WP-10 referring to WMO Technical Document TD 660 (SAT-13) "A Description of a Standard Small Satellite Ground Station for use by WMO Members".

CGMS congratulated WMO and the relevant CBS Working Group for this helpful information. In WMO-WP-09, CGMS was informed of the latest development of a project for low resolution satellite receiving equipment, and noted the important contribution by Switzerland.

F. COORDINATION OF INTERNATIONAL DATA COLLECTION & DISTRIBUTION

F.1 Status and Problems of IDCS

In its EUM-WP-06, EUMETSAT presented an overview of the utilization of the IDCS during the last year. In total, around 540 IDCP were registered for use with the system worldwide using 8 of the 33 available channels (I6, I7, I12, I13, I14, I15, I16, I18). Recently 4 additional channels (I4, I20, I25, I30) have been opened up to accommodate further growth in the system over the coming year and to provide reserve channels in case any DCP have to be reallocated because of interference. Within the Meteosat field of view around 140 IDCP are regularly reporting.

JAPAN-WP-06 reported that around 210 DCP were currently registered for use with GMS-4.

The Secretariat recalled that there had in the past been some IDCS allocations which had not been registered smoothly. It was proposed that the allocation notification procedure be addressed by the WG on telecommunications to determine if there was a requirement for additional fields specifying the area and frequency of operation of IDCP.

CGMS also noted that throughout 1994 the GMS, GOES and Meteosat IDCS regions were not seriously affected by radio interference. EUMETSAT commented that there had been some instances of below average performance of ASAP operating at the northern edge of the Meteosat field of view in the North Atlantic. Not all of these problems were related to interference, since on some occasions investigation had shown faulty equipment or incorrect antenna siting as primary causes of poor performance. In most cases, it had been shown that whilst interference would cause some garbling of characters, the content of message could still normally be decoded into usable data. It was noted in this context that a new ASAP monitoring facility had recently been established at Meteo France in Toulouse, who will undertake special end-to-end monitoring exercises involving all ASAP and satellite operators where appropriate. CGMS was invited to support this activity.

JAPAN-WP-07, whilst confirming the generally low level of interference in the Pacific regions, presented the results of a monitoring exercise carried out on IDCS channels 3 and 6 during 1994. The level of interference experienced did not affect the relay of messages.

CGMS were informed that there had been an exchange of the database containing the consolidated list of IDCS allocations between Members. It had been noted that a more regular exchange of this data might solve some of the allocation difficulties experienced recently. It was agreed that this matter would be discussed in more detail by the WG on Telecommunications, together with a request from EUMETSAT to re-visit the possible use of certain IDCS channels for regional meteorological applications in support of some future sponsored hydrometeorological and agrometeorological networks.

RUS-WP-05 described the planning in progress for the processing of DCP messages relayed through GOMS. All 33 IDCS channels would eventually be supported, however, for the time being the DCP reception centre in Moscow would support a total of 16 International and Regional Channels. Russia also reported that severe sweeping interference had been detected within the frequency band 401 - 403 MHz. An investigation into the source of the interference was in progress.

USA-WP-08, on IDCS assignment was presented and briefly discussed. It was noted that NOAA is planning to enhance its ground facility to automatically monitor the IDCS channels with respect to interference. This is planned to be implemented in early 1996.

In conclusion, problems were identified as regards the capacity of the IDCS systems and the corruption of the signal in some cases. The need for consideration of the long term development was also pointed out. CGMS invited the WG-I (Telecommunications) to review these three issues.

F.2/F.3 ASAP/ASDAR

In JAPAN-WP-08, Japan indicated that 148 ship IDCPs including ASAP were registered in the GMS DCS by the end of 1994 and were regularly relaying messages through the system. Japan recalled that the other satellite operators are expected to send to JMA telexes in accordance with the Annex 12 and Annex 14 of IDCS Users' Guide before any commencement of a ship IDCP operation. This request was duly noted by CGMS.

In WMO WP-13, CGMS was informed of the latest status of ASDAR and ASAP implementation. CGMS noted that of the 23 ASDAR units purchased, 14 units were installed with 10 of them operational, 6 units yet to be installed, 1 unit still seeking a carrier after being decommissioned and 2 units retained as spares. The WMO also indicated that the total number of ASDAR units will most probably not increase since they have been superseded by other technologies which are comprised of both the airborne and communication equipment. As of December 1994, 11 ASAP systems were operated by 4 countries and it was expected that Sweden will join the ASAP community in 1995. The USA has recently begun operation of one ASAP in the Pacific and an additional ship will be deployed in 1996.

In JAPAN-WP-09, it was noted that data from two of the ASDAR DCPs were not received.

F.4 Dissemination of DCP Messages (GTS or other means)

Japan provided in JAPAN-WP-10 a status report on the dissemination of DCP messages, indicating that 335 DCP were received via 8 international and 26 regional channels of the GMS-4 transponder.

The USA presented its USA-WP-09 which summarized the IDCS activity through the GOES for the period 1 January through 31 December 1994. It was noted that channel I16 had abnormally high interference as indicated by the significant number of DCP messages (about 55%) received with errors. The average error rate for the other active IDCS channels on GOES was noted to be about 8%.

G. COORDINATION OF DATA DISSEMINATION

G.1 Dissemination of Images Via Satellite

In its EUM-WP-07, EUMETSAT described the ongoing activities leading to the implementation of encryption of Meteosat High Resolution Image (HRI) data. Encryption of this data will commence in September 1995. Prior to that date some additional encrypted test formats are being regularly transmitted from the CMS Lannion uplink station. The working paper also detailed the various conditions of access to HRI data and presented a summary of applicable fees. EUMETSAT noted that a very large majority of NMS in developing countries would be granted free access to encrypted HRI data when used for normal internal purposes. Furthermore, EUMETSAT confirmed that the EUMETSAT Council agreed to provide HRI data free of charge to other satellite operators in the context of bilateral agreements.

JAPAN-WP-11 presented the dissemination plan of satellite images by GMS-5, equipped with water vapour and infrared channels.

In RUS-WP-07, the Russian Federation informed CGMS on the WEFAX Dissemination Schedule via GOMS, which will initially provide, every three hours, one image in four sectors plus a full disc. Further details and updates will be available from Roshydromet and NPO Planeta.

The USA briefly presented its USA-WP-10 on the status of NOAAPORT and highlighted the implementation of a "pathfinder" satellite broadcast (of limited data) in mid-1995. The development of the NOAAPORT documentation (i.e. Users' Guide) in an electronic format was noted.

G.2 Dissemination of Products Via GTS or Other Means

The status of operation of the Meteosat Meteorological Data Distribution (MDD) mission was presented in EUM-WP-08. EUMETSAT reported that there had been a steady growth in the use of this mission over the last two years, that there currently were around 80 operational users located in the field of view, many of then in the African region, and that the dissemination includes products from and for African meteorological centres. The most recent development in this respect is the implementation of the 3rd uplink in Toulouse, France, at the end of 1994, complementing the previous uplink in Rome, Italy and Bracknell, United Kingdom. The products disseminated by this station on MDD Channel 3 (1695.7562 MHz) had been recommended by a dedicated working group and would meet the needs of main data processing centres and NMS in the African region. Further refinement of this schedule was expected in the coming years as the experience in the use of the data further developed. CGMS noted that the MDD broadcasts had been encrypted since early 1993 and that only Meteorological Services were authorized to use the data. The encryption scheme had also allowed the distribution to ACMAD Member States of special ACMAD designated products created by ECMWF. It was confirmed that the content of MDD dissemination is directly taking account of requirements expressed by African users.

In USA-WP-11, NOAA reported on its plans to make ATOVS data and products available to the U.K. Meteorological Office and other NWP centres. Data transfer plans are expected to be finalized in advance of the NOAA-K launch.

NOAA's current Polar Satellite Active Archive (SAA) and the planned GOES SAA were briefly presented in USA-WP-12. The Polar SAA has been operational since March 1994 and has all NOAA AVHRR data (GAC, LAC and NOAA HRPT) since March 1994 on-line for user access via Internet. The GOES SAA design will be similar to the Polar SAA and will archive all GOES data (full resolution) for only a short time period (1 or 2 years) due to the large data volumes. After this period, the archived GOES data will be for synoptic periods and at reduced resolution. NOAA indicated other products and data (e.g. TOVS, SSM-I) will eventually be included in the on-line archive.

G.3 Global Exchange of Satellite Image Data

In EUM-WP-09, EUMETSAT recalled the global exchange of satellite images through the Meteosat system. Image data coverage of the western Atlantic, provided from 1991 to 1995 by X-ADC, and from 1 June 1995 by GOES-8, is regularly relayed by Meteosat via Météo-France/CMS at Lannion. Selected GMS WEFAX images, acquired from GOES-Tap were also accessed by CMS Lannion and disseminated through Meteosat every three hours. In the working paper plans were also presented for the possible acquisition of digital GMS data and GOMS WEFAX data. EUMETSAT added that it intended to continue this type of data exchange when the MSG satellite series came into operation around 2000.

It was confirmed that such distribution of foreign data was very useful for global general forecasting, aeronautical and marine forecasting. Japan noted that the distribution of GMS data may be subject to some limitations, and EUMETSAT confirmed that their distribution via Meteosat could be controlled in order to meet these requirements.

The Russian Federation indicated in RUS-WP-08 a proposal for retransmission via GOMS, of WEFAX data from GMS and Meteosat. CGMS welcomed this suggestion. Furthermore, the USA and EUMETSAT expressed their interest in obtaining High Resolution data from GOMS. The Russian Federation, the USA and EUMETSAT will give further consideration to this issue.

In WMO WP-11, CGMS was informed of the status of development of a WMO requirement for the exchange of digital satellite image data over the GTS. It noted that the CBS Working Group on Satellites (CBS WG/SAT) had developed a draft requirement that had been sent to all WMO World Meteorological Centres (WMCs) and Regional Specialized Meteorological Centres (RSMCs) for comment. Based on a consolidation of those comments, the requirement will be finalized at the next meeting of the CBS WG/SAT in 1996 for approval by CBS in the 4th quarter of 1996.

CGMS agreed that it was important to review these requirements.

ACTION 23.05 **CGMS members to review the draft requirement for the exchange of digital satellite image data over the GTS.**

H. OTHER ITEMS OF INTEREST

H.1 Applications of Meteorological Satellite Data for Environment Monitoring

The USA informed CGMS members about NOAA's application of meteorological satellite data for the purposes of environmental monitoring. As described in USA-WP-13, NOAA has developed an experimental Soil Wetness Index (SWI) from U.S. Defense Meteorological Satellite Program (DMSP) Special Sensor Microwave Imager (SSM/I). The SWI based on brightness temperatures at 85.5 and 19.35 GHz is an extremely useful tool for large area monitoring of flooding under sparse vegetation conditions. The high temporal resolution of the DMSP satellites assures a near global coverage on a near real time basis. The SWI can be used to quickly identify problem areas around the world. CGMS welcomed this information which opens very promising prospects.

H.2 Search and Rescue (S&R)

The USA provided in USA-WP-15 the Cospas-Sarsat System Data N° 17 and 18, which are status reports published by the Cospas-Sarsat Secretariat. In USA-WP-14, a detailed report was provided on the recent efforts to analyse geostationary earth orbit search and rescue (GEOSAR) satellite systems as a potential enhancement to the existing Cospas-Sarsat polar-orbiting system. The Cospas-Sarsat Council has directed that a Demonstration and Evaluation (D&E) phase be performed to confirm the expected benefits of a GEOSAR satellite system and establish its technical and operational performance characteristics. It is suggested to conduct the D&E activities in 1995, 1996 and beyond. NOAA invited each satellite operator to consider national or regional means to support satellite-aided search and rescue efforts through both low-earth orbit and geostationary systems, and provided technical guidelines for a D&E phase. Such a D & E will be conducted by US, Japanese, Russian and Indian satellite operators. CGMS noted the interest of these activities.

Japan reported in JAPAN-WP-15 about the GEOSAR experiment at 406 MHz, to be started in June 1995 with GMS-5 by the Ministry of Transport of Japan. CGMS expressed interest in being informed about the outcome of this experiment.

H.3 Anomalies from Solar and Other Events

No papers were submitted under this agenda item.

H.4 Information and Training

In response to Action 22.16 of CGMS XXII, EUMETSAT presented in EUM-WP-10 a first approach to a CGMS Directory of satellite applications. CGMS noted that comprehensive inputs had been received from two members as regards the expected content of such a Directory. For the practical implementation of such a project, several options were discussed regarding the language(s), the format, the material form, the funding and the management.

WMO strongly supported the concept of a CGMS directory of applications, which would help to promote satellite activities and extend the visibility of the benefits of CGMS satellite systems. CGMS noted that the intended audience would primarily be decision makers, but

that such a publication could also serve as an introductory teaching material. A possible option would be to adopt a format similar to the current EUMETSAT format, but with a revised selection of items and an increase in volume. It was noted that such a CGMS Directory would have to provide a balanced view of the applications conducted in the various parts of the world, that depend upon the different satellite systems of CGMS members. In addition to the inputs already provided (by EUMETSAT, NOAA and WMO), Japan, P.R.C and Russia expressed readiness to contribute to such an initiative by providing information and illustrations on activities within their regions. It was noted that CGMS has only one working language, which would help to keep the cost of such a CGMS Directory within affordable limits.

Following actions were agreed:

ACTION 23-06 **Japan, P.R.C, and the Russian Federation to indicate, by 30 November 1995, possible contributions to the CGMS Directory covering applications conducted in their respective regions.**

ACTION 23-07 **EUMETSAT to seek resources to initiate the project of a CGMS Directory of applications, and inform CGMS members by January 1996.**

ACTION 23-08 **CGMS members to provide WMO with names to be included in a list-server of points of contacts for the preparation a CGMS Directory.**

EUMETSAT then reported in EUM-WP-11 on the training activities conducted in cooperation with its Member-States. EUMETSAT has created a Foundation Course, is developing learning material to be distributed to the training establishments of its Member-States, intends to develop Computer Aided Learning Modules (CAL) and organizes or supports the advanced training of selected meteorologists and trainers. As regards developing countries, the activities initiated by EUMETSAT are a direct response to CGMS Action 22.18 requesting "CGMS Members to investigate possibilities to co-sponsor Regional Specialized Satellite Training Centres and report to CGMS XXIII." Building on the activities initiated within the Member-States, EUMETSAT made provisions to extend its training activities to developing countries, in particular in WMO Region I (Africa). The main orientations of this effort would be to train the trainers and to provide a long term support to two RSSTC in Africa, IMTR (Nairobi) and EAMAC (Niamey). A Forum of EUMETSAT Users in Developing Countries was recently convened in Niamey, where the participants from 30 African countries, representing most of the regional Meteosat users, had the opportunity *inter alia* to express their requirements for training and to jointly draw, with EUMETSAT and WMO representatives, the outline of a training programme fitted to the needs of the user community.

WMO recalled in WMO-WP-08 the latest status of the WMO strategy for education and training in satellite matters. WMO indicated that within the Programme & Budget proposal for 1996-1999 to be considered by its Congress in June 1995, there will be 8 training events in the next 4 years. WMO also congratulated EUMETSAT for its initiatives for training and encouraged all CGMS members to pursue their efforts to implement the strategy proposed by WMO in this area. NOAA expressed much interest and informed CGMS that it will consider

similar support to training activities in the Western hemisphere, subject to availability of funds and personnel.

H.5 Any other Business

CGMS noted the list of recent WMO publications presented in WMO-WP-03 including the "Annual Progress Report on Application of Satellite Technology", (WMO/TD 628) the "WWW/GOS Note WMO 411" and the "Description of Standard Small Satellite Groundstation for use by WMO members" (WMO/TD 660). CGMS was informed in WMO-WP-02 of the WMO initiative to identify commonality features for multipurpose computer workstations that will handle the various satellite-based meteorological broadcasts. WMO proposed to organize a consultant study on the hardware and software specifications to maximize commonality within such workstations, and to address in particular the feasibility and cost aspects. CGMS was informed of the readiness of the WMO Voluntary Cooperation Programme to consider recommendations from CGMS in this respect. CGMS was of the opinion that such a study would prove most useful and encouraged WMO's VCP to proceed with its plan for such a study. WMO furthermore encouraged EUMETSAT to renew the initiative of a Regional User Forum in Developing Countries, where technical questions related to e.g. MDD can be directly addressed with the interested users.

The USA indicated they would provide their technical specifications for multisatellite data receiving systems. EUMETSAT informed that the future MSG dissemination scheme would combine image data, MDD and DCP and that the use of an integrated workstation would then be facilitated. It was pointed out that a major element of the global cost of those stations is the maintenance of hardware and software.

CGMS was informed of the database available within WMO related to satellite receiving equipment, as described in WMO-WP-05, indicating that the total number of satellite user stations was around 7700. WMO invited CGMS satellite operators to cooperate in developing this database, through combining their respective databases. CGMS thanked and complimented WMO for this useful initiative and agreed to support it.

ACTION 23-09 **All CGMS satellite operators to contribute to the WMO database of satellite user stations, in providing information on geographical locations of the users of their respective satellites.**

ACTION 23-10 **All CGMS satellite operators to check the registration status of receiving stations of their users.**

PARALLEL WORKING GROUP SESSIONS

REPORT FROM WORKING GROUP I: TELECOMMUNICATIONS

I/0 Introduction

Mr. Robert Wolf (EUMETSAT) was elected as Chairman of Working Group I (Telecommunications), and Messrs. Bridge (EUMETSAT) and Staton (NOAA) as Rapporteurs.

I/1 Results of SFCG

The Chairman, being the nominated CGMS representative at Space Frequency Coordination Group (SFCG), introduced document EUM-WP-12 which reported upon the 14th meeting of the SFCG. The meeting took note, in particular, of ongoing discussions about the use of the band 1670 - 1710 MHz, the re-allocation of the Meteorological Satellite Service (Met SS) near 7.5 and 8.2 GHz, the protection of frequencies used by passive sensors, of frequencies to be used by wind profilers and the preparations for the World Radio Conferences (WRC) 1995 and 1997. The Chairman reminded the group that the 1997 WRC would be largely dedicated to "space" frequency allocations therefore it was very important that all matters requiring further study or notifications to the various authorities were carried out well in advance of the WRC. He added that it was planned to have a EUMETSAT presence at the 1995 WRC in order to ensure that any unforeseen matters arising, with regard to the use of Met SS frequencies by other services, would be properly addressed.

NOAA summarised USA-WP-16, also reporting on SFCG matters, and pointed out that there were several commercial activities in the USA who were actively making efforts to obtain the use of certain frequencies allocated to the Met SS. NOAA stressed the need to remain vigilant and work aggressively in order to protect these frequencies. NOAA also reminded the group that the continued protection of certain other met frequencies (e.g. those used by radio sondes) was necessary. There was a need to clearly demonstrate the continued and long term use of all these frequencies and to ensure that proper assignments of protection status, e.g. primary or secondary, be maintained. JMA confirmed that its agency was in close contact with the national radio authority and were making all efforts to ensure protection of frequencies in that part of the world.

The Chair recalled the good services of the WMO who were actively corresponding with its members concerning the need to protect the Met SS frequencies and instructing them on how to communicate with, and lobby, relevant PTT agencies well in advance of the WRC. It was clear that the highest priority of all concerned was to protect frequencies allocated to the Met SS - both present and planned. All CGMS Members were more that willing to assist WMO in its efforts to notify its members of the potential dangers regarding frequency protection.

To this end, it was agreed that the Secretariat, with the assistance of CGMS Members, would prepare an information note to be placed on the WMO-CGMS home page of the WMO Bulletin Board. This note would, in particular, inform users about future satellite programmes and missions, and list specific frequency bands requiring protection.

REPORT FROM WORKING GROUP I: TELECOMMUNICATIONS

I/0 Introduction

Mr. Robert Wolf (EUMETSAT) was elected as Chairman of Working Group I (Telecommunications), and Messrs. Bridge (EUMETSAT) and Staton (NOAA) as Rapporteurs.

I/1 Results of SFCG

The Chairman, being the nominated CGMS representative at Space Frequency Coordination Group (SFCG), introduced document EUM-WP-12 which reported upon the 14th meeting of the SFCG. The meeting took note, in particular, of ongoing discussions about the use of the band 1670 - 1710 MHz, the re-allocation of the Meteorological Satellite Service (Met SS) near 7.5 and 8.2 GHz, the protection of frequencies used by passive sensors, of frequencies to be used by wind profilers and the preparations for the World Radio Conferences (WRC) 1995 and 1997. The Chairman reminded the group that the 1997 WRC would be largely dedicated to "space" frequency allocations therefore it was very important that all matters requiring further study or notifications to the various authorities were carried out well in advance of the WRC. He added that it was planned to have a EUMETSAT presence at the 1995 WRC in order to ensure that any unforeseen matters arising, with regard to the use of Met SS frequencies by other services, would be properly addressed.

NOAA summarised USA-WP-16, also reporting on SFCG matters, and pointed out that there were several commercial activities in the USA who were actively making efforts to obtain the use of certain frequencies allocated to the Met SS. NOAA stressed the need to remain vigilant and work aggressively in order to protect these frequencies. NOAA also reminded the group that the continued protection of certain other met frequencies (e.g. those used by radio sondes) was necessary. There was a need to clearly demonstrate the continued and long term use of all these frequencies and to ensure that proper assignments of protection status, e.g. primary or secondary, be maintained. JMA confirmed that its agency was in close contact with the national radio authority and were making all efforts to ensure protection of frequencies in that part of the world.

The Chair recalled the good services of the WMO who were actively corresponding with its members concerning the need to protect the Met SS frequencies and instructing them on how to communicate with, and lobby, relevant PTT agencies well in advance of the WRC. It was clear that the highest priority of all concerned was to protect frequencies allocated to the Met SS - both present and planned. All CGMS Members were more that willing to assist WMO in its efforts to notify its members of the potential dangers regarding frequency protection.

To this end, it was agreed that the Secretariat, with the assistance of CGMS Members, would prepare an information note to be placed on the WMO-CGMS home page of the WMO Bulletin Board. This note would, in particular, inform users about future satellite programmes and missions, and list specific frequency bands requiring protection.

I/2 Co-ordination of frequency allocations

EUM WP-13 summarised the requirements for the protection of passive sensors for meteorological measurements. Technical details on the very specific use of frequencies were provided in the document in order to justify their protection. The Working Group endorsed the conclusion of the document whereby it was suggested that sharing at frequencies above 56 GHz appears to be possible but interference to passive microwave sensors will occur at frequencies below 56 GHz. It was therefore proposed to allocate the frequency band 54.25 - 56 GHz to Earth Exploration Satellites (EES) passive sensors and allowing the Fixed Satellite Services (FSS) to use the band above 56.0 GHz.

EUM-WP-14 presented the results of a study which investigated the feasibility of sharing frequencies between the Met SS and Mobile Sat Services (MSS) in the band 1670 - 1710 MHz. The results of this study will be presented to the ITU. The study relates, in particular, to EUMETSAT present and future systems, but would be of interest to other Members of CGMS, especially if they intend to carry out similar studies.

The study showed that there are possibilities for sharing the lower part of the frequency band (i.e. 1670 - 1690 MHz) where the main downlinks of geostationary meteorological satellites are operated. Since there are relatively few groundstations operating these links, sharing would be subject to guaranteed protection of these important links by the new services. Sharing appears to be impossible in the higher part of the band due to the large number of user stations operated on a world-wide basis and the required separation distance of 50 - 70 Km between MSS stations and meteorological user stations which was calculated in the study.

The WG took note of Russia-WP-09 which described measures which had been taken to protect frequencies used by GOMS-N1, METEOR-2, METEOR-3 and METEOR-3M satellites. Russia further confirmed that, to avoid any possible conflict with domestic DCP frequencies used by EUMETSAT and JMA, its domestic DCP frequencies would be located in a frequency band similar to that used by the domestic DCP service of the USA. For the time being, 8 IDCS channels and 8 domestic channels would be supported by the GOMS ground segment. Noting that DCP channel frequencies had not yet been decided, Russia was asked to provide details to CGMS in due course.

Action WG I.1 Russia to provide CGMS Members with details of IDCP channel frequencies as soon as possible.

The Group noted USA-WP-17 which described activities taking place to inform administrations about the coordination and protection of frequencies used by the Met SS. A report, prepared by the WMO CBS/WG on Telecommunications - Study Group on radio frequency coordination, was appended to the document.

In its USA-WP-18 and WP-19, the USA informed the Group about the registration of APT reception stations in order to protect them from interference from the MSS and the details of APT services to be provided by NOAA-N and -N´. The Group noted that the change would take place around the year 2000. Planning for the change from APT to LRPT had commenced and would be realized in the next decade. Concerning its estimate of the number of APT reception stations world-wide, the USA agreed to verify the number quoted in the document in due course.

Action WG I.2 **The USA to provide CGMS Members with information on the number of APT reception stations world-wide by 1 September 1995.**

In order to assist the WMO with its compilation of all Met Satellite reception stations, all CGMS Members were urged to regularly provide WMO with copies of databases of user stations.

Action WG I.3 **CGMS Members to regularly provide WMO with information on the number of meteorological satellite reception stations in their areas of responsibility.**

The Chairman commented that the large number of users indicated by the US registration process clearly demonstrated the need for adequate and long term protection of the frequency band in question (137 - 138 MHz).

The Group took note of USA-WP-20 and WMO-WP-15 which described the results of discussions of various Met SS topics in 1994 meetings of the ITU and commented that the ongoing activities would continue to be very important in the period leading up to the WRC.

I/3 Issues arising from the plenary session of CGMS XXIII

The Group addressed various actions arising from the plenary session, in particular :

(a) To study ways of estimating the number of lost DCP messages on the GTS

Having clarified the objective of this action the Working Group recommended that this action be removed from the "permanent" list and become a specific action of CGMS XXIII after suitable rewording. The Group suggested that there were two primary aspects of end to end monitoring of lost messages: those lost or corrupted by the satellite system, and those lost in the ground relay (e.g. GTS) part of the system. Following action was proposed:

Action WG I.4 **The Secretariat to establish a period in the next twelve months for the end to end monitoring of certain DCP, in consultation with the CGMS members supporting the IDCS. The WMO to address any resulting problems relating to the onward relay of messages via the GTS. A report of this monitoring to be prepared by the Secretariat for CGMS XXIV .**

(b) To confirm that one WMO admitting authority address had been allocated to PRC.

The Group confirmed that this was the case and noted that Annex 3 of the IDCS Users Guide should be updated accordingly. The first set of four bits denoting the PRC as admitting authority of a DCP is 1110 (E). The remaining WMO code is considered as "spare" and can be used for future allocation by CGMS.

Action WG I.5 **The Secretariat to update Annex 3 of the IDCS Users Guide, indicating the admitting authority address of the PRC.**

(c) To establish procedures for the monitoring of IDCS channels for interference

The Group recommended that since this activity was an element of the routine management of the IDCS by satellite operators, there was no requirement there for a "permanent" action.

(d) Coordination of downlink frequencies to be used by the PRC for the FY-1 series of polar orbiting satellites

The Group recalled that agreement had been reached during CGMS XXI. To avoid conflict with certain services provided by other CGMS Members, 1708 MHz would be used for this downlink in future.

(e) To evaluate new technologies to be used in future satellite DCS, in particular those which will render the DCS less susceptible to interference

Following a discussion of various techniques now under consideration by some satellite operators, e.g. spread spectrum techniques, forward error correction, other modulation schemes, the group suggested that all Members should continue to carry out studies of this topic and report back to CGMS XXIV.

Action WG I.6 All CGMS Members to study the possibilities for using spread spectrum techniques and higher bit rates for future DCS.

Noting that USA had already completed some studies of spread spectrum techniques applied to its DCS, the Group proposed that copies of the study results be made available to CGMS Members.

Action WG I.7 USA to provide CGMS with results of studies of DCS spread spectrum techniques and the use of higher bit rates by 1 July 1995.

(f) To confirm that current IDCS Admission procedures were adequate

The Group recalled IDCS admission procedures (IDCS Users Guide Annexes 12 and 14) and agreed that there was no need to modify the number of fields of information required. In the case of ship allocations, CGMS Members were urged to provide full information on both the areas and periods of operations of all vessels in order that the admitting authorities can be fully prepared *in advance* of the ship entering their areas of responsibility.

(g) Use of IDCS channel frequencies for certain regional DCP applications

The WG supported a request from EUMETSAT for the use of up to 5 IDCS channels (I29, I30, I31, I32 and I33) on a temporary basis to accommodate future network of regional DCP now being established within the framework of WMO sponsored agrometeorological and hydrometeorological programmes. Members of the Group commented that whilst no obvious large demands for IDCS capacity were expected in the coming years, if there was eventually

a requirement for the use of IDCS channels allocated to EUMETSAT, then alternative measures (e.g. reallocation) might have to be considered. EUMETSAT confirmed that this requirement for additional capacity was relatively short term (5-7 years maximum) since by 2000 the MSG DCS would support all DCP allocations. This system would provide 120 DCP channel frequencies for regional use. The above requested period would also allow around 2 years for the gradual transition of DCP from MTP to MSG.

I/4 Electronic bulletin boards

WMO presented its WMO-WP-7 describing CGMS Bulletin Boards. CGMS Member were invited to update the various mailing lists and to consider the setting up of an Internet home page. WMO advised that monitoring statistics of its home page had shown a very significant usage over recent months. The Group agreed that a CGMS home page would be a very useful asset and were pleased to accept the kind offer by the WMO to manage the page on its behalf. CGMS Members would be invited to submit material to be placed on the home page. WMO added that it now had the capability to handle many different types of graphical inputs.

The Chairman commented that the CGMS-EBB should also be used for the exchange of draft and final documents relating to frequency matters.

Action WG I.8 **CGMS Members to identify points of contacts to WMO CGMS representative, by 1 July 1995. Those points of contact would assist with the design, provision of material for, and dealing with enquiries resulting from, the CGMS home page.**

REPORT FROM WORKING GROUP II: SATELLITE PRODUCTS

The Working Group on Satellite Products was chaired by Dr Paul Menzel of NOAA and Ken Holmlund of ESA served as Rapporteur.

II/1 Imaging Processing Techniques

EUM-WP-15 summarized plans for and progress toward MPEF continuation of MIEC operational processing of Meteosat data. Products have been improved in several areas and the frequency of distribution has been increased; for example, the potential exists for winds to be extracted from all three spectral channels every 1.5 hours. The MPEF supports operations, commissioning, and product development with a performance margin of 50%. The transition from MIEC to MPEF is expected in November 1995.

RUS WP-10 described the ground microprocessing system for GOMS/Elektro real-time data reception, preprocessing and archiving. Interpretation of these data towards SST, winds and cloud parameters is under development. An archive of all raw GOMS data is included.

USA WP-21 gave a status on GOES-8 image navigation and registration. Good progress in characterizing and understanding Image Navigation and Registration (INR) performance and procedures was presented; after recent improvements, performance has been within specification in more than 90% of the images. Further improvements are still being sought.

USA WP-27 detailed algorithms for generating total precipitable water vapour products with 6.7, 10.7 and 12 μm radiances; good product quality has been evidenced with GOES-8 imager data. It was appreciated by the Japanese members as an information document, of potential use for comparison with their current algorithm.

The discussion emphasized that the use of satellite data should be viewed in the context of the total available observing system; full benefit of satellite data in defining the state of the atmosphere and earth surface is only realized through assimilation of all observing capabilities. The best mix of ground, airborne, and satellite measurements is under review in several countries and CGMS is encouraged to keep apprised of this.

II/2 Satellite Data Calibration

Several papers dealt with the problem of calibrating the visible and infrared sensors. EUM WP-16 outlined plans for an aircraft campaign aimed at calibrating the Meteosat-5 visible channel in summer 1995. Simultaneous calibration of Meteosat-6, as well as possible cross calibration, was also discussed. Subsequent monitoring of any drift in the visible calibration is foreseen with ground targets.

Action WG II.1 EUMETSAT to report at CGMS XXIV on their visible calibration campaign.

EUM WP-17 detailed the Meteosat infrared (IR) and water vapour (WV) vicarious calibration from forward calculated clear sky radiances. The achieved precision is of the order of 1% for the IR and 2-3% for the WV. It was also stressed that cross calibration between different satellites is highly desirable.

PRC WP-03 presented the Chinese efforts to establish ground calibration sites for the polar orbiting system. A land site with measured reflection characteristics, which are close to Lambertian, and a lake with measurable surface temperature have been selected and are now being prepared for use in 1997. The importance of such ground calibration capabilities was noted and the Working Group looked forward to hearing more from the Chinese members on their progress, at future CGMS meetings.

USA WP-22 reported on progress in characterizing the quality of the GOES-8 calibration. After corrections for variations in scan mirror emissivity as a function of scan angle, the IR window radiance brightness temperature is known to better than 0.5 K. This was confirmed in an extensive field experiment using class-sonde temperature and moisture profile determinations, ocean skin temperature measurements, and airborne interferometric radiance measurements. The value of such calibration campaigns was noted. USA WP-25 presented cross calibration results using HIRS, GOES, and Meteosat in response to action items 22.22 and 22.23 from the last CGMS. A precision of around 1 K is possible through intercalibration of polar orbiting with geostationary measurements as well as geostationary with geostationary measurements. Several intercalibration procedures were introduced. These promising results toward establishing uniform quality of most satellite radiance measurements prompted the following recommendation:

Recommendation. CGMS should take the initiative for planning periodic and on going cross calibration campaigns of all current geostationary and polar orbiting satellite infrared sensors in order to characterize diurnal, seasonal, and instrumental transitions.

II/3 Vertical Sounding

EUM WP-18 reported on agreements under discussion for EUMETSAT to distribute ATOVS ingest and pre-processing software. These intentions are very welcome to the ITOVS community, but distribution policy decisions must still be made by the EUMETSAT Council.

II/4 Other Parameter Extraction

EUM WP-19 reported on the present efforts by EUMETSAT to define Satellite Applications Facilities (SAF). The SAFs have been introduced as a distributed element of the EUMETSAT Ground System, aiming at an optimum use of meteorological satellite data and research resources in Europe. To validate this concept it is planned to select two pilot SAFs this year.

Action WG II.2 EUMETSAT to update CGMS XXIV on the progress of the pilot SAFs.

JAPAN WP-12 described the algorithms under development for GMS-5 applications. These include Upper Tropospheric Humidity (UTH), Sea Surface Temperature (SST), and total Precipitable Water vapour (PW). It was noted that several working papers stressed improved characterization of global moisture. The recent advances with GMS-5 and GOES-8 H_2O channel capabilities, together with the good Meteosat-5 H_2O sensing, now make coordinated

activities toward uniform product quality and NWP impact studies very important. The Working Group felt that this international commonality of satellite capability will be making important contributions to new applications and should foster significant progress in definition of global moisture and its movements in the near future.

Dr. Menzel, in his capacity of CGMS rapporteur to the International TOVS Working Group (ITWG), reported on the most recent ITWG meeting (USA WP-30), with all ITWG recommendations being noted by the WG participants. A few of these recommendations to CGMS were discussed in detail. The ITWG noted that some NWP centers were not informed of operational changes to NOAA TOVS processing. The Working Group noted the importance of this communication and recommended utilization of the WMO proposed CGMS "Home Page" as a means to improve the communication.

Action WG II.3 The USA (NOAA) to coordinate with the WMO to install, or link, TOVS operational processing change notifications to the CGMS Home Page and report at CGMS XXIV.

The Working Group also noted the ITWG comment on the absence of the HIRS channel at 8.2 μm and agreed with the expressed need for this window channel in cloud phase and cirrus cloud applications. In light of the number of ITWG recommendations and comments to CGMS, the Working Group suggested a formal response to the ITWG.

Recommendation. The Working Group on Satellite Products recommends that the CGMS Plenary nominate two members to: review the ITWG report, recommend items to which the CGMS should provide specific response, draft such responses for member review by 30 September 1995, and provide feedback to ITWG by 30 November 1995.

II/5 New Products and their use in Numerical Weather Prediction

USA WP-23 reported on recent NMC efforts to use GOES IR precipitation estimates in global precipitation models. An algorithm combining IR and microwave observations is also being developed. It was commented that several initiatives for the direct use of radiances in NWP models are currently underway and that progress in this area and the availability of suitable data is of great interest to satellite data users.

II/6 Coordination Code Forms for Satellite Data (No papers were presented.)

II/7 Coordination of Data Formats for the Archive and Retrieval of Satellite Data

Two papers (RUS WP-11 and -12) spelled out the data archiving and distribution formats for the Russian meterological and earth resource satellite sensors. Digital Universal Format (DUF) is planned for GOMS and Hierarchical Data Formats (HDF) are planned for RESURS and OKEAN. USA WP-24 gave an update of CEOS activities with regard to data formats. The CEOS Working Group on Data noted the importance of CGMS staying informed on data format matters and requested CGMS become more involved.

The Working Group felt that data format issues were the purview of CEOS and that current communications were keeping both groups well informed of each other's activities.

REPORT FROM WORKING GROUP III: GLOBAL CONTINGENCY PLANNING

The working group comprised representatives of the three satellite operators - EUMETSAT, Japan, USA - which have fully operational geostationary satellites systems, together with a representative of the WMO. It was chaired by John Morgan, assisted by Jérôme Lafeuille as Secretary.

III/1 Review of Actions from the CGMS XXII

The working group reviewed CGMS Action 22.30, in which EUMETSAT was to coordinate a dialogue with Japan and the USA concerning a global contingency plan. EUMETSAT recalled that there were practical examples of a joint contingency actions between the USA and EUMETSAT, and a long term agreement on joint contingency planning. This had demonstrated the practical and political possibilities for such joint actions when appropriate. Discussions had taken place between Japan and the other partners on this issue. There was a sincere wish on each side to find a joint solution, but it had not yet proved possible to define any practical initiatives before an actual contingency situation would occur.

Although in principle technical solutions exist and have been demonstrated (the "bent-pipe" Atlantic Data Coverage continency operation), there are two main obstacles to a common CGMS wide solution. The first is the lack of financial resources. Like any other country, Japan would find it difficult to make financial provision for unexpected failure. The second is more technical, arising from the new dual-function MTSAT satellite concept, in which spare satellites need to be kept available at specific geographical locations for back-up support of essential national services.

In the light of this discussion, the working group recommended to close Actions 22.30 and 22.31.

III/2 Global Contingency Strategy

The working group nevertheless determined that there is a strong motivation amongst participants to keep open all possibilities for mutual support during contingency situations. The working group proposed that this motivation should be formalised through a non-binding CGMS declaration of good will and support to the extent possible when the occasion arises. Such a statement should be modelled on the existing EUMETSAT-USA Agreement, taken into account recent experience and lessons learned which the working group felt should be recorded for future reference. This should address both the requirements of the respective satellite operators as well as, to the extent possible, the wider WMO requirements.

The proposed form of the declaration was:

CGMS Members noted that one of the primary objectives of an operational satellite system is data continuity. Satellite and launch technology is still a high risk business and individual satellite operators may not always be able to maintain sufficient spare satellite

capacity to cover all possible contingencies. However, because of the need to prepare for contingency situations, satellite operators may, during some periods, have reserve capacity in orbit which is not being utilised with the same priority as its primary systems.

Accordingly, the CGMS may base its joint contingency strategy on the possible use, through bi-lateral arrangements, of any spare capacity available to other CGMS satellite operators, on a "Help your neighbour" principle. It is agreed that a contingency arises if a satellite operator is no longer in a position to provide priority satellite based services, or expects that such a situation will arise in the near future. In this context, priority satellite based services includes key missions such as image generation and dissemination, the data collection system and the global distribution of products used in NWP, such as Cloud Track Winds.

In accordance with this principle, any CGMS satellite operator faced with a contingency situation, whereby priority satellite based services cannot be supported, should immediately discuss the situation with the other satellite operators. All CGMS satellite operators undertake to discuss possible options in good faith, without prior commitment, to try to help solve the problem in the most effective way. There is no general obligation of any Member to help another on an ad-hoc basis without exchange of funds, although this is the basis of the Long Term Agreement between EUMETSAT and the USA, which assumes a long term balance of obligations. The possible financial aspects will be discussed on a case by case basis, but CGMS satellite operators will try to minimise any possible financial impact on either party to a contingency action.

A possible technical solution, which might be evaluated in future contingency events, is for a satellite operator, having a spare capacity in orbit beyond its priority needs, to move a spare satellite to support the operator having a contingency situation. The baseline is that the owner of the satellite will continue to operate the satellite in question, to avoid duplication of expensive control facilities, while the host operator makes all necessary provision for the regional utilisation of the satellite. Where possible, direct control of the satellite will be implemented. When this is not feasible, indirect control, through some form of "bent-pipe" telecommunications relay, may be used.

To provide the best possible level of services in a contingency situation it is essential that the satellite operator and the host operator come to an early agreement concerning their respective responsibilities. In order to provide guidance for such arrangements, it is suggested that the following guidelines, based on practical experience, shall be followed:

a) The satellite owner shall:

- Continue to own and operate the spare satellite so as to generate and disseminate imagery within available resources, in accordance with the normal standards of the satellite owner,

- Use the satellite to the extent possible in support of the International Data Collection System as a priority and the Regional Data Collection System if possible,

- Continue to support international programmes such as ISCCP and GPCP through the continued production of standard products based on data from the spare satellite,

- Continue the global distribution of key products used in NWP, such as Cloud Track Winds.

- Seek to operate the satellite in accordance with the data policy of the host operator, in order to minimise any impact on third parties.

b) The host operator shall:

- Make efforts to ensure that its users continue to be provided with services, such as access to image data, through a combination of the services provided by the satellite owner and those provided by the host,

- Seek to provide specialised support for the Regional Data Collection System where facilities permit,

- Continue to take responsibility, as far as possible, for specialised regional and other requirements not addressed by the satellite operator.

- Make every effort to restore normal service as soon as possible through the successful launch of a replacement satellite.

III/3 Preparation of Working Group Report

In compiling this report, the working group recommended that the above text be incorporated in the Report of CGMS XXIII and that, in due course, it be added to the Consolidated CGMS Report as a standard CGMS Strategy.

Furthermore, the working group recommended that it was no longer necessary to maintain a permanent working group on this subject, but that the topic should be discussed at the plenary level during each meeting of the CGMS.

REPORT FROM WORKING GROUP IV: SATELLITE-TRACKED WINDS

The Working Group on Satellite-Derived Winds was chaired by Dr Johannes Schmetz of EUMETSAT. Timothy Stryker of NOAA served as Rapporteur.

The Working Group noted the progress since the Second Meeting of the International Winds Workshop, held in Japan in December 1993. Working Group participants also discussed plans for the next workshop, tentatively scheduled for 1996 in Europe. To facilitate further progress on winds intercomparison methods, the Working Group expressed the desire for scheduling the 1996 Winds workshop in advance of the next CGMS Plenary. Specifically, the Working Group wishes to change the current CGMS method of winds comparison described in the CGMS Consolidated Report. The Working Group recommended that the CGMS Plenary in turn arrange to hold CGMS XXIV after the next International Winds Workshop.

IV/1 Winds Verification Statistics

EUM WP-21 provided an update on METEOSAT cloud motion winds (CMW) verifications based on comparisons against collocated radiosonde measurements. The paper addressed the performance of METEOSAT high, medium, and low level CMW and water vapour winds (WVW). The new WVW are of comparable quality to the high level CMW, and improvement at medium and low level is also apparent. The introduction of the new rectification scheme had a noticeable positive impact on CMW at all three levels. The transition from METEOSAT-4 to METEOSAT-5 in February 1994 had an initial negative effect on CMW quality due to a rotating lens problem on Meteosat-5, but was mitigated with software modifications in September 1994. The present speed biases at all three levels have been reduced to less than 1.0 m/s. Root Mean Square (RMS) vector differences versus radiosondes are also reduced. Efforts for further improvement continue.

JAPAN WP-13 reported on the status of GMS CMW derivation. Monthly mean differences between CMW and radiosondes were calculated according to the standard CGMS method. The quality of low-level CMW has been good. Since 1991, RMS vector differences have been smaller than 5.0 m/s. Absolute values of speed differences have generally been below 0.5 m/s.

USA-WP-26 provided a summary of modifications to NESDIS winds processing and the resulting improvements to CMW quality. Operational GOES-7 CMW have been stabilized. GOES-8 CMW show an improvement over those of GOES-7. GOES-8 winds are planned to become operational in the summer of 1995, when they will be transmitted to other NWP centres over the GTS. Wind vector production every three hours is envisaged in 1996. NOAA also informed the Working Group of plans to modify the GOES-M satellite to add a CO_2 channel at 8 km resolution. The Working Group welcomed the reappearance of a CO_2 channel aboard the GOES satellites since the CO_2 slicing for height assignment has advantages over the water vapour methods.

USA WP-28 provided the CGMS standard winds intercomparison report. It was recognized by the Working Group that the current CGMS guidelines for CMW statistics need revision. Detailed specifications should be provided by the International Winds Workshop for the next CGMS Plenary Meeting (XXIV). Thus the Working Group agreed upon the following:

Action WG IV.1 CGMS members develop a new standardized reporting method on winds quality, in coordination with the International Winds Workshop, and propose a new method at CGMS XXIV. Coordination via electronic bulletin board is requested from WMO.

Action WG IV.2 EUMETSAT will provide over this bulletin board an electronic copy of the winds statistics section of the CGMS Consolidated Report.

Recommendation: The next International Winds Workshop should be held prior to the next CGMS Plenary Meeting.

As an interim step the Working Group agreed on the following recommendation:

The Working Group members should provide the following information to one another and to the CGMS secretariat.

(1) Monthly means of speed bias and RMS vector difference between radiosondes and satellite winds for low- (>700 hPa), medium- (700-400 hPa), and high- (<400 hPa) levels together with the radiosonde mean wind speed. This procedure should be done for three latitude bands: North of 20 North, the tropical belt (20 North to 20 South), and South of 20 South.

(2) Figures of the monthly CMW and WVW statistics through the last 12 months.

(3) Information on recent significant changes in the wind retrieval algorithm.

Furthermore the Working Group participants agreed to revise Permanent Action 5 so that it reads:

"CGMS members generating CMW check that the following monthly statistics are sent and received on a quarterly basis: number of co-locations, temporal and spatial co-location thresholds, and radiosonde inclusion/exclusion criteria."

IV/2 Procedures for the Exchange of Inter-comparison Data

No papers were presented under this agenda item.

IV/3 Derivation of Wind Vectors

ESA WP-04 provided an update on the status of ESOC's water vapour wind extraction. These operational WVW show comparable quality to CMW and provide better horizontal coverage. Additionally, the water vapour channel provides an easy alternative to image filtering of high level cloud scenes. Recent research at ESOC has developed an approach for assigning a quality mark to each of the derived vectors. This mark provides an indication of the representativeness of the WVW vector as a single level wind measurement. The dissemination of these quality marks together with the derived vector is highly desirable and would improve the utilisation of these data.

The Working Group noted that quality marks are needed by NWP centres, which can use all quality levels for improved synoptic analyses. The Working Group added that charts of WVW including lower quality vectors are very useful for synoptic analyses in tropical regions due to the very good spatial coverage; MDD dissemination of these was suggested. These charts are in particular useful in developing countries which may lack other detailed observations. The following action was proposed:

Action WG IV.3 **CGMS winds operators to explore the establishment of standard guidelines for quality marking and report on their progress at CGMS XXIV. CGMS winds operators to propose a special session on this topic at the next International Winds Workshop.**

ESA WP-05 reported on the development of low level CMW derivation using visible METEOSAT images. The technique is similar to the infrared low level cloud motion wind retrieval method, but is restricted to marine regions. The height assignment of the visible CMW relies on the cloud brightness temperature obtained in the METEOSAT IR channel. Validation of these winds show that they are of operational quality. High spatial resolution visible imagery warrant shorter time intervals for monitoring winds; additional improvements are likely when this is possible.

JAPAN WP-14 presented its CMW and WVW extraction methods planned for GMS-5. GMS-5 WVW are expected to become operational after adjustment of the pattern selection and the evaluation of data quality. WMO noted that, in all cases, users would like the CMW and WVW to be provided as distinguishable datasets.

The Working Group invited EUMETSAT to report, at CGMS XXIV, on any differences between MPEF and MIEC wind processings.

The Working Group noted that a new milestone was within reach. Very soon JMA, ESA/EUMETSAT, and NOAA will be using similar height assignment techniques. Russia intends to use the experimental water vapour channel on GOMS to develop similar capabilities. The use of similar height assignments will be a major step forward for global winds modelling efforts.

FINAL PLENARY SESSION: SENIOR OFFICIALS MEETING

J.1 APPOINTMENT OF CHAIRMAN

The CGMS XXIII Senior Officials meeting was convened at 9 a.m. on 19 May 1995, with Mr. J. Morgan elected as Chairman.

J.2 REPORTS FROM THE WORKING GROUPS

The reports from the four Working Groups were presented by their Chairmen: Mr. R. Wolf (WG I. on Telecommunications), Dr P. Menzel (WG II on Satellite Products), Mr J. Morgan (WG III on Global Contingency Planning) and Dr J. Schmetz (WG IV on Satellite-tracked Winds).

The Senior Officials took note of the reports and thanked the participants and Chairmen for their active and fruitful discussions. They endorsed the proposed actions and recommendations formulated with minor modifications.

In particular, CGMS thanked the Working Group I for its very efficient and comprehensive action. CGMS took note of the outcome of SFCG and confirmed the need to list the frequencies requiring protection. It was noted that Action WG I.3 should become a Permanent Action. Furthermore, CGMS agreed to delete Permanent Action No.7 since the issue is normally addressed within the agenda of CGMS plenary.

Working Group II and its Chairman were also complimented for their very comprehensive report. CGMS agreed that the use of satellite data should be viewed within the context of the total available observing system, taking benefit of the assimilation of all observing capabilities. CGMS endorsed the recommendation that CGMS should undertake periodic cross calibration campaigns of all current geostationary and polar satellite infrared sensors in order to establish a record of diurnal, seasonal and instrumental transitions, and formulated an Action on that issue. CGMS appreciated the significant progress which is expected to result from the international commonality of satellite capabilities with regard to global moisture sensing. CGMS agreed that NOAA and EUMETSAT should each nominate one contact to review the ITWG report in order to recommend items to which the CGMS should provide specific responses, to draft such responses and to provide feedback to ITWG. CGMS agreed on the actions proposed by the Working Group. CGMS also proposed a new action regarding CEOS-CGMS interaction.

The CGMS endorsed the report of Working Group III on Global contingency planning, and stressed that it was in the interest of the whole community to address these issues as early as possible. The Senior Officials unanimously endorsed the strategy as described in Annex 5. CGMS furthermore agreed that it was currently not necessary to maintain a permanent working group on this subject and decided to close Actions 22-30, 22-31 and 21-32, but added that Global contingency planning should be a regular agenda item for CGMS plenary.

CGMS thanked Working Group IV on Satellite-tracked winds and endorsed its conclusions. CGMS welcomed the offer from EUMETSAT to host a new Winds Workshop in early 1996. CGMS also agreed to the proposed actions, and endorsed the recommendation made to the Working Group members.

J.3 NOMINATION OF CGMS REPRESENTATIVES AT WMO AND OTHER MEETINGS

The Senior Officials agreed that :

- Dr. Menzel will represent CGMS at the next meeting of the ITWG,
- Mr. Morgan will represent CGMS at the WMO Congress in June 1995,
- The Secretariat will represent CGMS at the WMO EC in May 1996,
- Dr. Szejwach will represent CGMS at the WMO CBS/WG-Sat,
- Dr. Szejwach will be Rapporteur at the Wind Workshop,
- Mr. Wolf will represent CGMS interests at the SFCG and WRC,
- The Secretariat will represent CGMS at CEOS plenary.

Furthermore, the points of contacts of CGMS Members for the various activities were reviewed. The updated lists are given in the annexes.

J.4 ANY OTHER BUSINESS

CGMS took note with a special sense of satisfaction that the long planned network of five coordinated geostationary meteorological satellites had been achieved after many years of planning, following the successful launch of GOMS-N1. The CGMS congratulated Russia on this event and expressed the hope that GOMS could soon be made operational.

CGMS also noted that this new satellite, filling an important gap over the Indian Ocean region, would provide vital data for routine forecasts, for aviation meteorology, for climate studies and for many other applications. Wide access to these data is vital for operational purposes and CGMS hopes the Roshydromet will establish the facilities needed for processing GOMS data and dissemination of products to the wider user community. CGMS expressed the wish that ongoing discussions between EUMETSAT and Russia, as well as the interest expressed by NOAA for receiving GOMS digital data, will result in the routine exchange and re-distribution of digital data.

The CGMS congratulated EUMETSAT as a host and as the Secretariat for their efforts in arranging this plenary session.

J.5 APPROVAL OF DRAFT FINAL REPORT

The plenary session, with all Senior Officials present, reviewed the draft Final Report of the meeting. Noting a few modifications and the new actions resulting from the Working Groups, the Senior Officials approved the report. The Secretariat agreed to include all the amendments into a revised version which would be distributed to CGMS Members for final comment prior to publication.

J.6 SUMMARY LIST OF ACTIONS

(i) Permanent actions, as reworded during CGMS XXIII

1. The Secretariat to review the tables of current and planned polar and geostationary satellites, and to distribute this updated information, via the WWW Operational Newsletter, via Electronic Bulletin Board, or other means as appropriate.

2. All satellite operators to circulate regular satellite operational reports.

3. All satellite operators to provide NOAA/NESDIS with information on unexplained anomalies for study, and NOAA to provide solar event information to the satellite operators on request and a status report on the correlation study at each meeting.

4. USA to issue quarterly to all other admitting authorities the consolidated DCP assignments.

5. All satellite operators to regularly provide WMO with information on the number of Met satellite reception stations in their areas of responsibility.

6. All CGMS Members to inform users to register user stations within their area of responsibility.

7. CGMS members generating CMW check that the following monthly statistics are sent and received on a quarterly basis: number of co-locations, temporal and spatial co-location thresholds, and radiosonde inclusion/exclusion criteria.

(ii) Outstanding actions from previous meetings (as reviewed in Section A5)

ACTION 21.17 All CGMS Members are requested to indicate planned introduction dates of LRIT.

ACTION 21.24 CGMS Members to consider the possible technical measures for the reorganization of the IDCS to include the PRC and any other changes necessary to meet currently foreseen uses of the IDCS.

ACTION 22.05 EUMETSAT to consider the possibility of moving a "spare" Meteosat satellite, if necessary, in order to provide coverage over the Indian Ocean.

ACTION 22.06 NOAA and WMO to investigate the possibility of making Special Sensor Microwave Imager (SSM/I) data and products available on the GTS, so that they could be received by all NWP centres, tropical cyclone RSMCs and regional forecast offices.

(iii) Actions from CGMS XXIII

ACTION 23-01 USA/NOAA to distribute by 1 November 1995 the definition of the LRPT format.

ACTION 23-02 CGMS Members are requested to notify the Secretariat of their agreement on the proposed LRPT format by CGMS XXIV.

ACTION 23-03 WMO to provide CGMS Members with a copy of the GCOS Space Plan version 1.0.

ACTION 23-04 CGMS Members to review and comment on the GCOS Space Plan version 1.0, with respect to achievability and proposed priority of implementation into their own plans.

ACTION 23-05 CGMS to investigate the feasibility of meeting the draft requirement for the exchange of digital satellite image data over the GTS.

ACTION 23-06 Japan, P.R.C, and the Russian Federation to indicate, by 30 November 1995, possible contributions to the CGMS Directory covering applications conducted in their respective regions.

ACTION 23-07 EUMETSAT to seek resources to initiate the project of a CGMS Directory of applications, and inform CGMS Members by January 1996.

ACTION 23-08 CGMS members to provide WMO with names to be included in a list-server of points of contacts for the preparation of a CGMS Directory. WMO to establish such a list-server.

ACTION 23-09 All CGMS Satellite operators to contribute to the WMO database of satellite user stations, in providing information on geographical locations of the users of their respective satellites.

ACTION 23-10 All CGMS satellite operators to check the registration status of receiving stations of their users.

ACTION 23-11 The CGMS Secretariat, with the assistance of CGMS Members, to prepare for the WMO-CGMS home page of the WMO Bulletin Board, an information note about future satellite programmes and missions, and the specific frequency bands requiring protection.

ACTION 23-12 Russia to provide CGMS Members with details of IDCP channel frequencies as soon as possible.

ACTION 23-13 The USA to provide CGMS Members with information on the number of APT reception stations world-wide by 1 September 1995.

ACTION 23-14 The Secretariat to establish a period in the next twelve months for the end to end monitoring of certain DCP, in consultation with CGMS Members supporting the IDCS, and report to CGMS XXIV.

ACTION 23-15 The WMO to address any resulting problems relating to the onward relay of DCP messages via the GTS and report to CGMS XXIV.

ACTION 23-16 The Secretariat to update Annex 3 of the IDCS Users Guide, indicating the admitting authority address of the PRC.

ACTION 23-17 All CGMS Members to study the possibilities for using spread spectrum techniques and higher bit rates for future DCS.

ACTION 23-18 The USA to provide CGMS with results of studies of DCS spread spectrum techniques and the use of higher bit rates by 1 July 1995.

ACTION 23-19 CGMS Members to identify to WMO, by 1 July 1995, points of contacts who would assist with the design of, provision of material for, and dealing with enquiries resulting from, the CGMS home page.

ACTION 23-20 EUMETSAT to report on visible calibration campaign at CGMS XXIV.

ACTION 23-21 CGMS Members to nominate points of contacts to coordinate the preparation of a procedure for cross-calibration of satellites.

ACTION 23-22 EUMETSAT to update CGMS XXIV on the progress of the pilot SAFs.

ACTION 23-23 USA (NOAA) to coordinate with the WMO to install or link TOVS operational processing change notifications to the CGMS Home Page and report at CGMS XXIV.

ACTION 23-24 NOAA and EUMETSAT to each nominate one contact to review the ITWG report, consider any appropriate response, draft such response for Member review by 30 September and provide feedback to ITWG by 30 November 1995.

ACTION 23-25 CGMS to forward CGMS CAL/VAL working papers to CEOS CAL/VAL working group and maintain close communication on these issues.

ACTION 23-26 People's Republic of China to report at CGMS XXIV on progress regarding its calibration sites.

ACTION 23-27 The rapporteur of the Wind workshop to discuss and recommend standardized reporting method on winds quality, in coordination with the International Winds Workshop, and propose a new method at CGMS XXIV.

ACTION 23-28 EUMETSAT will provide over an Electronic Bulletin Board a copy of the winds statistics section of the CGMS Consolidated Report.

ACTION 23-29 CGMS winds operators to explore the establishment of standard guidelines for quality marking and report on their progress at CGMS XXIV. CGMS winds operators to propose a special session on this topic at the next International Winds Workshop.

ACTION 23-30 EUMETSAT to report at CGMS XXIV on any differences between MPEF and MIEC wind processing.

J.7 DATE AND PLACE OF NEXT MEETINGS

CGMS was pleased to accept the offer by WMO to host CGMS XXIV in April/May 1996 in Switzerland. CGMS noted that optimum arrangements for its annual meetings require suitable facilities for meetings during the day and during the evenings. CGMS felt it important that the venue be at a secluded site to meet best such requirements. Such arrangements in the past had greatly enhanced working group, sub-group and informal discussions. It encouraged WMO to take these factors into consideration when selecting the venue in Switzerland.

CGMS also encouraged the Russian Federation to consider hosting the CGMS XXV.

Annex 1

AGENDA OF THE CGMS XXIII PLENARY MEETING DARMSTADT, GERMANY, 15-19 MAY 1995

A. PRELIMINARIES

A.1 Introduction
A.2 Election of Chairman
A.3 Adoption of agenda and work plan of W/G Sessions
A.4 Arrangements for the Drafting Committee
A.5 Review of Action Items

B. REPORT ON THE STATUS OF CURRENT SATELLITE SYSTEMS

B.1 Polar Orbiting Meteorological Satellite Systems
B.2 Geostationary Meteorological Satellite Systems

C. REPORT ON FUTURE SATELLITE SYSTEMS

C.1 Future Polar Orbiting Meteorological Satellite Systems
C.2 Future Geostationary Meteorological Satellite Systems

D. OPERATIONAL CONTINUITY AND RELIABILITY

D.1 Global planning, including orbital positions
D.2 Inter-regional contingency measures

E. METEOROLOGICAL SATELLITES AS PART OF WMO PROGRAMMES

E.1 World Weather Watch
E.2 Other Programs

F. COORDINATION OF INTERNATIONAL DATA COLLECTION & DISTRIBUTION

F.1 Status and Problems of IDCS
F.2 Ships, including ASAP
F.3 ASDAR
F.4 Dissemination of DCP messages (GTS or other means)

G. COORDINATION OF DATA DISSEMINATION

G.1 Dissemination of images via Satellite
G.2 Dissemination of products via GTS or other means
G.3 Global exchange of satellite image data

H. OTHER ITEMS OF INTEREST

H.1 Applications of Meteorological Satellite Data for Environment Monitoring
H.2 Search and Rescue (S&R)
H.3 Anomalies from Solar and Other Events
H.4 Information and Training
H.5 Any other business

--------- PARALLEL WORKING GROUP SESSIONS ----------

WORKING GROUP I - TELECOMMUNICATIONS

I/1 Results of SFCG - Secretariat Report
I/2 Coordination of Frequency Allocations
I/3 Matters arising from the plenary
I/4 Electronic Bulletin Boards (EBB)

WORKING GROUP II - SATELLITE PRODUCTS

II/1 Image processing techniques
II/2 Satellite Data Calibration
II/3 Vertical sounding
II/4 Other Parameter Extraction
II/5 New Products & their use in Numerical Weather Prediction
II/6 Coordination of Code forms for satellite Data
II/7 Coordination of Data Formats for the Archive and Retrieval of Satellite Data

WORKING GROUP III - GLOBAL CONTINGENCY PLANNING

III/1 Review of Actions from the CGMS XXII
III/2 Global contingency strategy
III/3 Preparation of WG Report

WORKING GROUP IV - CLOUD MOTION WINDS

IV/1 Wind verification statistics
IV/2 Procedures for the exchange of inter-comparison data
IV/3 Derivation of Wind vectors

---------- SENIOR OFFICIALS MEETING ----------

J.1 Appointment of Chairman of final session
J.2 Reports from the Working Groups
J.3 Nomination of CGMS Representatives at WMO and other meetings
J.4 Any Other Business
J.5 Summary List of Actions from CGMS XXIII
J.6 Approval of Draft Final Report
J.7 Date and Place of Next Meetings

WORKING PAPERS SUBMITTED TO CGMS-XXIII

		(Agenda item)
	ESA	
ESA-WP-01	The Extended Atlantic Data Coverage Mission (XADC)	(B.2)
ESA-WP-02	Meteosat spacecraft anomalies	(B.2)
ESA-WP-03	Correction of the Meteosat-6 radiometric anomaly	(B.2)
ESA-WP-04	Present status of water vapour wind extraction at ESOC	(IV/3)
ESA-WP-05	Cloud-Motion Winds from visible Meteosat images	(IV/3)
	EUMETSAT	
EUM-WP-01	Review of actions items (Secretariat report)	(A.5)
EUM-WP-02	Status of the Meteosat system	(B.2)
EUM-WP-03	Status and plans for MTP	(B.2)
EUM-WP-04	Status of the EPS Preparatory Programme	(C.1)
EUM-WP-05	Status and plans for MSG	(C.2)
EUM-WP-06	Status and problems of IDCS	(F.1)
EUM-WP-07	Implementation of HRI encryption	(G.1)
EUM-WP-08	Status of Meteorological Data Distribution (MDD)	(G.2)
EUM-WP-09	Global exchange of satellite images	(G.3)
EUM-WP-10	CGMS Directory of Applications	(H.4)
EUM-WP-11	EUMETSAT training activities	(H.4)
EUM-WP-12	Report from the 14th meeting of the SFCG	(I/1)
EUM-WP-13	Protection of passive sensor frequencies Use of the Oxygen absorbtion band around 60 GHz	(I/2)
EUM-WP-14	Sharing of the frequency band 1670-1710 MHz between meteorological and mobile satellite services	(I/2)
EUM-WP-15	The MPEF in the new EUMETSAT ground segment	(II/1)
EUM-WP-16	Absolute calibration of the Meteosat Visible Channels	(II/2)
EUM-WP-17	Calibration of Meteosat IR and WV channels	(II/2)
EUM-WP-18	ATOVS software development	(II/3)
EUM-WP-19	Status of EUMETSAT SAF concept	(II/4)
EUM-WP-21	Wind verification statistics	(IV/1)
	JAPAN	
JAPAN-WP-01	Review of action items from previous CGMS meetings	(A.5)
JAPAN-WP-02	Status of Geostationary Meteorological Satellite-4 (GMS-4)	(B.2)
JAPAN-WP-03	Report on status of satellite systems: present status of the Geostationary Meteorological Satellites	(B.2)
JAPAN-WP-04	Progress and plans for GMS-5	(C.2)
JAPAN-WP-05	Plans for Multi-functional Transport Satellite (MTSAT)	(C.2)
JAPAN-WP-06	Status and problems of IDCS	(F.1)
JAPAN-WP-07	Interference monitoring of IDCS channels	(F.1)
JAPAN-WP-08	Status of ship IDCPs including ASAP	(F.2)
JAPAN-WP-09	Status of the ASDAR	(F.3)
JAPAN-WP-10	Dissemination of DCP messages	(F.4)
JAPAN-WP-11	Dissemination plan of satellite images by GMS-5	(G.1)
JAPAN-WP-12	Products utilizing data of GMS-5 new sensors	(II/4)

JAPAN-WP-13	Current Status of GMS wind derivation	(IV/1)
JAPAN-WP-14	Derivation of cloud motion and water vapor motion winds	(IV/3)
JAPAN-WP-15	GMS-5 GEOSAR experiment in Japan	(H.2)
	PEOPLE'S REPUBLIC OF CHINA	
PRC-WP-01	The Status of FY-1 Program	(C.1)
PRC-WP-02	The Status of FY-2 Program	(C.2)
PRC-WP-03	The progress on preparing radiometric calibration sites	(II/2)
	RUSSIAN FEDERATION	
RUS-WP-01	Current polar orbiting meteorological satellite system (METEOR-2, -3)	(B.1)
RUS-WP-02	Geostationary Operational Meteorological Satellite GOMS-Elektro	(B.2)
RUS-WP-03	Report on the status of future polar orbiting meteorological satellite systems	(C.1)
RUS-WP-04	Geostationary Operational Meteorological Satellite GOMS N2	(C.2)
RUS-WP-05	GOMS retransmission system components and status	(F.1)
RUS-WP-06	DCP status in Russia	(F.4)
RUS-WP-07	WEFAX imagery preparation and dissemination via GOMS	(G.1)
RUS-WP-08	Global exchange of satellite image data	(G.3)
RUS-WP-09	Coordination of frequency allocation: satellite networks	(I.2)
RUS-WP-10	An overview of the ground microprocessing system for GOMS data receiving, processing and archiving	(II.1)
RUS-WP-11	GOMS N1 data archiving and distribution formats	(II.7)
RUS-WP-12	Data formats for RESURS and OCEAN satellites	(II.7)
	USA	
USA-WP-01	Status of NOAA actions from CGMS XXII	(A.5)
USA-WP-02	Report on the status of current polar orbiting meteorological satellite systems	(B.1)
USA-WP-03	Report on the status of current geostationary meteorological satellite systems	(B.2)
USA-WP-04	Status report on NOAA-K, -L, -M	(C.1)
USA-WP-05	GOES-J spacecraft status	(C.2)
USA-WP-06	Status report on GOES-K, L, M	(C.2)
USA-WP-07	Post GOES M follow-on plan	(C.2)
USA-WP-08	Report of IDCS assignments	(F.1)
USA-WP-09	Dissemination of DCP Messages (GTS or Other Means)	(F.4)
USA-WP-10	NOAAPORT Satellite Broadcast Network	(G.1)
USA-WP-11	NOAA/NESDIS ATOVS data transfer to the U.K. Meteorological Office	(G.2)
USA-WP-12	Polar Satellite Active Archive (SAA) (Information Paper)	(G.3)
USA-WP-13	Applications of the DMSP SSM/I derived experimental soil wetness index for large area flood monitoring	(H.1)
USA-WP-14	COSPAS-SARSAT demonstration and evaluation of geostationary earth orbit Search and Rescue satellite systems	(H.2)
USA-WP-15	Update on the International COSPAS-SARSAT Program	(H.2)

USA-WP-16	Report of the Fourteenth Space Frequency Coordination Group Meeting	(I/1)
USA-WP-17	Coordination of frequency allocations	(I/2)
USA-WP-18	Registration of NOAA Automatic Picture Transmission (APT) Earth Stations	(I/2)
USA-WP-19	Proposed changes to the Automatic Picture Transmission (APT) frequencies for NOAA-N and NOAA-N'	(I/2)
USA-WP-20	1994 International Telecommunication Union meetings concerning meteorological satellite frequencies	(I/2)
USA-WP-21	GOES-8 image navigation and registration system status	(II/1)
USA-WP-22	GOES-8 calibration and radiometric performance	(II/2)
USA-WP-23	Use in global numerical models of precipitation estimates derived from geostationary satellite imagery	(II/5)
USA-WP-24	Committee on Earth Observation Satellite (CEOS) Working Group on Data (WGD)	(II/7)
USA-WP-25	Comparison of HIRS, GOES, and Meteosat calibration	(II/2)
USA-WP-26	Derivation of wind vectors and wind performance statistics	(IV/1)
USA-WP-27	Derived product imagery for GOES I-M	(II/1)
USA-WP-28	Report on the Initial Joint Polar Orbiting Operational Environmental Satellite System	(C.1)
USA-WP-29	Report on the U.S. National Polar Orbiting Operational Environmental Satellite System and U.S.-EUMETSAT long term cooperation in polar satellites	(C.1)
USA-WP-30	International TOVS Working Group Report to CGMS	(II.4)
USA-WP-31	Status report on semi-annual CGMS international comparison of satellite winds	(IV/1)

WMO

WMO-WP-01	Dissemination of information on typhoons via satellites	(E.1)
WMO-WP-02	Requirement for a multi-purpose computer workstation for handling satellite-based meteorological broadcasts	(H.5)
WMO-WP-03	List of WMO publications	(H.4)
WMO-WP-04	Review of action items from previous CGMS meetings	(A.5)
WMO-WP-05	WMO databases	(H.5)
WMO-WP-06	Satellite image interpretation message	(E.1)
WMO-WP-07	CGMS Electronic Bulletin Boards	(I/3)
WMO-WP-08	WMO Strategy for Education and Training in Satellite Matters Status Report	(H.4)
WMO-WP-09	Low Cost Low Resolution Satellite Receiving Project	(E.2)
WMO-WP-10	Matters Related to APT/WEFAX and Conversion	(E.1)
WMO-WP-11	Status Report on WMO Requirements for Global Contingency Planning	(G.3)
WMO-WP-12	WMO Satellite Data Requirements Status Report	(E.1)
WMO-WP-13	ASDAR and ASAP	(F.2)
WMO-WP-14	The GCOS Space-based Observation Plan	(D.1)
WMO-WP-15	Radio Frequency Matters Related to Meteorological Satellite Activities	(I.2)

Annex 3

LIST OF PARTICIPANTS IN CGMS XXIII

ESA

Dr. Dave **ANDREWS**
Head of Earth Observation Missions
ESA/ESOC

Dr. Volker **GÄRTNER**
Head of Meteorologists
ESA/ESOC

Mr. Ken **HOLMLUND**
MOP/MEP
Theoretical Meteorologist
ESA/ESOC

EUMETSAT

Mr. Gordon **BRIDGE**
CGMS Secretariat
Meteosat Operational Programme Manager

Mr. Jérôme **LAFEUILLE**
CGMS Secretariat
International Affairs Officer

Mr. John **MORGAN**
Director

Mr. Mikael **RATTENBORG**
MPEF Manager

Dr. Johannes **SCHMETZ**
Head of Meteorological Division

Dr. Gerard **SZEJWACH**
Head of Technical Department

Mr. Heinrich **WOICK**
Meteorological Expert

Mr. Robert **WOLF**
Head of Ground Support Division

JAPAN

Dr. Tetsu **HIRAKI**
Head, Office of Meteorological Satellite Planning
Japan Meteorological Agency

Mr. Koichi **KIMURA**
Head, System Engineering Division Data Processing Dpt.
Meteorological Satellite Center

Mr. Motoi **OKAWARA**
Earth Observation Satellite Group
National Space Development Agency of Japan

PEOPLE'S REPUBLIC OF CHINA

Mr. Huang **HANWEN**
Senior Engineer
National Satellite Meteorological Center

Mr. Jianping **XU**
Senior Engineer
Satellite Meteorology Center
China Meteorological Administration

RUSSIA

Mr. Vladimir **KHARITONOV**
Chief of Space Observation Systems Department
Roshydromet

Mr. Yury **TRIFONOV**
Deputy Director
VNIIEM

Mr. Alexander **USPENSKY**
General Director
NPO "Planeta"

USA

Mr. Paul **MENZEL**
SDAB
NOAA/NESDIS

Mr. John **HUSSEY**
Director Office of Systems Development
NOAA/NESDIS

Mr. Carl **STATON**
Deputy Chief, Information Processing Division
NOAA/NESDIS

Mr. Tim **STRYKER**
International Relations Specialist
NOAA/NESDIS

Mr. Fred **ZBAR**
Chief, System Requirements Branch
NOAA/National Weather Service

WMO

Dr. Don **HINSMAN**
Senior Scientific Officer
WMO Satellite Activities

Mr. Stefan **MILDNER**
Head of Technical Department
Deutscher Wetterdienst
(Vice-president of CBS)

Annex 4

MEMBERS OF WORKING GROUP I: TELECOMMUNICATIONS

Mr.	R. Wolf (Chairman)	EUMETSAT
Mr.	G. Bridge (Secretary)	EUMETSAT
Dr.	T. Hiraki	JMA, JAPAN
Mr.	M. Okawara	NASDA, JAPAN
Mr.	H. Hanwen	SAST/SISE, PRC
Mr.	J. Xu	SMC, PRC
Mr.	V. Kharitonov	ROSHYDROMET, RUSSIA
Mr.	Y. Trifonov	VNIIEM, RUSSIA
Mr.	J. Hussey	NOAA/NESDIS, USA
Mr.	C. Staton	NOAA/NESDIS, USA
Mr.	F. Zbar	NATIONAL WEATHER SERVICE, USA
Dr.	D. Hinsman	WMO
Mr.	S. Mildner	WMO/CBS

MEMBERS OF WORKING GROUP II: SATELLITE PRODUCTS

Dr.	P. Menzel (Chairman)	NOAA/NESDIS, USA
Mr.	K. Holmlund (Secretary)	ESA/ESOC
Dr.	V. Gärtner	ESA/ESOC
Dr.	J. Schmetz	EUMETSAT
Mr.	H. Woick	EUMETSAT
Mr.	K. Kimura	MSC, JAPAN
Mr.	M. Okawara	NASDA, JAPAN
Mr.	J. Xu	SMC, PRC
Mr.	H. Hanwen	SAST/SISE, PRC
Mr.	V. Kharitonov	ROSHYDROMET, RUSSIA
Dr.	A. Uspensky	NPO PLANETA, RUSSIA
Mr.	C. Staton	NOAA/NESDIS, USA
Mr.	F. Zbar	NOAA/NWS, USA

MEMBERS OF WORKING GROUP III: GLOBAL CONTINGENCY PLANNING

Mr.	J. Morgan (Chairman)	EUMETSAT
Mr.	J. Lafeuille (Secretary)	EUMETSAT
Dr.	T. Hiraki	JMA, JAPAN
Mr.	M. Okawara	NASDA, JAPAN
Mr.	J. Hussey	NOAA/NESDIS, USA
Mr.	T. Stryker	NOAA/NESDIS, USA
Dr.	D. Hinsman	WMO

MEMBERS OF WORKING GROUP IV: CLOUD MOTION WINDS

Dr.	J. Schmetz (Chairman)	EUMETSAT
Mr.	T. Stryker (Secretary)	NOAA/NESDIS, USA
Mr.	H. Woick	EUMETSAT
Dr.	V. Gärtner	ESA/ESOC
Mr.	K. Holmlund	ESA/ESOC
Mr.	K. Kimura	MSC, JAPAN
Dr.	A. Uspensky	NPO Planeta, RUSSIA
Dr.	P. Menzel	NOAA/NESDIS, USA
Dr.	D. Hinsman	WMO

Annex 5

STRATEGY FOR GLOBAL CONTINGENCY PLANNING

endorsed at CGMS XXIII

One of the primary objectives of an operational satellite system is data continuity. Satellite and launch technology is still a high risk business and individual satellite operators may not always be able to maintain sufficient spare satellite capacity to cover all possible contingencies. However, because of the need to prepare for contingency situations, satellite operators may, during some periods, have reserve capacity in orbit which is not being utilised with the same priority as its primary systems.

Accordingly, the CGMS may base its joint contingency strategy on the possible use, through bi-lateral arrangements, of any spare capacity available to other CGMS satellite operators, on a "Help your neighbour" principle. It is agreed that a contingency arises if a satellite operator is no longer in a position to provide priority satellite based services, or expects that such a situation will arise in the near future. In this context, priority satellite based services includes key missions such as image generation and dissemination, the data collection system and the global distribution of products used in NWP, such as Cloud Track Winds.

In accordance with this principle, any CGMS satellite operator faced with a contingency situation, whereby priority satellite based services cannot be supported, should immediately discuss the situation with the other satellite operators. All CGMS satellite operators undertake to discuss possible options in good faith, without prior commitment, to try to help solve the problem in the most effective way. There is no general obligation of any Member to help another on an ad-hoc basis without exchange of funds, although this is the basis of the Long Term Agreement between EUMETSAT and the USA, which assumes a long term balance of obligations. The possible financial aspects will be discussed on a case by case basis, but CGMS satellite operators will try to minimise any possible financial impact on either party to a contingency action.

A possible technical solution, which might be evaluated in future contingency events, is for a satellite operator, having a spare capacity in orbit beyond its priority needs, to move a spare satellite to support the operator having a contingency situation. The baseline is that the owner of the satellite will continue to operate the satellite in question, to avoid duplication of expensive control facilities, while the host operator makes all necessary provision for the regional utilisation of the satellite. Where possible, direct control of the satellite will be implemented. When this is not feasible, indirect control, through some form of "bent-pipe" telecommunications relay, may be used.

To provide the best possible level of services in a contingency situation it is essential that the satellite operator and the host operator come to an early agreement concerning their respective responsibilities. In order to provide guidance for such arrangements, it is suggested that the following guidelines, based on practical experience, shall be followed:

a) The satellite owner shall:

- Continue to own and operate the spare satellite so as to generate and disseminate imagery within available resources, in accordance with the normal standards of the satellite owner,

- Use the satellite to the extent possible in support of the International Data Collection System as a priority and the Regional Data Collection System if possible,

- Continue to support international programmes such as ISCCP and GPCP through the continued production of standard products based on data from the spare satellite,

- Continue the global distribution of key products used in NWP, such as Cloud Track Winds.

- Seek to operate the satellite in accordance with the data policy of the host operator, in order to minimise any impact on third parties.

b) The host operator shall:

- Make efforts to ensure that its users continue to be provided with services, such as access to image data, through a combination of the services provided by the satellite owner and those provided by the host,

- Seek to provide specialised support for the Regional Data Collection System where facilities permit,

- Continue to take responsibility, as far as possible, for specialised regional and other requirements not addressed by the satellite operator.

- Make every effort to restore normal service as soon as possible through the successful launch of a replacement satellite.

Annex 6

CGMS MEMBERS' SATELLITES IN GEOSTATIONARY ORBIT

Status as of June 1995

Operator	Satellite	Launched	Location	Status
EUMETSAT	Meteosat 3	06/1988	75°W	Stand-by
	Meteosat 4	03/1989	10°	Back-up to Meteosat 5
	Meteosat 5	03/1991	0°	**Operational**
	Meteosat 6	11/1993	0°	In commissioning
	Meteosat 7 (MTP)	---	0°	Projected launch mid-1997
	MSG 1	---	0°	Projected launch 2000
	MSG 2	---	0°	Projected launch 2002
	MSG 3	---	0°	Projected launch 2006
INDIA	INSAT I-d	06/1990	83° E	Domestic operational use
	INSAT II-a	07/1992	74° E	Domestic partly operat. use
	INSAT II-b	07/1993	93.5° E	Domestic operational use
	INSAT II-e	---	TBD	Projected launch 1997/98
JAPAN	GMS-4	09/1989	120°	Back-up of GMS-5
	GMS-5	**03/1995**	**140° E**	**Operational**
	MTSAT-1	---	140° E	Projected launch in 1999
USA	**GOES - 7**	02/1987	135°W	**Operational**
	GOES - 8	04/1994	75°W	**Operational Demonstration**
	GOES - J	05/1995		In commissioning
	GOES - K	---		Projected launch in 1999
	GOES - L	---		Projected launch in 2000
	GOES - M	---		Projected launch in 2004
RUSSIA	Elektro-1	11/94	76° E	In commissioning
	Elektro-2	---	76° E	Projected launch in 1997
CHINA	FY-2	---	105° E	Projected launch end 1996

CGMS MEMBERS' SATELLITES IN POLAR ORBIT

Status as of June 1995

Operator	Satellite	Launched	Orbit	Status
EUMET-SAT	Metop-1	---	AM 827 km	Projected launch in 2001
	Metop-2	---	AM 827 km	Projected launch in 2006
	Metop-3	---	AM 827 km	Launch date TBD
USA	NOAA-11	09/1988	PM 850 km	Available for support
	NOAA-12	**05/1991**	**AM 850 km**	**Operational**
	NOAA-14	**12/1994**	**PM 850 km**	**Operational**
	NOAA-K	---	AM 850 km	Projected launch 04/1996
	NOAA-L	---	PM 850 km	Projected launch in 1997
	NOAA-M	---	AM 850 km	Projected launch in 1999
	NOAA-N	---	PM 850 km	Projected launch in 2000
	NOAA-N'	---	PM 850 km	Projected launch in 2002
	NPOESS-1	---	824 km	Projected launch in 2006
	NPOESS-2	---	824 km	Launch date TBD
	NPOESS-3	---	824 km	Launch date TBD
CHINA	FY-1 C	---	870 km	Projected launch 1997/1998
	FY-1 D	---	870 km	Launch date TBD
RUSSIA	Meteor 2-21	08/1993	950 km	Operational
	Meteor 3-5	**08**/1991	1200 km	**Operational**
	Meteor 3-7	01/1994	1200 km	**Operational**
	Meteor 3-8	----	1200 km	Projected launch in 1996
	Meteor 3M-1	----	925 km	Projected launch in 1998
	Meteor 3M-2	----	925 km	Projected launch in 2000

Appendix A:

SELECTED PAPERS SUBMITTED TO CGMS XXIII

CGMS-XXIII RUS-WP-02
Prepared by RUSSIA
Agenda Item: B.2

GEOSTATIONARY OPERATIONAL METEOROLOGICAL SATELLITE GOMS/ELECTRO

The Russian geostationary meteorological satellite GOMS N1 (ELECTRO) was launched on November 1, 1994 into orbit with inclination of less than 1.3 deg. and orbital period of about 24 hours to the point at 90^0 East.

Within the first 24 hours the problems arised in the process of the spacecraft insertion into orbit that made impossible to set up three-axes orbital attitude as planned. The analiysis cleared up that the local vertical sensor had failed.

GOMS N1 was inserted into nominal position of 76^0 East on November 29, 1994.

During December 1994 - January 1995 onboard computer controlling complex was checked on ground-based simulation test-beds and modified in order to restore the nominal spacecraft orientation. The corrections were transmitted to the spacecraft by radiolink. These corrections complemented with imagery control on the ground processing centre allowed to perform the spacecraft orientation manoeuvre on February 1, 1995 successfully. Since that three-axes orbital orientation is maintained with the precise sun-angle sensors and the Polar star sensor.

The satellite eclipse season ended on April 27, 1995. All onboard systems nave been checked and are nominally operating. At present, the satellite is kept at 76^0 E, supporting imaging mode. Infra red imagery (10.5-12.5 μm) is considered to be quite accurate for distribution after subsequent geometrical and radiometrical correction. Due to malfunctions in onboard optical instrumentation partial utilization of visible images (0.46-0.7μm) is discussing at the meantime. No anomalies occur with helio-geophisical information which is receiving and processing hourly. The water vapour channel (6.0-7.0 μm) is operating in experimental mode.

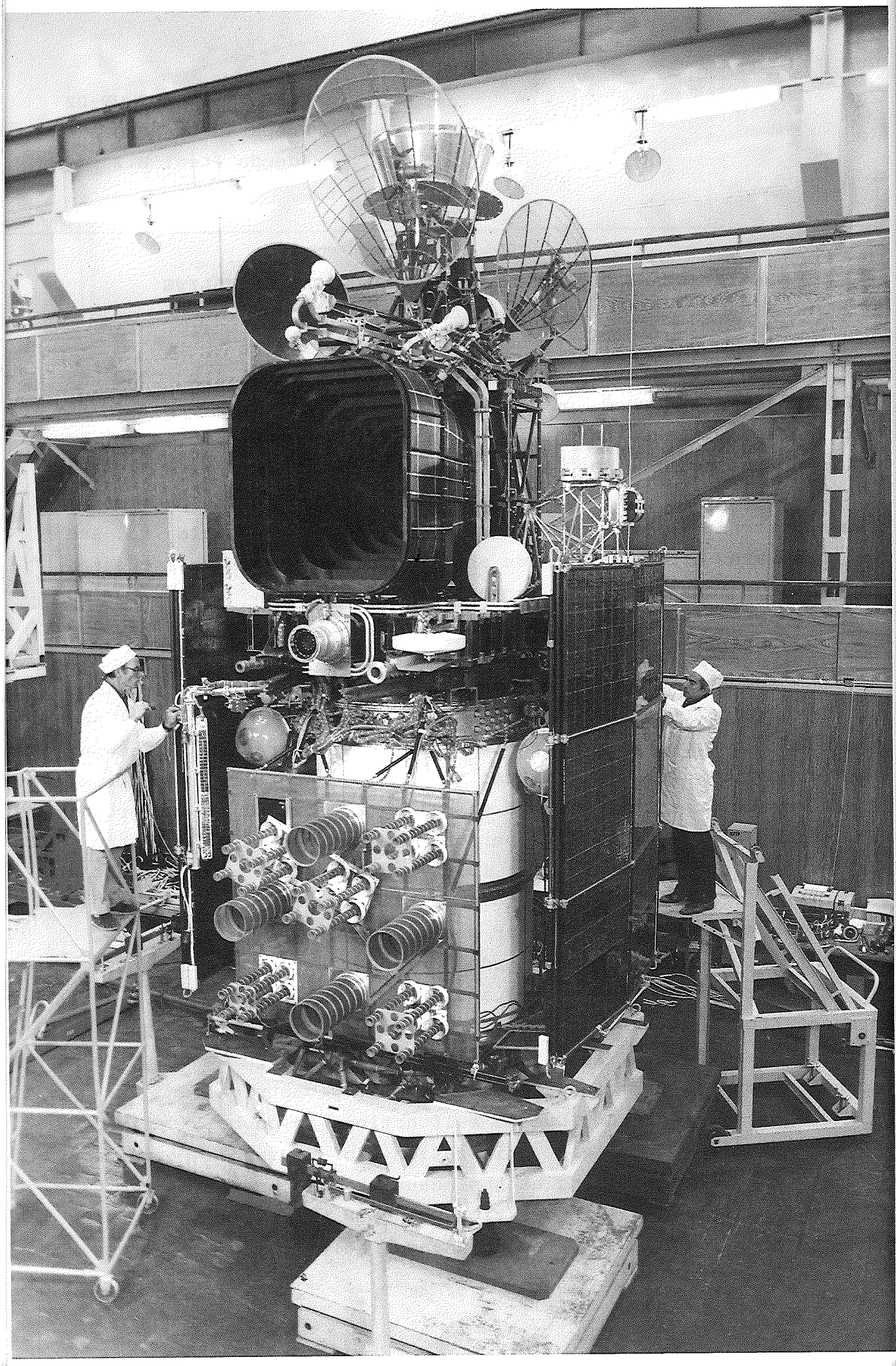

Geostationary weather Satellite “Electro - 1”

Table 1

S/C "GOMS" Performances
(space platform)

1. Orbit	
• type	geostationary
• altitude	36,000 km
• inclination	less 1.3°
• revolution period	86,164±1 s
• position longitude	76±0.1° E
2. Orientation	
• type	fly-wheel triaxial
• co-ordinate system (see Fig. 1)	bank axis X along the s/c flight direction pitch axis Y attitude towards the Polar star yaw axis Z attitude from the Earth's center towards the s/c center of mass
• orientation accuracy in the standard mode:	
– for bank and pitch	±2 arcmin
– for yaw	±5 arcmin
• uprated accuracy mode:	
– for bank and pitch	±1 arcmin
– for yaw	±2 arcmin
• angular stabilization velocity	less 0.0005 arc.deg./s
3. Power supply	
• solar panel maximum capacity	3,700 W
• daily average capacity	more than 1,700 W
4. Lifetime	more than 3 years
5. Mass	2,650 kg
• payload mass	950 kg
6. Dimensions	
• height along Y	6.35 m
• diameter in the XY plane for the lift-off state	2.9 m
• s/c size (along X) in flight	15 m
7. Launcher	"Proton" with a booster

Table 2

Characteristics of the GOMS Data Radio Technical Complex

1. TV radiometer (TRS)	
• spectral bands:	
– visible	0.46-0.7 μm
– IR I	10-12.5 μm
– IR II	6-7 μm
• IFOV /ground resolution	
– VISIBLE	31.5 μrad/1.25 km
– IR I-II	160 μrad/6.5 km
• data transmission sessions	
– session frequency	30 min
– frame length	12 min
– band	1.7 & 7.5 GHz (S-band & X-band)
– informativity	2.56 Mbit/s
2. Radiation and measurement system (RMS)	
• energy bands for measuring density of the electron, proton, α-particle fluxes and galaxy radiation	from 0.04 up to 600 meV
• four bands for measuring solar radiation	from 0.4 μm up to 1.3 μm
• interval of the Earth's magnetic field measurement for three axes	±180 nT
• frequency of the data transmission sessions	60 min
3. Radio relay complex (BRRK)	
• data collection from platforms (DCP):	
– sampling band	401–403 MHz
– number of simultaneously sampled platforms	133
– informativity	100 B/s
• band for data transmission from DCP to the weather service centers	1.7 GHz (S-band)
• relay bands for the processed in the WEFAX mode data between the weather service centers	1.7 and 7.5 GHz (S-band & X-band)
• informativity	1,200 B/s
• band for transmitting the same data to small stations (APPI)	1.7 GHz (S-band)
• band for re-transmitting high rate digital data	7.5 GHz (X-band)
• informativity	up to 0.96 MB/s
• band for the platform (DCP) calling	469 MHz

CGMS-XXIII PRC WP-01
Prepared by China
Agenda Item : C.1

THE STATUS OF FY-1 PROGRAM

China is continuing FY-1 program. FY-1 C is being designed now. It is expected that FY-1 C will be launched in the time frame 1997-1998.

The specifications of FY-1 C and FY-1 D are as follows:

- **Orbit altitude : 870 Km**
- **Inclination : 98.85 Degree**
- **Excentricity : less than 0.005**
- **Orbital period : 102.3 minute**
- **Sensor :**

Multispectral Visible and IR Scan Radiometer (MVISR) is the major sensor of FY-1 C and D. The wavelength of MVISR is as follows:

Channel No.	Wavelength (μm)
1	0.58-0.68
2	0.84-0.89
3	3.55-3.93
4	10.3-11.3
5	11.5-12.5
6	1.58-1.64
7	0.43-0.48
8	0.48-0.53
9	0.53-0.58
10	0.90-0.965

The resolution at sub satellite point is about 1.1 Km.

Transmission:

The high Resolution Picture Transmission of FY-1 C and D is named CHRPT. The bit rate of CHRPT is 1.3308 Mbps and the modulation of CHRPT is BPSK/Bi-phase.

Progress and Plans for GMS-5

GMS-5 was successfully launched at 08:01 UTC on 18 March 1995. The satellite is located in synchronous orbit at a temporary location, 160°E above the equator. After post-launch checkouts, GMS-5 will be moved to and stationed at 140° E, and take the place of GMS-4 to initiate routine operation in mid-June 1995.

Instead of current sensors, the infrared sensors of GMS-5 increase from one to three. A water vapor sensor is newly equipped and split window sensors are replaced a current window sensor as shown in Table 1. Space Environmental Monitor (SEM) is not loaded into the GMS-5. The other functions of the GMS-5 are identical to those of the GMS-4.

Major GMS-5 products are summarized in Table 2.

Table 1. Sensor channels on board GMS-4 and GMS-5

Channel		GMS-4	GMS-5
Visible		0.50 - 0.75 μm	0.55 - 0.90 μm
Infrared	Water Vapor	None	6.5 - 7.0
	Window	10.5 - 12.5	10.5 - 11.5
			11.5 - 12.5

Table 2 Major GMS-5 products

Images broadcasted by GMS-5

Type of data	Description	Region of interest	Output frequency	Data distribution via GMS to
Stretched VISSR	Real-time digital VISSR image	Full disk picture	hourly	M-DUS
WEFAX	Analogue image produced by the computer system using VISSR image data with various processings; sampling, brightness conversion, superimposing grid and coastal lines, and adding annotation	Four-sectorized each disk pictures IR (A ~ D) WV (K ~ N) Polar-stereographic pictures IR (H) VIS (I) Enhanced IR (J)	 3-hourly 12-hourly hourly hourly (daytime) hourly (nighttime)	 S-DUS

For users via GTS

Type of data	Description	Region of interest	Output frequency	Data distribution
Cloud motion wind	Cloud motion wind derived from time-sequential IR and VIS images	50°N ~ 50°S 90°E ~ 170°W	00UT, 06UT, 12UT, 18UT (SATOB)	Global Exchange
Water vapor wind	Water vapor wind derived from time-sequential WV images	50°N ~ 50°S 90°E ~ 170°W	00UT, 06UT, 12UT, 18UT 4 times/day	Global Exchange
Sea surface temperature	Five days Mean of the sea surface temperature in 1.0° lat. × 1.0° lon. area	50°N ~ 50°S 90°E ~ 170°W	1 time/5days	Global Exchange
Typhoon analysis	Location of the typhoon center (Special hourly observation)	For the typhoon in 100°E ~ 180°E, and in the northern hemisphere	8 times/day (24 times/day)	Global Exchange
	Estimation of typhoon intensity		4 times/day	

For domestic users

For domestic users

Type of data	Description	Region of interest	Output frequency	Data distribution via ADESS to
Cloud amount data	Mean and anomaly of the total, high-level, and low-level cloud amount in 1°lat.× 1°lon. area	60°N ～ 60°S 80°E ～ 160°W	1 time/5days (chart and GRID) 1 time/month (ditto) 1 time/3months (chart)	Forecast Dep. of JMA
Equivalent black blackbody temperature (TBB)	Mean and standard deviation of equivalent blackbody temperature in 2.5°lat. ×2.5°lon. area	60°N ～ 60°S 80°E ～ 160°W	1 time/5days (chart and GRID) 1 time/month (ditto) 1 time/3months (chart)	Forecast Dep. of JMA
Outgoing longwave radiation	Mean and standard deviation of outgoing longwave radiation in 0.5°lat.×0.5°lon. area	50°N ～ 50°S 90°E ～ 170°W	3-hourly (GRIB)	Forecast Dep. of JMA
	Mean and standard deviation of outgoing longwave radiation in 2.5°lat.×2.5°lon. area	60°N ～ 60°S 80°E ～ 160°W	1 time/5days (chart and GRID) 1 time/month (ditto)	Forecast Dep. of JMA
Upper tropospheric air humidity	Mean relative humidity between middle and upper troposphere in 0.5°lat. ×0.5°lon. area	50°N ～ 50°S 90°E ～ 170°W	6-hourly (GRIB)	Forecast Dep. of JMA
Precipitable water amount	Precipitable water amount in 0.5°lat. ×0.5°lon. area	50°N ～ 50°S 90°E ～ 170°W	6-hourly (GRIB)	Forecast Dep. of JMA

Note : ADESS means Meteorological Communication Circuits in Japan

For domestic users

Type of data	Description	Region of interest	Output frequency	Data distribution via ADESS to
Satellite-derived index of precipitation intensity	Precipitation intensity estimated from GMS data	Near Japan	hourly (digital data)	Forecast Dep. of JMA
Satellite cloud analysis chart	Characteristics and temporary change of cloud distribution, cloud top height etc.	Vicinity of Japan	3-hourly (chart)	Forecast Dep. of JMA
Satellite cloud information chart (Far East)	Cloud distribution, cloud top height, convective cloud location etc.	60°N ～ Equator 90°E ～ 170°W	hourly (chart)	Forecast Dep. of JMA
VISSR grid point value	Minimum TBB, cloud amount in five layers, mean and standard deviation of TBB for cloudy area and cloud amount of convective clouds in 0.5°lat. ×0.5°lon. area	50°N ～ 50°S 90°E ～ 170°W	6-hourly (GRIB)	Forecast Dep. of JMA
Sea surface temperature	Daily mean of the sea surface temperature in 0.5°lat. ×0.5°lon. area	50°N ～ 50°S 90°E ～ 170°W	1 time/ day (GRIB)	Marine Dep. of JMA
	Five days, ten days and monthly mean of the sea surface temperature in 1.0°lat. ×1.0°lon. area	50°N ～ 50°S 90°E ～ 170°W	1 time/ 5days (chart) 1 time/ 10days (chart) 1 time/ month (chart).	Marine Dep. of JMA

For domestic users

Type of data	Description	Region of interest	Output frequency	Data distribution via ADESS to
Low-level cloud motion wind in a typhoon vicinity	Low-level cloud motion wind in a typhoon vicinity derived from 15-minute interval IR and VIS images.	For the typhoon in 100°E ~ 180°E, and in the northern hemisphere	04UT (BUFR) 1 time/day	Forecast Dep. of JMA
Solar irradiation	Solar irradiantion at the surface of the earth in 0.25°lat.×0.25°lon.	60°N ~ 60°S 80°E ~ 160°W	1 time/day (GRIB)	Forecast Dep. of JMA
Index of snow ice cover	An index for examining the presence of snow ice cover in 0.25 ° lat.×0.25° lon. area	60°N ~ 20°N 80°E ~ 160°W	1 time/day (GRIB)	Forecast Dep. of JMA

For WMO/WCRP

Type of data	Description	Region of interest	Output frequency	Data distribution by mail with magnetic tape
ISCCP data (AC data)	Original VISSR for inter-calibration between images from different geostationary satellites	2000×2000 km² (Area selected by SCC)	5 times/month	Satellite Calibration Center (France)
ISCCP data (B1 and B2 data)	Nominally 10km spatial resolution full disk data for B1 data, 30km for B2 data	Full earth disk coverage	8 times/day	Global Processing Center (USA)
GPCP data	Five day mean histogram of TBB in 16 clases in 2.5°lat. ×2.5°lon. area.	40°N ～ 40°S 90°E ～ 170°W	1 time/5days	Climate Analysis Cnter (USA)

CGMS-XXIII WP-05
Prepared by Japan
Agenda Item: C.2

Plans for Multi-functional Transport Satellite

JMA started procedures for procurement of the Multi-functional Transport Satellite (MTSAT) as a successor to GMS-5 in cooperation with the Civil Aviation Bureau (CAB), Ministry of Transport in fiscal year (FY) 1994 (April 1994 - March 1995). The MTSAT has two kinds of functions; one is for continuation of meteorological services in JMA and the other for air-traffic control services in CAB. The MTSAT will be launched in geostationary orbit at 140°E in around August 1999.

A tender for MTSAT was carried out in accordance with Procedures for Procurement of Non-R&D Satellites adopted as a policy of the goverment of Japan in June 1990, which provides the transparent, open and non-discriminatory competitive procedures. The successful bidder is a supplier of GOES-8 to NOAA/NASA. The proposed MTSAT is a three axis stabilized satellite based on a bus of INTELSAT-VII. The same type of imager for the meteorological mission as one loaded on the GOES-8 is adopted for MTSAT.

The fundamental specification for the meteorological mission of MTSAT is as an attached paper. As for the meteorological mission, the specifications of GMS-5 will be fundamentally succeeded and an infrared sensor with a wavelength of 3.5 - 4.0 μm will be added. High resolution digital data, WEFAX signal and DCP data relay function of MTSAT are basically same as those of GMS-5. The details of high resolution digital data and WEFAX have not been determined as yet.

Fundamental Specification of the MTSAT

Design Life: more than 5 years for meteorological mission more than 10 years for air−traffic control mission
Estimated Survival Probability: 0.89 or greater 5 years for meteorological mission 0.81 or greater 10 years for air−traffic control mission
Orbital Position: ±0.1° north−south and east−west from its nominal position of 140° E longitude
Imaging Period: within 27.5 minutes
Imager Characteristics: Visible 0.55 − 0.85 μm IR 1 10.3 − 11.3 IR 2 11.5 − 12.5 IR 3 6.5 − 7.0 IR 4 3.5 − 4.0
Signal Quantizing: 10 bits for both Visible and IR
Resolution at the sub−satellite point: 1 km for Visible, 4 km for IR
Imager Data Transmission Rate: 2.62 Mbps
Telecommunication Function: Transmission of raw image data Relay of high resolution digital data (equivalent to S−VISSR of GMS) Relay of WEFAX signal Relay of DCP reports Relay of DCP interrogation

WEFAX IMAGERY PREPARATION AND DISSEMINATION VIA GEOSTATIONARY OPERATIONAL METEOROLOGICAL SATELLITE (GOMS)

1 The WEFAX Imagery Preparation

The Weather Facsimile images originates from the raw GOMS data. The raw data reception and operational processing is performed in RPA PLANETA's GOMS Ground Processing Centre (Moscow). The PC-based technology implemented allows to perform the raw data pre-processing including particulary:

- data quality primary control;
- single binary noise data filters;
- data radiometrical correction and calibration;
- imagery geometrical correction;
- data sampling and archiving;
- imagery navigation and mapping.

The Weather Facsimile Service is designed to meet various requirements of the analogue data users. The principal features of WEFAX production technology are: the data sampling, brightness conversion and equalization, superimposing grid and coastal line, adding annotation. The data automated framing and scaling is available to produce both compressed image of the full disk and the globe frame of full resolution (up to 5 km at subsatellite point).

Presently the entire image is sectorized into 4 WEFAX images (labelled W1 through W4). The full disk image is labelled W0. Examples of full-disk image and its four sectors are shown on fig.1.

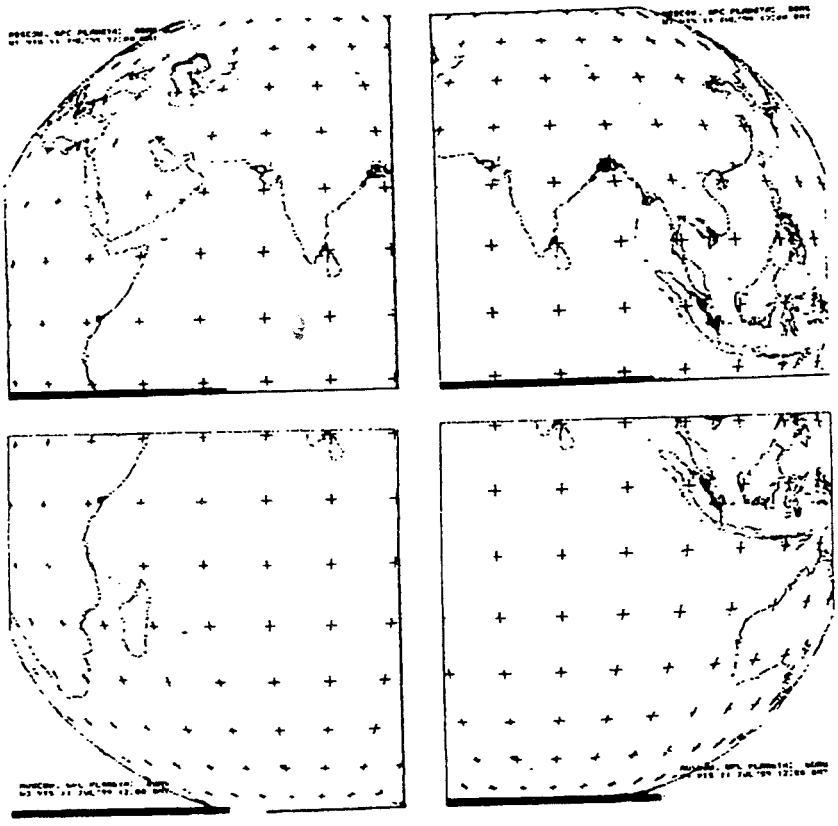

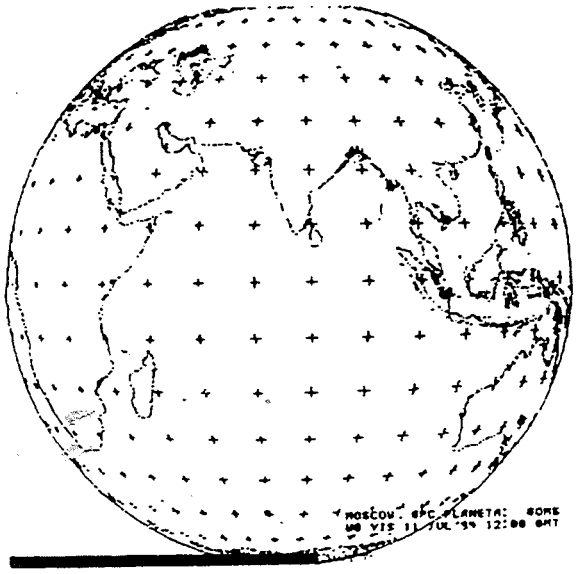

Figure 1. Examples of GOMS WEFAX formats

2 GOMS N1 WEFAX Dissemination Format

The GOMS WEFAX image dissemination format is similar to METEOSAT WEFAX format. The GOMS-M WEFAX image dissemination format is such that a complete image transmission consists of four parts:

- the starting tone;
- the phasing signal;
- the data signal;
- the stopping tone.

The complete transmission consists of 852 lines, each of 250 milliseconds duration. The starting tone is 3 sec or 12 lines in duration and consists of the 2400 Hz subcarrier being modulated by a 300 Hz square wave.

The phasing signal is 5 sec or 20 lines in duration. The modulation of the subcarrier in this portion of the transmission is such that the first 12.5 milliseconds of each line is fully modulated. This is minimum subcarrier level (equivalent to black level). For the remainder of each line, 237.5 milliseconds, the subcarrier is unmodulated and the 2400 Hz level is maximum or white.

During the data portion of the transmission, 200 sec or 800 lines in duration, the first 1/21 part of each line is modulated by a 840 Hz signal. The remainder of each line is modulated by the analog data signal.

The stopping signal is 5 sec or 20 lines in duration and consists of the 2400-Hz subcarrier being modulated by a 450-Hz square wave signal. There will be a 30 seconds pause between the end of one image transmission and the start of the next transmission. Figure 2 depicts the image format as it will appear at the receicer/recorder.

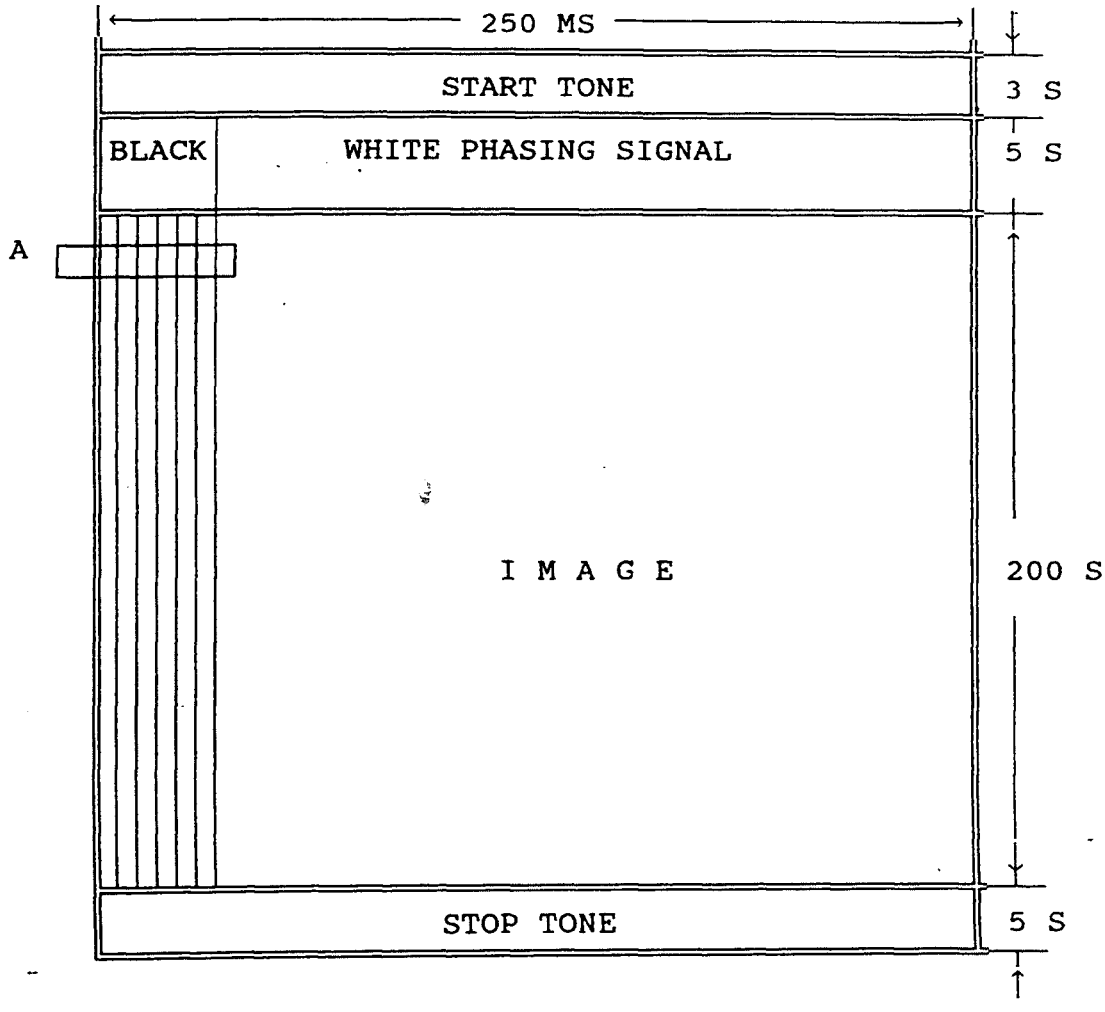

START TONE 300 Hz square wave 3 seconds (12 lines) duration

PHASING SIGNAL 5 seconds duration (20 lines)
Each line: 12.5 ms BLACK 237.5 ms WHITE

DATA SIGNAL PHASE BAR A

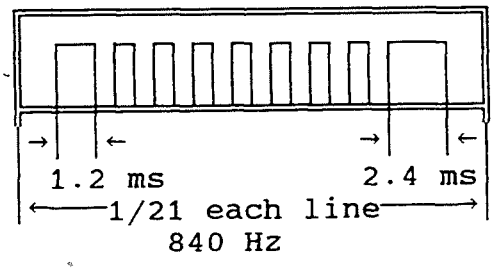

DATA 200 seconds (800 lines)

STOP TONE 450 Hz square wave 5 seconds duration

Figure 1: GOMS N1 WEFAX dissemination format

3 GOMS N1 WEFAX Downlink Characteristics

Channel	Parameter							
	1	2	3	4	5	6	7	8
WEFAX 1	FM	18K0F3C	1671.48 -1698.8	3.8	-38.7	0.018	lin.	0.024
WEFAX 2	FM	18K0F3C	1674.48 -1691.4	3.8	-38.7	0.018	lin.	0.024

1 - modulation type;
2 - phase encoding;
3 - frequency range (MHz);
4 - transmitter output power (dBW);
5 - signal strength (dBW/Hz);
6 - RF bandwidth (MHz);
7 - antenna polarisation;
8 - bit rate (Mbps).

WEFAX transmission schedule is corrected at the meantime and will be distributed to the beginning of GOMS operations.

CGMS XXIII
USA WP-13
Agenda Item H.1

Applications of the DMSP SSM/I Derived Experimental Soil Wetness Index for Large Area Flood Monitoring.

Rao Achutuni and Norman C. Grody
NOAA/NESDIS Office of Research and Applications
Room 601, NOAA Science Center
Washington D.C. 20233

Microwave Techniques for Large Area Flood Monitoring.

Microwave remote sensing systems can be broadly categorized as either active or passive sensors, each having clear advantages. Active microwave sensors, such as the Synthetic Aperture Radar (SAR), provide their own source of energy or illumination. Passive microwave systems, on the other hand, can detect extremely low levels of microwave radiation emitted and/or reflected by the Earth. Passive microwave systems have found numerous hydrological applications such as for monitoring sea-ice, snow melt, soil wetness and soil temperature. An added advantage in using microwave remote sensing systems is that they do not depend on the sun as a source of illumination, and can therefore provide day or night coverage over the area of interest (Ullaby et al., 1982).

The underlying principle in microwave remote sensing of surface moisture status is the large contrast between the dielectric properties of liquid water and of dry soil. The dielectric constant of the soil increases with the volumetric soil moisture content (Engman and Chauhan, 1995; Hall et. al., 1995; Schmugge, 1983). Radiation in the microwave frequencies has the unique ability to penetrate clouds, light rain, snow, ice crystals, haze and smoke.

The surface-related effects of surface roughness and vegetative cover must be taken into account during soil moisture retrievals from space. Microwaves also have the ability to penetrate vegetation more deeply than radiation in the visible and thermal infrared portion of the spectrum. The presence of vegetation as well as variations in the surface roughness are known to reduce the sensitivity to soil moisture. Lambertian (rough) surfaces tend to increase surface emissivity, thereby reducing the sensitivity to soil moisture. On the other hand, vegetation attenuates the microwave emission from the soil. The extent of attenuation is a function of canopy structure, canopy water content and the radar wavelength (Dobson *et al.*, Hall *et al.*, 1995; RADARSAT, 1994a&b). The lower frequencies provide better vegetation and ground penetration than the higher frequencies, and are therefore better suited for studying surface soil conditions (Choudhury *et al.*, 1987; McFarland and Neale, 1991; Schmugge *et al.*, 1986).

In active microwave systems, such as the synthetic aperture radar (SAR), the backscatter from bare soil is expressed as a function of surface roughness and the volumetric soil moisture. In SARs the P-band (.45GHz) is found to be better suited than either the L-band (1.26GHz) or the C-band (5.3GHz) for detecting flooding especially under densely vegetated stands (Hess *et al.*, 1990). The European Space Agency's ERS-1 & ERS-2 (1995 launch), as well as the Canadian RADARSAT (September 1995 launch) satellites carry the C-band SAR having a spatial resolution of 30 meters. The Japanese JERS-1 carries a L-band SAR also with a 30 meter spatial resolution (RADARSAT, 1994a). Key disadvantages of these Earth resource satellites for operational large area flood monitoring is their poor temporal coverage and the high cost of acquiring the data. The spacecraft repeat cycle ranges from 24 days for RADARSAT to 41 days for JERS-1. However, the temporal disadvantage can eventually be overcome in the future with the launch of additional satellites.

In passive microwave systems, the radiometer measures the brightness temperature T_B, defined as the product of the temperature and emissivity, of the target. Emissivity is dependent on the dielectric constant of the soil and the surface roughness. Studies show that there is a nonlinear relationship between the dielectric constant and soil moisture(Engman and Chauhan, 1995; Schmugge *et al.* 1986). For bare soil surfaces, experimental studies suggest that the microwave brightness temperature T_B decreases approximately linearly with soil moisture content. The radiometric sensitivity to soil moisture decreases with both increasing surface roughness and the frequency .

The Defense Meteorological Satellite Program (DMSP) is designed to provide global meteorological, oceanographic, and solar-geophysical data in support of the U.S. Department of Defense operations. The Special Sensor Microwave/Imager (SSM/I) aboard the DMSP series of polar orbiting satellites is a seven channel, four frequency, linearly polarized, passive microwave radiometer. It measures radiation emanating from the Earth at frequencies of 19.35, 22.235, 37.0, and 85.5 GHz. All channel measurements are made in both the vertical (V) and horizontal (H) polarizations with the exception of the 22.235 GHz channel, which measures only vertically polarized radiatio (Hollinger, 1991).

The DMSP series of satellites operate in a sun-synchronous orbit with a period of about 102 minutes. Such an orbit assures that the satellite passes over all places on Earth having the same latitude, twice daily at the same local Sun time. The SSM/I has a scan angle of 102.4°, resulting in a scene swath width of about 1400 km. For 85.5 Ghz, sampling is done every 12.5kms along the orbital track and every 25km for the lower frequencies (Hollinger et. al., 1987). The high orbital inclination of the satellite is designed to optimize coverage

at high latitudes, and this leads to considerable data gaps at lower latitudes. This problem can be somewhat minimized by combining data from the DMSP F-10, F-11 and the recently launched F-12 satellites. A key advantage in using the DMSP series of satellites for flood monitoring

Schmugge *et al.* (1977) showed that satellite microwave observations at the 1.55cm wavelength from the Electrically Scanning Microwave Radiometer (ESMR) were responsive to soil moisture variations within a depth comparable in magnitude to the wavelength itself. They emphasize that meaningful soil moisture retrievals can be made only if the target area consists of either bare soil or sparse vegetation, such as crops in their early stages of development. Recognizing these caveats, one can still obtain useful information from satellite derived brightness temperatures for detecting changes in soil moisture near the surface layer at a spatial resolution of about 25km.

McFarland and Neale (1991) used the 19.35(H) GHz and the 37.0(V) GHz channels of the SSM/I for surface moisture retrievals in the form of a normalized brightness temperature T19H/T37V. However, they also observed that the 85.5 GHz channels were excellent for identifying water bodies within the SSM/I footprint. They used the (i) 85.5 (V) - 37.0 (V) and (ii) 85.5 (H) - 37.0 (H) combinations to discriminate both moist soil surfaces and large water bodies from dry surfaces. Numerous classification rules were formulated to identify flooded soil, moist soil surface, composite water and soil or wet soil surface, composite water and vegetation. Flooding due to heavy rain or melting snow, and large bodies of water were identified using a brightness temperature threshold of 4 K or less for the difference between the 22.235 (V) GHz and the 19.35 (V) GHz brightness temperatures.

Choudhury (1989) quantified the spatial and temporal variabilities of microwave brightness temperature (T_B) over the U.S. Southern Great Plains in terms of vegetation and soil wetness. Daytime brightness temperatures were derived from NIMBUS-7 Scanning Multichannel Microwave Radiometer (SMMR) observations at the 6.6 GHz (horizontal polarization) frequency. The NOAA-7 Advanced Very High Resolution Radiometer (AVHRR) derived Normalized Difference Vegetation Index (NVI) was used to examine the spatial and temporal variability of vegetation. The spatial and temporal variability of soil wetness was examined in terms of an Antecedent Precipitation Index (API). The API was found to explain only about 50 percent of the variability in T_B. They suggest that the 6.6 GHz horizontally polarized T_B, corrected for vegetation by the NDVI, can serve as an indicator of surface wetness.

Both active and passive microwave remote sensing systems have their distinct advantages and disadvantages for retrieving soil surface characteristics. The high temporal coverage and the relatively low

data cost associated with the DMSP series of satellites makes them ideal for large area flood monitoring. On the other hand, SAR systems provide good vegetation penetration with high spatial coverage that is necessary for flood impact analysis at the local level. Both these systems complement each other and have a unique role in flood monitoring and flood impact analysis.

The SSM/I Soil Wetness Index

Large area flood monitoring on a real-time basis induces the need for developing a satellite derived algorithm that: 1) is easy to implement operationally; 2) provides useful information on the areal extent of flooding under all weather conditions, especially under persistent cloudiness; 3) utilizes data that are available operationally, and 4) is cost-effective as well.

The SSM/I channel data are ingested into the NOAA\NESDIS Visible Infrared Spin Scan Radiometer (VAS) Data Utilization Center (VDUC) system daily at 0000Z, 00006Z, 0012Z and 0018Z, respectively. The VDUC system also supports the Man Computer Interactive Data Access System (McIDAS) developed by the University of Wisconsin, Madison. All of the Soil Wetness Index algorithm development and testing was done on the McIDAS.

The NOAA/NESDIS SSM/I derived experimental Soil Wetness Index (SWI) was developed during the summer of 1993 as a prognostic tool for the near real-time monitoring of large area flooding in the U.S. Midwest (Achutuni *et al.*, 1994). The SWI is defined as follows

$$SWI\text{-}85.5(H)\text{-}19.35(H)$$

where: 85.5(H) = the 85.5GHz horizontal polarization T_B,
19.35(H) = the 19.35GHz horizontal polarization T_B, and
10 <= SWI <= 30.

The SWI as defined above indicates a wide range of soil wetness conditions. Our primary interest in developing the SWI is for flood monitoring. Consequently, we have to assign upper and lower thresholds for the index in order to identify soil surfaces that are either extremely wet, contain large puddles of standing water, or are simply flooded. Field reports from the United States Department of Agriculture, Crop Reporting Service (USDA/CRS) located in Des Moine, Iowa were used in the qualitative calibration of the index over the U.S. Midwest into the 'extremely wet' to 'flooded' categories. The index values from representative pixels located over the Great Lakes

were used to calibrate the index to reflect large bodies of water.

The scaled SWI images have to be digitally enhanced in order to improve their visual interpretability. The SWI brightness temperature values are then enhanced using histogram-equalized stretch over the range 0-255 in order to improve image interpretatbility.

The nature of large area flood monitoring using passive microwave instruments such as the SSM/I is such that one cannot infer any quantitative information on the depth of flooding. This difficulty arises from the fact that the instrument can only detect moisture conditions within the surface layer of the soil. For example, a pixel representing a soil surface predominantly covered by a thin film of water will appear radiometrically identical to a pixel located over a body of deep water. Familiarity with the local terrain is essential for the proper interpretation of satellite imagery.

Another important factor to consider in inferring flooding using the SWI imagery is the temporal persistence of the observed feature. Transient mesoscale convective complexes can produce very heavy rainfall, rendering the soil surface to be extremely wet and perhaps producing localized flash floods. Flooding can generally be inferred from the SWI imagery on the basis of temporal persistence of the flooded features.

It is true that heavily precipitating clouds, containing large water droplets and/or ice crystals will scatter radiation at the higher microwave frequencies such as the 85.5GHz, resulting in lower index values. However, this problem can be minimized by compositing the images temporally and retaining the maximum SWI value for each pixel during that period.

Global Flood Monitoring with the Soil Wetness Index

The experimental SWI is being produced by ORA on a daily basis. In addition to flood monitoring, the index is also being used by meteorologists at NOAA's National Precipitation Prediction Unit (NPPU) to provide flash flood guidance and advisories to the regional River Forecast Centers (RFCs). Heavy precipitation falling upon soil that is already extremely saturated can lead to flash floods.

1993 Midwestern Flooding

Farmers in the U.S. Midwest cultivate predominantly corn and soybeans during the summer months. The 1993 growing season in the Midwest was plagued by delayed planting, excessive lodging of plants, and

unfavorable field conditions. Field reports indicate that much of the crop land in Iowa experienced various degrees of ponding and flooding.

The experimental SWI for selected days in June and July, 1993 are shown in the four-panel image (Fig.1). The gray tones indicate various levels of soil wetness, ranging from extremely wet (light gray) to puddles/flooded conditions (dark gray/black). The SWI image for June 6, 1993 (Fig. 1a) indicates the presence of vast areas with excessive ponding in southeastern Nebraska and east central Illinois, following heavy precipitation events. The above situation did not persist for more than a few days, suggesting a transient phenomenon. However, from an agricultural point of view much of the damage to crops in their vegetative stage had already taken place. Such extremely wet field conditions can result in severe crop losses due to lodging, flooding, and the spread of disease and pests.

The imagery for July 15, 1993 (Fig. 1b) indicates the situation at a peak flood stage along the Missouri and Mississippi Rivers. The spatial resolution of the SSM/I instrument does not permit the identification of individual rivers and streams. However, the SWI can provide useful information on the status of soil wetness over large geographic areas such as at the county or crop reporting district level. The large dark spot over southern Minnesota and north central and north central Iowa was a persistent feature in the late June through mid-July imagery.

The situation as of July 12, 1993 was summed up as follows by the *Iowa Crops & Weather* (IAS, 1993), a weekly crop-weather bulletin:

"... the greatest (wettest) weekly average since such statistics have been kept, followed eight consecutive months of above normal precipitation and has resulted in the worst natural disaster in the state's history... Heavy rains continued over the state last week causing severe flooding along many streams. The wet conditions have taken their toll on this years crops as ponding and flooding have caused yellowing and slow growth in areas that have not been destroyed by the flooding"

Large areas of ponding or flooding are also indicated in south central Kansas and along the track of the Missouri River, near St. Joseph, Boonville and St. Louis areas.

The situation as of July 20, 1993 (Fig. 1c) reveals continued flooding problems over much of Iowa and parts of Missouri. Extremely saturated soil conditions are also evident in many parts of South Dakota, Minnesota, southeastern Nebraska, Kansas, and Illinois.

By July 29th (Fig. 1d), the situation in many parts of the Midwest appears to have improved significantly. However, some large pockets of flooding are still evident in Missouri near St. Joseph, Kansas City, Boonville, Moberly, St. Louis and in the Bootheel region. These areas continued to indicate flooding problems through August, as evident from subsequent SWI imagery.

The SWI was also compared with other products such as the Palmer Crop Moisture Index and the NOAA Advanced Very High Resolution Radiometer (AVHRR) derived Normalized Difference Vegetation Index. For example, Figure 2 shows the Crop Moisture Index for the week ending July 17, 1993 (USDA, 1993). A comparison with the SWI for July 14, 1993 (Fig. 1) indicates a close agreement between the two products in delineating wet areas over the Midwest.

1995 Flooding in California

Since early January 1995, California has been experiencing one of the wettest periods on record. The Sierra Nevada mountains experienced record amounts of snowfall, whereas the Sacramento-, San Joaquin-, and the Imperial Valley regions experienced torrential rains. Extensive flooding occurred during both January and March of 1995. By the middle of March about 39 counties in the state were declared as federal disaster areas. Damage to property and agricultural crops was quite extensive, running into the billions of dollars.

Figure 3 shows the comparison of the SWI for January 11, 1994 (no flooding) with that on January 11, 1995 (flooded). The flooded or extensively puddled areas can easily be identified along the Sacramento-, San Joaquin-, and the Imperial Valley regions . This pattern of flooding recurred during the first two weeks of March when the same areas experienced very heavy precipitation amounts.

1995 Flooding in N. Europe

Record heavy precipitation in Northern Europe resulted in severe flooding problems over vast areas of Belgium, France, Germany, and the Netherlands. In the British Isles, very heavy precipitation contributed to extremely saturated soil conditions and resulted in some localized flooding.

The time series of the SWI from January 12, 1995 (pre-flooding), and January 23-27, 1995 (flooding) are shown in Figure 4. The SWI imagery indicates flooding related problems in parts of the British Isles,

Belgium, France, Germany, the Netherlands, Poland and Hungary.

SUMMARY AND CONCLUSIONS

The DMSP SSM/I derived experimental Soil Wetness Index, developed within the NOAA/NESDIS Office and Research and Applications, is an extremely useful tool for large area monitoring of flooding under sparsely vegetated conditions. The high temporal resolution of the DSMSP series of satellites assures near global coverage on a near real-time basis. The SWI can be used to quickly identify problem areas around the world. High resolution SAR imagery can then be used to identify the impact of flooding at the local level. The USDA World Agricultural Outlook Board is currently using the SWI to identify flood impacted areas around the world. Efforts are under way to validate the SWI with SAR imagery from ERS-1 and RADARSAT.

REFERENCES

Achutuni, V.R., LaDue, J.L., Scofield, R.A., Grody, N., and Ferraro, R., 1994: A soil wetness index for monitoring the Great Flood of 1993. Paper presented at the *Seventh Conference on Satellite Meteorology and Oceanography,* Monterey, California, June 6-10, 1994, pp. 580-584.

Choudhury, B.J., 1989: Monitoring global land surface using Nimbus-7 37GHz data: theory and examples. *Int. J. Remote Sensing*, **10**, 1579-1605.

Choudhury, B.J., M. Owe, S.N. Goward, RE. Golus, J.P. Ormsby, A.T.C. Chang, and J.R. Wang, 1987: Quantifying spatial and temporal variabilities of microwave brightness temperature over the Southern Great Plains. *Int. J. Remote Sensing*, **8**, No. 2, 177-191.

Dobson, M.C., Ulaby, F.T., and Pierce, L.E., 1995: Land-cover classification and estimation of terrain attributes using synthetic aperture radar, *Remote Sens. Environ.* **51**:199-214.

Engman, E.T., and Chauhan, N., 1995: Status of microwave soil moisture measurements with remote sensing, *Remote Sens. Environ.* **51**:189-198.

Hall, F.G., Townshend, J.R., and Engman, E.T., 1995: Status of remote sensing algorithms for estimation of land surface state parameters,

Remote Sens. Environ. 51:138-156.

Hess, L.L., Melack, J.M., and Simonett, D.S., 1990, Radar detection of flooding beneath the forest canopy: a review, *Int. J. Remote Sensing,* **11**, No. 7, 1313-1325.

Hollinger, J., R. Lo, G. Poe, R. Savage, and J. Pierce, 1987: *Special Sensor Microwave/Imager User's Guide,* Naval Research Laboratory, Washington, D.C., 120 pp.

Hollinger, J., 1991: *DMSP Special Sensor Microwave/Imager Calibration/Validation,* Final Report, Volume 2. Naval Research Laboratory, Washington, DC 20375-5000.

IAS, 1993: *Iowa Crops and Weather,* Vol. 93-15 (July 12, 1993). Produced by Iowa Agricultural Statistics, Des Moines, Iowa 50309.

Mc Farland, M.J., and C.M.U. Neale, 1991: Land Parameter Algorithm Validation and Calibration, pp. 91-1 to 9-39, In DMSP Special Sensor Microwave/Imager Calibration/Validation, Final Report, Volume 2. Naval Research Laboratory, Washington, DC 20375-5000.

RADARSAT., 1994a: RADARSAT ADRO Program Announcement Volume I. Published jointly by the Canadian Space Agency and NASA pp.50.

RADARSAT., 1994b: RADARSAT ADRO Program Announcement Volume II: RADARSAT System Description. Published jointly by the Canadian Space Agency and NASA pp.35.

Schmugge, T.J., 1983: Remote sensing of soil moisture:Recent advances, *IEEE Trans. Geosci. Remote Sens.* GE 21(3):336-344.

Schmugge, T.J., J.M. Meneely, A. Rango, and R. Neff, 1977: Satellite microwave observations of soil moisture variations. American Water Resources Association, *Water Res. Bull.,* Vol. **13**, NO. 2, pp. 265-281.

Schmugge, T., O'Neil, P.E., and Wang, J.R., 1986: Passive microwave soil moisture research. I.E.E.E. *Trans. Geosci. Remote Sensing,* **24**, 12.

Ulaby, F.T., Moore, R., and Fung, A.K., 1982, Microwave Remote Sensing: Active and Passive (Volume II) - Radar Remote Sensing and Surface Scattering nission Theory, published by the Addison-Wesley Publishing Company, pp. 457-1047.

USDA, 1993: *Weekly Weather and Crop Bulletin,* 24pp. Vol. 80, No. 29 (July 20, 1993). Produced jointly by USDA and NOAA/NWS, Washington, DC.

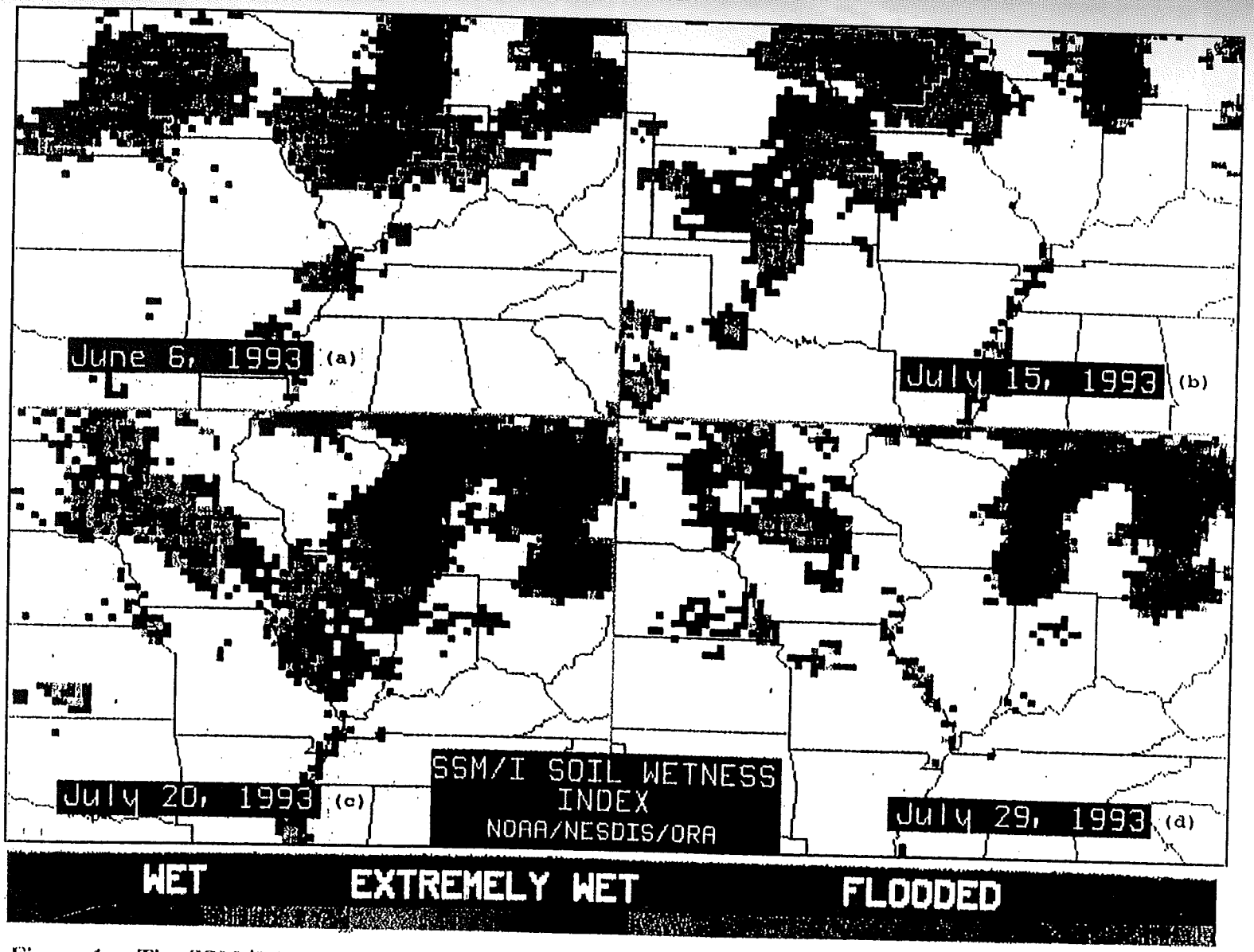

Figure 1. The SSM/I Soil Wetness Index for: (a) June 6, (b) July 15, (c) July 20, and (d) July 29, 1993.

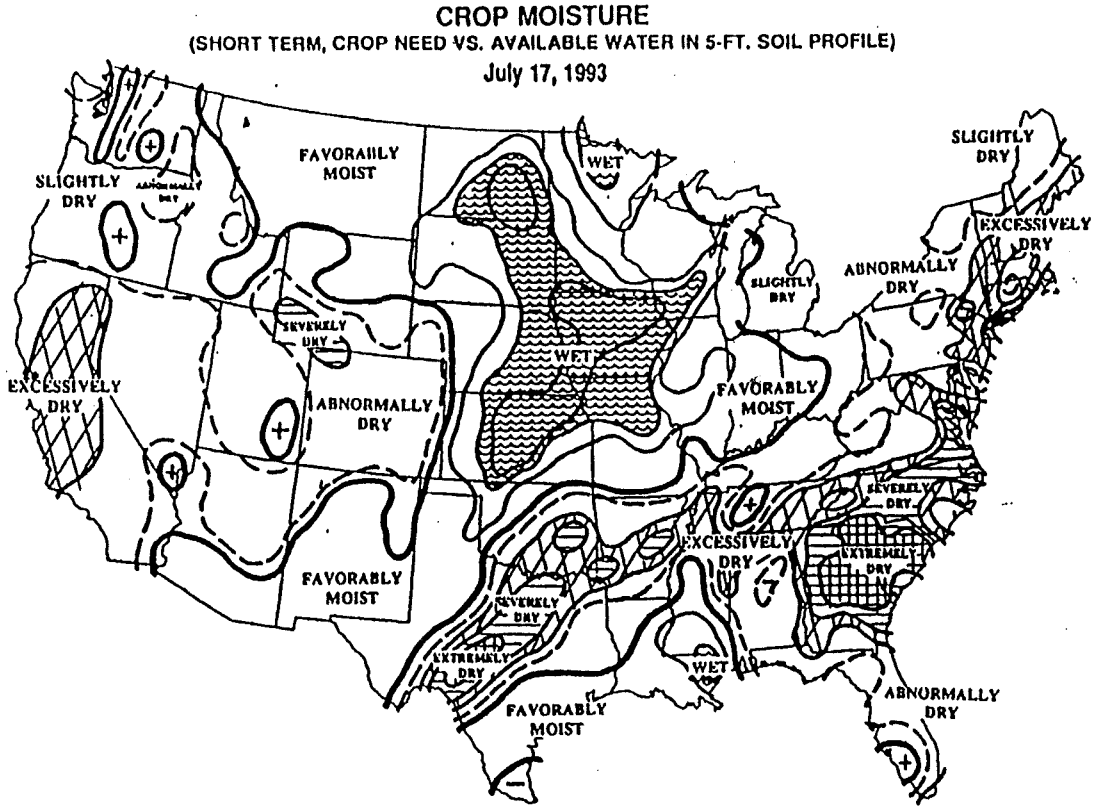

Figure 2. Crop moisture status for the week ending July 17, 1993 (After USDA, 1993).

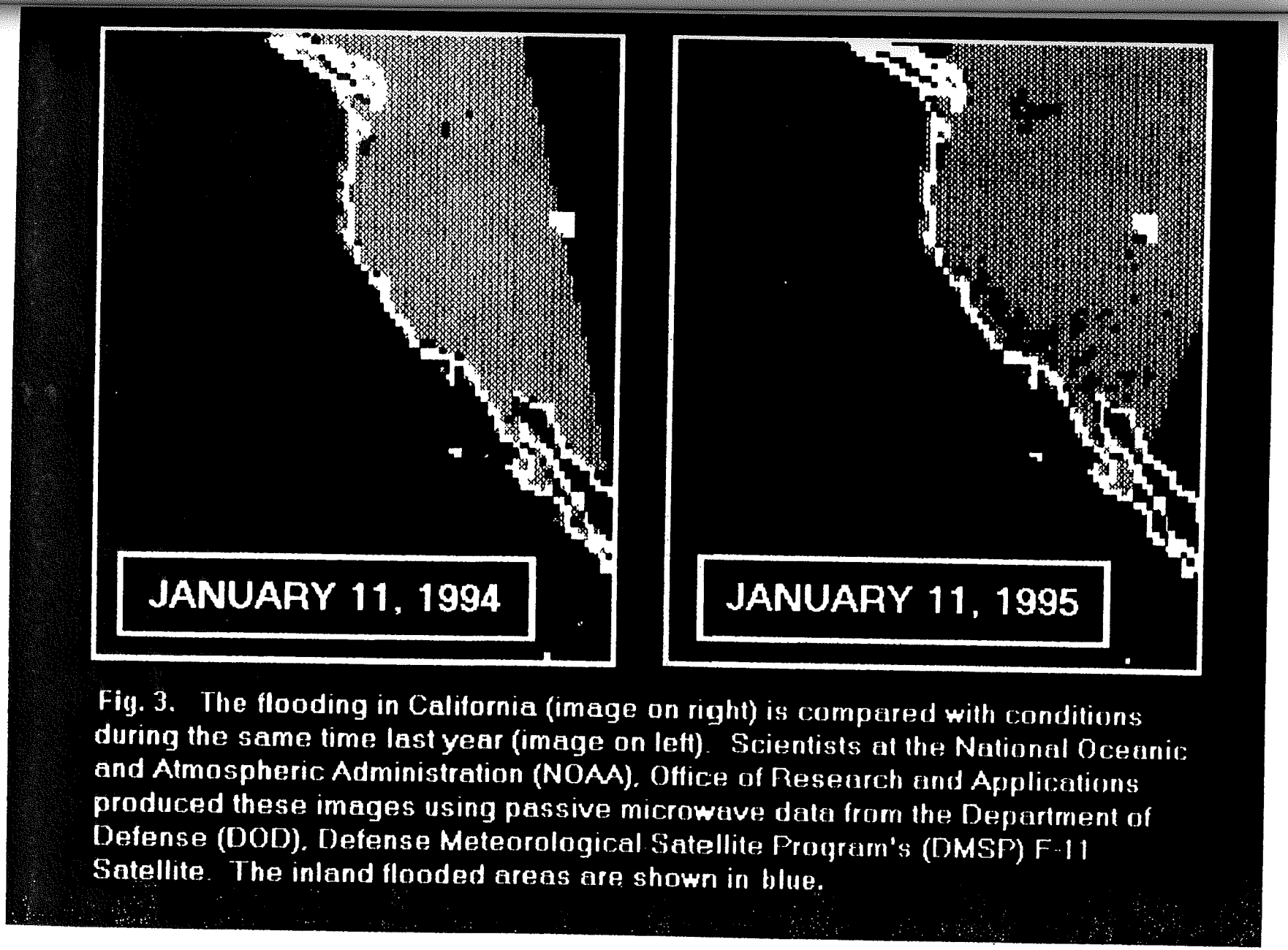

Fig. 3. The flooding in California (image on right) is compared with conditions during the same time last year (image on left). Scientists at the National Oceanic and Atmospheric Administration (NOAA), Office of Research and Applications produced these images using passive microwave data from the Department of Defense (DOD), Defense Meteorological Satellite Program's (DMSP) F-11 Satellite. The inland flooded areas are shown in blue.

MONITORING FLOODING IN THE BRITISH ISLES AND
USING DMSP SSMI DERIVED NOAA NESDIS SOIL
January 12
January 24
January 20
January 27
FIGURE 4

PROTECTION OF PASSIVE SENSORS USE OF THE OXYGEN ABSORPTION BAND AROUND 60 GHz

The following document was edited with inputs from CNES, METEO FRANCE and EUMETSAT and shall support discussions on agenda points 3.2 and 6.

1 Present status of allocations in the 50.2-66 GHz frequency range

The present regulatory status in the oxygen absorption band around 60 GHz, as resulting from the 1979 WARC, is summarized in figure 1 which emphasize the slots which are shared between "Passive" and "Active" services. The 54.25 - 58.2 GHz region, one of the slots where such sharing is permitted, is currently allocated to the following services on a primary basis:

- EARTH EXPLORATION-SATELLITE (passive),
- FIXED,
- INTER-SATELLITE,
- MOBILE,
- SPACE RESEARCH (passive).

This band is specifically considered in this document, because plans are developing fast in Europe to introduce Fixed Services in this slot. In the UK in particular, such services are already operating in significant number in the upper part within 57.2 - 58.25 GHz.
The introduction of mobile services is also under consideration.

2 Meteorological satellite service utilisation of 54.25 - 58.2 GHz band

2.1 Mechanism of passive atmospheric sounding

2.1.1 Basic principle:

Absorbing gas at wavelength λ radiates an energy (at the same frequency) at a level which is proportional to its temperature T and to its absorption ratio $\alpha = f(\lambda)$.

This is governed by the equation:

$$I = \alpha * L \qquad \text{(Kirchoff's law)},$$

Where: I is the spectral brightness of the gas at temperature T,

$L = 2*k*T/\lambda^2$ is the spectral brightness of the black body at T ($w.m^{-2}.str^{-1}.Hz^{-1}$),
$k = 1.38*10^{-23}$ ($J.K^{-1}$) is the Boltzman's constant,
α characterizes the gas (O_2, CO_2, H_2O, O_3...).

*Two atmospheric gases, CO_2 and O_2, are playing a predominant role, because their concentration and pressure in the atmosphere (two parameters which determine the absorption ratio α), are almost constant and known all around the globe.

It is therefore possible to retrieve atmospheric temperature profiles from radiometric measurements at various frequencies in the appropriate absorption bands (typically around 15μm for CO_2, and around 57 GHz for O_2).

* Radiometric measurements in the specific absorption bands of other chemically and radiatively important atmospheric gases of variable and unknown concentration (H_2O, O_3, CH_4, ClO... see Figure 2) are also implemented. But in that case, the knowledge of atmospheric temperature profiles is mandatory in order to retrieve the vertical concentration profiles of these gases.

2.1.2 Application to vertical atmospheric sounding:

In case of vertical atmospheric sounding from space, the radiometer measures at various frequencies (infrared or microwave) the total contribution of the atmosphere from the surface to the top.

- Each layer (characterized by its altitude) radiates energy proportionally to its local temperature and absorption ratio. The upwards energy (in direction of the radiometer) is partly absorbed by the upper layers and in turn, the layer absorbs partly upwards emissions from the lower layers.

- Integration of the radiative transfer equation along the path from earth's surface to the satellite reflects this mechanism, and results in a weighting function which describes the relative contribution of each atmospheric layer, depending on its altitude.

- The peak of the weighting function occurs at an altitude which depends on the absorption ratio at the frequency considered. A sounder incorporates several frequency channels. They are carefully selected within the absorption band, covering a wide range of absorption levels in order to optimise the sampling of the atmosphere from the surface up to stratospheric altitudes. (See typical weighting functions of a microwave temperature sounder on figure 3.)

2.2 Why microwave sounding around 60 GHz ?

Atmospheric temperature profiles are amongst the essential parameters which are routinely used by meteorological services for operational weather forecast, and by the scientific community involved in climate and environment monitoring and studies. These applications do not generate direct commercial return. However, they have an important impact on all economic activities and contribute heavily to human welfare and life conservation.
Atmospheric temperature profiles are currently obtained from spaceborne sounding instruments working in the infrared spectrum and in the microwave spectrum (oxygen absorption around 60 GHz).

As compared to IR techniques, the all-weather capability (the ability for a spaceborne sensor to "see" through most clouds) is probably the most important feature that is offered by microwave techniques.
This is fundamental for operational weather forecast and atmospheric sciences applications, because approximately 50% of the earth's surface is, on average, totally overcast by clouds, and only 5% of any 20x20 km² spot (corresponding to the typical spatial resolution of the IR sounders) are completely cloud-free. This situation severely hampers operations of IR sounders, which have very little or no access to large, meteorological active regions.

The next O_2 absorption spectrum around 118 GHz has a lower potential due to its particular structure (monochromatic, as compared to the rich multi-line structure around 60 GHz) and is more heavily affected by the attenuation caused by atmospheric humidity, as it is shown on figure 4. The 50/70 GHz band offers a unique possibility to perform all-weather measurements of the vertical atmospheric temperature profiles from a satellite's orbit.

2.3 Current plans and instrumentation:

Since 1978, the Meteorological Satellite Service has used sections of the 50.2 - 58.2 GHz band for passive microwave sounding of the atmosphere. These measurements are provided by the Microwave Sounding Unit (MSU) instrument which is flown on the operational series of polar-orbiting weather satellites operated by NOAA. MSU is a 4 channel radiometer (see table 1 for channel characteristics) with two channels in the frequency band under discussion (at 54.76 - 55.16 GHz and 57.75 - 58.15 GHz).

On the basis of experience gained with the MSU data, NOAA will upgrade the microwave sounding capability on its operational polar-orbiting satellites in the near future. This capability will be provided by two new instruments: the Advanced Microwave Sounding Unit - A (AMSU-A), for determining atmospheric temperature profiles, and the Advanced Microwave Sounding Unit - B (AMSU-B), for determining atmospheric water vapour profiles. Together, these two instruments have 20 microwave channels, of which 9 AMSU-A channels fall within the 54.25 - 58.2 GHz band.

Further upgrading of the microwave sounding capability will be achieved (in the 2000 timeframe) by the addition of "stratospheric" channels in the frequency range 60.4 - 61.2

GHz. Such channels will increase the maximum height at which the atmospheric temperature is retrieved from approximately 45 km to approximately 70 km. This technique relies on a special interaction between the Earth's magnetic field and particular O_2 absorption lines (Zeeman splitting).

The channel characteristics of these instruments are given in tables 2 and 3 respectively. Figure 5 shows the location of the AMSU-A channels within the oxygen absorption band. Figure 4 shows the atmospheric attenuation at microwave frequencies due to oxygen and water vapour together with the 20 AMSU channel positions.

The service provided by the MSU instrument is likely to continue through until the end of 1997.

The first flight of the AMSU-A an AMSU-B instruments, on NOAA-K, is currently scheduled for 1995. These instruments will be operated continuously until about 2005, before being replaced with new improved instruments.

The other following microwave sounding instruments must also be mentioned:

- The SSM/T (Special sensor microwave/Temperature) has 7 channels (50.5 to 58.4 GHz), and is currently operated on the US defense meteorological polar satellites DMSP.

- The SSMIS is a new sensor under development for the DMSP series. It integrates into one unique instrument microwave channels previously distributed amongst three distinct sensors: SSM/I (surface sensing), SSM/T (atmospheric temperature profiles), and SSM/H (atmospheric humidity profiles). In particular, SSMIS has 13 channels within 50-61 GHz, and 3 channels around 183 GHz.

- The MTZA is a 10 channels (52 to 57 GHz) temperature sounder, which is going to be operated on the Russian METEOR-3M (from 1996 onwards).

3 Operations of the microwave temperature sounders

A network composed of two NOAA operational weather satellites carrying identical payloads (Vis/IR imagers, IR and MW sounders...), is currently being maintained and operated for the benefit of the whole international meteorological and scientific communities. Meteorological sensors have a wide field of view enabling each of them to yield two complete coverage per day of the earth and of its atmosphere.

The two satellites are in co-ordinated "morning" (around 7.30 a.m local time at equator's crossing) and "afternoon" (around 1.30 p.m local time) sun-synchronous orbits respectively, in such a way that an almost 6-hourly repeat cycle is achieved by the network (4 times global coverage daily, for each type of sensor).

Instruments are operated continuously. Besides the real time data dissemination to regional or local users, global data are stored on board the satellites, and dumped at regular intervals over a limited number of central ground data acquisition stations at

selected geographical positions in order to avoid loosing any piece of data. Typically, each user station can acquire real-time data four times a day, during up to three successive satellite passages.

From around 2000 onwards Europe, through EUMETSAT and ESA, will assume responsibility for the "morning" orbit service. The European METOP satellite is going to occupy the "morning" orbit position (probably with a slightly different local time at equator's crossing), and will replace the corresponding NOAA satellite which will be discontinued.

The remaining "afternoon" NOAA satellite and the "morning" METOP satellite will continue to carry essentially identical meteorological core instruments.

In a longer timeframe, it can be anticipated that other meteorological satellites carrying similar instruments, for instance the Russian METEOR-3M, will be integrated in this network. This would improve the number of coverages per day, and local times at equator's crossing would be adjusted accordingly.

4 Typical characteristics of microwave sounders in the 50 - 60 GHz frequency range

	Present :	**Future :**
Antenna diameter :	15 cm	45 cm
IFOV 3dB points :	3.3°	1.1°
FOV (cross-track) :	+/- 50°	+/- 50°
Antenna gain :	36 dBi	45 dBi
Side lobes :	- 10 dBi	-10 dBi
Beam efficiency :	> 95%	> 95 %
Radiometric resolution:	0.3 K	0.1 K
Swath width :	2300 km	2300 km
Pixel size (nadir) :	49 km	16 km
Number of pixels/line :	30	90
Orbit altitude (circular) :	850 km	850 km
Orbit inclination (sun synchronism):	98.8 °	98.8 °

Note: Viewing usually is "cross-track" in a plane perpendicular to satellite's orbit (for instance mechanically scanned MSU and AMSU-A, and future "push-broom" instrument). The mechanically scanned instruments SSMIS and MTZA have adopted conical viewing around nadir direction providing constant incidence angle of about 53 degrees on the ground.

5 Evaluation of sharing possibilities

AMSU-A, which will enter into operation in 1995, represents a major advance as compared to MSU. It incorporates the best of the technology available at the time of its design, and its optimization reflects the present knowledge in atmospheric physics and modelisation.

However, it is expected that further scientific expertise which shall be gained through utilization of AMSU-A data, and that the technological advances which can be anticipated in the fields of antenna and microwave technologies will generate the need for, and render possible, further enhancements of microwave sounders, in particular:

- optimized selection of frequency channels,
- improved radiometric and geometric resolutions,
- improved vertical resolution.

This is a usual and unavoidable iterative practice in the field of instrument design for sensing complex geophysical parameters from a satellite's orbit, where improvements of instrument performances and improvement of scientific expertise and modelisation proceed along two parallel paths in a kind of "pushpull" process.

5.1 Characterization of a microwave sounder:

Sounders are designed to accurately measure atmospheric parameters, and to optimize the vertical and horizontal sampling of the atmosphere on a global basis. Their performances are characterized by the following main parameters:

- The ground resolution (the "pixel", or the elementary measurement cell) which depends on antenna aperture and on altitude. The pixel is typically the 3dB footprint of the antenna.

- The vertical resolution (represented by the sharpness of the weighting functions), which depends in particular on the channel bandwidth B(Hz),

- The radiometric resolution ΔTe (K) represents the smallest scene temperature variation that the radiometer can detect. It is expressed by the following equation (for a total-power radiometer):

(1) $$\Delta Te = Ts / \sqrt{B.\tau}$$

Where:
* Ts (K) is the radiometer system noise temperature, which includes the receiver temperature and the antenna contribution. The antenna contribution itself is essentially the temperature of the scene as seen by the main lobe of the antenna,
* B (Hz) is the receiver (channel) bandwidth,
* τ (s) is the integration time, during which the elementary measurement cell is "seen" by the radiometer.

- The radiometer threshold Δp (W), the smallest power variation that the instrument is able to detect, is expressed by the equations :

(2) $$\Delta p = k.\Delta Te.B \quad \left(\text{or} \quad \Delta p = k.Ts.\sqrt{\frac{B}{\tau}}\right)$$

Where $k=1.38\times10^{-23}$ J/K is the Boltzman constant.

Note 1: The integration time τ allocated to each pixel is an important parameter. It depends basically on the size of the pixel, on the velocity of the satellite, and because the instrument has to sample a great number of pixels within a scanning line (cross-track or conical about nadir), on the efficiency of the scanning. The scanning efficiency is lower if the pixels in a line are sampled in sequence (case of a mechanically scanned sensor); it is high if all pixels in a line are sampled simultaneously (case of a "push-broom" type instrument).

Note 2: The design of the instrument must realize a difficult trade-off between radiometric resolution (requiring a wide channel bandwidth), and vertical resolution (requiring a narrow channel bandwidth). On AMSU-A, this difficulty is overcome at the expense of hardware complexity in the following way:
Some channels are built with the sum of up to 4 narrow band sub-channels carefully selected at, ideally, almost identical absorption levels of the O_2 spectrum, on the slopes of neighbouring absorption peaks. This technique is illustrated on figure 6, which represents a "zooming" on channels 9 to 14.

5.2 Anticipated performances improvements:

The following assumptions have been made regarding technological improvements. These improvements are based on what is currently anticipated, but cannot be considered as absolute limits:

- Adoption of microwave low-noise pre-amplifiers based, for instance, on HEMT's (High Electronic Mobility Transistors). A receiver noise figure of 3dB can be expected. The receiver contribution to the system noise temperature Ts is then 300K.

- Adoption of a radiometer layout which enables full optimization of the integration time τ (for instance a "push-broom" technique). Optimum τ is taken as the full time that is necessary for the satellite, to travel across the dimension of a pixel: Therefore, τ is directly proportional to the pixel's size and inversely proportional to satellite's velocity. For instance τ =1s for a 7 km pixel (satellite velocity typically around 7 km/s).

- The improvement potential which can be achieved by using these techniques will be optimally distributed amongst the parameters which characterize the performances of the instrument (ref.section 5-1) in a way which is difficult to appreciate today, but which is likely to privilege the vertical resolution (sharper weighting functions and increased number of channels, thus following the continuous improvement process of numerical weather forecast models), and the horizontal resolution.

This improved ("push-broom") sensor was introduced in 1993, in the ITU documentation. A sample of the achievable performances, (as an example), and the permissable interference levels are presented in Recommendations UIT-R SA.515-2, UIT-R SA.1028, and UIT-R SA.1029 respectively, for the scanning sounder and for the "push-broom" sounder.

5.3 Interference threshold:

- An interferer which produces at the input of the radiometer a signal reaching 20% of the radiometer sensitivity is considered harmful:

(3) $$Ph = 0{,}2.k.\Delta Te.B$$

Where *Ph* (W) is the interference threshold at the input of the radiometer.

- The Interference threshold at the radiometers input is given in ITU recommendation UIT-R SA.1029:

Ph = -166 dBW (for the "push-broom" sounder)
Ph = -161 dBW (for the scanning sounder)

This interference threshold refers to a 100 MHz reference bandwidth. This interference threshold in the radiometer channels reflects the difference between the channel bandwidth and the reference bandwidth.

5.4 Sharing criteria

- Several direct or indirect propagation mechanisms can produce interferences at the radiometer's input. Only the direct propagation in the zenithal direction is considered in this document.

- Interference threshold can be converted into **maximum acceptable EIRP** in the zenith direction. The following formula is used:

(4) $$Ph = \left(\frac{\lambda}{4.\pi.R}\right)^2 .Gr.(EIRP).(Att)$$

Where:

* *Ph* (w) is the interference threshold at radiometer's input.
* λ (m) is the wavelength.
* *R* (m) is the distance, which is the altitude of the satellite in the "zenith" case.
* *Gr* is the gain of the radiometer antenna.
* *EIRP* (W) is the total interferer power radiated in the zenith direction.
* *Att* is the total oxygen and water vapour attenuation at the frequency considered.

The maximum acceptable EIRP spectral density (dBW/Hz) is also a useful parameter, because it takes into account possible differences of channel bandwidth optimization.

- At this stage of the evaluation, it is necessary to have a precise knowledge of the frequencies, in order to introduce the oxygen and water vapour attenuation. The following assumptions were made:

  * US standard atmosphere 1976 and LIEBE 89 microwave propagation model for the computation of atmospheric attenuation.
  * Two initial altitudes are considered for fixed terminals: 0 km and 1 km.

  * The shared bands between 50.2 - 50.4 GHz and between 54.25 - 57.2 GHz band are split into several slots separated by the absorption peaks. The atmospheric attenuation taken for the evaluation is the attenuation which appears in the valleys.

Eight frequency slots are identified:

- Slot nr. 1: 50.2 - 50.4 GHz
- Slot nr. 2: 54.25 - 54.67 GHz (valley: 54.25 GHz)
- Slot nr. 3: 54.67 - 55.22 GHz (valley: 54.74 GHz)
- Slot nr. 4: 55.22 - 55.78 GHz (valley: 55.31 GHz)
- Slot nr. 5: 55.78 - 56.26 GHz (valley: 55.89 GHz)
- Slot nr. 6: 56.26 - 56.36 GHz (valley: 56.29 GHz)
- Slot nr. 7: 56.36 - 56.96 GHz (valley: 56.57 GHz)
- Slot nr. 8: 56.96 - 57.20 GHz (valley: 57.19 GHz)

Two instrument scenarios were considered (see section 4):

* A scanning instrument comparable to the AMSU-A as it is currently specified (pixel size, radiometric resolution).
* A "push broom" instrument along the lines defined in section 5.2.

Referring to the specification document MTP 1416 issued by the Radiocommunication Agency (Issue 4, October 1992), the maximum EIRP radiated by an unique FIXED terminal in the zenith direction can reach the following values:

EIRP = -10 dBW (high performance directional antenna)
EIRP = -10 dBW (omnidirectional antenna)
EIRP = +3 dBW (standard directional antenna)

The maximum total EIRP and EIRP spectral density in the pixel were computed in each frequency slot for the two initial altitudes 0 and 1 km, and in the zenith direction only. The results are presented in tables 4.1 and 4.2.

To illustrate possible practical consequences of this threshold, the maximum number of FIXED terminals that can be accepted within one pixel is also computed for each type of

FIXED terminal as specified in document MPT 1416 (standard antenna, high performance antenna, omnidirectional antenna). Instrument performances and results of the simulation are presented in tables 4.1 and 4.2.

Results above are valid for the zenithal direction. The variations of the total path loss (atmospheric attenuation + propagation loss) are computed in tables 5.1 and 5.2 for the various elevation angles. These variations can be compared to the antenna pattern masks provided in document MPT 1416, in order to verify if the zenith case is the worst case. Depending on frequency, this is marginal in case of FIXED terminals fitted with omnidirectional antennas.

6 Conclusion

Under the assumptions made the following preliminary conclusions can be drawn:

- Sharing is probably feasible at frequencies above 56 GHz, because the EIRP threshold shows a significant margin.
- Calculations show that interference to passive microwave sensors will occur at frequencies below 56 GHz.

Therefore it is proposed to allocate the frequency band 54.25 - 56 GHz to Earth Exploration-Satellite (passive) allowing FSS to use the remaining part of the band (56 - 58.2 GHz).

Table 1: MSU channel characteristics.

INSTRUMENT: Microwave Sounding Unit			
Channel	Frequency (GHz)	Bandwidth (MHz)	NEΔT (K)
1	50.30	± 200	0.21
2	53.74	± 200	0.22
3	54.96	± 200	0.18
4	57.95	± 200	0.21

Table 2: AMSU-A channel characteristics.

INSTRUMENT: Advanced Microwave Sounding Unit - A			
Channel	Frequency (GHz)	Bandwidth (MHz)	NEΔT (K)
1	23.8	± 135	0.2
2	31.4	± 90	0.2
3	50.3	± 90	0.3
4	52.8	± 200	0.2
5	53.596	± 200	0.2
6	54.4	± 200	0.2
7	54.94	± 200	0.2
8	55.5	± 165	0.2
9-14	57.290344	± 390	0.2
15	89.0	± 3000	0.5
Additional stratospheric channels on upgraded AMSU-A			
-	60.79267	± 361	1.5

Table 3: AMSU-B channel characteristics.

INSTRUMENT: Advanced Microwave Sounding Unit - B			
Channel	Frequency (GHz)	Bandwidth (MHz)	NEΔT (K)
16	89.0	± 1500	0.3
17	150.0	± 1500	0.6
18a	182.311	± 250	0.6
18b	184.311	± 250	0.6
19a	180.311	± 500	0.6
19b	186.311	± 500	0.6
20a	176.311	± 1100	0.6
20b	190.311	± 1100	0.6

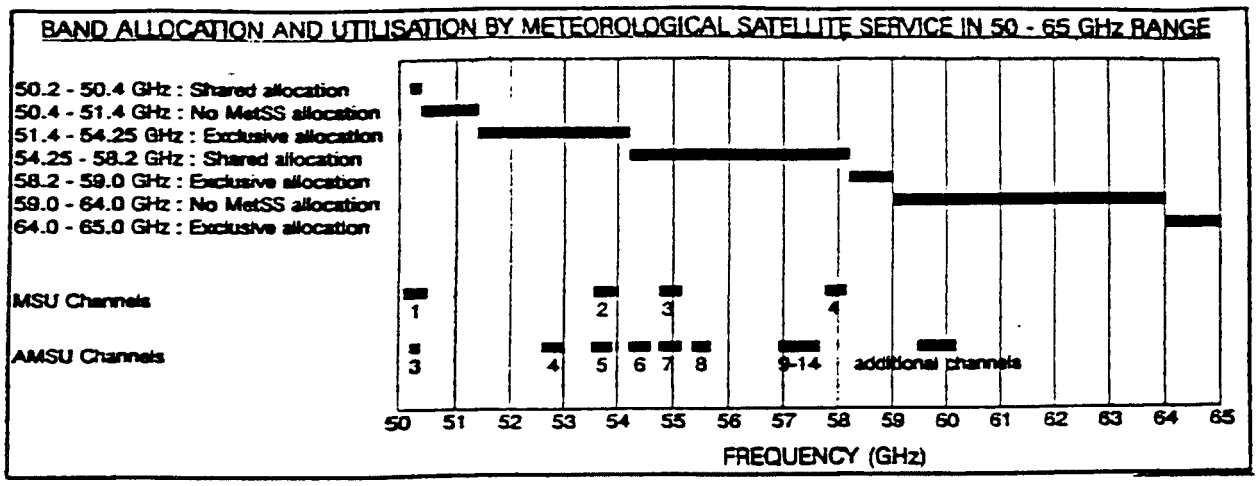

Figure 1: Band allocation as regards the Meteorological Satellite Service, and utilisation by the Meteorological Satellite Service in the 50 - 65 GHz range.

Preferred Frequency Bands for Passive Microwave Sensors

	Frequency (GHz)	Bandwidth (MHz)	Measurements
SURFACE	Near 1.4	100	Soil Moisture; salinity
	Near 2.7	60	Salinity; soil moisture
	Near 5	200	Estuarine temperature
	Near 6	400	Ocean temperature
	Near 11	100	Rain; snow; lake ice; sea state
	Near 15	200	Water vapor; rain
	Near 18	200	Rain; sea state; ocean ice; water vapor
	Near 21	200	Water vapor; liquid water
	22.235	300	Water vapor; liquid water
	Near 24	400	Water vapor; liquid water
	Near 30	500	Ocean ice; water vapor; oil spills; clouds; liquid water
	Near 37	1000	Rain; snow; ocean ice; oil spills; clouds
	Near 55	250 Multiple*	Temperature
	Near 90	6000	Clouds; oil spills; ice; snow
ATMOSPHERE	100.49	2000	Nitrous oxide
	110.80	2000	Ozone
	115.27	2000	Carbon monoxide
	118.70	2000	Temperature
	125.81	2000	Nitrous oxide
	150.74	2000	Nitrous oxide
	164.38	2000	Chlorine oxide
	167.20	2000	Chlorine oxide
	175.86	2000	Nitrous oxide
	183.31	2000	Water vapor
	184.75	2000	Ozone
	200.98	2000	Nitrous oxide
	226.09	2000	Nitrous oxide
	230.54	2000	Carbon monoxide
	235.71	2000	Ozone
	237.15	2000	Ozone
	251.21	2000	Nitrous oxide
	276.33	2000	Nitrous oxide
	301.44	2000	Nitrous oxide
	325.10	2000	Water vapor
	346.80	2000	Carbon monoxide
	364.32	2000	Ozone
	380.20	2000	Water vapor

*Several bands each of 250 MHz bandwidth

Figure 2: Preferred frequency bands for passive microwave sensors

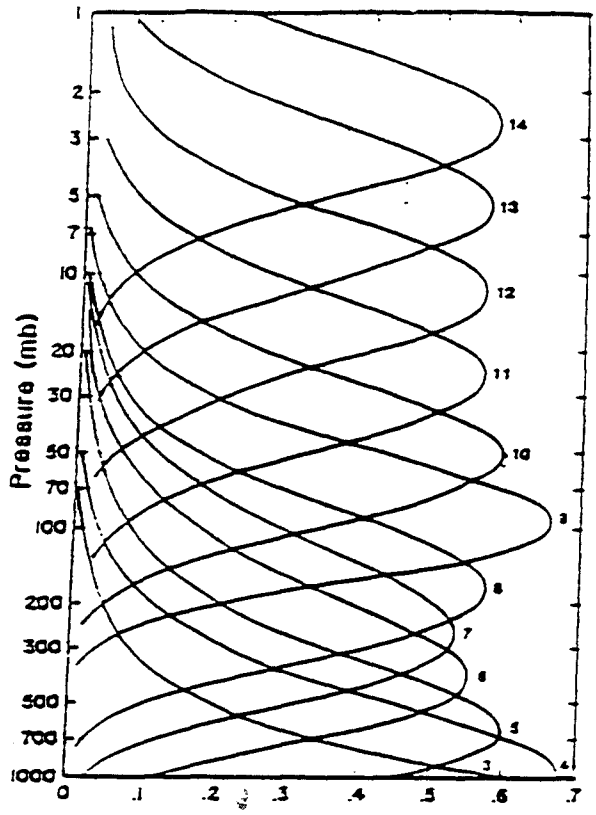

Figure 3: Typical weighting functions of a microwave temperature sounder

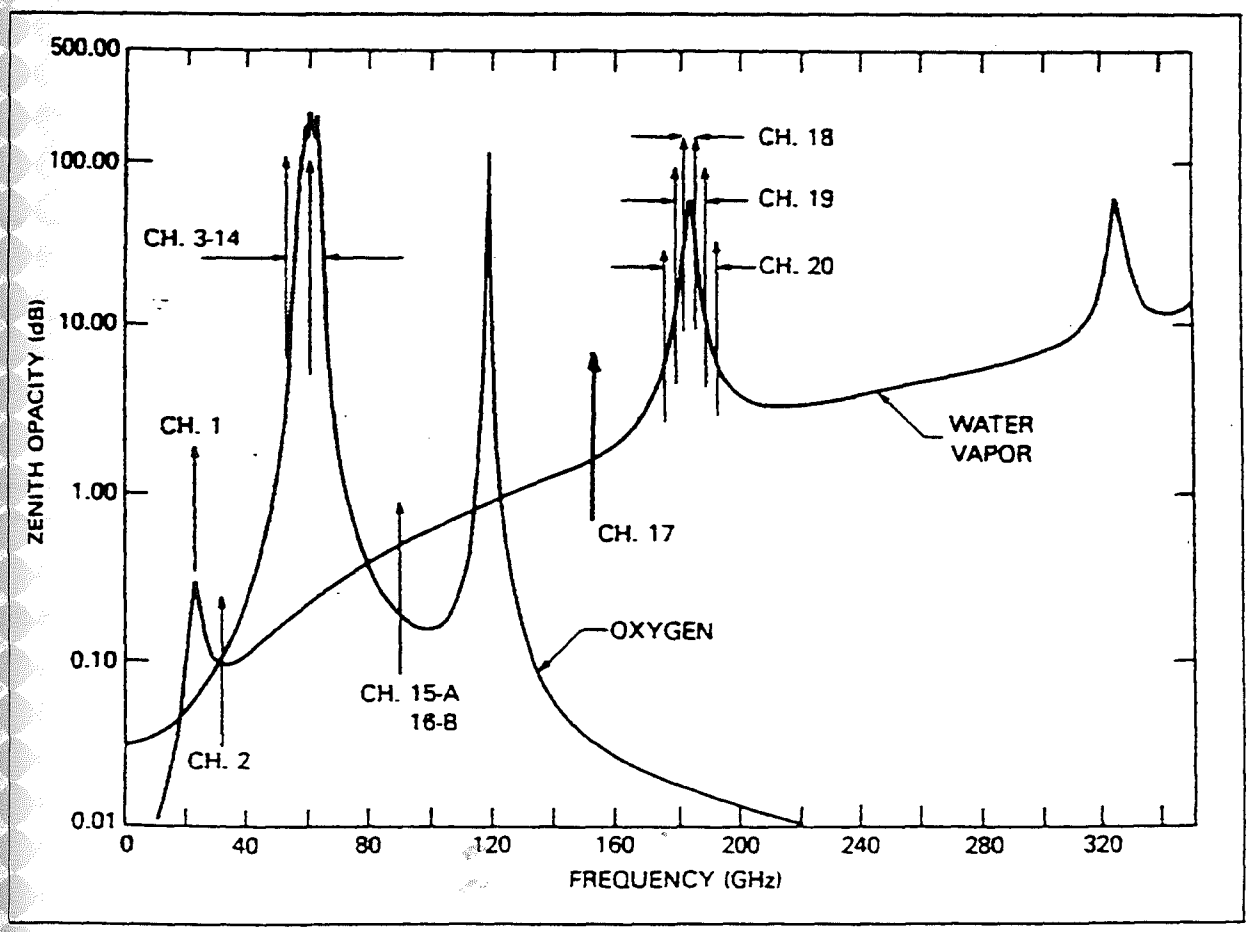

Figure 4: Atmospheric attenuation at microwave frequencies due to oxygen and water vapour molecules, together with the AMSU (A and B) channel positions.

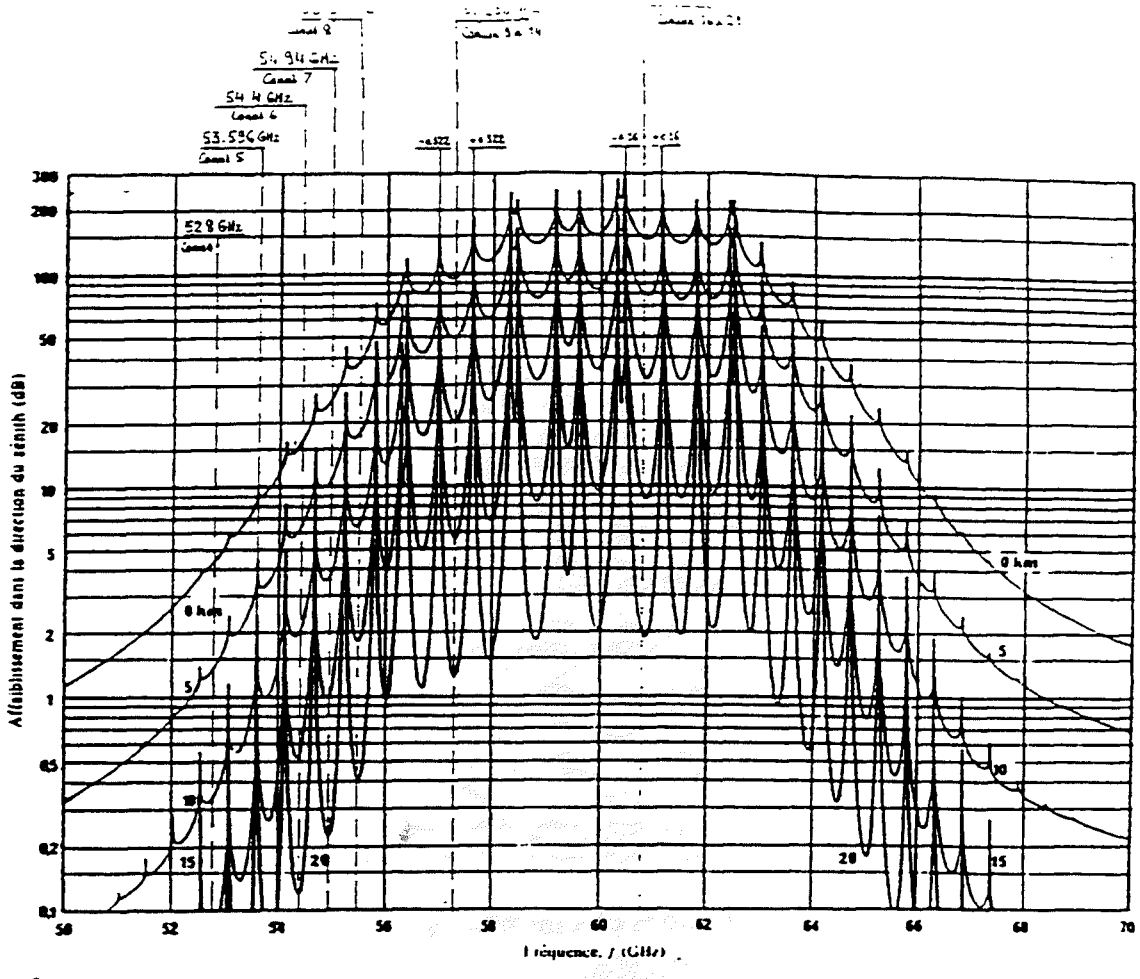

Figure 5: Location of the AMSU-A channels within the oxygen absorption spectrum

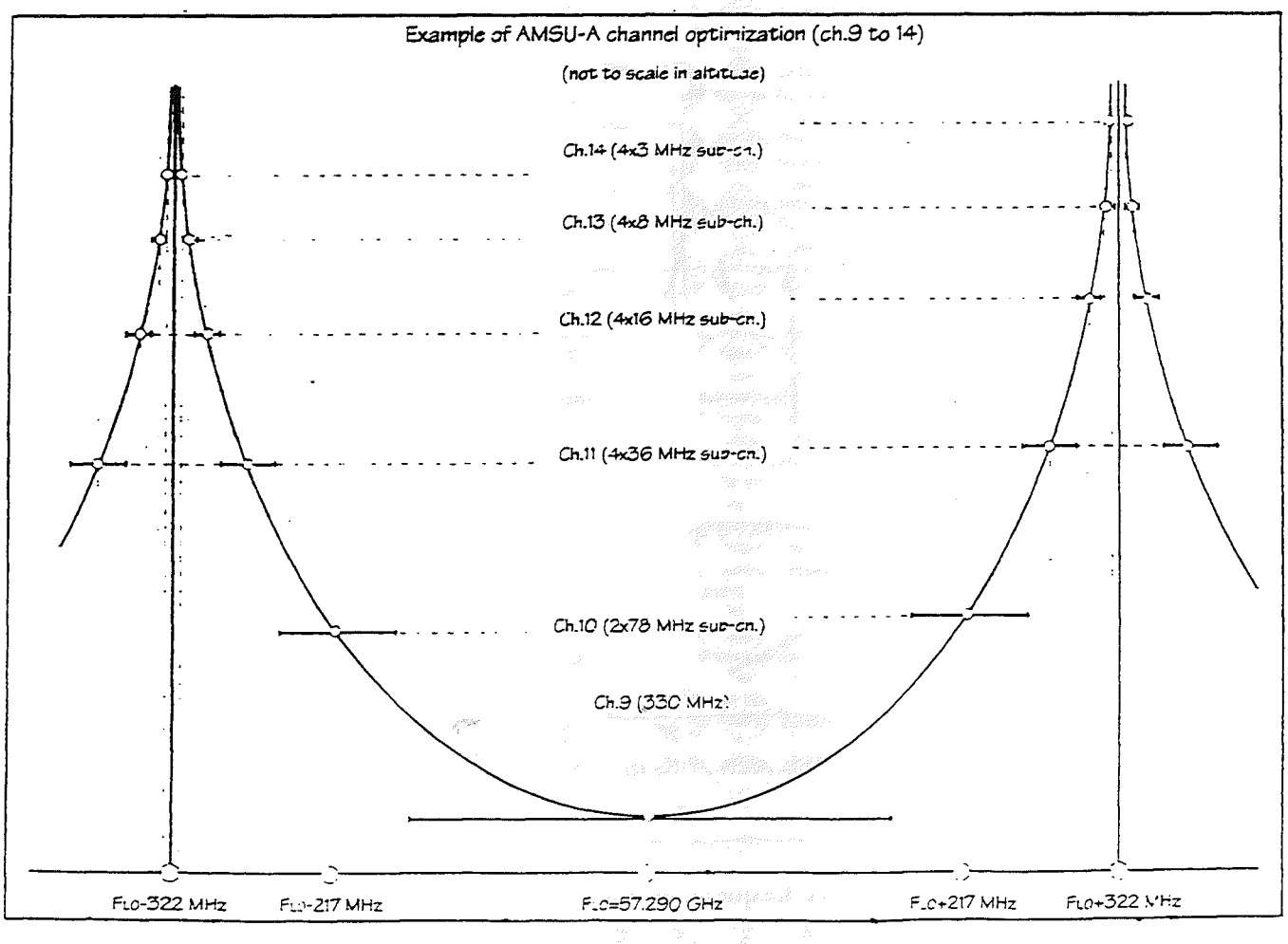

Figure 6: Example of AMSU-A channel optimization

18-Aoû-94	"PUSH-BROOM" SOUNDER - Zenith case							
"Fixed" terminal max.EIRP to zenith (dBW)	(assumed within 140 MHz bw)							
Standard antenna:		3	3	3	3	3	3	3
High performance antenna:		-10	-10	-10	-10	-10	-10	-10
Omnidirectional antenna:		-12	-12	-12	-12	-12	-12	-12

Frequency slots (GHz)	50.2-50.4	54.25-54.67	54.67-55.22	55.22-55.78	55.78-56.26	56.26-56.36	56.36-56.96	56.96-57.2
Slot n°	1	2	3	4	5	6	7	8
Center frequency (GHz)	50,3	54,25	54,74	55,31	55,89	56,29	56,57	57,19
Wavelength (cm)	0,596	0,553	0,548	0,542	0,537	0,533	0,530	0,525
Altitude (km)	850	850	850	850	850	850	850	850
Propagation loss (dB)	-185,1	-185,7	-185,8	-185,9	-186,0	-186,0	-186,1	-186,2
System noise temp.(K)	550	550	550	550	550	550	550	550
O2 abeorp.0 km init.(dB)	-1,6	-15,3	-23,7	-37,0	-57,4	-86,4	-80,2	-58,8
O2 abeorp.1 km init.(dB)	-1,3	-12,8	-20,3	-32,2	-50,9	-78,5	-71,5	-88,3
PIXEL nadir (km)	16	16	16	16	16	16	16	16
Integration time (s)	2,45	2,45	2,45	2,45	2,45	2,45	2,45	2,45
Antenna gain (dB)	45	45	45	45	45	45	45	45
Channel bandwidth (MHz)	15	15	15	15	15	15	15	15
Rad.sensitivity (K)	0,1	0,1	0,1	0,1	0,1	0,1	0,1	0,1
Rad.threshold (dBW)	-167,3	-167,3	-167,3	-167,3	-167,3	-167,3	-167,3	-167,3
Interf.threshold in channel bw (dBW)	-174,3	-174,3	-174,3	-174,3	-174,3	-174,3	-174,3	-174,3
Interf.threshold in 100 MHz ref.bw (dBW)	-166,0	-166,0	-166,0	-166,0	-166,0	-166,0	-166,0	-166,0
Interf.spectral dens.(dBW/Hz)	-246,0	-246,0	-246,0	-246,0	-246,0	-246,0	-246,0	-246,0
0 km initial altitude								
Max EIRP (dBW/pxl):	-33,0	-18,7	-10,2	3,2	23,7	52,7	46,6	65,3
Max EIRP spectral density in slot (dBW/Hz):	-104,8	-90,5	-82,0	-68,6	-48,1	-19,1	-25,2	-6,5
Max number of terminals/pixel								
Standard antenna:		0	0	10	1096	871053	213971	15733388
High performance antenna:		1	9	194	21870	17379791	4269278	313922363
Omnidirectional antenna:		2	14	307	34682	27545113	6766349	497533416
Hyp. "-10dBW/400MHz, -10dBi terminal":		36	252	5516	621902	494215684	121402152	8926767408
1 km initial altitude								
Max EIRP (dBW/pxl):	-33,4	-21,2	-13,6	-1,6	17,2	44,9	37,9	54,8
Max EIRP spectral density in slot (dBW/Hz):	-105,1	-93,0	-85,4	-73,4	-54,6	-26,9	-33,9	-17,0
Max number of terminals/pixel								
Standard antenna:		0	0	3	243	144228	28864	1402240
High performance antenna:		1	4	64	4851	2877694	575910	27978360
Omnidirectional antenna:		1	6	102	7689	4560837	912755	44342712
Hyp. "-10dBW/400MHz, -10dBi terminal":		20	115	1822	137950	81830748	16376700	795598983

	SCANNING SOUNDER - Zenith case							
"Fixed" terminal max.EIRP to zenith (dBW)	(assumed within 140 MHz bw)							
Standard antenna:		3	3	3	3	3	3	3
High performance antenna:		-10	-10	-10	-10	-10	-10	-10
Omnidirectional antenna:		-12	-12	-12	-12	-12	-12	-12

Frequency slots (GHz)	50.2-50.4	54.25-54.67	54.67-55.22	55.22-55.78	55.78-56.26	56.26-56.36	56.36-56.96	56.96-57.2
Slot n°	1	2	3	4	5	6	7	8
Center frequency (GHz)	50,3	54,25	54,74	55,31	55,89	56,29	56,57	57,19
Wavelength (cm)	0,596	0,553	0,548	0,542	0,537	0,533	0,530	0,525
Altitude (km)	850	850	850	850	850	850	850	850
Propagation loss (dB)	-185,1	-185,7	-185,8	-185,9	-186,0	-186,0	-186,1	-186,2
System noise temp.(K)	2300	2300	2300	2300	2300	2300	2300	2300
O2 absorp.0 km init.(dB)	-1,6	-15,3	-23,7	-37,0	-57,4	-86,4	-80,2	-98,8
O2 absorp.1 km init.(dB)	-1,3	-12,8	-20,3	-32,2	-50,9	-78,5	-71,5	-88,3
PIXEL nadir (km)	49	49	49	49	49	49	49	49
Integration time (s)	0.20	0.20	0.20	0.20	0.20	0.20	0.20	0.20
Antenna gain (dB)	36	36	36	36	36	36	36	36
Channel bandwidth (MHz)	400	400	400	400	400	400	400	400
Rad.sensit.(K)	0.3	0.3	0.3	0.3	0.3	0.3	0.3	0.3
Rad.threshold (dBW)	-148.5	-148.5	-148.5	-148.5	-148.5	-148.5	-148.5	-148.5
Interf.threshold in channel bw (dBW)	-155.5	-155.5	-155.5	-155.5	-155.5	-155.5	-155.5	-155.5
Interf.threshold in 100 MHz ref.bw (dBW)	-161.5	-161.5	-161.5	-161.5	-161.5	-161.5	-161.5	-161.5
Interf.spectral dens.(dBW/Hz)	-241.5	-241.5	-241.5	-241.5	-241.5	-241.5	-241.5	-241.5
0 km initial altitude								
Max EIRP (dBW/pxl):	-4,5	9,8	18,3	31,7	52,2	81,2	75,1	93,8
Max EIRP spectral density in slot (dBW/Hz):	-90,5	-76,3	-67,8	-54,4	-33,8	-4,8	-10,9	7,7
Max number of terminals/pixel								
Standard antenna:		2	12	258	29032	23071532	5867432	416729389
High performance antenna:		33	235	5138	579271	460337583	113080129	8314844450
Omnidirectional antenna:		53	372	8144	918083	729585902	179219926	13178140365
Hyp. "-10dBW/400MHz, -10dBi terminal":		944	6679	146114	16472295	13090283767	3215572144	236442799825
1 km initial altitude								
Max EIRP (dBW/pxl):	-4,9	7,3	14,8	28,9	45,6	73,4	66,4	83,3
Max EIRP spectral density in slot (dBW/Hz):	-90,9	-78,7	-71,2	-59,2	-40,4	-12,6	-19,6	-2,8
Max number of terminals/pixel								
Standard antenna:		1	5	85	6440	3820115	764515	37141046
High performance antenna:		19	107	1698	128494	76221314	15254090	741061292
Omnidirectional antenna:		30	169	2690	203649	120802642	24176103	1174502996
Hyp. "-10dBW/400MHz, -10dBi terminal":		532	3039	48272	3653879	2167446556	433768747	21072986716

Link-budgets for various elevation angles and frequencies

0 km initial altitude								
Sat.altitude (km)	850	850	850	850	850	850	850	850
Frequency (GHz)	50,3	54,25	54,74	55,31	55,89	56,29	56,57	57,19
Elevation (°)	90	90	90	90	90	90	90	90
O2 absorption (dB)	-1,60	-15,25	-23,67	-36,98	-57,41	-86,35	-80,21	-98,78
Spreading loss (dB)	-129,58	-129,58	-129,58	-129,58	-129,58	-129,58	-129,58	-129,58
Attenuation (dB)	-131,18	-144,83	-153,25	-166,56	-186,99	-215,93	-209,79	-228,36
Elevation (°)	80	80	80	80	80	80	80	80
O2 absorption (dB)	-1,62	-15,49	-24,04	-37,55	-58,30	-87,68	-81,45	-100,30
Angle/nadir (°)	8,814	8,814	8,814	8,814	8,814	8,814	8,814	8,814
Slant range (km)	861,54	861,54	861,54	861,54	861,54	861,54	861,54	861,54
Spreading loss (dB)	-129,70	-129,70	-129,70	-129,70	-129,70	-129,70	-129,70	-129,70
Attenuation (dB)	-131,32	-145,18	-153,73	-167,25	-187,99	-217,38	-211,14	-230,00
Increment/nadir (dB)	-0,14	-0,35	-0,48	-0,69	-1,00	-1,45	-1,35	-1,64
Elevation (°)	70	70	70	70	70	70	70	70
O2 absorption (dB)	-1,70	-16,23	-25,19	-39,35	-61,09	-91,89	-85,36	-105,12
Angle/nadir (°)	17,566	17,566	17,566	17,566	17,566	17,566	17,566	17,566
Slant range (km)	897,61	897,61	897,61	897,61	897,61	897,61	897,61	897,61
Spreading loss (dB)	-130,05	-130,05	-130,05	-130,05	-130,05	-130,05	-130,05	-130,05
Attenuation (dB)	-131,76	-146,28	-155,24	-169,41	-191,15	-221,95	-215,41	-235,17
Increment/nadir (dB)	-0,58	-1,45	-1,99	-2,85	-4,16	-6,02	-5,62	-6,81
Elevation (°)	60	60	60	60	60	60	60	60
O2 absorption (dB)	-1,85	-17,61	-27,33	-42,70	-66,29	-99,71	-92,62	-114,06
Angle/nadir (°)	26,181	26,181	26,181	26,181	26,181	26,181	26,181	26,181
Slant range (km)	962,96	962,96	962,96	962,96	962,96	962,96	962,96	962,96
Spreading loss (dB)	-130,66	-130,66	-130,66	-130,66	-130,66	-130,66	-130,66	-130,66
Attenuation (dB)	-132,51	-148,27	-158,00	-173,37	-196,96	-230,37	-223,28	-244,73
Increment/nadir (dB)	-1,33	-3,44	-4,75	-6,80	-9,97	-14,44	-13,49	-16,37
Elevation (°)	50	50	50	50	50	50	50	50
O2 absorption (dB)	-2,09	-19,91	-30,90	-48,27	-74,94	-112,72	-104,71	-128,95
Angle/nadir (°)	34,555	34,555	34,555	34,555	34,555	34,555	34,555	34,555
Slant range (km)	1067,02	1067,02	1067,02	1067,02	1067,02	1067,02	1067,02	1067,02
Spreading loss (dB)	-131,56	-131,56	-131,56	-131,56	-131,56	-131,56	-131,56	-131,56
Attenuation (dB)	-133,64	-151,46	-162,45	-179,83	-206,50	-244,28	-236,26	-260,50
Increment/nadir (dB)	-2,46	-6,63	-9,20	-13,27	-19,51	-28,35	-26,47	-32,14
Elevation (°)	40	40	40	40	40	40	40	40
O2 absorption (dB)	-2,49	-23,72	-36,82	-57,53	-89,31	-134,34	-124,78	-153,67
Angle/nadir (°)	42,529	42,529	42,529	42,529	42,529	42,529	42,529	42,529
Slant range (km)	1226,90	1226,90	1226,90	1226,90	1226,90	1226,90	1226,90	1226,90
Spreading loss (dB)	-132,77	-132,77	-132,77	-132,77	-132,77	-132,77	-132,77	-132,77
Attenuation (dB)	-135,26	-156,49	-169,59	-190,30	-222,08	-267,11	-257,55	-286,44
Increment/nadir (dB)	-4,08	-11,66	-16,34	-23,74	-35,09	-51,17	-47,76	-58,08

Table 5.1

SNDGEO02 XLS

Link-budgets for various elevation angles and frequencies

1 km initial altitude								
Sat.altitude (km)	850	850	850	850	850	850	850	850
Frequency (GHz)	54,25	54,25	54,74	55,31	55,89	56,29	56,57	57,19
Elevation (°)	90	90	90	90	90	90	90	90
O2 absorption (dB)	-1,50	-11,70	-19,40	-30,50	-50,10	74,00	-70,20	-83,80
Spreading loss (dB)	-129,58	-129,58	-129,58	-129,58	-129,58	-129,58	-129,58	-129,58
Attenuation (dB)	-131,08	-141,28	-148,98	-160,08	-179,68	-55,58	-199,78	-213,38
Elevation (°)	80	80	80	80	80	80	80	80
O2 absorption (dB)	-1,52	-11,88	-19,70	-30,97	-50,87	75,14	-71,28	-85,09
Angle/nadir (°)	8,814	8,814	8,814	8,814	8,814	8,814	8,814	8,814
Slant range (km)	861,54	861,54	861,54	861,54	861,54	861,54	861,54	861,54
Spreading loss (dB)	-129,70	-129,70	-129,70	-129,70	-129,70	-129,70	-129,70	-129,70
Attenuation (dB)	-131,22	-141,58	-149,40	-160,67	-180,57	-54,56	-200,98	-214,79
Increment/nadir (dB)	-0,14	-0,30	-0,42	-0,59	-0,89	1,02	-1,20	-1,41
Elevation (°)	70	70	70	70	70	70	70	70
O2 absorption (dB)	-1,60	-12,45	-20,65	-32,46	-53,32	78,75	-74,71	-89,18
Angle/nadir (°)	17,566	17,566	17,566	17,566	17,566	17,566	17,566	17,566
Slant range (km)	897,61	897,61	897,61	897,61	897,61	897,61	897,61	897,61
Spreading loss (dB)	-130,05	-130,05	-130,05	-130,05	-130,05	-130,05	-130,05	-130,05
Attenuation (dB)	-131,65	-142,50	-150,70	-162,51	-183,37	-51,30	-204,76	-219,23
Increment/nadir (dB)	-0,57	-1,22	-1,72	-2,43	-3,69	4,28	-4,98	-5,85
Elevation (°)	60	60	60	60	60	60	60	60
O2 absorption (dB)	-1,73	-13,51	-22,40	-35,22	-57,85	85,45	-81,06	-96,76
Angle/nadir (°)	26,181	26,181	26,181	26,181	26,181	26,181	26,181	26,181
Slant range (km)	962,96	962,96	962,96	962,96	962,96	962,96	962,96	962,96
Spreading loss (dB)	-130,66	-130,66	-130,66	-130,66	-130,66	-130,66	-130,66	-130,66
Attenuation (dB)	-132,40	-144,17	-153,07	-165,88	-188,51	-45,22	-211,72	-227,43
Increment/nadir (dB)	-1,32	-2,89	-4,08	-5,80	-8,83	10,36	-11,94	-14,05
Elevation (°)	50	50	50	50	50	50	50	50
O2 absorption (dB)	-1,96	-15,27	-25,32	-39,81	-65,40	96,60	-91,64	-109,39
Angle/nadir (°)	34,555	34,555	34,555	34,555	34,555	34,555	34,555	34,555
Slant range (km)	1067,02	1067,02	1067,02	1067,02	1067,02	1067,02	1067,02	1067,02
Spreading loss (dB)	-131,56	-131,56	-131,56	-131,56	-131,56	-131,56	-131,56	-131,56
Attenuation (dB)	-133,51	-146,83	-156,88	-171,37	-196,96	-34,96	-223,20	-240,95
Increment/nadir (dB)	-2,43	-5,55	-7,90	-11,29	-17,28	20,63	-23,41	-27,57
Elevation (°)	40	40	40	40	40	40	40	40
O2 absorption (dB)	-2,33	-18,20	-30,18	-47,45	-77,94	115,12	-109,21	-130,37
Angle/nadir (°)	42,529	42,529	42,529	42,529	42,529	42,529	42,529	42,529
Slant range (km)	1226,90	1226,90	1226,90	1226,90	1226,90	1226,90	1226,90	1226,90
Spreading loss (dB)	-132,77	-132,77	-132,77	-132,77	-132,77	-132,77	-132,77	-132,77
Attenuation (dB)	-135,10	-150,97	-162,95	-180,22	-210,71	-17,64	-241,98	-263,14
Increment/nadir (dB)	-4,02	-9,69	-13,97	-20,14	-31,03	37,94	-42,20	-49,76

Table 6.2

SNDGEO02.XLS

CGMS XXIII
USA WP-19
Agenda Item WG I/2

PROPOSED CHANGES TO THE AUTOMATIC PICTURE TRANSMISSION (APT) FREQUENCIES FOR NOAA-N AND NOAA-N'

The NOAA Configuration Control Board, on 16 June 1994 approved the use of the following frequencies for the Automatic Picture Transmission (APT) links of the NOAA N and N' satellites: 137.1 and 137.9125 MHz. These frequencies, approved for use by NOAA's National Weather Service, were changed to maintain protection through use an International Telecommunication Union (ITU) primary allocation for meteorological satellites, and where the Mobile Satellite Service (MSS) retains only a secondary status. Use of the existing frequencies at 137.50 MHz and 137.62 MHz must be accomplished on a coprimary status with the MSS. Possible future spectrum battles with the new MSS are thus avoided by adopting these frequency changes.

The programmatic impacts to NOAA are slight. Costs are avoided by waiting until NOAA-N to implement the change in frequencies. Schedule impacts are also avoided. The minor change in frequencies involves little technical risk.

Table 6.2

APT imagery provides a source of weather data available worldwide to users operating relatively inexpensive ground receiving stations. The World Meteorological Organization (WMO) continues to be a strong advocate for disseminating this information, particularly to Third World countries. Corruption of this service from interference produced by future mobile satellites could limit the useful data available to areas of the world whose only dependable weather images are broadcast on the APT frequencies.

In addition to the frequency changes, the change in the transmitted satellite signal from analog to digital format must be considered. The digital Low Rate Picture Transmission (LRPT) link foreseen on the METOP satellites and the converged U.S. polar satellites will replace the analog APT during the next decade. Close coordination between NOAA and EUMETSAT is required in designing the new transmission link.

The WMO through the former EC Panel of Experts on Satellites has been involved in this LRPT frequency issue since 1987. The WMO will be kept informed of the planned changes in transmission frequencies and modulation to assure that satellite data users will have as much notice as possible of the changes. Regarding the frequency change, the planned launch date of NOAA-N is 2000.

CGMS-XXIII EUM-WP- 15
Prepared by EUMETSAT
Agenda Item: II/1

THE METEOROLOGICAL PRODUCTS EXTRACTION FACILITY (MPEF) IN THE NEW EUMETSAT GROUND SEGMENT [1]

ABSTRACT

This paper describes the MPEF, part of the newly developed EUMETSAT Ground Segment, which will process the data from all MOP and MTP satellites from December 1995.

The MPEF is a near real time processing system designed as a stand-alone facility imbedded in the Mission Control Centre (MCC). Successor of the current MOP MIEC operated by the European Space Operations Centre, it features increased modularity and a number of improved processing and algorithms implementation. It includes three processing chains for operational product extraction, commissioning and test support, and a separate development environment with a performance margin of at least 50%.

The algorithms are extensions of the MIEC algorithms and incorporate improvements in several areas, e.g. Fast Fourier Transform (FFT) based cross-correlation method for the Cloud Motion Wind (CMW) product. The product extraction and distribution frequency has been increased and will allow the distribution of the CMW product, derived from all three spectral channels of the Meteosat satellite, every 1.5 hours.

The new Automatic and Manual Quality Control concept will guarantee a flexible quality control and will allow the inclusion of quality control information in the individual products. The Meteorological Workstation for manual quality control, visualisation and analysis of MPEF products and images is based on off-the-shelf software and guarantees a state-of-the-art graphics display and development facility.

[1] H.B Faas, R.A. Francis, Y. Buhler, D. Quingley, R. Schraidt (EUMETSAT), V. Gärtner (EAS/ESOC)

THE METEOROLOGICAL PRODUCTS EXTRACTION FACILITY (MPEF) IN THE NEW EUMETSAT GROUND SEGMENT

1 MPEF as part of the MTP Mission Control Centre (MCC)

A new ground segment is being developed by EUMETSAT to take full control of all Meteosat satellites from the start of the Meteosat Transition Programme (MTP) on 1st December 1995. The MTP ground segment includes a Mission Control Centre (MCC) and a Primary Ground Station (PGS). This will replace the system currently operated from the European Space Operations Centre (ESOC) in Darmstadt, Germany.

The MCC will be located in a new EUMETSAT headquarters building in Darmstadt and the PGS will be located in Fuccino, Italy. The MCC is divided into four main facilities, each being developed by European industry under direct contracts from EUMETSAT. The Core Facility is the central element of the MCC and includes the functions of mission management, satellite control, ground segment control and the pre-processing of satellite data.

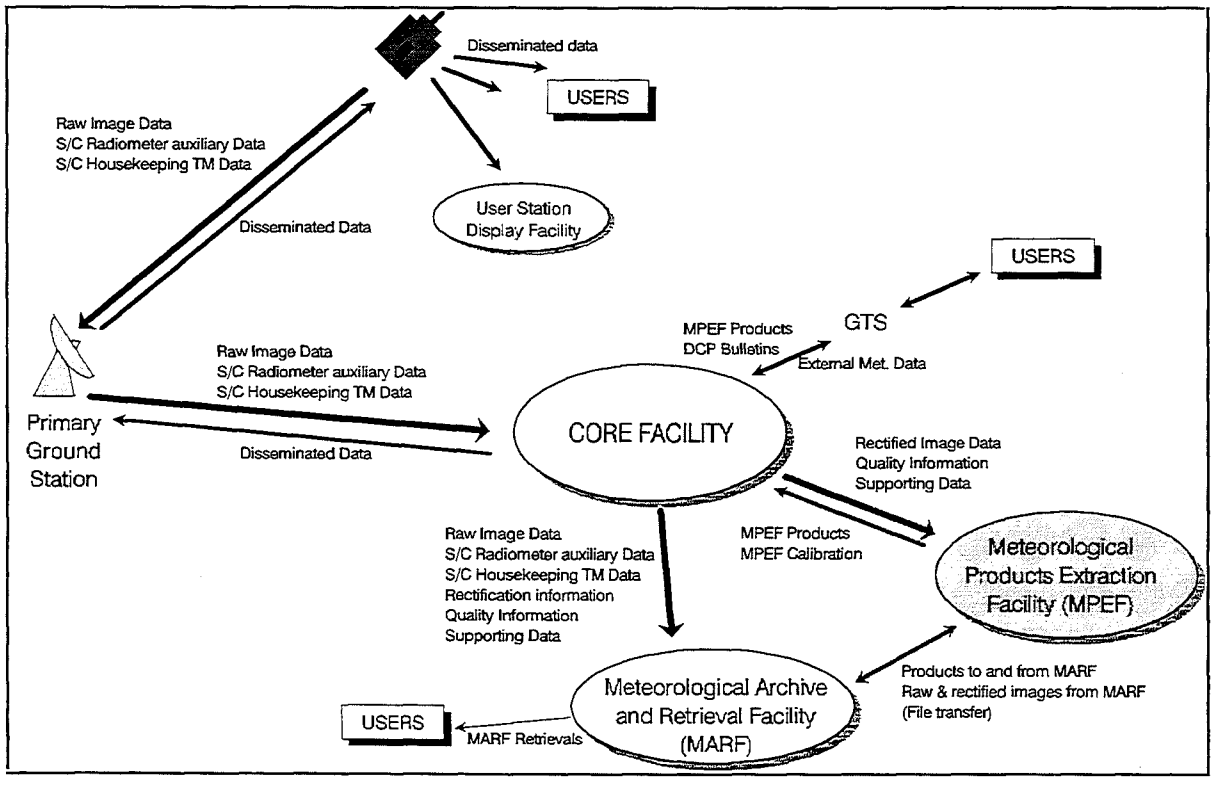

Figure 1 MPEF as part of the MTP Ground Segment

The Meteorological Archive and Retrieval Facility (MARF) provides the capability for the users to access the historical data from Meteosat satellites. The User Station Display Facility (USDF) provides real-time visibility of the end products to operations staff within the MCC. The MPEF processes rectified image data to derive a range of meteorological products for the end users. The overall MTP ground segment architecture is shown in Figure 1.

2 MPEF Architecture

The MPEF will be implemented on a distributed workstation system and will include three processing chains each comprised of two workstations. These chains will be used for operational product extraction, support for satellite commissioning and test support. One of the two non-operational chains can function in parallel to the operational chain in hot stand-by mode to guarantee high availability of an operational system. MPEF has been specified

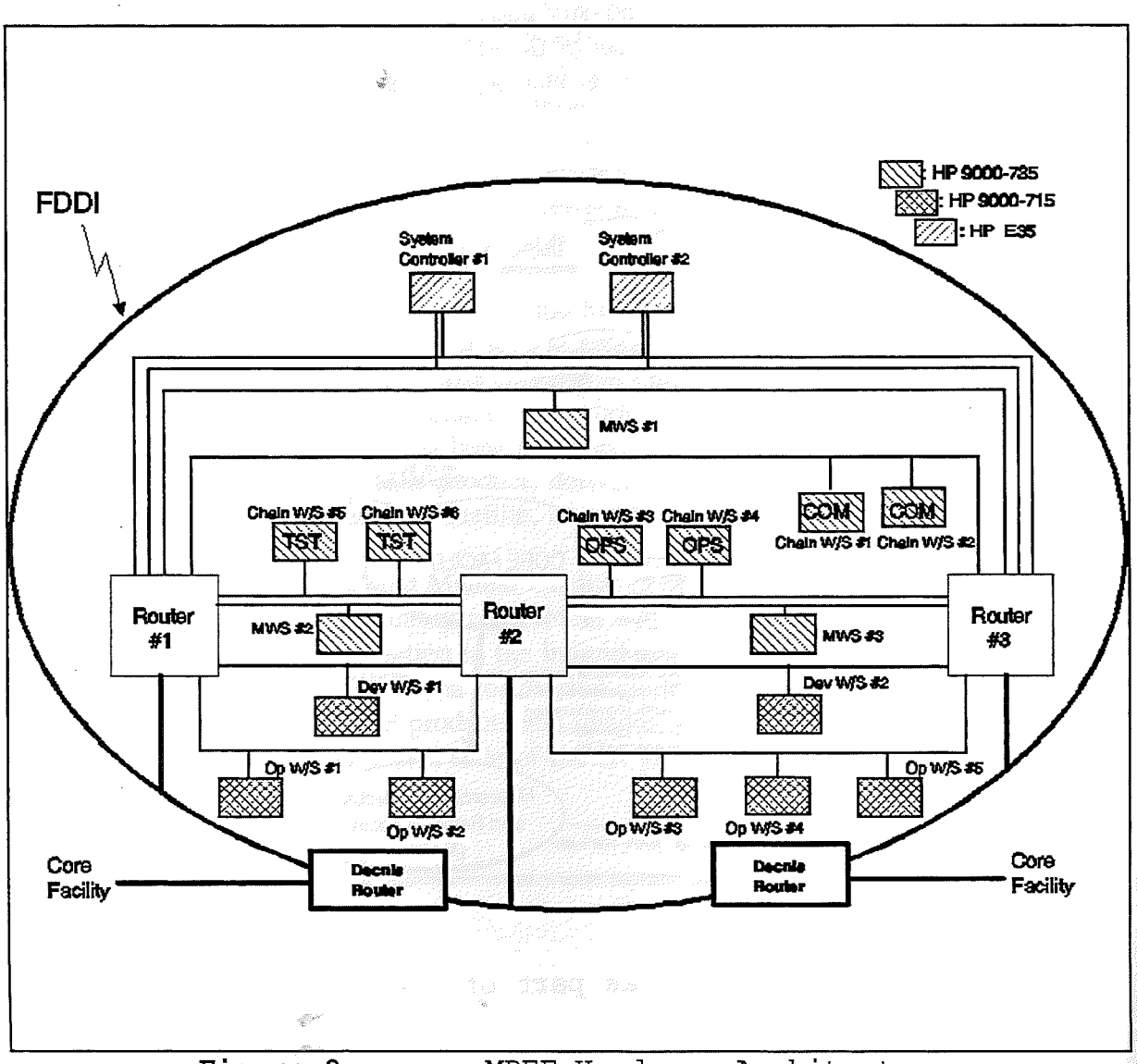

Figure 2 MPEF Hardware Architecture

with a performance margin of 50% for all hardware elements and also with the possibility of re-allocating processes to different workstations. This will provide sufficient flexibility for future developments, improvements and the inclusion of new operational products. The use of off-the-shelf hardware will further improve the availability and will reduce maintenance costs. The MPEF architecture is depicted in Figure 2.

The MPEF workstations and system controllers are inter-connected through a local area network (LAN) based on an FDDI ring with routers providing connections to the hardware elements via Ethernet spurs. The interface to the Core Facility is via two redundant routing devices connected to both the MPEF LAN and the CF LAN.

Each processing chain consists of two Hewlett Packard 9000/735 workstations. When acting as hot stand-by the commissioning chain or the test chain will receive the same data and perform the same processing as the operational chain, but will not normally distribute the derived products. In the event of a failure of the operational chain no manual intervention will be necessary to bring the stand-by to operational status.

Up to two parallel image data streams may be processed by the chain workstations so that MPEF can support the commissioning of a new satellite without interrupting its operational processing activities.

The system controller consists of two (redundant) Hewlett Packard E35 servers connected to a dual ported, mirrored disk system. The main functions of these servers is to provide support for the monitoring of system performance, the scheduling of processes and the maintenance of a relational database containing a wide variety of system information such as logged parameters, display definitions, user details, etc.

In addition to the two system controllers and six chain workstations there are three other types of workstations in MPEF, namely operator workstations (five Hewlett Packard 9000/715s), development workstations (two Hewlett Packard 9000/715s) and MWS workstations (three Hewlett Packard 9000/735s with enhanced graphics). These provide access to all operational functions although the manual quality control of MPEF products and the visualisation of products and images can only be performed from the MWS workstations which have enhanced graphics capabilities. The prime function of the operator workstation is to facilitate hardware and software monitoring along with other operator functions. The development workstations can be used for the development and testing of new application and system software. The MWS workstations are based on off-the-shelf software and feature a state-of-the-art graphics display and development facility. Three printers are connected to the network to provide hardcopy facilities and a video subsystem provides the capability to record and print graphical information from any of the MWS workstations.

3 General Concept of the MPEF Design

The MTP MPEF is the successor to the current Meteosat Information Extraction Centre (MIEC) for MOP. It features modular software design and incorporates a number of improvements in image data processing and product generation algorithm implementations. In addition the product algorithms are configured at run-time by a set of user-defined

The Meteorological Archive and Retrieval Facility (MARF) provides the capability for the users to access the historical data from Meteosat satellites. The User Station Display Facility (USDF) provides real-time visibility of the end products to operations staff within the MCC. The MPEF processes rectified image data to derive a range of meteorological products for the end users. The overall MTP ground segment architecture is shown in Figure 1.

2 MPEF Architecture

The MPEF will be implemented on a distributed workstation system and will include three processing chains each comprised of two workstations. These chains will be used for operational product extraction, support for satellite commissioning and test support. One of the two non-operational chains can function in parallel to the operational chain in hot stand-by mode to guarantee high availability of an operational system. MPEF has been specified

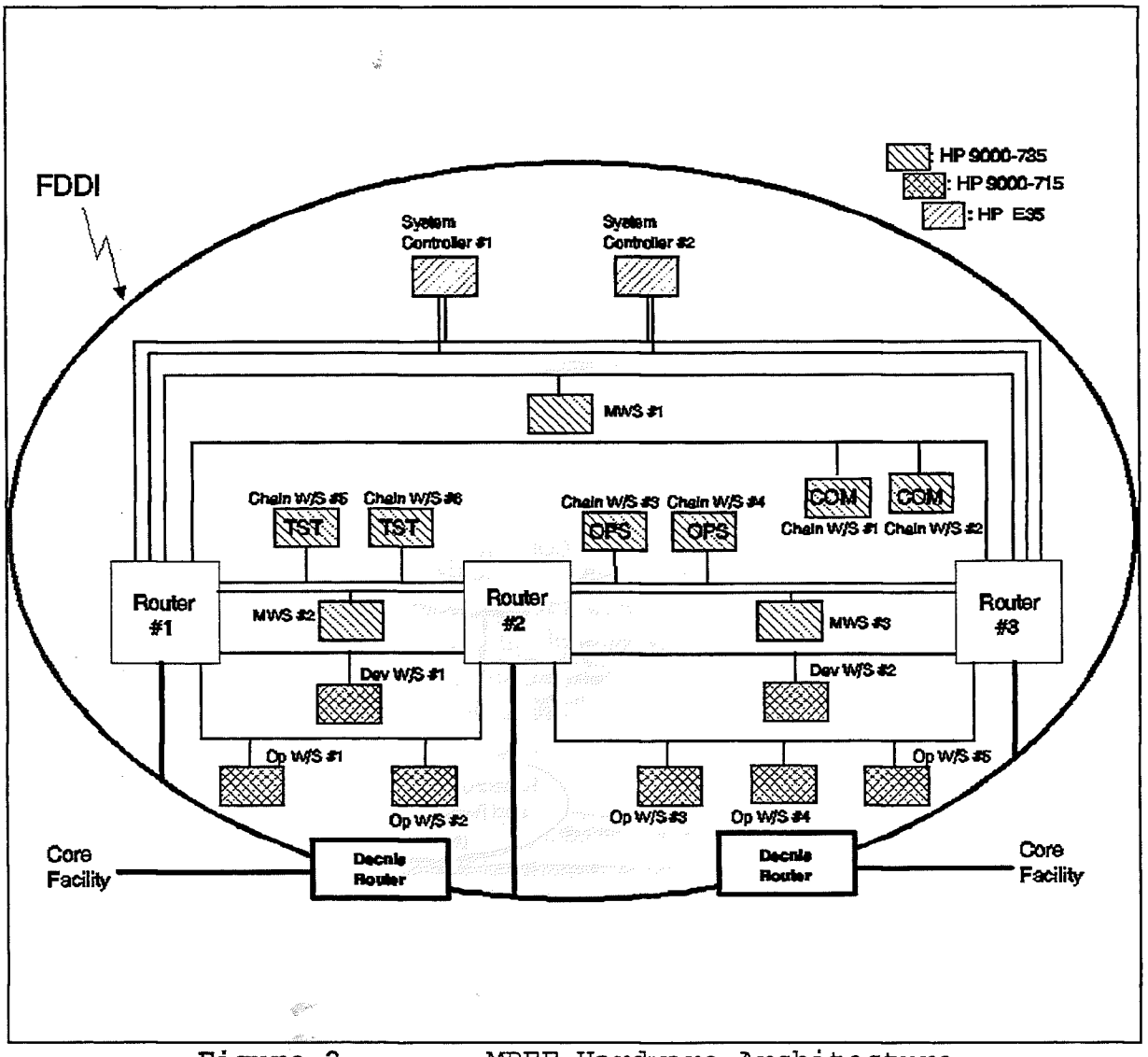

Figure 2 MPEF Hardware Architecture

with a performance margin of 50% for all hardware elements and also with the possibility of re-allocating processes to different workstations. This will provide sufficient flexibility for future developments, improvements and the inclusion of new operational products. The use of off-the-shelf hardware will further improve the availability and will reduce maintenance costs. The MPEF architecture is depicted in Figure 2.

The MPEF workstations and system controllers are inter-connected through a local area network (LAN) based on an FDDI ring with routers providing connections to the hardware elements via Ethernet spurs. The interface to the Core Facility is via two redundant routing devices connected to both the MPEF LAN and the CF LAN.

Each processing chain consists of two Hewlett Packard 9000/735 workstations. When acting as hot stand-by the commissioning chain or the test chain will receive the same data and perform the same processing as the operational chain, but will not normally distribute the derived products. In the event of a failure of the operational chain no manual intervention will be necessary to bring the stand-by to operational status.

Up to two parallel image data streams may be processed by the chain workstations so that MPEF can support the commissioning of a new satellite without interrupting its operational processing activities.

The system controller consists of two (redundant) Hewlett Packard E35 servers connected to a dual ported, mirrored disk system. The main functions of these servers is to provide support for the monitoring of system performance, the scheduling of processes and the maintenance of a relational database containing a wide variety of system information such as logged parameters, display definitions, user details, etc.

In addition to the two system controllers and six chain workstations there are three other types of workstations in MPEF, namely operator workstations (five Hewlett Packard 9000/715s), development workstations (two Hewlett Packard 9000/715s) and MWS workstations (three Hewlett Packard 9000/735s with enhanced graphics). These provide access to all operational functions although the manual quality control of MPEF products and the visualisation of products and images can only be performed from the MWS workstations which have enhanced graphics capabilities. The prime function of the operator workstation is to facilitate hardware and software monitoring along with other operator functions. The development workstations can be used for the development and testing of new application and system software. The MWS workstations are based on off-the-shelf software and feature a state-of-the-art graphics display and development facility. Three printers are connected to the network to provide hardcopy facilities and a video subsystem provides the capability to record and print graphical information from any of the MWS workstations.

3 General Concept of the MPEF Design

The MTP MPEF is the successor to the current Meteosat Information Extraction Centre (MIEC) for MOP. It features modular software design and incorporates a number of improvements in image data processing and product generation algorithm implementations. In addition the product algorithms are configured at run-time by a set of user-defined

parameters whose values are under operator control. In this way the product generation processes may be tuned to produce optimum results. An example of these parameters are the thresholds used in the automatic quality control of the products.

The whole MTP ground segment is defined as a near real-time processing system in which the MPEF is embedded. The MPEF will receive pre-processed (rectified) satellite image data from the Core Facility normally on a line-by-line basis, it will process these data to derive meteorological products and it will return the products to the Core Facility for distribution. The near real-time derivation and distribution of the MPEF products will minimise the delay for product distribution and will reduce the overall processing load on the system. The system will, for instance, enable products extracted from a half-hourly image slot to be computed for the southern hemisphere when Meteosat is still scanning the northern part of the earth disk.

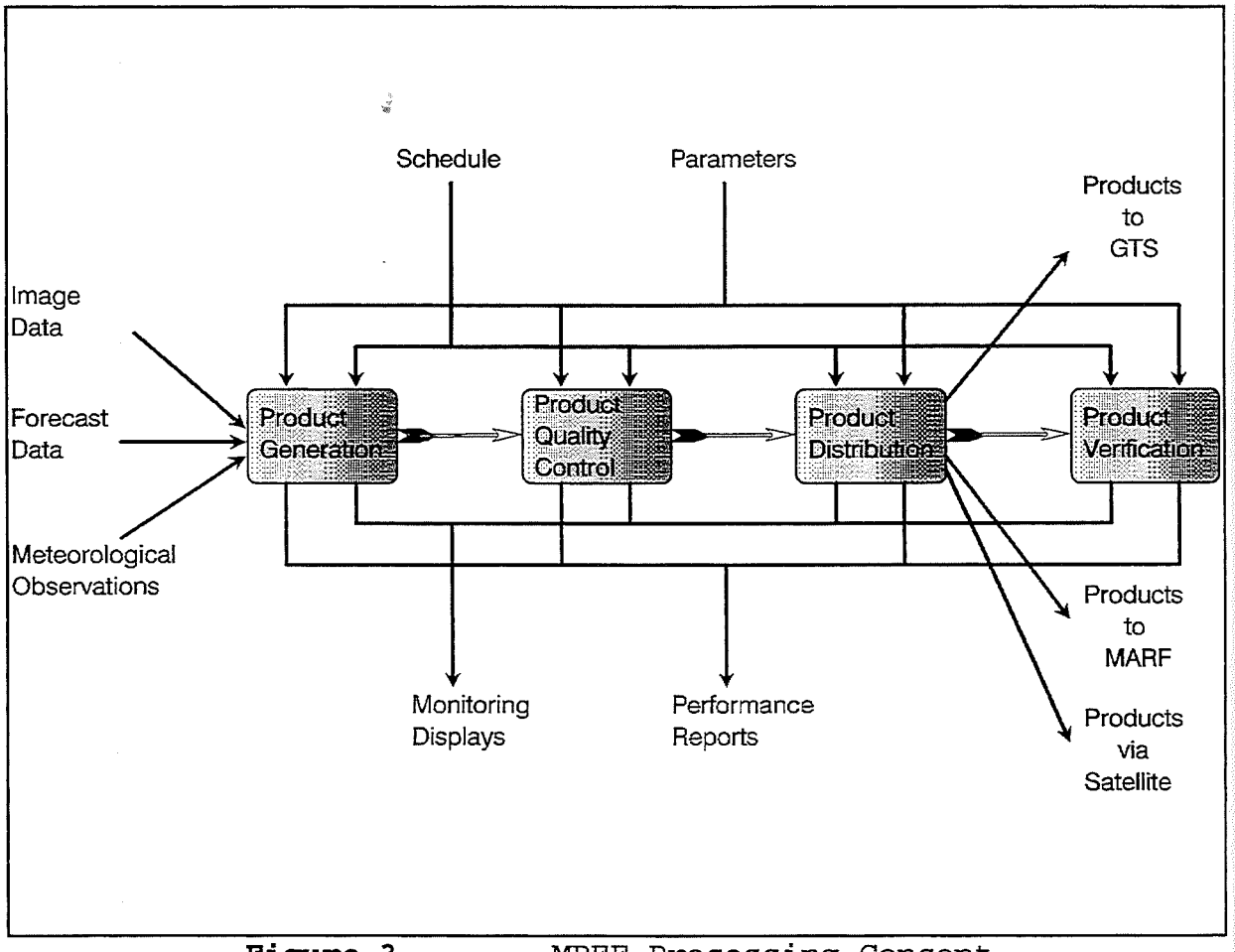

Figure 3 MPEF Processing Concept

A standardised human-computer interface, based on OSF/Motif, has been developed with all operator interaction taking place through a system of user rôles and associated menus. All operational user rôles are accessed from the workstations by invoking a system menu. The following rôles have been defined in order to fulfil the operational requirements : Monitoring & Control (M&C), Scheduling, Analysis & Reporting (A&R), Database Preparation & Administration, Manual Quality Control, Visualisation & Analysis and System & Software Maintenance.

For M&C and for A&R a parameterised approach has been adopted in which system parameters are continuously logged and automatically checked against their expected state. This enables the dynamic monitoring of hardware elements as well as application processes. Parameters may also be combined to derive other parameters to enable, for example, the monitoring of parameter means and percentage completion of activities. Another set of application parameters are logged and used for algorithm related analysis and form the basis for the generation of reports on system performance and product quality.

The Scheduling rôle enables an operator to exert control over the various processes in terms of their initialisation, mode of operation and expected completion. Such is the nature of the product derivation processes and the predictability of the various input data that such a system lends itself well to control by repeating schedules of this type. This approach allows complete flexibility in the derivation, quality control and dissemination of the products.

This overall concept is illustrated in Figure 3.

4 MPEF Product Processing

4.1 General Description

The MPEF algorithms are extensions of the MIEC algorithms incorporating improvements in several areas. For instance, different cross correlation methods for the Cloud Motion Wind (CMW) product derivation (including a Fast Fourier Transform (FFT) based method) will be implemented. It will be possible to select the correlation method independently for each spectral channel. The baseline product extraction and distribution frequency for a number of products has been increased and will, for instance, allow the distribution of the CMW product, derived from all three spectral channels (IR, WV andVIS), every 1 hours.The SST product will be derived for every slot in order to monitor the IR calibration but will be distributed to end-users twice a day. The CTH product will be produced four times a day and the CLA and UTH products every 3 hours. The extraction of the CDS product will be at hourly intervals which should make the product useful for detailed analysis of daily variations of the extracted cloud features. Table 1 summarises the MPEF products to be extracted and the baseline schedule for their extraction frequency. It is important to note, however, that the extraction times can be configured and the performance margin of the system will allow increased extraction frequency if required.

MPEF Product	Extraction Times (UTC)
Cloud Motion Wind (CMW)	0000, 0130, 0300 . . . . 2100, 2230
Sea Surface Temperature (SST)	0000, 1200
Cloud Analysis (CLA)	0000, 0300, 0600 . . . . 1800, 2100
Upper Tropospheric Humidity (UTH)	0000, 0300, 0600 . . . . 1800, 2100
Cloud Top Height (CTH)	0300, 0900, 1500, 2100
Climate Data Set (CDS)	0000, 0100, 0200 . . . . 2200, 2300
Precipitation Index (PI)	Extracted at 0000, 0300, 0600 . . . . 1800, 2100 and accumulated for 5 days
ISCCP Data Set (IDS)	0000, 0300 . . . . 1800, 2100 (for B1 and B2 data sets) AC data set according to coordinated schedule

Table 1: List of MPEF products and their daily extraction times

A combination of automatic and manual quality control processes will ensure the quality of the disseminated products and, with the introduction of BUFR code for the products disseminated over the GTS (instead of the currently used SATOB code), selected quality information may then be distributed along with the product parameters.

The CMW, SST, CLA and UTH products will be distributed to users via the GTS in WMO coded form, the CTH in pictorial form as part of the Meteosat Wefax dissemination schedule and the CDS, PI and IDS products will be sent to the Meteosat Archive and Retrieval Facility (MARF) from where they will be disseminated to users.

4.2 CMW Extraction

To illustrate the way in which MPEF derives products the extraction of the CMW product is described in some detail below. Much of the following can be found in [1] along with a detailed description of the algorithms used in the CMW extraction process.

4.2.1 Overview

The Cloud Motion Wind (CMW) product is computed by identifying and localizing the same cloud pattern ("tracer") in consecutive METEOSAT images. Using the knowledge of the tracer displacement, combined with the measurement of its temperature, the following values are extracted which constitute the CMW product : wind location, wind speed, wind direction, temperature and pressure level. The overall internal structure of the CMWprocess is shown in Figure 4.

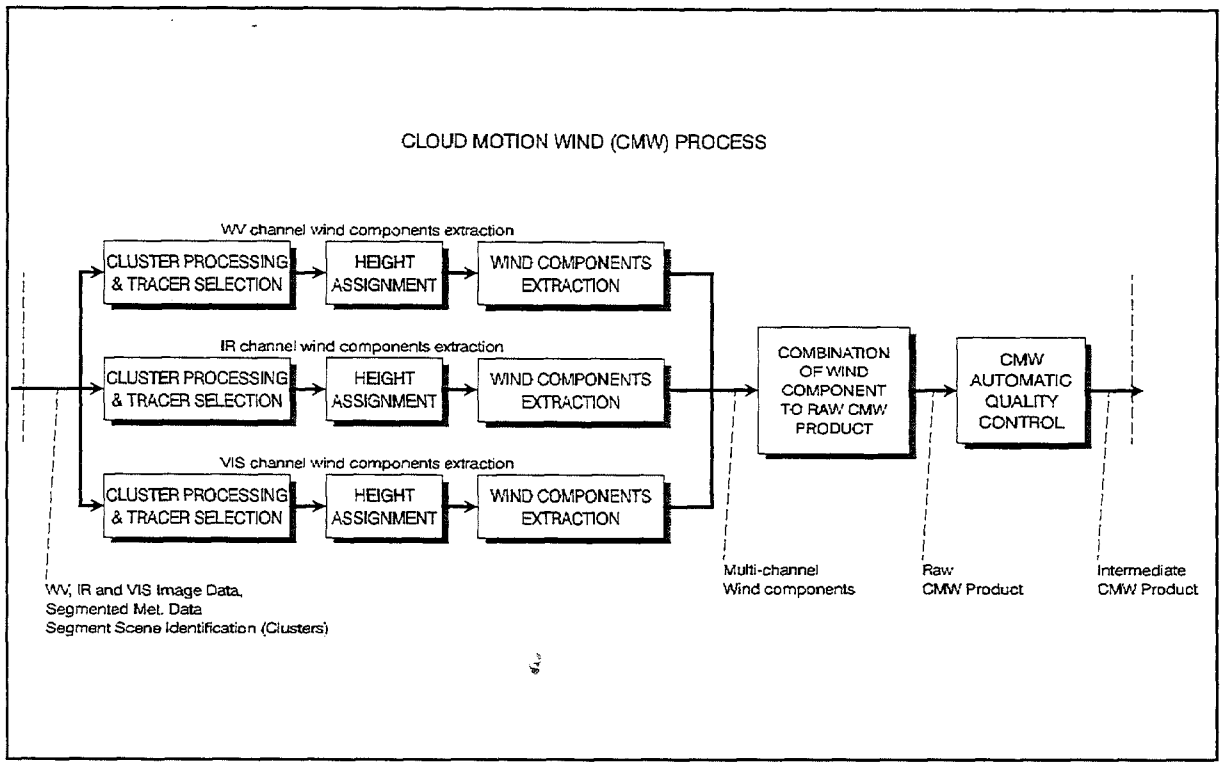

Figure 4 The structure of the CMW extraction process

The first operation performed is the selection of the clusters that will be used as the tracers, based on the information provided by the Segment Processing. This tracer selection is done in a channel-specific way, including cluster merging or rejection when necessary. When a useful tracer has been identified, height assignment is performed and the corresponding wind component can be extracted. The wind-component extraction process comprises the definition of the Target and Search areas taken from the current and previous image, their enhancement, followed by their cross-correlation. This is done for all three spectral channels in a parallel manner. This parallel operation is an important feature of product extraction since it enables the possibility of relocating these high-load processes onto different workstations, therefore providing further potential for growth. The extracted wind components are thereafter combined to generate the raw CMW product. Finally, this raw product is analysed by the Automatic Quality Control decision network and the results are issued as a refined product to the (optional) MQC process.

4.2.2 Near real-time operation

Near real-time operation has been selected as the baseline for the definition of the MPEF processing, and is specially applied to the CMW product extraction, as it allows the spreading of the most computationally intensive process of the whole MPEF (more than 85 %of the total MPEF load) over the duration of the image slot being processed. For this reason, the CMW extraction processing is based on a real-time "pipelined" processing scheme : the rectified images are received line-by-line (South to North) in real-time from the Core Facility, they are packed into the MPEF segment structure (32 lines by 32 pixels) and made available to the CMW process a row of segments at a time.

4.2.3 The Quality Control concept

The Automatic Quality Control of the CMW product is an integral part of the product generation. The general concept for all products is that each of the component processes that participate in the product extraction also generate one or more so-called quality marks which are a measure of the 'confidence' in the derived results. An example for the CMW product are the quality marks generated by the tracer selection process which are based on the measurement of the entropy and the size of the tracer in the target area. All the quality marks so generated are gathered by the AQC process and combined into a global processing mark for each individual result. The AQC process then performs a battery of consistency checks on the product (temporal, spatial, forecast) with each of these checks also generating a specific mark. Finally the AQC process combines all quality indicators for each result (using configurable weights) and compares this combined quality mark against a configurable quality threshold resulting in acceptance or rejection of each result. All parts of the product, including those which were rejected by the AQC, may then be made available for an MQC process. This provides a final opportunity for an operator, using tools provided on the MWS workstations, to reject suspect results and possibly reinstate results previously rejected by AQC.

This concept is illustrated in Figure 5.

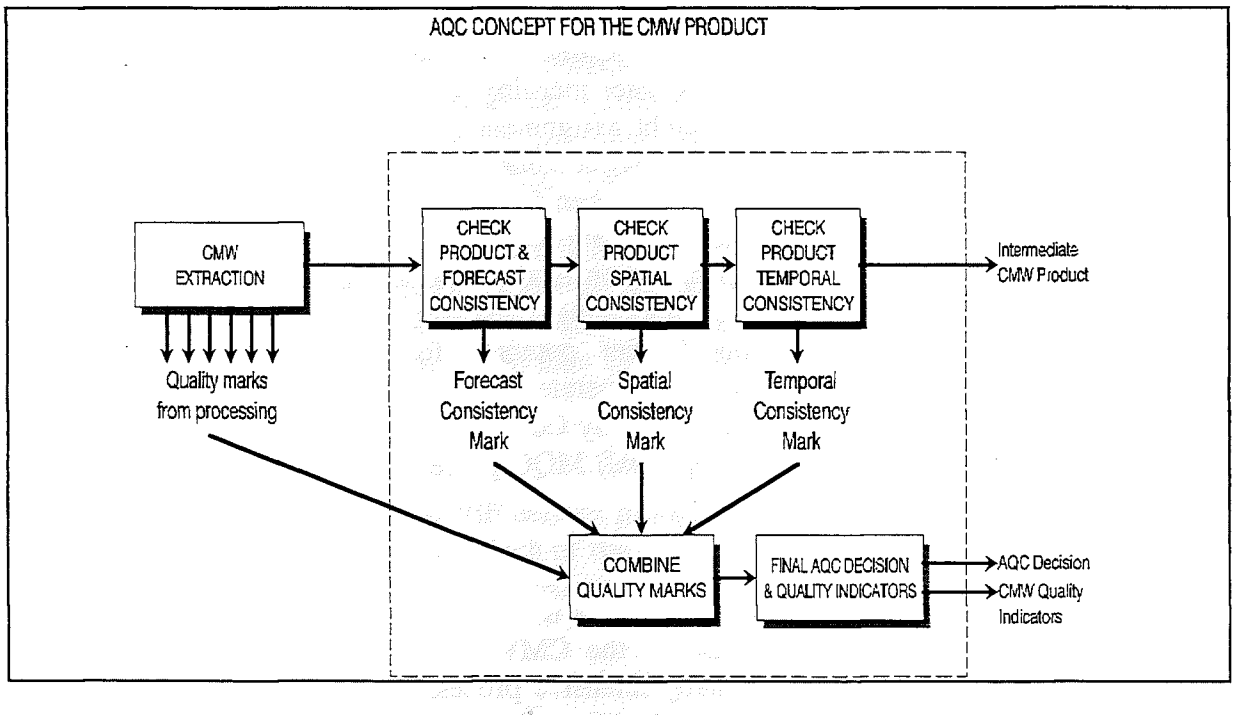

Figure 5 AQC Concept for the CMW Product

5 Conclusion

The MTP MPEF as the successor of the MOP MIEC features increased modularity and a number of new or improved processing and algorithms implementations.

The near real-time processing in the whole MTP ground segment will minimise the delay for product distribution. The MPEF architecture with three processing chains, including one hot-standby, and the use of off-the-shelf hardware guarantees high availability of the operational system. The possibility to reallocate application processes and a performance margin of at least 50% of all hardware elements will leave sufficient flexibility for future developments, improvements and the possible addition of new operational products.

The modular design of the algorithms software will reduce maintenance effort and allow future improvements in this area. The separate development environment and the test chain will provide the necessary facilities for research and development activities.

BIBLIOGRAPHY

[1] Y. BUHLER & K. HOLMLUND, "The CMW Extraction Algorithm for MTP/MPEF", 2nd International Wind Workshop, Tokyo, Dec. 1993, pp 205 - 217

AN OVERVIEW OF THE GROUND MICROPROCESSING SYSTEM FOR GOMS DATA RECEIVING, PROCESSING AND ARCHIVING

1. THE SYSTEM MAIN FEATURES

The Ground Microprocessing System for GOMS data receiving processing and archiving is developed and implemented in Research and Production Association PLANETA (RPA PLANETA). The main features of the Ground System are the following:

- providing the raw GOMS data reception and extensive operational multispectral processing (pre-processing);
- imagery video terminal processing;
- satellite imagery mapping and combination for video terminal analysis in weather forecasting;
- data archiving and retrieval facilities.

The digital data real-time interpretation facilities is developing to provide particularry:

- sea surface temperature;
- wind direction and velocity;
- cloud characteristics (cloud top temperature and height, quantity of clouds etc.).

2. THE SYSTEM DESIGN

The principles of the system in general terms are formulated as follows: the UNIX-based *operative technology* provides:

- raw digital high resolution data reception and primary processing;
- automatic scheduling and *reception of full set* of digital data transmitted;
- automatic *real time multispectral pre-processing* of full set of the data ingesting;,
- automatic data framing and packing for data storage according to user requests.

3. THE DATA SET

GOMS high resolution raw data (2.56 Mbps, 1685 MHz)
spectral channels: 0.46 - 0.7 μm (VIS)
10.5 - 12.5 μm (IR)

4. MAIN SYSTEM COMPONENTS

4.1 Hardware

- TNA-57 12 m antenna (Russia);

- CPU Intel 486 DX2-66 (optional);
- Hard Disk storage 2 * 500 Mbytes;
- Hard Disk Array 5 * 1000 Mbytes;
- Video board SVGA, 1 Mb RAM;
- 14'' SVGA monitor 1024*768;
- Xilinx-based data Frame Formatter Board (RPA PLANETA);

- CPU Intel Pentium-90;
- 21'' Ultra VGA monitor 1280*1028;

- HP JetStore 5000i, 4 Gb;
  DDS (4 mm) data cartridges, 90 m;
- LaserJet IV;
- ETHERNET Connection for local area network.

4.2 Software

- SCO UNIX Operating System Release 3.2 Version 4.2
- Data Receiving Software Package (RPA PLANETA)
- Pre-processing Software Package (RPA PLANETA)
- SATellite image GRAphics tool kit (SATGRAF)

5. DATA RECEPTION

The reception of raw data from GOMS is handled by a system consisting of 12 meter TNA-57 antenna. Automated reception scheme is used in order to receive the full set of the data available.

PC Direct Memory Access (DMA) 16-bit channel is used for data input from the receiver or from the bit synchroniser via the data Frame Formatter Board (FFB). The FFB is plugged into standard ISA bus. The incoming information is formatted as a UNIX binary data file and is dumped into the PC backing storage.

Total size of single raw data file amounts up to 256 Mb. Up to 48 images are daily received and processed. The original data is stored in PC till next data transmission and is therefore processed in real time. The total time of reception - 14 min, pre-procession time period (depending on processing programm) is not more than 12 min.

6. PRIMARY PROCESSING

Primary processing involves:

- bit and frame synchronization (if necessary);
- incoming data quality primary control and decoding;
- single binary noise data filtering;
- the imagery data geometrical correction;
- earth scan data radiometrical correction and calibration;
- data sampling and archiving;
- imagery navigation and mapping;
- the WEFAX production: sampling, brightness conversion, superimposing grid and coastal line, adding annotation

Primary processing (pre-processing) operative technology is designed as an automatic background UNIX process. The Figures 1-3 are given as an example of GOMS IR image hard copy.

7. THE DATA ARCHIVE

An operational archive and retrieval facility for digital data from GOMS N1 is designed to store data, to allow users to search through these data and to provide users with copies of data requested. This document provides the information on the format and media in which the data files are distributed on the meantime. With advancing in technology since the beginning of GOMS N1 operations, the utilisation and application of standarts recomended CGMS and a layered approach of data handling will be implemented.
At present Digital Universal Format (DUF) is used for the GOMS data distribution Transportaion madia presently available are: photographic papers, LaserPrinted hard copies, 4 mm data cartriges Digital Data Starage and local network (ETHERNET) service. The DUF description is given in CGMS-XXIII RUS-WP-12.

8. SATELLITE GRAPHICS SYSTEM (SATGRAF)

The SATGRAF tool kit is designed for satellite imagery visualization as well as videoterminal analisys. The general facilities of the SATGRAF system are shown in fig.4, some of those are:

- sampling, zooming
- contrast operations (both fixed and image related)
- color operations (false colouring, resetting palette)
- filter procedures
- superimposing grid and coastal line (fixed or contrast)
- geometrical resampling
- simple graphical operations (editing, drawing, writing text)
- updating and printing images

GOMS N1 Infra Red Image Mar 15, 1995 09:06:16

RPA Planeta, Dep. 1.4.2

Figure 1

GOMS N1 Infra Red Image Mar 28, 1995 09:33

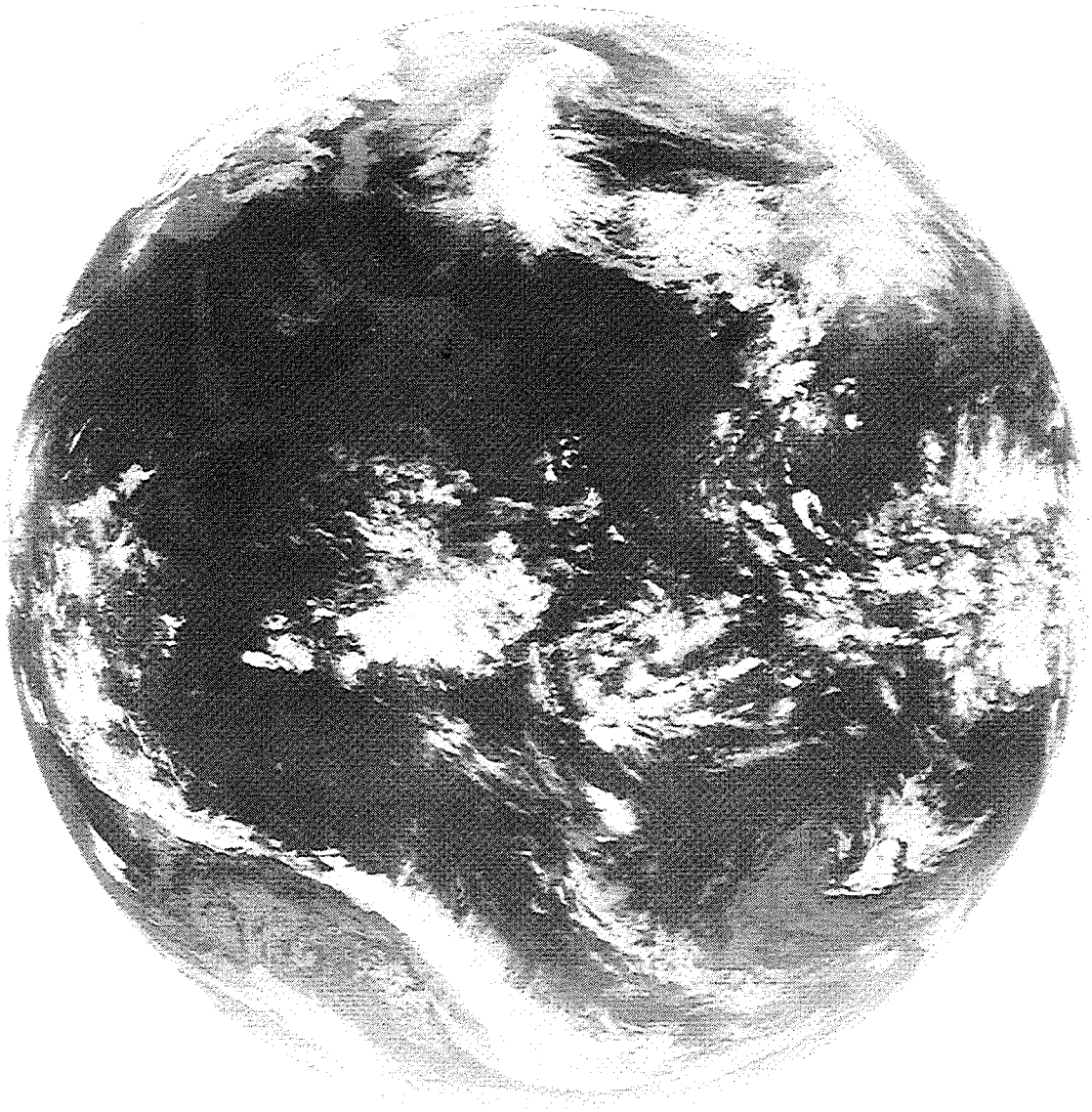

RPA Planeta, Dep. 1.4.2

Figure 2

GOMS N1 Infra Red Image May 12, 1995 10:04:35

RPA Planeta, Dep. 1.4.2

Figure 3

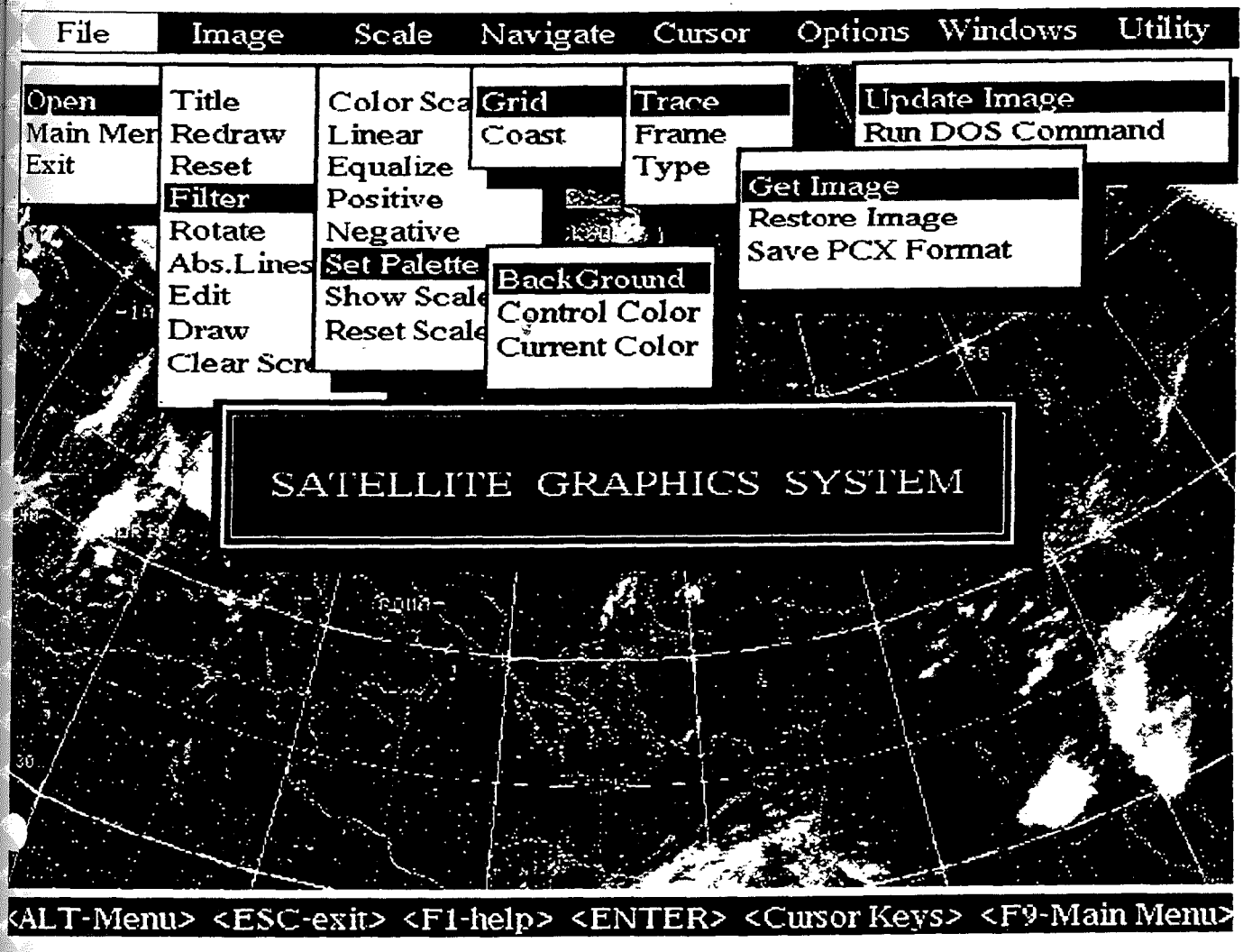

Figure 4. The Satellite Graphics System.

EARLY EXAMPLES OF GOES-8 DATA AND PRODUCTS

W. Paul Menzel

Advanced Satellite Products Project
National Environmental Satellite Data and Information Service
NOAA, Madison, Wisconsin

James F. W. Purdom

Regional and Mesoscale Meteorology Branch
National Environmental Satellite Data and Information Service
NOAA, Ft. Collins, Colorado

ABSTRACT

In April 1994, the first of NOAA's next generation of geostationary satellites, GOES-I now referred to as GOES-8, was successfully launched. The introduction of this major component of NOAA's modernization represents a significant advance in geostationary remote sensing that has been under development for the last decade. All components of the GOES-8 system are new or greatly improved: (1) the satellite is earth oriented to improve instrument performance; (2) sounding and imaging operations are now performed by different and separate instruments; (3) a five band multispectral radiometer with higher spatial resolution improves imaging capabilities; (4) a sounder with higher radiometric sensitivity enables operational temperature and moisture profile retrieval from geostationary altitude for the first time; (5) a different data format is used to retransmit raw data to direct receive users; and, (6) a new ground data processing system handles the high data volume and distributes advanced products to a variety of users. This paper presents early examples of GOES-8 imager and sounder radiometric performance and derived products and makes comparisons with GOES-7 and Meteosat-5.

1 INTRODUCTION

On 13 April 1994, the first of NOAA's next generation of geostationary satellites, GOES-8, was launched. After four weeks of orbit maneuvers to achieve geostationary orbit, the first GOES-8 visible image was taken on 9 May 1994. After the radiation coolers were opened, the first infrared images were taken on 31 May 1994. Shortly thereafter the first soundings were accomplished on 6 June 1994. Figure 1 shows these GOES-8 firsts.

2 THE GOES-8 IMAGER

The GOES-8 imager has a five band multispectral capability with 10 bit precision and high spatial resolution: a) 0.52 - 0.72 μm (visible) at 1 km useful for cloud, pollution, and haze detection and severe storm identification; b) 3.78 - 4.03 μm (shortwave infrared window) at

4 km useful for identification of fog at night, discriminating between water clouds and snow or ice clouds during the daytime, detecting fires and volcanoes, and nighttime determination of sea surface temperature; c) 6.47 - 7.02 μm (upper level water vapor) at 8 km useful for estimating regions of mid-level moisture advection and drying and tracking mid-level atmospheric motions; d) 10.2 - 11.2 μm (longwave infrared window) at 4 km familiar the most users for cloud-drift winds, severe storm identification, and location of heavy rainfall; and, e) 11.5 - 12.5 μm (infrared window more sensitive to water vapor) at 4 km useful for identification of low-level moisture, determination of sea surface temperature, and detection of airborne dust and volcanic ash. On-board calibration provides brightness temperatures with 0.3 K relative precision; inflight determinations of noise levels indicate reduction by 2 to 10 times over those from GOES-7. Table 1 indicates the in flight noise performance of the GOES-8 imager and compares it with the GOES-7 and Meteosat-5 performance.

The improved performance is most notable in the visible band, where 10 bit data from silicon detectors shows much better low light sensitivity and detector to detector consistency. Figure 2 illustrates the improvement in the visible images; in the upper panel Tropical Storm Alberto in the eastern Gulf of Mexico from 2 July 1994 as seen by GOES-8 clearly shows radial outflow features in the western portion of Alberto. Hard "bubbling" convection is also evident, particularly in the northeast quadrant. Unfortunately, the poor detector matching in the GOES-7 (bottom panel) imagery makes resolution of those features very difficult, if at all. Because, GOES-8 oversamples the 1 km visible field of view by a factor of 1.75, the aspect ratio of the GOES-8 image is stretched in the east-west direction.

Band	Bit Depth G-8 / G-7 / M-5	Resolution (km) G-8 / G-7 / M-5	Noise G-8 (spec) / G-7 / M-5
Visible			(counts)
.65 μm	10 / 6 / 8	1 / 1 / 2.5	3 (7) / 1 / 1
Infrared			(deg C at 300 K)
3.9 μm	10 / 10 / X	4 / 16 / ---	0.23 (1.40) / 0.25 / ---
10.7 μm	10 / 10 / 8	4 / 8 / 5	0.14 (0.35) / 0.15 / 0.20
12.0 μm	10 / 10 / X	4 / 16 / ---	0.26 (0.35) / 0.40 / ---
			(deg C at 230 K)
6.7 μm	10 / 10 / 8	8 / 16 / 5	0.22 (1.0) / 1.00 / 0.40

Table 1: GOES-8, GOES-7, and Meteosat-5 Imager Comparisons of Inflight Performance (with GOES-8 specified noise values indicated).

The water vapor band performance of GOES-8 is also improved by an order of magnitude over GOES-7 (twice the spatial resolution and one fifth the noise); this brings GOES-8 in line with the very good noise performance of the Meteosat-5 water vapor band. Figure 3 shows 31 May 1994 water vapor images where GOES-8 data is noticeably sharper and delineates more gradations of moisture in the atmosphere than GOES-7.

It has also become obvious that the high spatial resolution and the good signal to noise of the imager data make it very useful at satellie viewing angles up to 75 degrees. Examples over Hudson Bay and near the Arctic Circle reveal details not seen in the GOES-7 images.

3 THE GOES-8 SOUNDER

The GOES-8 sounder has 18 thermal infrared bands plus a visible band that are sensitive to temperature, moisture, and ozone. The field of view is 8 km and is sampled every 10 km; 13 bit data is transmitted. The full time availability of the GOES-8 sounder enables operational sounding products for the first time; this has the potential for significant contributions to mesoscale forecasting over the conterminous United States, monitoring thermal winds over oceans, and supplementing the Automated Surface Observing System (ASOS) with upper level cloud information. More shortwave bands enhance low-level vertical resolution, an accurate split window provides atmosphere corrected views of the earth surface, and three moisture-sensing bands improve the vertical resolution for moisture sounding. Improved soundings in severe storm and hurricane situations are expected to further understanding and improve forecasts of those weather phenomena. As with the imager, on-board calibration provides brightness temperatures with 0.3 K relative precision. The quality of the absolute calibration is evident in Figure 4 where collocated GOES-8 sounder and NOAA-12 HIRS (High resolution Infrared Radiation Sounder) radiances are compared; the brightness temperatures for the different spectral bands on each instrument are charted as a function of wavenumber. The absorption bands of CO2, O3, H2O, and N2O/CO2 show up as low brightness temperatures. Agreement in surface viewing window bands is within 2°C. Initial calibration of GOES-8 seems to be working well. Table 2 indicates the in flight noise performance of the GOES-8 sounder and compares it with the GOES-7 VAS (Visible Infrared Spin Scan Radiometer Atmospheric Sounder) and NOAA-12 HIRS performance. Noise equivalent temperatures (NEDT) are calculated at 290K. Noise equivalent radiance is indicated by NEDR. Ratios of NEDR adjusted for field of view (FOV) sizes are shown in the last two columns. GOES-8 sounder radiances show noise reduction by factors of 1 to 12 over those from VAS and .6 to 5 over HIRS. In the midwave band, GOES-8 has the best water vapor performance ever. However, in the longwave band, specs are not being met.

Figure 5 shows examples of the long-, mid-, and short-wave sounder data from June 6. CO2 sensitive longwave band 4 (13.7 μm) sees the middle to upper level tropospheric temperature patterns. Smooth transitions showing the cooling further north are evident in clear areas; this is proof of the good signal to noise accomplished in these difficult bands. Water vapor (H20) sensitive midwave band 11 (7.0 μm) sees the middle tropospheric moisture patterns. Dry (warm) pockets are obvious in Colorado/New Mexico, Texas, Louisiana/Mississippi, and Michigan. Carbon dioxide (CO2) sensitive shortwave band 14 (4.5 μm) sees the middle to lower level tropospheric temperatures; comparison with band 4 indicates the warming in the lower atmosphere.

Wavelength (μm)	Ch.	NEDT (290K)	NEDR (mW/m2/ster/cm-1)			G8/G7	G8/N12
			G-8 (spec)	G-7	HIRS	(FOV adjusted)	
Longwave							
14.7	1	1.02	1.63 (0.66)	5.1*	0.67	1/6	1 / 1
14.4	2	0.87	1.41 (0.58)	2.1*	0.50	1/3	1.5/1
14.1	3	0.60	0.94 (0.54)	2.5	0.31	1/2.5	1.5/1
13.9	4	0.40	0.65 (0.45)	1.7	0.21	1/2.5	1.5/1
13.4	5	0.45	0.74 (0.44)	1.7	0.20	1/2	1.5/1
12.7	6	0.20	0.32 (0.25)	1.3		1/4	
12.0	7	0.13	0.21 (0.16)				
Midwave							
11.0	8	0.10	0.15 (0.16)	0.2	0.10	1/1	1/1.5
9.7	9	0.14	0.20 (0.33)		0.15		1/1.5
7.4	10	0.11	0.091 (0.16)		0.20		1/5
7.0	11	0.13	0.091 (0.12)	1.3	0.19	1/12	1/5
6.5	12	0.21	0.119 (0.15)	0.3		1/2	
Shortwave							
4.57	13	0.13	0.012 (0.013)		0.006		1/1
4.52	14	0.13	0.011 (0.013)	0.03*	0.003	1/5	1.5/1
4.45	15	0.16	0.012 (0.013)	0.04*	0.004	1/6	1.5/1
4.13	16	0.10	.0042 (0.008)				
3.98	17	0.17	.0052 (.0082)	.008*	0.002	1/3	1/1
3.7	18	0.10	.0023 (.0036)		0.001		1/1
FOV size			8km	7km (* 14km)	17km		

Table 2: GOES-8 Sounder Comparison to GOES-7 VAS and NOAA-12 HIRS

4 EARLY RESULTS

NOAA begins operational geostationary sounding for the first time with GOES-8. The first soundings from GOES-8 have been of excellent quality. Several GOES-8 sounder products are planned initially; they include the clear field-of-view (FOV) brightness temperatures, profile retrievals of temperature and moisture, as well as their layer mean values, lifted indices, and thermal wind profiles.

Vertical temperature profiles from sounder radiance measurements are produced at 40 pressure levels from 1000 to 0.1 mb using a physical retrieval algorithm that solves for surface skin temperature, atmospheric temperature, and atmospheric moisture simultaneously. Also, estimates of surface emissivity, cloud top pressure, and cloud amount are obtained as by-products. The retrieval begins with a first guess temperature profile that is obtained from a space/time interpolation of fields provided by NWS forecast models. Hourly surface observations and sea surface temperature from AVHRR help provide surface boundary information. Soundings are produced from a 5x5 array of FOVs whenever 9 or more FOVs are determined to be either clear or contaminated by "low cloud". Figure 6 shows a moisture profile retrieval using sounder data from 7 June 1994 over Stephenville, Texas. Agreement with a nearby radiosonde is quite good. GOES-8 is able to track the radiosonde measured dewpoint temperature changes in height better than the TOVS/HIRS, probably because it has more moisture sensitive channels (one more), better signal to noise, and better spatial resolution.

The total column precipitable water vapor (PW), derived from integrating the retrieved moisture profile, is displayed in Figure 7 as a derived product image. Using the radiance measurements in the longwave split windows, the shortwave window, and the 6.7 mm water vapor bands, the derived product imagery is formed from pixel-by-pixel retrievals of atmospheric temperature and moisture profiles wherever the atmosphere is quasi-clear. The images appear as the derived product with the cloud cover superimposed. Comparison of GOES-7 and -8 derived product images of PW from July 1 reveals the improvement in this nowcasting product. The better delineation of the dry tongue in southern Michigan is readily apparent. Ample moisture sources are evident for thunderstorms in Oklahoma and the Mississippi River valley. The cloud and surrounding region in west central Texas is well defined. Southeastern Texas is moister in GOES-8 than GOES-7. GOES-8 is describing atmospheric moisture features with an order of magnitude more detail.

More information regarding the GOES-8 sounder and examples of data are accessible on the World Wide Web at htpp://cloud.ssec.wisc.edu/sounder/g8.html.

The full time availability of the GOES-8 sounder enables operational hourly sounding products for the first time; this has the potential for significant contributions to mesoscale forecasting over the conterminous United States, monitoring thermal winds over oceans, and supplementing the Automated Surface Observing System (ASOS) with upper level cloud information. More shortwave bands enhance low-level vertical resolution, an accurate split window provides atmosphere corrected views of the earth surface, and three moisture-sensing bands improve the vertical resolution for moisture sounding. Improved soundings in severe storm and hurricane situations are expected to further understanding and improve forecasts of those weather phenomena.

5 CONCLUSIONS

Since all components of the GOES-8 system come from new designs, the spacecraft has undergone an extensive checkout before routine operations began mid-October 1994. As the complicated ground operations of the GOES-8 are being mastered, the data quality and the inherent information are proving that the NOAA geostationary observing capability has been greatly enhanced.

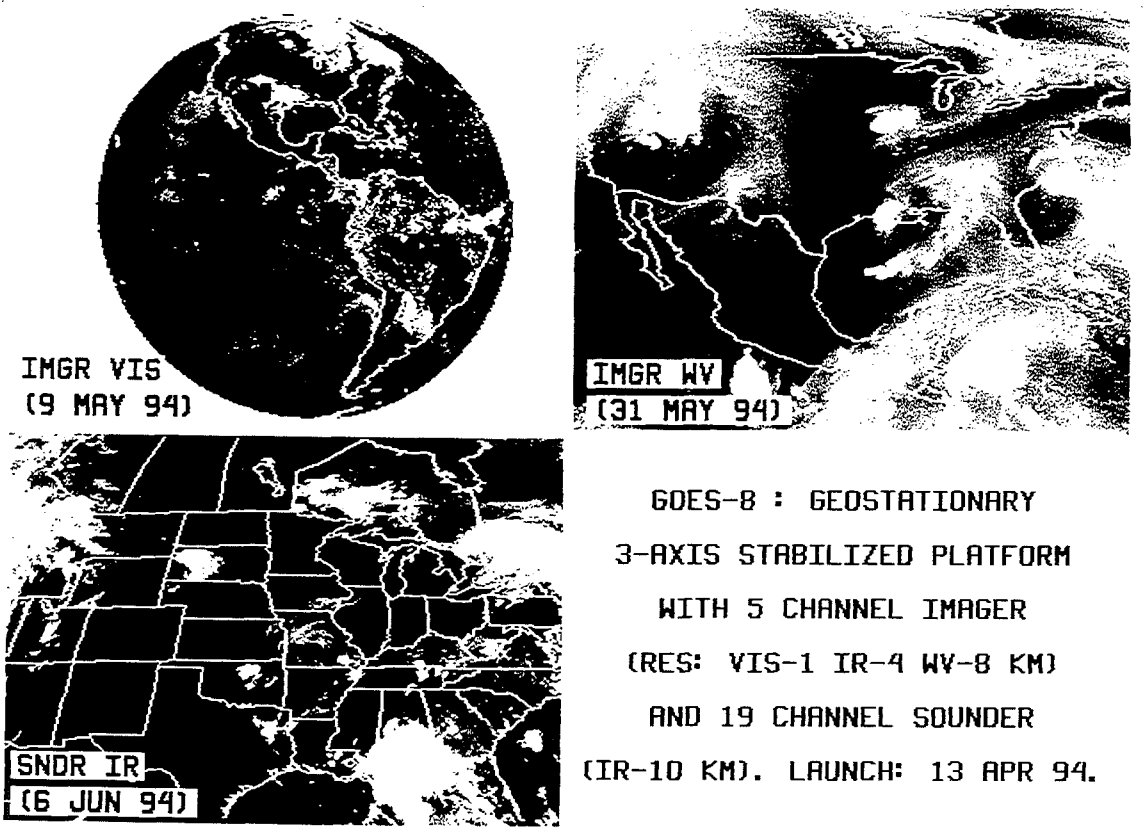

Figure 1. First GOES-8 data and products. Upper left is the first visible full disk image (May 9) from the imager. Upper right is the first water vapor image (May 31) from the imager. Lower left is the first sounder infrared window image (June 6).

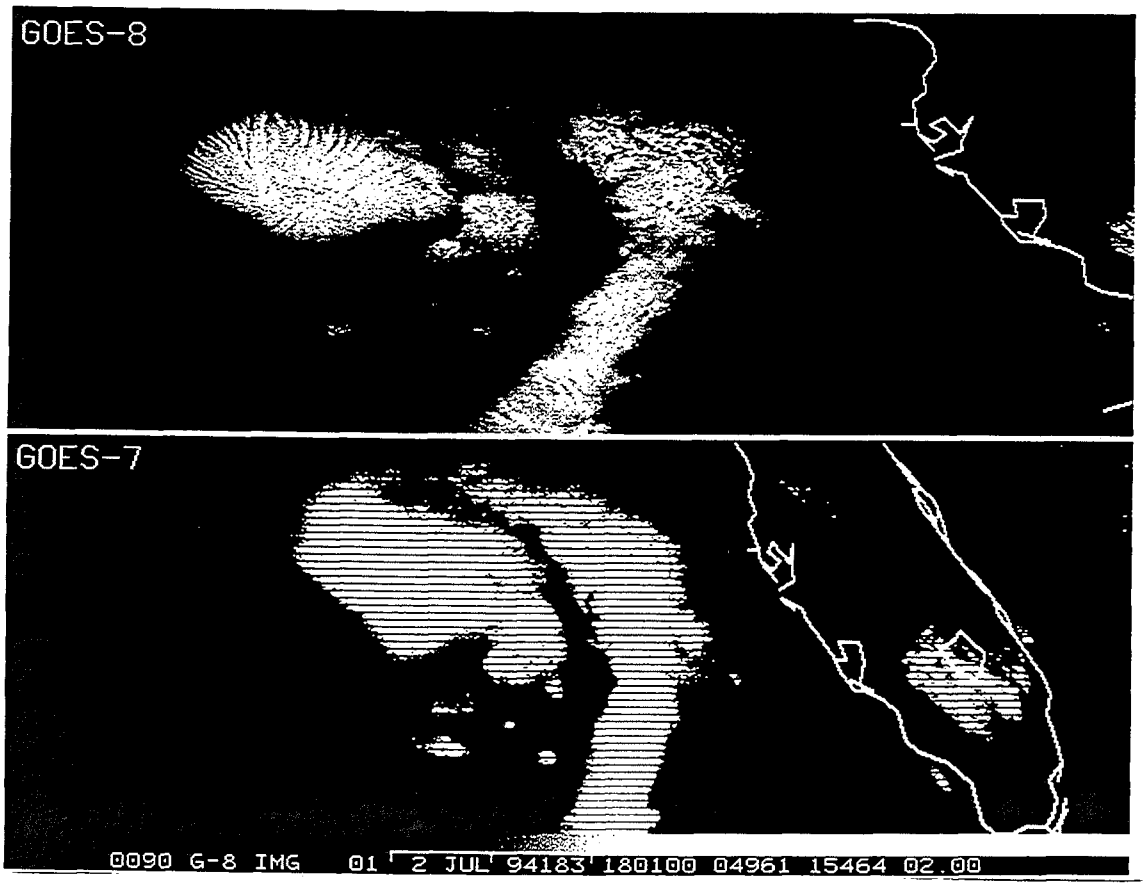

Figure 2. Tropical storm Alberto in the Eastern Gulf of Mexico from 2 July as seen by GOES-8 (upper) and GOES-7 (lower).

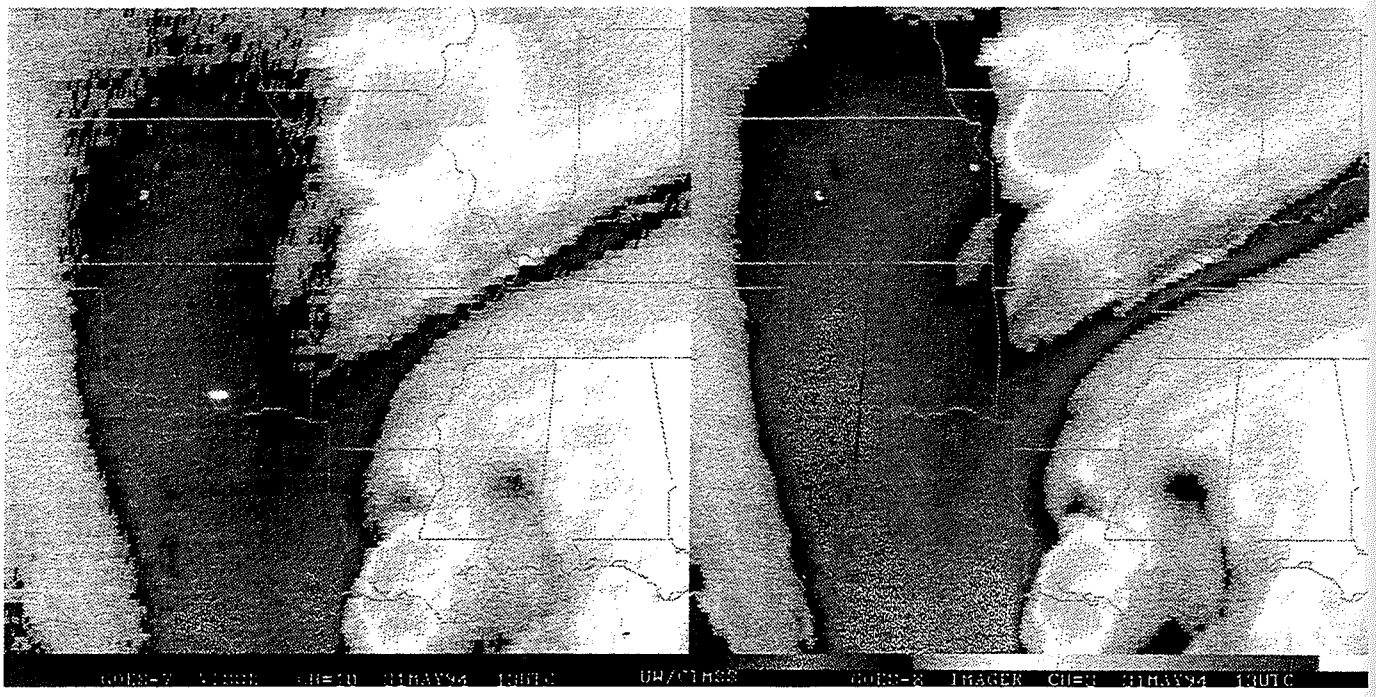

Figure 3. Comparison of GOES-7 and GOES-8 water vapor bands from May 31. Better resolution (8km versus 16km) and reduced noise (.2 versus 1.0°C) in GOES-8 (right) versus GOES-7 (left) water vapor band are apparent.

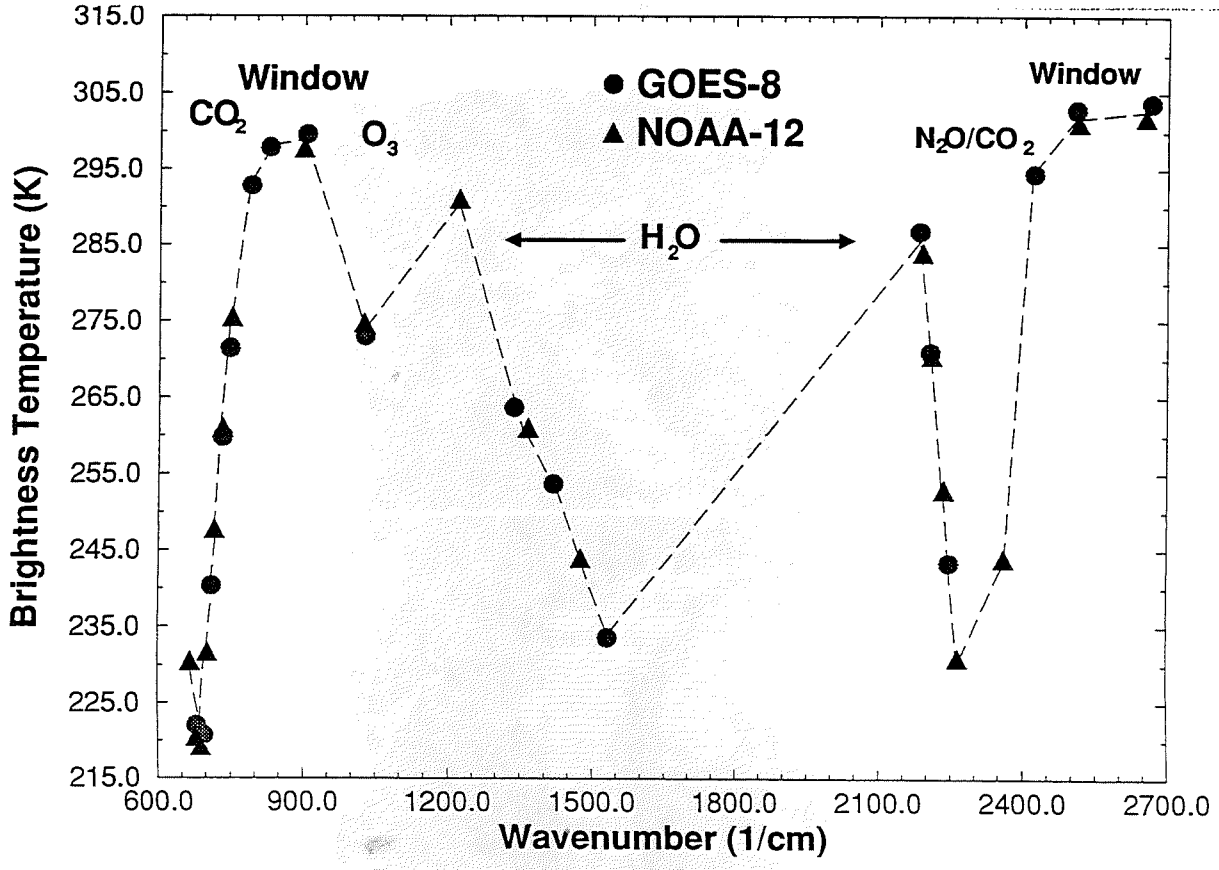

Figure 4. Comparison over Stephenville, Texas of GOES- and POES sounder calibration from June 7. Brightness temperatures for the different sounding bands on GOES-8 and NOAA-12 are plotted as a function of wavenumber.

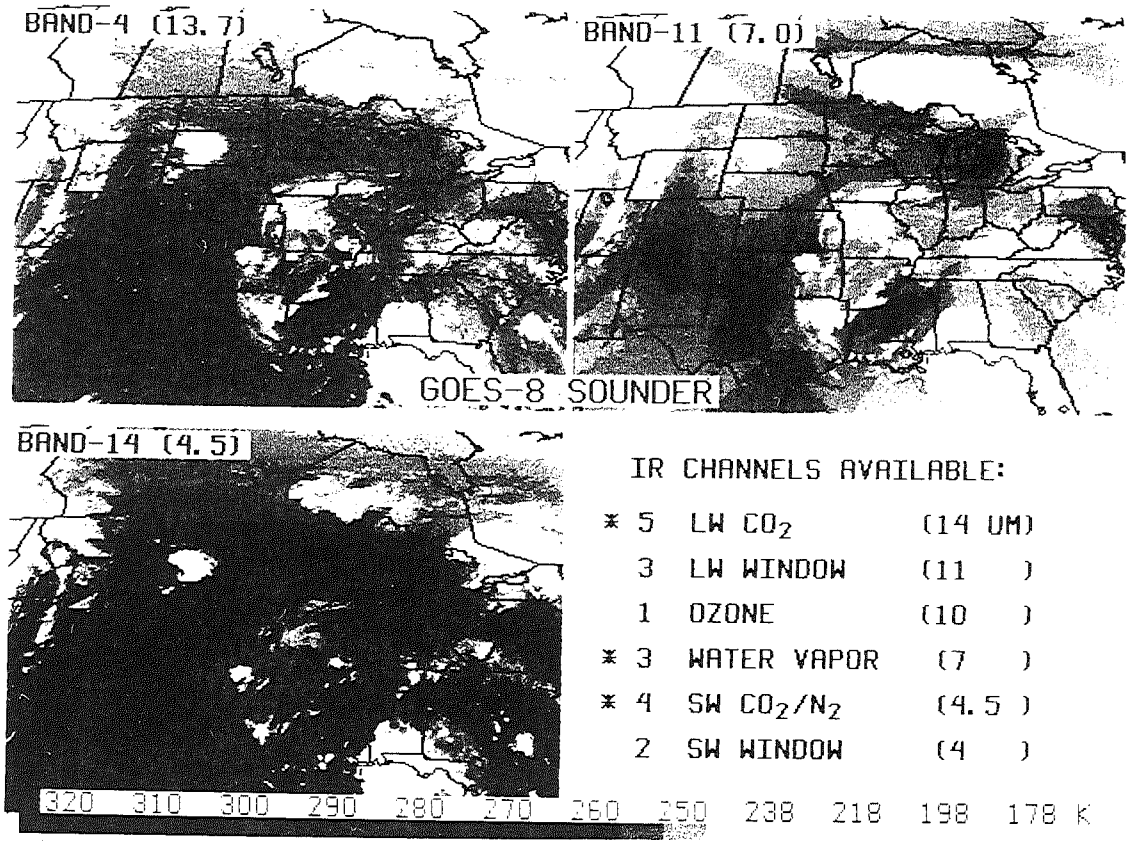

Figure 5. Long-, mid-, and short-wave sounder data from June 6.

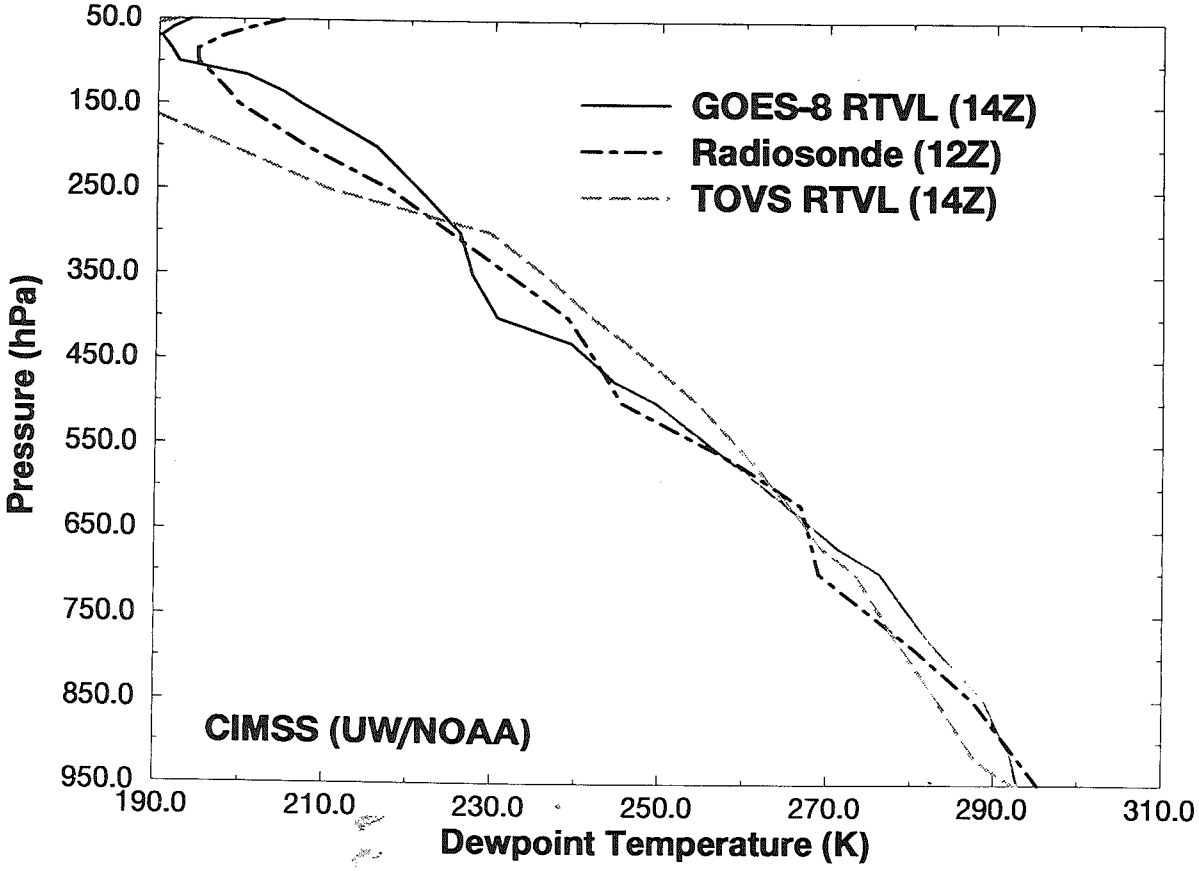

Figure 6. A moisture profile retrieval using the GOES-8 sounder data over Stephenville, Texas from 7 June 1994; a nearby radiosonde report as well as the TOVS/HIRS profile retrieval are shown for comparaison.

Figure 7. Comparison of GOES-7 and -8 derived product images of Total Precipitable Water Vapor (PW) from July 1. Improvement in this nowcasting product is evident. Note better delineation of the dry tongue in southern MI. Ample moisture sources are evident for thunderstorms in OK and the Mississippi River valley. The cloud and surrounding region in west central TX is well defined. Southeastern TX is moister in G-8 than G-7. GOES-8 is describing atmospheric moisture features with an order of magnitude more detail.

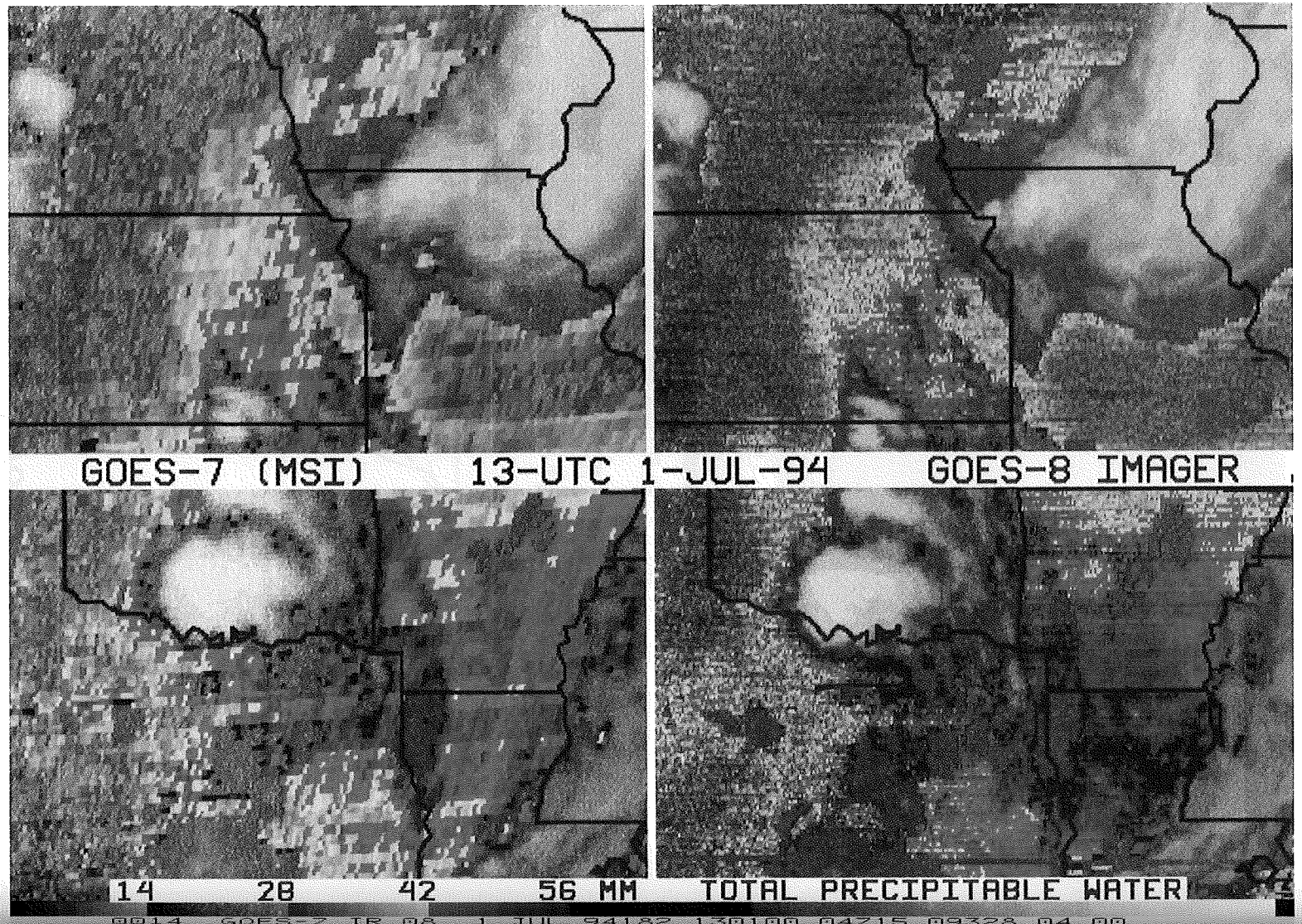

DERIVED PRODUCT IMAGERY FROM GOES-8

Christopher M. Hayden[1], Gary S. Wade[1] and Timothy J. Schmit[2]

ABSTRACT

Derived product imagery (DPI) is a method of presenting quantitative meteorological information, derived from satellite measurements, as a color coded image at full spatial resolution. Its intended use is as animated sequences to observe trends in the displayed quantities, which for the GOES-8 are total precipitable water, lifted index, and surface skin temperature. These products will be produced operationally, once per hour, over the continental Unites States and the Gulf of Mexico. This paper reviews the development of the DPI and details the algorithm used for GOES-8. The quality of the products is discussed and an example is given. The greatest value of the DPI probably lies in comparing a sequence of the satellite product with a sequence derived from a numerical forecast. In this way, deviation of the forecast from reality is readily exposed.

1 INTRODUCTION

The new series of Geostationary Operational Environmental Satellites (GOES) beginning with GOES-8, launched in April 1994, have been designed with separate imaging and sounding instruments to support the requirements of the modernized National Weather Service (NWS) in the 1990s. The imager is a 5 band instrument measuring at the wavelengths specified in Table 1. Its primary function is to provide the visible (band 1), longwave infrared window (band 4), and water vapor (band 3) imagery which has become a fundamental tool of the operational forecaster. Additional windows (bands 2 and 5) have been added for cloud/fog detection at night and surface temperature determinations. The sounder is a 19 band extension of the 12 band VISSR Atmospheric Sounder (VAS) which has been carried on the GOES since September 1980. Its primary function is to provide temperature and moisture profiles of the atmosphere with high spatial and temporal resolution. More complete details can be found in Menzel and Purdom (1994).

As follow-on to the VAS, the day-1 products for GOES-8 are essentially a continuation of the VAS products. Among these are derived product images (DPI) which are image presentations of meteorological products, presented at the full resolution of the imager or sounder. This report reviews the development of the derived product image and presents an example of the day-1 products developed for GOES-8.

1: NOAA/NESDIS System Design and Applications Branch
Madison, Wisconsin

2: Cooperative Institute for Meteorological Satellite Studies
University of Wisconsin, Madison, Wisconsin

Band	Wavelength (μm)	IGFOV (km)	Nominal Noise (NEDR)
1	0.52-0.72	1.0x1.0	10bit; 8 counts=3σ
2	3.78-4.03	4.0x4.0	.006
3	6.47-7.02	8.0x8.0	.04
4	10.2-11.2	4.0x4.0	.20
5	11.5-12.5	4.0x4.0	.35

Table 1: GOES-8 imager characteristics. IGFOV: Instantaneous Geometric Field Of View. NEDR: Noise Equivalent Delta Radiance, bandwidth cm-1.

2 BACKGROUND

Products from the VAS underwent a lengthy development and evaluation before operational implementation at the VAS Data Utilization Center (VDUC) at the Word Weather Building in Washington in 1987. The "derived product image" evolved during this development and evaluation period. The concept was initiated at NASA, where Petersen et al. (1984) introduced images of atmospheric moisture derived from the VAS. The concept was further developed at the Cooperative Institute for Meteorological Satellite Studies (CIMSS) and incorporated into quasi -operational products offered for evaluation to the National Severe Storms Forecast Center (NSSFC) (Smith et al., 1985). DPI of total precipitable water and lifted index were provided. The latter was also demonstrated at NASA by Chesters et al. (1986). The VDUC and NASA approaches are similar in concept, the major difference being that the VDUC product incorporates the National Meteorological Center forecast as part of a full physical retrieval. The NASA approach is statistical, using contemporary radiosondes for training.

Derived product imagery is used in time-sequenced loops to animate the changes in atmospheric moisture or stability (and more recently surface skin temperature). It was favorably, though not enthusiastically, received by the NSSFC in their evaluation. Their product application is heavily dependent on frequency and timelinesss, and both proved to be persistent problems in providing the VAS DPI. Normally, VAS sounding data were available only every 90 minutes and had to be collected in two 10 minute pieces (to permit operational VISSR coverage). This contributed to a 30 minute delay from real-time. Also, due to computational limitations of the VDUC, an additional 15 minutes was required for processing. Product quality suffered further from the necessity of operating in venetian blind mode whereby four lines of data are alternately processed or skipped. Only by using this mode could the continental U.S. be covered in the time available. This necessitated a fill-in process for the missing lines which was never satisfactorily accomplished. On the suggestion of NSSFC forecasters, the timeliness was improved by turning from the full dwell sounding to the multispectral imaging (MSI) mode of the VAS. In this mode only three of the VAS channels are utilized; but, the spatial coverage is complete, the data are available half hourly, and data collection is accomplished in 7 minutes. To further improve timeliness, the processing algorithm was changed to preprocess "coefficients" so that DPI image production could be accomplished in only 2 minutes.

Timeliness continues to be a concern with GOES-8 insofar as the sounder requires approximately 40 minutes to scan the continental U.S. Consequently the imager will be used to produce operational DPI in much the same manner as with the VAS MSI. A large benefit with GOES-8, however, is that the measurement spatial resolution is improved by a factor of 2, and the noise greatly reduced, especially for band 5. In the following section the algorithm is presented. Section 3 provides an example of the products, and a summary is presented as Section 4.

3 METHOD

(a) Algorithm

The GOES-8 algorithm for processing DPI is a close analogue to the VAS algorithm for temperature and moisture retrieval detailed in Hayden (1988), hereafter referred to as (I). The method is a linearized, simultaneous solution for perturbations to a first guess temperature profile, moisture profile, and skin temperature estimate. The first guess profiles are provided by a time/space interpolation of NMC forecasts generated with either the Regional Analysis and Forecast System (RAFS) or the Eta models. The first guess skin temperature is a statistical regression estimate using the GOES infrared window measurements. The regression coefficients are fixed, derived with radiance temperatures simulated from a set of 117 radiosonde profiles (carefully selected to represent the full variance of the atmosphere), regressed against the radiosonde surface air temperature, randomly perturbed. The retrieval algorithm is designed to use any or all of the sounding (or imaging) bands available on the GOES-8. Estimates of surface air temperature and mixing ratio are also included as "measurements" to assist in determining the lower atmospheric structure. These "measurements" are interpolated from objective analyses of surface network data using the time-interpolated NMC forecast as a background field. In current practice, the 3.95 μm shortwave window (band 2) is used only for cloud clearing and to determine (in the absence of reflected solar radiation) a first guess skin temperature. Thus the imager DPI is generated from 3 bands and the two surface measurements.

The inversion algorithm described in (I) has been slightly extended to include variable surface emissivity. Thus the deviation of observed radiance temperatures from those calculated from the first guess δT^* is apportioned into three terms related to the surface skin temperature Ts, the temperature profile $\delta T(p)$, and the precipitable water profile $\delta u(p)$ according to:

$$\delta T^* = \delta T_s \left(\frac{(\partial B_s^0 / \partial T_s^0)}{(\partial B_s^0 / \partial T_s^*)} \right) \varepsilon \tau_s^0 - \int_0^{P_s} \delta T(p) \Re(p)^0 \left(\frac{(\partial B^0 / \partial T(p)^0)}{(\partial B^0 / \partial T^*)} \right) d\tau^0 + \int_0^{P_s} \delta u(p) \left(\frac{1}{u(p)^0} \frac{\partial \tau(p)^0}{\partial \ln u(p)^0} \right) \Re(p)^0 \left(\frac{(\partial B^0 / \partial T(p)^0)}{(\partial B^0 / \partial T^*)} \right) dT^0 \qquad (1)$$

$$\Re(p) = 1 \div (1 - \varepsilon)(\frac{\tau_s}{\tau(p)})^2$$

where R represents the correction for surface reflection caused by non-unit emissivity ϵ. Note that the frequency dependence of radiance temperature, Planck radiance B, and transmittance τ in (1) is omitted for simplicity. Superscript 0 is used to denote prior estimate", initially the first guess and thereafter the result of the previous iteration. The perturbations of the three meteorological variables are represented in terms of pressure dependent basis functions φ(p) with one function assigned to the skin temperature, five functions assigned to the moisture profile, and seven functions assigned to the temperature profile:

$$\delta T_s = \alpha_0 \varphi_0$$
$$\delta U(p) = \sum_{i=1}^{5} \alpha_i \int_0^p q(p)\varphi_i(p)dp \qquad (2)$$
$$\delta T(p) = -\sum_{i=6}^{12} \alpha_i \phi_i(p)$$

The retrieval problem is reduced to finding the coefficient vector α which may be applied to (2). The manner in which this is accomplished is given in (I), reducing to expressions of the form:

$$\alpha = \left(\tilde{\Phi}^T \tilde{\Phi} + \gamma I\right)^{-1} \tilde{\Phi}^T \delta\tilde{T}^* = \chi \delta\tilde{T}^* \qquad (3)$$
$$\tilde{\Phi}_{i,k} = \Phi_{i,k}/e_k \quad ; \quad \delta\tilde{T}_k^* = \delta T_k^* e_k$$

where the matrices Φ have dimension 20 x 12 reflecting the maximum number of observations (k, 18 bands plus two surface measurements) and the number of basis functions (i,13). The stabilizing term γI and the confidence vector e are described in (I).

In providing GOES-8 soundings, the process of computing χ, applying it to the measurement vector to find α, and updating the meteorological variables from (2) is iterated through three passes. The result is accepted if all elements of δT* are within twice the value of the corresponding element in e. In providing DPI, however, the solution is not iterated, and so χ depends only on the first guess profiles and can be precomputed as soon as forecast fields are available. χ and ϕ are readily combined in (2) to provide a single set of coefficients to be applied to the radiance temperature vector δT* when the measurements become available.

As mentioned earlier, the DPI consists of skin temperature, total precipitable water, and lifted index. The first two correspond to the first two equations of (2) while the third involves the second and third equation. Note that by solving for only the total column of precipitable water, the pressure dependence of the second equation is removed. It is similarly removed from the third equation by our choice to solve for temperature at only one level, the quadrature level immediately above the surface pressure, to represent the boundary layer. (The complete derivation of the lifted index is defined below.) Thus the solution of each equation in (2) involves only the application of five coefficients to be applied to the five measurements.

In physical schemes for retrieving temperature and moisture profiles it is customary to make a bias correction to the observed brightness temperatures. The procedure is empirical, intended to account for uncertainties in transmittance and radiative transfer calculations. We have found that, quantitatively, the GOES DPI are improved by including a bias correction, and we employ the same technique used with temperature soundings (Hayden, 1994) following the method of Fleming et al. (1991).

(b) Radiance Data

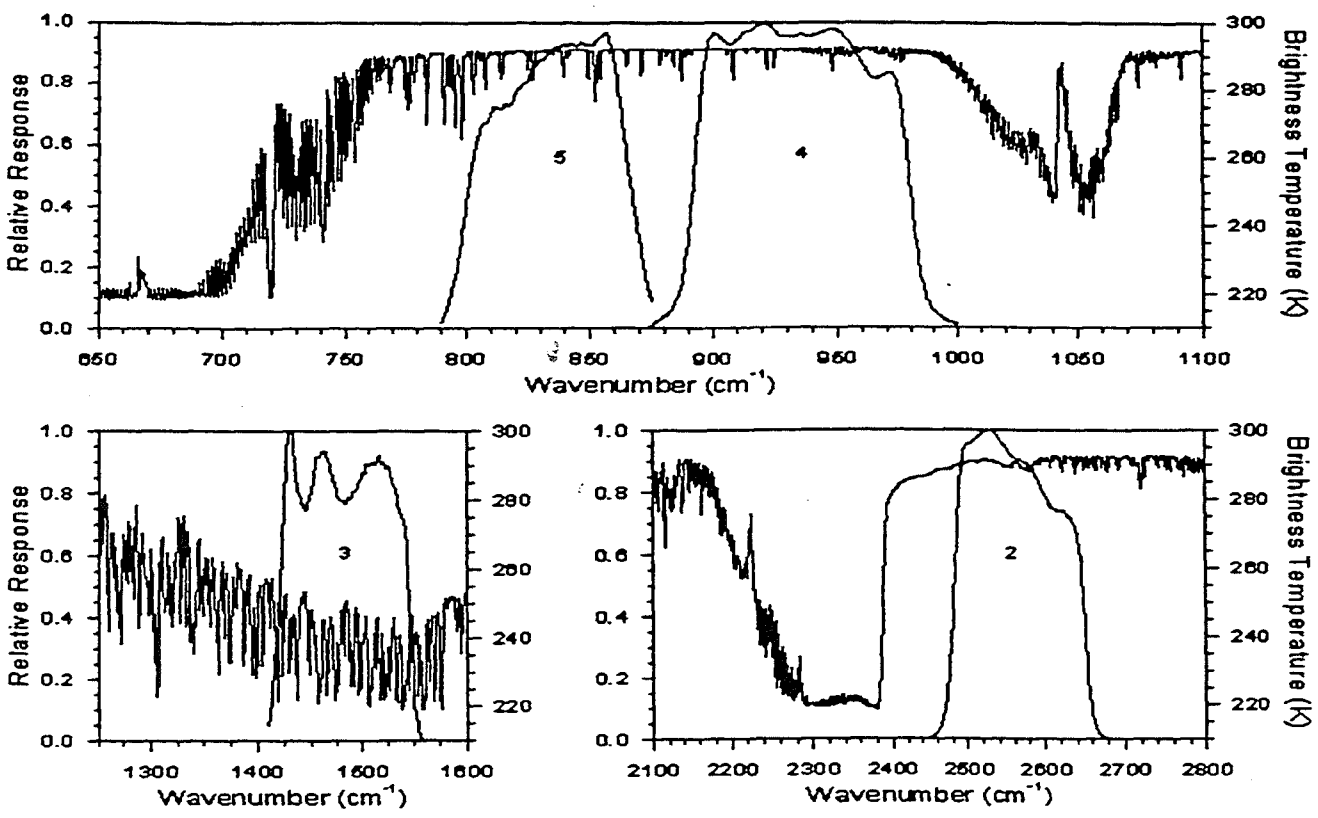

Figure 1. GOES-8 imager filter functions superimposed over high resolution spectrum. Infrared band numbers corresponding to Table 1 are plotted inside filter functions.

Fig. 1 shows the spectral intervals covered by the imager infrared bands described in Table 1. Instrument response functions for each band are plotted over a spectrum calculated at the resolution of the High resolution Interferometer Sounder (HIS) which has been developed at the CIMSS as a prototype for future sounding systems (Smith et al. 1990). The top figure shows bands 4 and 5 in the longwave window region of the spectrum. Water vapor absorption is shown by the dips in the full resolution spectrum. The lower left figure depicts the midwave water vapor band 3, whereas the shortwave window band 2 is displayed on the lower right. As will be discussed in more detail below, the primary signal for the DPI is obtained from the difference between bands 4 and 5. This is used to indicate the low level moisture content in modifying the total precipitable water estimate and also to remove that influence in determining the skin temperature (for a detailed review see Prata, 1993). To improve the fidelity of the split window over that of the VAS, GOES-8 band 5 (sometimes referred to as the dirty window because of greater moisture sensitivity) has been moved spectrally closer to band 4. However, this improvement is at the cost of reduced moisture absorption, and the consequently reduced signal-to-noise becomes a paramount

consideration. As an example, Fig. 2 shows the spatial variation of bands 4 and 5 for the conditions at 15 UT on 14 March 1995, which is used as our demonstration case in this paper. Full resolution radiance temperatures are shown, west to east, along the line AB drawn over the first image of Fig. 3. The pixel to pixel variation shows the surface/atmosphere outgoing radiance. The western edge is over the hot surface of coastal TX. The following cooling represents shelf water which gives way to the warmer offshore water of the Gulf of Mexico. The spacing between the lines represents the variation of the split window or the moisture attenuation. It is apparent that on the large scale, the variation in spacing along the line AB is quite small, although there is clearly more moisture (greater spacing) in the midportion than on either end. The more noticeable feature is the small scale variation in the spacing caused by measurement noise. There are, for example, pixels where the dirty window is warner than the clean window, and while this phenomenon can occur over low cloud or where there is a strong boundary layer temperature inversions, neither is present in this example. It is obviously undesirable to retain this noise in deriving the DPI, and it can be controlled by adjusting in (3) as discussed in the following section.

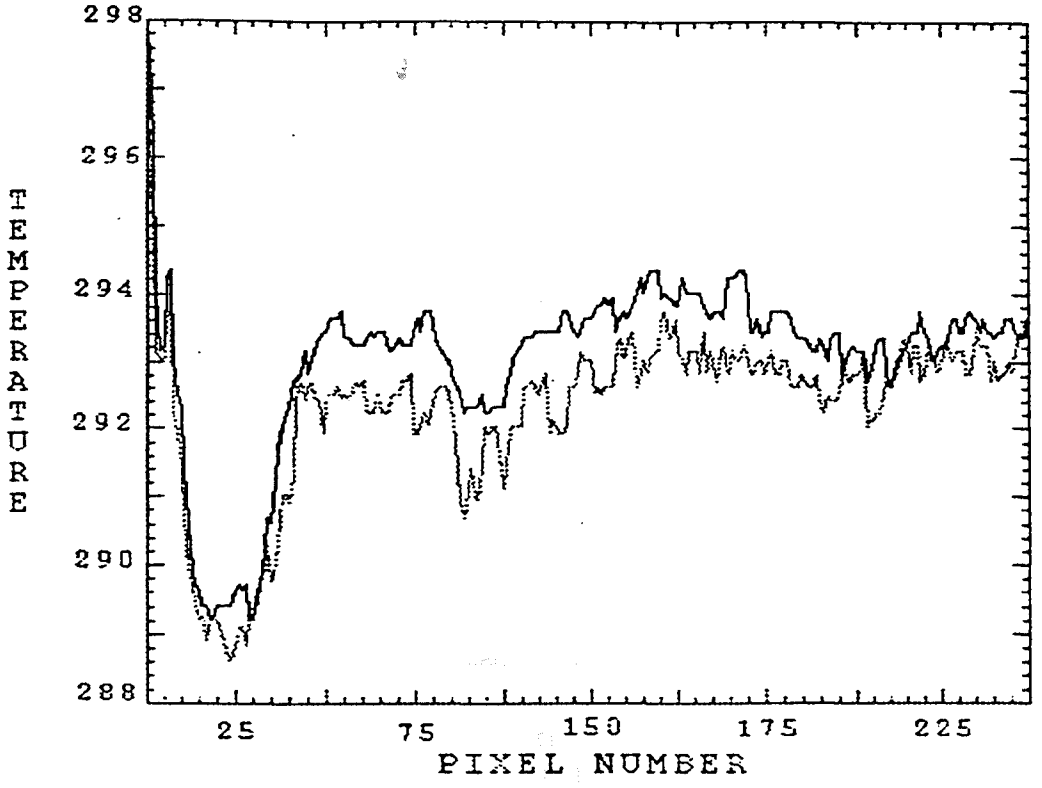

Figure 2. Band 4 (upper) and band 5 (lower) radiance temperature observations along the line shown in Fig. 3.

(c) Coefficient fields

The production of the three imager DPI involves 3 sets of 5 coefficients. These are computed as grid point fields from the RAFS (or Eta) forecasts for valid times 12 and 18 hours after the 00 and 12 UT runs (available approximately 6 hours after the initial time). By using 12 and 18 hour forecasts, instead of more timely 6 and 12 hour forecasts, we are afforded a time cushion for receiving the forecasts and processing the coefficients. The procedure involves the calculation of coefficients from a data set in which the forecasts at

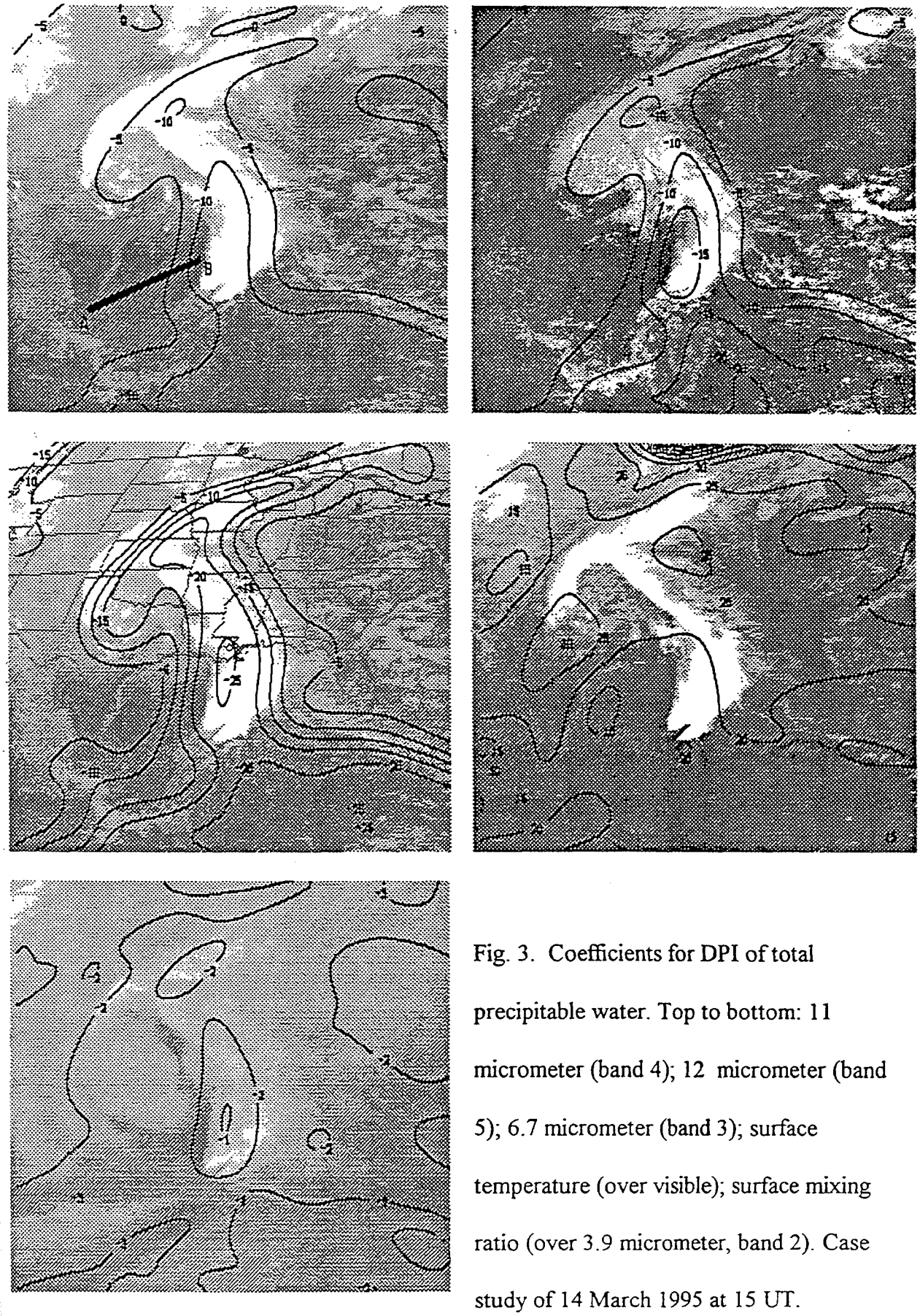

Fig. 3. Coefficients for DPI of total precipitable water. Top to bottom: 11 micrometer (band 4); 12 micrometer (band 5); 6.7 micrometer (band 3); surface temperature (over visible); surface mixing ratio (over 3.9 micrometer, band 2). Case study of 14 March 1995 at 15 UT.

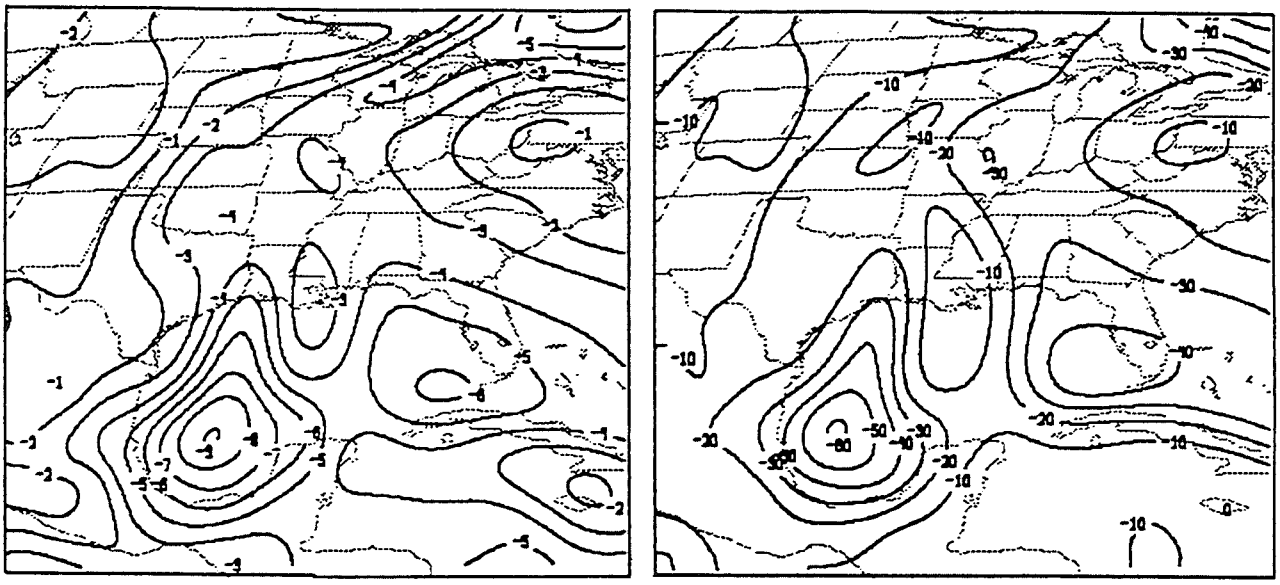

Fig. 4. Band 5 coefficients for estimating boundary layer temperature (for lifted index). Left: loose tolerance (large e). Right: tight tolerance (small e).

In preparing the first guess temperature and moisture profiles for the DPI we use the same interpolation approach as used with the coefficients (Table 2). We initially tried using more timely forecasts (i.e. the 6 hour) but found that this introduced a visible discontinuity in the DPI near 6 and 18 UT. The discontinuity was related to the arrival of a 6 hour forecast (for processing the 7 or 19 UT data) to replace an 18 hour forecast (for processing the 6 or 18 UT data). This feature is a further manifestation of the well known dependence of the retrieval on the first guess.

(d) Cloud clearing

The derived products can be produced only from cloud cleared measurements. The DPI procedure for cloud clearing is very similar to that used in producing retrievals. In both cases the data are treated as contiguous X*X fields of view (fov). For the imager DPI we use 5X5 fov (approximately 20 by 12 km accounting for oversampling) to derive a box averaged clear radiance temperature vector. Using a complex decision tree, each fov is flagged as usable or unusable for deriving the average. The usable fov are further classified as certainly or probably clear. Preference is given to the former in retrieval processing, but for the DPI, where coverage is a major concern, no distinction is made. The usable fov for each band are ordered, and each one falling within 2σ of the warmest is included in the average. Those falling outside this limit are redefined as unusable. The value of σ varies with band, with surface characteristics, and the variance of the local first guess. The algorithm includes the option of requiring coregistration of the band samples, but this feature is not currently invoked.

In making up the images, unusable fov are given a scaled value of the 11 micrometer measurement to provide gray shading denoting cloud. Usable fov are processed to provide estimates of the derived product which are color coded according to magnitude. For boxes which contain usable measurements, the box average radiance temperature vector is corrected for bias and coefficients are interpolated to the centroid of the usable fov to calculate the average value of the DPI parameter. Individual fov are processed as deviations from the box estimate using the same coefficients. Because of the box processing, the DPI

suffer from boxiness , particularly when an entire box is deemed unusable. This unfortunate feature is especially prevelant in the hours before dawn for boxes which contain water bodies large enough to significantly impact individual measurements. The heat retaining, warmer water fools the cloud clearing algorithm because our topography file is insufficiently detailed. The boxiness is mitigated by reducing the size of the box, but at the cost of accurate cloud clearing and processing expense.

(e) Surface data

Surface data over land are extracted from objective analyses of the local hourly surface data. The analyses use a background from the time interpolated NMC forecast. Over oceans (and the Great Lakes) the temperatures are replaced by sea surface temperatures derived and mapped from an AVHRR global composite (if available), and surface dewpoint depressions are fixed at 5K. As currently used, the surface temperature is blended into the lowest 100 hPa of the guess profile, and the guess temperature at the surface is the observation. This means that for the DPI (with no iteration), the surface air temperature observation does not interact in the retrieval because the δT^* is zero. The surface mixing ratio observation is allowed some interaction because the first guess is set to the average of the observation and the forecast. Thus the δT^* is not zero. Values of the surface data are calculated for the four corners of each retrieval box and interpolated to the individual fov. The interpolation is adjusted by topography which is obtained from a 10 minute latitude/longitude topography file.

(f) Lifted Index

The lifted index is formed by lifting a boundary layer parcel to 500 hPa and comparing the resultant temperature of the parcel with the ambient temperature. A negative value denotes that the parcel is warmer than the environment and therefore may be expected to rise (unstable) and vice versa. For the DPI estimate, an incremental temperature for the boundary layer is retrieved using the third equation in (2). This is added to the forecast temperature profile (blended with the surface observation), averaged over the first 100 hPa above the surface. The average mixing ratio for the boundary layer is also derived from the forecast and multiplied by the ratio of the retrieved to forecast total precipitable water. These averaged quantities form the temperature and moisture for the parcel which is lifted (from 50 hPa above the surface) to 500 hPa. The 500 hPa temperature, from which the lifted temperature is subtracted to form the lifted index, is taken directly from the forecast. In practice we find that the boundary layer temperature is changed very little by the retrieval. This is appropriate, because the window bands have little signal to adjust the low level atmospheric temperature. Most of the impact on the lifted index is generated by the change in moisture, derived from the change in total precipitable water.

4 PRODUCTS

An example of the three DPI products for the case shown in Fig. 3 is given in Fig. 5. As explained above, cloud replaces pixels where the products cannot be generated. The figure also shows each of the products derived without using the satellite measurements, but still using the surface observations and topography (note, for example, the low values of total precipitable water over the Appalachian mountains in the eastern U.S.) to modify the forecast. (The horizon in the figure is given by a local zenith angle of 60o and is not the earth s edge.) One is first struck by how similar the satellite and no-satellite images are, but

this is somewhat deceiving. Very close agreement exists over land, because the forecast is generally very accurate over the U.S. Close inspection shows that the agreement is not nearly as good over the Gulf of Mexico. The moisture lobes in the southern part of the no-sat image are removed by the data, and the moisture maximum associated with the cyclone is apparently repositioned beneath the cloud. This change is not easily seen in the separate images of the figure, but note the width of the blue area between the storm and the western Gulf coast. Differences amount to as much as 15 mm. This latter feature is particularly interesting because it defines a phase error in the forecast. There is also an area of low moisture (somewhat noisy, apparently due to SST variations) in the forecast west of Florida which is not preserved in the DPI.

The lifted index DPI also provides information not available in the no-sat representation. For this product the differences over the continent are more pronounced, though still quite modest. Over the far western mountains the stability of the forecast has been increased, in the direction suggested by the radiosondes. The biggest change is again in the cyclone where the precipitable water delineates the phase error. The DPI adds detail to what is essentially a blob from the forecast (though let us point out that this is not the highest resolution forecast available from NMC!). Interestingly, the synoptic scale phase error is not nearly as easily seen in the lifted index as in the precipitable water DPI.

The surface skin temperature DPI is the parameter most influenced by the satellite radiances. Excellent horizontal detail is apparent in the imagery, corresponding to, but not duplicating, the detail of the infrared window image. It is particularly exciting to see how well variations in the sea surface temperature are captured, and there is good integrity in these from hour to hour (as often as the DPI are currently produced). We have composited the DPI over a day and find that it is possible to produce an SST image which is mostly cloud free. Over the land, the diurnal temperature cycle is readily captured (in clear air), and we have even seen a diurnal cycle in the surface temperature of Lake Erie.

5 SUMMARY

This report has defined the process for the production of derived product imagery from the GOES satellites. The product has been refined over more than 10 years, seeking to overcome many difficulties. Principal among these is the recognition of cloud. This can be surprisingly difficult over the land even during the day when visible measurements are available. An obvious future refinement will include a composited albedo to assist in the cloud definition, but the current method works quite well, even where there is snow cover. Another significant problem is measurement noise. This is more critical for the DPI than for normal retrievals, since the single pixel representation limits the application of spatial averaging to reduce noise (though the initial box processing includes this aspect). Experience has shown that the most important consideration in producing DPI is the horizontal averaging. The smaller the box, the more cosmetic the image, but at the same time the greater the probability of cloud contamination. We have found that the box size of 5X5 seems optimal for the GOES-8 imager. Furthermore, it is our consensus that the imager product is preferable to the sounder product, even though the latter has obvious advantages in the greater number of measurements. The reasons are simply timeliness and the imager better (4 vs. 10 km) resolution. From an historical perspective it is interesting to note that the GOES-I DPI seem considerably better than anticipated from before launch simulations (Hayden and Schmit, 1991). Much of this apparent improvement is due to improved processing technique and the remainder due to the improved resolution (which could not be

simulated using VAS measurements).

There remains the question of the utility of the DPI. The total precipitable water image is being delivered on an experimental basis to the National Weather Service Forecast Office at Sullivan, Wisconsin. They report that they have found some utility for predicting minimum temperatures, based on the assumption of greater radiative cooling in dry atmospheres. The feature of the forecast phase error discussed above also suggests an application. We are not currently planning to provide the no-sat product to the field, but if it were, the forecasters could clearly see the error in the model forecast and apply this information to adjust the timing of their local forecast. There are further implications with respect to data assimilation. If, as is the current plan, GOES-8 data are introduced to the NMC models only in the form of precipitable water (rather than more complete profiles of temperature and moisture), there is no hope of correcting this type of phase error. We also feel that the skin temperature DPI should have application for frost or fog forecasting, and we have begun providing this product to Sullivan as well.

No claim is made for a high degree of absolute accuracy in the DPI. It is intended to be used in time sequenced mode, especially the lifted index, so that the observer can follow and extrapolate trends in the weather. At the same time, the accuracy is not bad, held in check by the forecast first guess. We have had no success in showing,with radiosonde match-up statistics that the DPI is an improvement over the forecast. Yet it obviously is, as demonstrated qualitatively in Fig. 5. Estimates of total precipitable water and lifted index from radiosondes are simply too sparse in space and time, and in themselves not accurate enough. It is hoped that these DPI products will soon be routinely available to the field. In the meantime, examples can be found on the CIMSS Home Page on the World Wide Web at: http://cloud.ssec.wisc.edu.

Figure 5 (Facing page): Derived Product Imagery (DPI) from the GOES-8 imager at 1445 UT on 14 March 1995. On the left are the satellite products; on the right are the first-guess products (composed of the NMC forecast and an analysis of the hourly surface reports). From top to bottom, the DPI parameters displayed are: total precipitable water vapor, lifted index, and surface skin temperature. Radiosonde values at 1200 UT are plotted over the first two satellite DPI. The color enhancement wedges are marked with a scale at the bottom of each image; clouds are depicted in gray in the satellite DPI.

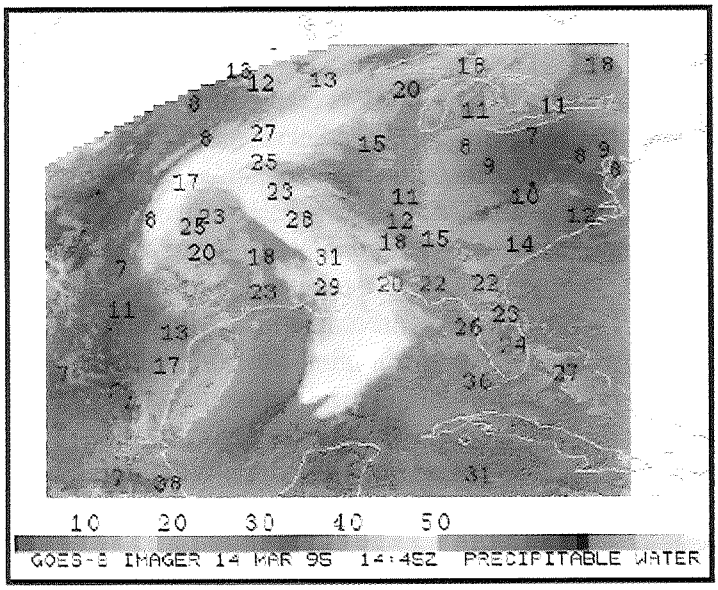
10 20 30 40 50
GOES-8 IMAGER 14 MAR 95 14:45Z PRECIPITABLE WATER

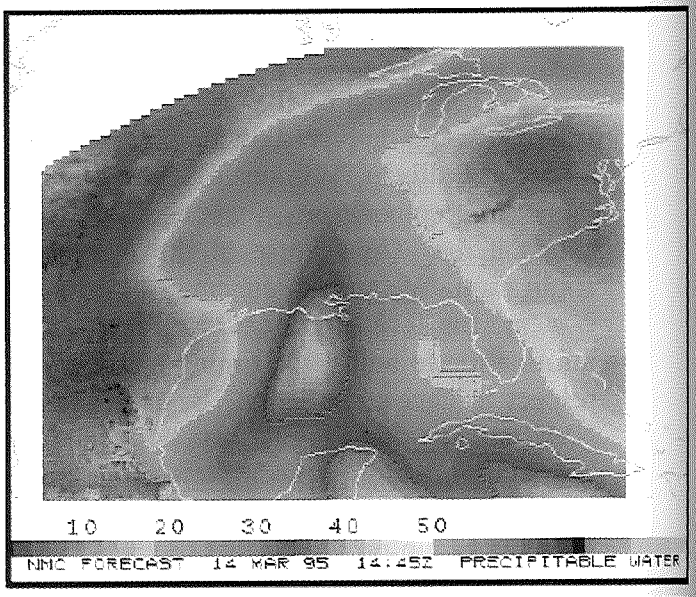
10 20 30 40 50
NMC FORECAST 14 MAR 95 14:45Z PRECIPITABLE WATER

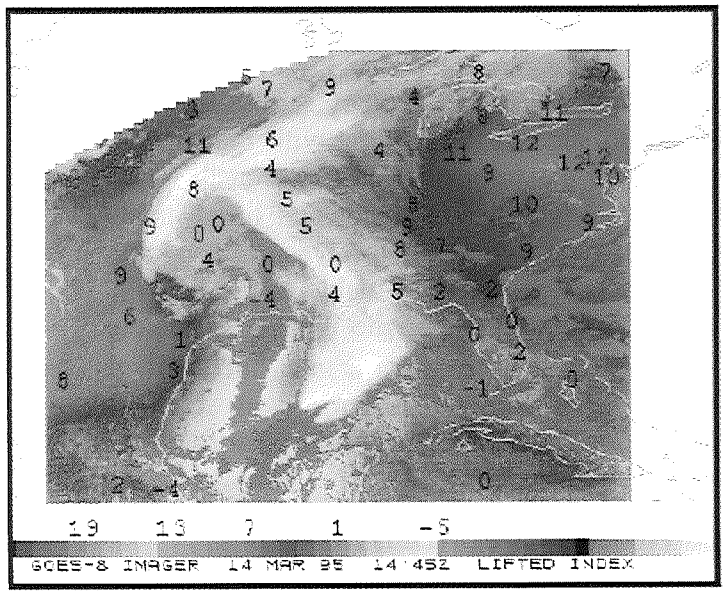
19 13 7 1 -5
GOES-8 IMAGER 14 MAR 95 14:45Z LIFTED INDEX

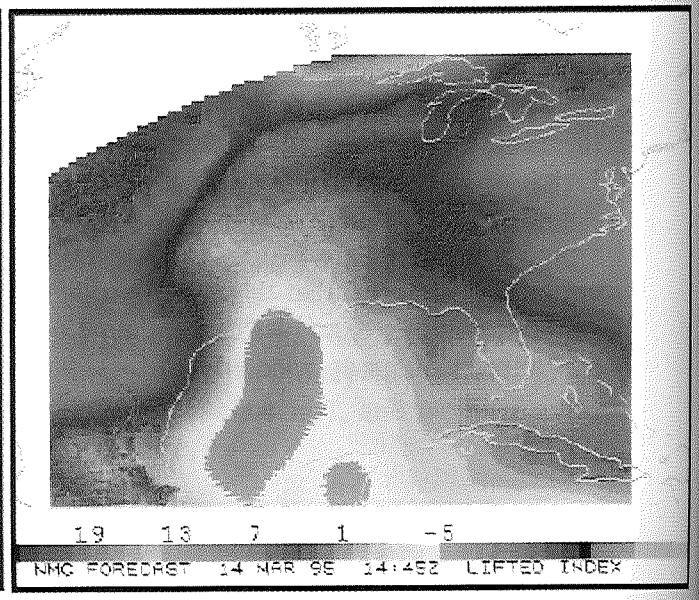
19 13 7 1 -5
NMC FORECAST 14 MAR 95 14:45Z LIFTED INDEX

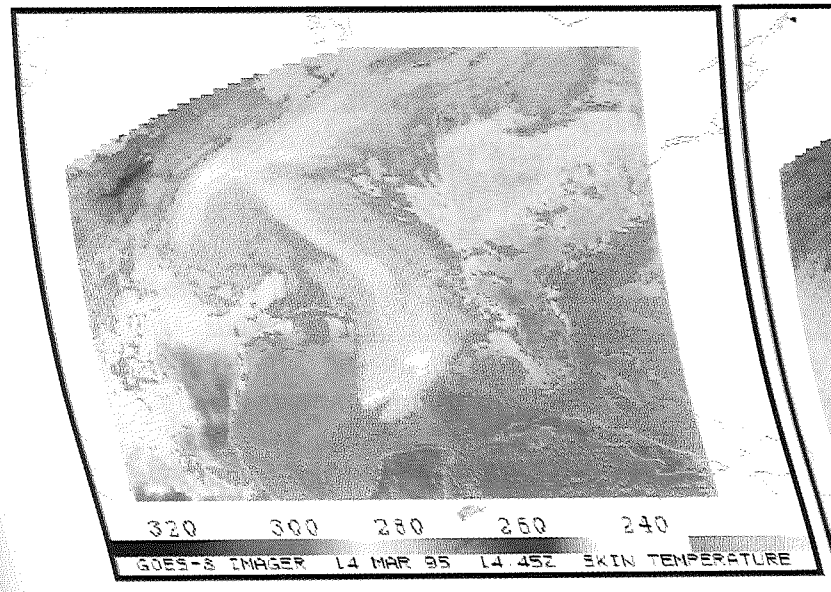
320 300 280 260 240
GOES-8 IMAGER 14 MAR 95 14:45Z SKIN TEMPERATURE

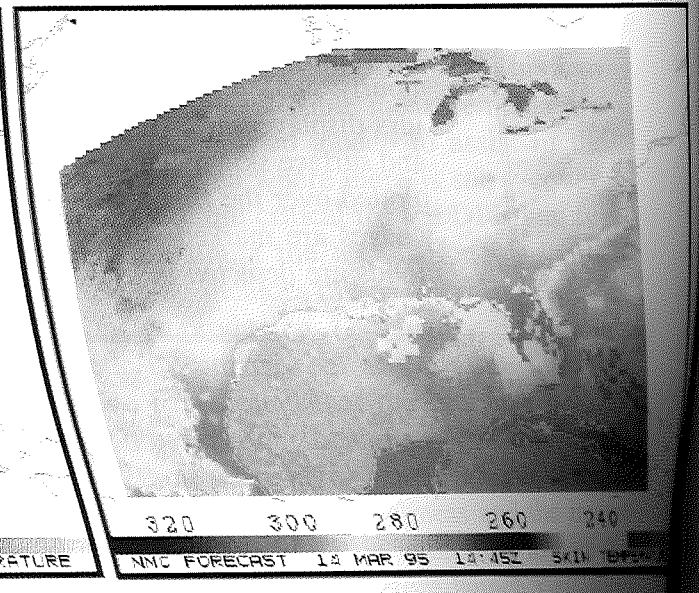
320 300 280 260 240
NMC FORECAST 14 MAR 95 14:45Z

Acknowledgements. Thanks to Paul van Delst of CIMSS for providing Fig. 1.

References:

Chesters, D., A. Mostek, and D. A. Keyser, 1986: VAS sounding images of atmospheric stability. Wea. and Fore., 1, 5-22.

Fleming, H. E., N. C. Grody, and E. J. Katz, 1991: The forward problem and corrections for the SSM/T satellite microwave temperature wounder. IEEE Transactions of geoscience and remote sensing., 29, 571-583.

Hayden, C. M.,1988: GOES VAS simultaneous temperature moisture retrieval algorithm. J. Appl. Meteor., 27, 705-733.

_____, and T. J. Schmit, 1991: The sounding capabilities of GOES-I and beyond. Bull. Amer. Met. Soc., 72, 1835-1846.

_____, 1994: GOES-I Sounder, Pre-launch investigations in simulation. Proceedings of the 7th Conference on Satellite Meteorology and Oceanography, June 6-10, 1994 Monterey, CA, Amer. Meteor. Soc. 484-488.

_____, and R. J. Purser, 1994: Recursive filter objective analysis of meteorological fields, applications to NESDIS Operational Processing, J. Appl. Meteor. 34, 3-15.

Menzel, W. P., and J. F. W. Purdom, 1994: Introducing GOES-I; the first of a new generation of geostationary operational environmental satellites. Bull. Amer. Met. Soc., 75, 757-781.

Petersen, R. A., L.W. Uccellini, A. Mostek, and D. A. Keyser, 1984: Delineating mid- and low-level water vapor patterns in pre-convective environments using VAS moisture channels, Mon. Wea. Rev. 112, 2178-2198.

Prata, A. J., 1993: Land surface temperatures derived from the advanced very high resolution radiometer and the along-track scanning radiometer 1. Theory. J Geophys Res., 98, 16689-16702.

Smith, W. L., G. S. Wade, and H. M. Woolf, 1985: Combined atmospheric sound ing/cloud imagery - a new forecasting tool. Bull. Amer. Met. Soc., 66, 138-141.

_____, H.E. Revercomb, H. B. Howell, H.-L. Huang, R. O. Knuteson, E. W. Koenig, D. D. LaPorte, S. Silverman, L. A. Sromovsky, and H. M. Woolf, 1990: GHIS - the GOES high resolution interferometer sounder. J. Appl. Meteor. 29, 1189-1204.

CALIBRATION OF THE METEOSAT IR AND WV CHANNELS [1]

ABSTRACT

The present operational procedures for the calibration of the METEOSAT infrared (IR: 10.5 - 12.5 μm) and water vapour (WV: 5.7 - 7.1 μm) channels are reviewed. Since no adequate onboard calibration is available vicarious calibration techniques have been developed. The operational calibration techniques for both the IR and WV channel rely on radiation model calculations for clear-sky which take independent data on the atmospheric and surface state as model input.

For the IR calibration clear-sky satellite observations (counts) over the ocean are correlated with radiances calculated from independent sea surface temperature analyses and short-term forecast fields on temperature and humidity. The WV calibration is based on radiation calculations with radiosonde data on temperature and humidity in areas with no clouds in the upper troposphere.

Two appendices provide an analytic relationship between radiance and brightness temperature and the radiometric noise characteristics of the IR and WV channel, respectively.

1 INTRODUCTION

The quantitative use of satellite radiometer data requires an absolute calibration of the instrument which relates the observed digital counts to radiances. For thermal infrared radiometers this is commonly achieved by viewing a blackbody. Preferably this is done by putting the blackbody in front of the complete optical chain, which is, however, impossible on a spinning geostationary satellite where the prime mirror (on Meteosat) is as large as 40 cm in diameter.

The necessity to calibrate the radiometer including the foreoptics is due to the fact that the detector responds to the combined thermal radiation from the Earth and the optical parts of the radiometer. In the case of Meteosat this includes seven mirrors, filters, a contamination window and lenses. All these elements contribute to the radiation received at the detector by emitting at their own temperature. A quasi-complete calibration can be realized by a blackbody put into the optical path and an additional monitoring of the temperature of contributing optical elements and correcting for them. This also requires accurate knowledge of the optical properties of the foreoptics (i.e. transmittance and reflectance).

Such a method is used for the operational calibration of the VAS instrument aboard GOES-7 and its predecessors (Menzel et al., 1981). Unfortunately this is not possible

---

[1] The paper is based on a presentation given at the 10th Meteosat Scientific Users' Meeting in Cascais, Portugal, by J. Schmetz (EUMETSAT), L. van de Berg and V. Gaertner (ESA/ESOC)

with the current series of Meteosats since neither the optical properties of the relevant mirrors and filters are known with sufficient accuracy nor can their temperatures be monitored.

Meteosat-4, -5 and -6 also have an onboard blackbody calibration for both the IR and WV channel, however it occurred that the blackbody calibration for Meteosat-4 and Meteosat-5, which would be a useful tool for monitoring the detector response, cannot be utilized at all for technical reasons.

It is interesting to note that it was the perception during the design of the Meteosat satellites that 'external calibration' would be needed. Reynolds (1976) discussed the matter and suggested various alternatives including the use of the moon as calibration target or the use of the total earth radiance from the full disc as a stable source. After in-depth study the suggestions did not emerge as viable solutions to the problem.

2 OPERATIONAL CALIBRATION

In conclusion to the above it is necessary to perform the absolute calibration of the Meteosat IR (10.5 - 12.5 μm) and WV channel (5.7 - 7.1 μm) within targets on Earth of known radiative properties, i.e. with properties that can be either calculated or measured with other calibrated satellites. Eyre (1980) calibrated the WV channel of Meteosat-1 via radiative transfer calculations based on accurate measurements of the atmospheric profiles of humidity and temperature from an aircraft. Beriot et al. (1982) used a calibrated satellite radiometer to derive a calibration from collocated satellite radiance measurements. While the methods work well, they are as case studies only of limited use to the operational exploitation of the satellite data, since the IR and WV channels require a continuous monitoring and recalibration since significant calibration changes can occur due to ageing, contamination or heating cycles (Jones and Morgan, 1981). For instance, the Meteosat-3 WV channel calibration coefficient increased by 6% over a period of less than 50 days after launch mainly due to contamination (Schmetz, 1989).

The concept of the operational vicarious calibration is as follows:

- Calculate a radiance R for an area with defined radiative characteristics
- Associate the radiance with a measured raw count
- Assume a linear relationship between count C and radiance

$$R = \int_{\lambda 1}^{\lambda 2} R\lambda \; \Phi \; \lambda \; d\lambda = \alpha \; (C - C_0) \qquad [1]$$

where λ denotes wavelength, R is the spectral radiance, $\lambda_1$and λ_2 the cut-off wavelengths of the spectral response function ϕ_{λ} C_0 is the offset (space view) and α the calibration coefficient (in $Wm^{-2}sr^{-1}$).

The actual calibration coefficients are distributed to the users in the headers of PDUS image data and/or with the Quarterly Calibration Reports.

2.1 IR Channel

The operational calibration of the IR channel is based on the collocation of clear-sky counts over the ocean with calculated radiances from a radiative transfer model with short-term forecast profiles from ECMWF and sea surface temperature analyses of NOAA (Reynolds, 1991). The radiative transfer model has been presented in Schmetz (1986) and the main features are:

i) it resolves the channel with 6 spectral sub-intervals (see Figure 1).

ii) transmittance in each sub-interval is treated by exponential-sum fits

iii) the model considers H_2O line absorption, H_2O continuum absorption, aerosol absorption, and viewing angle dependent sea surface emissivity.

The IR calibration is determined as follows:

i) Calibration coefficients α_{IR} are computed from hourly images

ii) For an update the hourly values of the last 12 hours are considered, that is:

$$\alpha_{new}^{IR} = 1/12 \sum_{i=1}^{12} \alpha_i^{IR}$$

and if: $| \alpha_{IR} - \alpha_{new}^{IR} | < 0.002$ Wm^{-2}sr^{-1} then update: $\alpha_{IR} = \alpha_{new}^{IR}$

iii) During eclipse α_{new}^{IR} is computed twice daily from slots 22 and 46 for the last six days.

iv) The precision of the calibration is $\approx$ 1 % which corresponds to ΔT = 0.7 K at 300 K, and ΔT = 0.4 K at 220 K.

v) The mean bias error in the range of SST (see Figure 2) is about 1 K. Slightly larger bias errors may occur for low temperatures (high clouds) due to nonlinearity effects (see below).

2.2 WV Channel

The operational calibration of the WV channel is based on the collocation of clear-sky WV counts with radiances computed from a radiation model with radiosonde profiles of temperature and humidity (Schmetz, 1989). Since the radiosonde humidity measurements in the upper troposphere are problematic a careful quality screening of the sonde data is required (Schmetz and van de Berg, 1994). An improved quality control of radiosondes has been operationally introduced on 4 February 1994 along with some other changes, which reduced the calibration coefficient α_{WV} by about 6 - 8% compared to the previous method.

Further details of the calibration procedure are:

i) The radiative transfer model considers water vapour absorption. Figure 3 shows a comparison with results from LOWTRAN-7.

ii) The radiative transfer model uses radiosonde profiles, where soundings are excluded if the mean radiosonde upper tropospheric relative humidity (UTH) between 600 and 300 hPa. is less than 4%.

iii) No radio soundings are taken outside 55° viewing angle.

iv) An expected count is computed from the current α_{WV} and the computed radiance.
Soundings are rejected if the difference between expected count and measured count exceeds a certain threshold, which is 32 counts for radiosonde UTH values below 50% and 16 counts else.

v) Calibration runs are performed twice daily with radiosoundings for noon and midnight UTC.

vi) For an update of α_{WV} we consider the last 6 values (3 days):

$$\alpha_{new}^{WV}=1/6\sum_{i=1}^{6}\alpha_i^{WV}$$

vii) If the difference between α_{WV} and α_{new}^{WV} is less than 1 %, the coefficient is α_{WV} is kept, otherwise it is replaced by α_{new}^{WV}

viii) For the computation of α_{new}^{WV} we exclude values outside the one - σ range of the six values.

ix) The precision of the calibration is $\approx$ 2-3 % which corresponds to ΔT = 0.9 K at 260 K and ΔT = 0.6 K at 220 K.

3 EFFECT OF CONTAMINATION

A passive cooling system, consisting of a sunshield and a two stage cooler, is used to ensure that the detectors for the IR and WV can be operated at a low temperature. A temperature regulation in the form of a heating resistor and a thermistor is used to maintain a temperature of 90 K throughout the year. Keeping the detectors at a constant temperature is essential since the spectral detector response changes with temperature which would in turn affect the filter function and consequently the relationship between incident radiance and the output (voltage or counts).

The IR and WV channels are also affected by contamination due to water vapour which evaporates and tend to condense at the coldest parts of the satellite. The effect of contamination on the cooler performance has been discussed by Mason and Diekmann (1990). A question which has not been addressed before is to what extent a thin layer

of ice on parts of the optical path affects the overall filter function of the different channels.
A relevant test has been performed by Matra Espace, the manufacturer of the radiometer: The transmission loss of an optical Germanium window has been measured before and after a contamination with a layer of about 1 μm of water vapour. The resulting transmittance changes have been applied to the original non-contaminated normalized filter functions and IR results are plotted in Figure 4. Only the six values representing the six spectral bands of the radiation model used for calibration are shown and fitted with a smooth curve. The important result is that the original curve differs from the one for contamination only by a constant factor to within the measuring errors. That is, the relative contribution of a spectral band to the overall response remains constant and no corresponding change to the filter function in the radiation calculations is required when contamination occurs. A detailed test with the radiation model shows that brightness temperature errors are less than 0.2 K.

A further interesting result is that an ice layer of 1 μm changes the transmittance by a factor of about 0.7. A gain change of about two steps (each a factor 1.2) would be needed to maintain the dynamic range of the images.

4 CONCLUSION

The present generation of METEOSAT satellites requires a vicarious calibration concept for the operational calibration of the IR and WV channel. The IR channel is calibrated via a collocation of clear-sky counts over sea versus radiances calculated from short-term forecast profiles (ECMWF) and SST analysis (NOAA). The WV channel is calibrated by collocations of clear-sky counts and radiances calculated from radiosonde profiles.

The precision is about 1% for the IR and 2 - 3% for WV, respectively. Bias errors are difficult to estimate and should be less than 2 % for the IR and less than 5 % for the WV. Since the relationship between counts and radiances is assumed to be linear a possible nonlinearity could cause a cold bias for cold clouds in the IR channel.

On 4 February 1994 the WV calibration has been changed with a transition from Meteosat-4 to Meteosat-5. The new calibration procedure lowered the values of α_{WV} by 6 - 8 % in comparison to the previous method.

The condensation of ice on elements of the optical path of the radiometer does not significantly change the relative shape of the filter functions in both the IR and WV channel. Corresponding errors are less than 0.2 K in brightness temperature.

Last but not least it should be mentioned that an onboard calibration for the next generation of European geostationary satellites (MSG) is currently being designed which will alleviate problems occurring with the current generation of Meteosats.

REFERENCES

Beriot, N., N. Scott, A. Chedin and P. Sitbon, 1982: Calibration of geostationary satellite radiometers using the TIROS-N vertical sounder. Application to Meteosat-1. J. Appl. Meteorol., 21, 84 -89.

Eyre, J., 1980: Calibration and some exploratory uses of the
Meteosat water vapour channel imagery, Second Meteosat Scientific Users' meeting, p. A1 - A14.

Jones, M. and J. Morgan, 1981: Adjustment of the Meteosat-1 radiometer response by ground processing. ESA Journal, 5, 305 - 320.

Gaertner, V., 1989: MIEC IR calibration coefficients derived from cloud free sea pixels. Proc. of the 7th Meteosat Scientific Users' Meeting, Madrid, Eumetsat, EUM P04, 15 - 18.

Mason, B.D. and F.J. Diekmann, 1990: IR detector contamination - causes and effects. Proceedings of the 8th Meteosat Scientific Users' Meeting. Norrkoping 28 - 31 August 1990, EUM P 08, p. 45 - 50.

Menzel, W.P., W.L. Smith and L.D. Herman, 1981: Visible infrared spin- scan radiometer atmospheric sounder radiometric calibration: an inflight evaluation from intercomparisons with HIRS and radiosonde measurements. Appl. Opt., 20, 3641 - 3644.

Menzel, W.P., S. Wanzong, S. Nieman, F. Wu, C. Velden and J. Schmetz, 1994: Comparison of GOES and Meteosat calibration and products. Proceedings of the 10th Meteosat Scientific Users' Meeting.

Reynolds, M., 1976: On the problem of infra-red calibration of the radiometer. ESA - Meteorological Programme Office, Internal note MET/TN/074-76 of 3 March 1976, 9 pp.

Schmetz, J., 1986: An atmospheric correction scheme for operational application to Meteosat infrared measurements. ESA Journal, 10, 145 - 159.

Schmetz, J., 1989: Operational calibration of the Meteosat water vapor channel by calculated radiances. Appl. Opt., 28, 3030 - 3038.

Schmetz, J. and L. van de Berg, 1994: Upper tropospheric humidity observations from Meteosat compared with short-term forecast fields. Geophys. Res. Letters, 21, 573 -576.

Conversion of Radiances to Brightness Temperatures

The calibration equation (see Equ. 1) provides radiances. Often it is useful to convert those to equivalent blackbody or brightness temperatures. The radiance-to-temperature relationship for each satellite has been provided to the users in the METEOSAT CALIBRATION REPORTs in tabular form only. Those tables can be accurately fitted with the following expression:

$$R(T) = \exp(A + \frac{B}{T}) \qquad [A1]$$

where R is the radiance (in $Wm^{-2}sr-1$) and T the temperature (in K) and A and B (in K^{-1}) are regression coefficients. Equation A1 fits the relationship with an rms error of less than 0.2 K over the range between 200 K and 330 K. Table A1 provides the regression coefficients for the different Meteosat satellites.

	METEOSAT-2	METEOSAT-3	METEOSAT-4	METEOSAT-5	METEOSAT-6
IR: A	6.1401	6.1694	6.7300	6.7348	6.7615
IR: B	-1267.0	-1262.7	-1272.2	-1272.2	-1267.2
WV: A	8.7698	8.8812	9.0921	9.2361	9.1124
WV: B	-2180.5	-2167.9	-2255.7	-2266.7	-2264.9

Table A1: Regression coefficients for the relationship between radiance ($W\ m^{-2}sr^{-1}$) and brightness temperature (K) for the IR-1 and WV-2 channels of Meteosat-2 through Meteosat-6.The analytic form of the relationship is given by Equation A1.

Radiometric Noise

Table A2 provides the radiometric noise characteristics of Meteosat-3, 4, 5 and 6 at reference temperatures of 290 K for IR and 260 K for WV, respectively. The single pixel noise for a given brightness temperature can be obtained from:

$$NE\Delta T(T) = NE\Delta R\left(\frac{\partial R}{\partial T}\right)^{-1} = NE\Delta R \frac{T^2}{-B\,R(T)} \qquad [A2]$$

Of note is the greatly improved performance of the WV channel from Meteosat-3 to the MOP satellites Meteosat-4, 5 and 6. For instance, at a brightness temperature of 200 K the single pixel noise is about 7 K for Meteosat-3 but only 1.6 K for Meteosat-5.

Satellite	Channel	NEΔT	NEΔR in $Wm^{-2}sr^{-1}$
METEOSAT-3	IR-1	0.27 K at 290 K	0.025
	WV	0.95 K at 260 K	0.053
METEOSAT-4	IR-1	0.30 K at 290 K	0.047
	WV-2	0.39 K at 260 K	0.02
METEOSAT-5	IR-1	0.33 K at 290 K	0.053
	WV-2	0.20 K at 260 K	0.011
METEOSAT-6	IR-1	0.23 K at 290 K	0.038
	WV-2	0.17 K at 260 K	0.009

Table A2: Radiometric noise characteristics of Meteosat-3 through Meteosat-6. Values for Meteosat-4 are from commissioning while other values are from a campaign in weeks 23 and 24 in 1994 (Diekmann, personal communication). The values of NEΔR are relative with respect to the Planck radiances folded with the filter function of the corresponding channel.

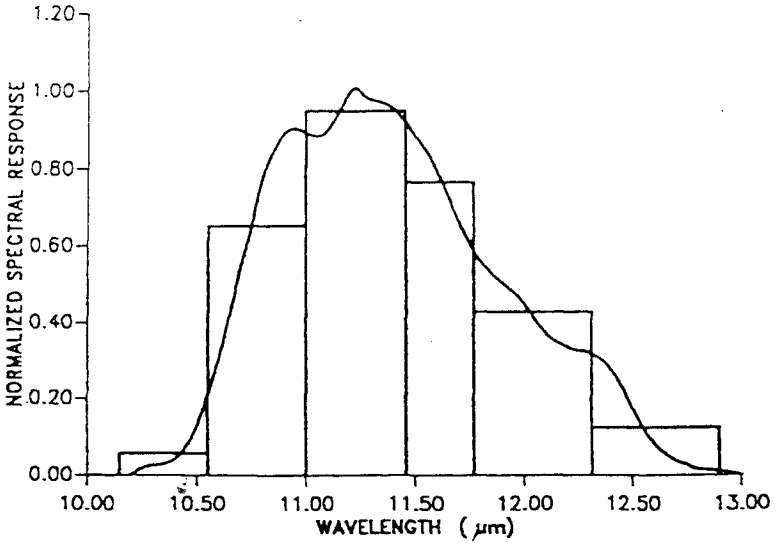

Figure 1: Normalized spectral response for the Meteosat-4 IR-1 channel at 90 K. The histogram depicts the width of the spectral intervals of the radiation model and the weights of each sub-interval.

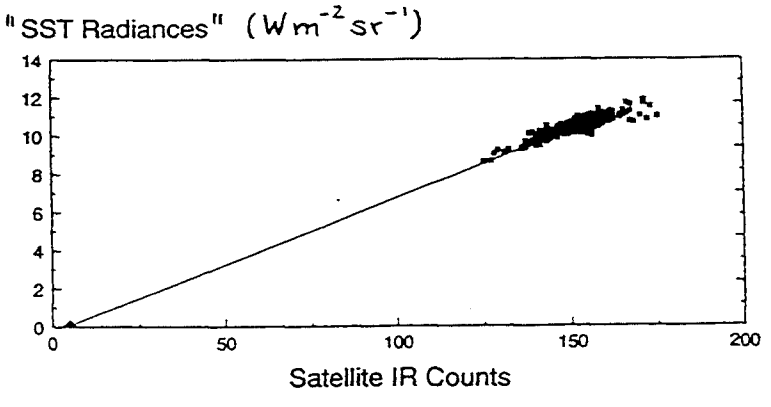

Figure 2: Example of an IR calibration. The radiances obtained from calculations for clear-sky ocean are plotted versus the observed counts. The actual instantaneous calibration coefficient is obtained from a straight line between the space count C_0 and the mean value of all collocations. The number of collocations is typically between 1200 and 1400 per calibration run. Runs are performed hourly but α_{IR} is only updated as described in section 2.1.

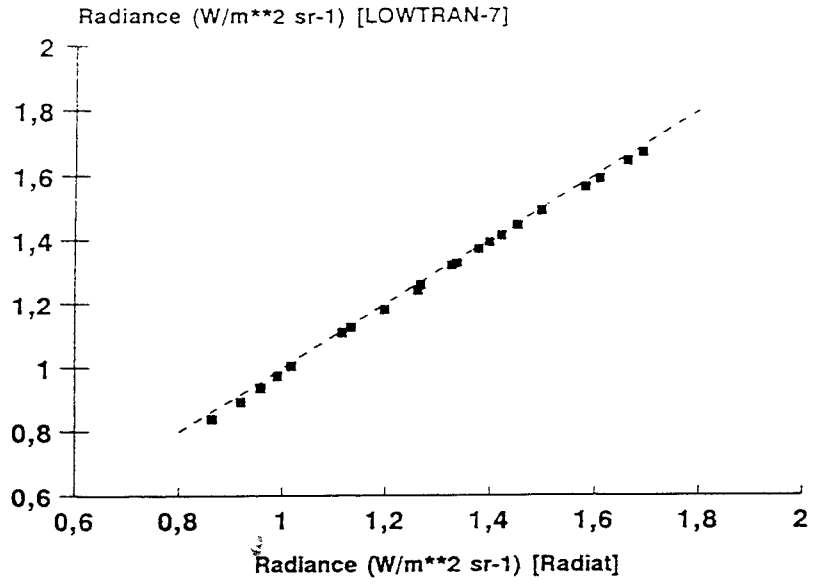

Figure 3: Comparison of the radiation model ('Radiat') used for calibrating the WV channel with results from LOWTRAN-7. No radiometer filter function has been applied to weigh the spectral sub-intervals. The rms difference corresponds to about 0.15 K.

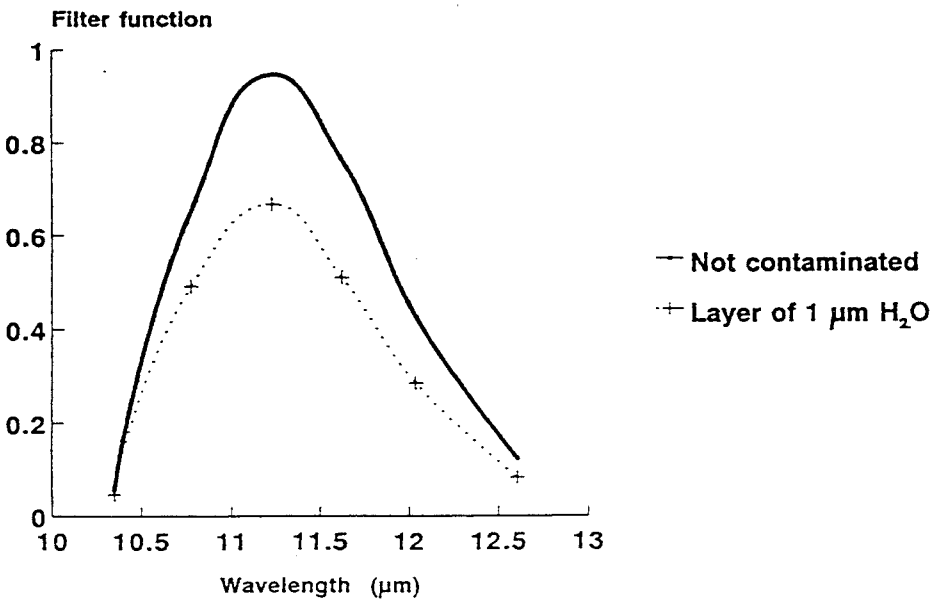

Figure 4: Effect on the radiometer filter function of an ice layer of 1 μm deposited on a Germanium window within the optical path. Note that filter functions remain similar, i.e. they are different by a nearly constant factor. Curves are fits to the six values representing the spectral bands of the radiation model (see Figure 1).

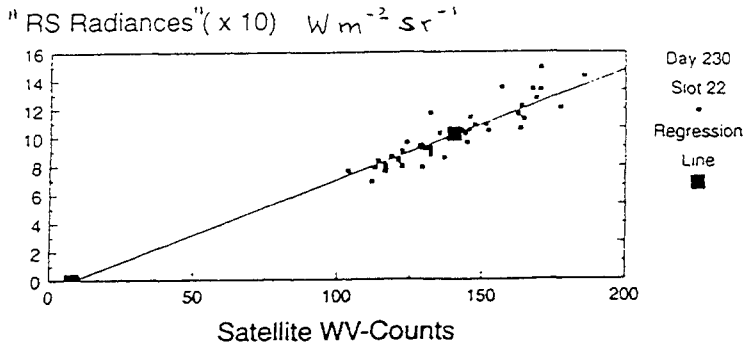

Figure 5: Example of a WV calibration. The radiances calculated from radiosoundings are plotted versus the observed counts. The actual instantaneous calibration coefficient is obtained from a straight line between the space count C_0 and the mean value of all collocations. The number of collocations is typically between 30 and 50 per calibration run. Runs are performed twice daily but α_{wv} is less frequently updated as described in section 2.1.

CGMS XXIII
USA WP-25
Agenda Item WG II/2

COMPARISON OF HIRS, GOES, AND METEOSAT CALIBRATION

W. Paul Menzel

Advanced Satellite Products Project
Office of Research and Applications
National Environmental Satellite Data and Information Service
NOAA, Madison, Wisconsin

Steve Wanzong

Cooperative Institute for Meteorological Satellite Studies
University of Wisconsin - Madison
Madison, Wisconsin

Johannes Schmetz

Meteorological Division
EUMETSAT
Darmstadt, Germany

1. INTRODUCTION

Meteosat-3 (M-3), positioned at 70 or 75 W during the Extended Atlantic Data Coverage (deWaard et al., 1992), afforded new opportunities for collaborative research projects between the United States and Europe. Collaboration between the European Space Operations Center (ESOC) of ESA, the Meteorological Division of EUMETSAT, and the Cooperative Institute for Meteorological Satellite Studies (CIMSS) of NESDIS has suggested techniques for cross-calibration of the geostationary and polar orbiting sensors that have temporally and spatially collocated measurements. Initial focus has been on comparison of the infrared window and water vapor channels radiances measured by these systems.

2. CALIBRATION COMPARISONS OF GOES AND METEOSAT

M-3 is calibrated operationally by using M-4 (or M-5) measurements as reference radiances in an area viewed by both satellites. The M-3 calibration procedure was initially found to be noisy, but recent work (Menzel et al., 1993) suggested several methods to reduce the variability of the M-3 calibration coefficients. The GOES-7 (G-7) calibration, which occurs every spin (.6 seconds), was used to verify improvements in the Meteosat operational calibration procedures performed twice daily. Over a period of 4 days in July 1993, 17 comparsions were made of equatorial clear sky radiances in areas equally distant from either satellite. Table 1 shows the results. The G-7 calibration was found to be .1 C warmer than M-3 with a scatter of .7 C. A correction has been made for the different atmospheric absorption caused by the different spectral response functions of the two sensors.

Table 1. Comparison of Meteosat-3 and GOES-7 IRW clear sky radiances for 17 events in Jul 1993. Mean deviation (G-7 minus M-3) is after correction for spectral response differences.

G-7 - M-3 (17 cases from Jul 93)

	Mean Deviation (C)	Sigma about the Mean (C)
IRW	0.1	0.7

Comparisons of the water vapor channels are difficult because the viewing angle difference of more than 40 degrees precludes assuming that the atmospheric water vapor absorption is the same for the two sensors.

3. CALIBRATION COMPARISONS OF HIRS AND METEOSAT

The geostationary satellites can only be calibrated directly with respect to one another if their earth views have some overlap. However the polar orbiting High resolution Infrared Radiation Sounder (HIRS) offers a fixed reference for all of the geostationary satellites and suggests another approach to instrument cross calibration. The nineteen channel HIRS has both an infrared window and a water vapor channel (for more information on the HIRS, see Smith et al., 1979).

The geostationary and polar orbiting data can be compared with histograms of brightness temperatures of similar spectral channels from the two sensors for an area within 10 degrees of the geostationary sub-satellite point (Schmit and Herman, 1992). This minimizes viewing angle differences and the need for high accuracy navigation. The geostationary data should be averaged to approximately the same resolution as the HIRS data (roughly 20 km) so that the same distribution of warm and cold radiance values can be expected; for the Meteosat-3 5 km resolution data 16 fovs (fields of view) are averaged, and for the GOES-7 7 km resolution data 9 fovs are averaged. The clearest scene (highest temperature) from each satellite is compared. Spectral response differences are accounted for with forward calculations of the expected radiance for each satellite for the current atmospheric state. Observed radiance difference minus forward calculated radiance difference is than attributed to calibration differences.

The M-3 and G-7 calibration was monitored with respect to the HIRS for several months in 1993 and 1994. Figure 1 shows the two histograms over the same region on 24 August 1993 for both the M-3 and NOAA-12 HIRS water vapor brightness temperatures, respectively. The collocation in time was better than 30 minutes. Both capture the peaks associated with the mean temperature in the upper atmosphere. The apparent brightness temperature difference (M-3 minus N-12) associated with the clearest scene temperature is about 4.7 C. Spectral response differences (M-3 minus N-12) are about -1.1 C; clear radiances for each satellite were computed from the NMC 12 and 24 hour global forecast interpolated to the correct time and the radiance difference due to spectral response was then inferred. Thus the brightness temperature difference (M-3 minus N-12) that can be attributed to calibration differences is 5.8 C. Table 2 shows the results for several M-3 comparisons with HIRS, as well as several G-7 comparisons with HIRS. IRW comparisons are typically show less scatter than WV comparisons.

Table 2. Comparison of Meteosat-3 and GOES-7 IRW and WV clear sky radiances with NOAA polar orbiting HIRS measurements for ten case study days. Mean deviation (geostationary minus HIRS) is after correction for spectral response differences.

M-3 - HIRS (seven cases from Aug 93 to Jan 94)

	Mean Deviation (C)	Sigma about the Mean (C)
IRW	2.5	1.9
WV	8.4	2.8

G-7 - HIRS (ten cases from Aug 93 to Jan 94)

	Mean Deviation (C)	Sigma about the Mean (C)
IRW	-0.3	0.9
WV	1.2	1.7

4. EMPIRICAL DISTRIBUTION FUNCTION COMPARISONS

Another approach for intercalibration of different sensors involves matching empirical distribution functions (Weinreb et al., 1989). If two sensors with similar spectral response and similar horizontal spatial resolution view the same scene, the distribution of their respective outputs will be nearly identical. Therefore, one sensor can be used as a reference (in this work, GOES-7). The other sensor (Meteosat-3), can be adjusted to match the reference channel. A scene with large variations is necessary to ensure that most of the raw count range of each channel will be used (Menzel et al., 1994).

The calibration of M-3 using collocated G-7 data proceeds as follows. The distribution of M-3 counts is matched to the distribution of G-7 counts (assuring that there is sufficient variation in the scene so that as much of the range of possible counts is involved); for each M-3 count value a corresponding G-7 count value is established. Then with M-3 counts matching G-7 counts, M-3 counts are converted to with G-7 radiances (via look up table or linear fit). G-7 radiances are connected to M-3 radiances by correlating clear sky forward calculations for the given atmospheric state and the respective spectral response functions; for the infrared windows, a simple quadratic fit from one Planck function to another (adjusted for spectral band width as noted in Menzel et al., 1993) is adequate. Then M-3 radiances calibrated with the G-7 reference are compared with the operationally calibrated radiances. Figure 2 shows the procedure applied to IRW data on 31 August 1994 in four panels: 2a is the histogram of counts for the collocated scene (note that G-7 is 10-bit and M-3 is 8-bit); 2b plots the empirical distribution functions (EDF) for both sensors that establishes a one to one relationship between the two sensors; 2c shows the linear relationship of G-7 radiances to M-3 counts; and 2d shows the difference of recalibrated minus operational brightness temperatures over the range of observed temperatures. The temperature differences are larger in the colder range (2 to 3 C) but are within 1 C for all temperatures warmer than 240 K. The mean difference for the whole temperature range is 0.5 C and the standard deviation about that mean is about 0.5 C.

Both histograms (Figure 2a) show that each sensor is viewing the same scene. The difference in bit depth between the two satellites explains the disparity in the counts (x axes). GOES-7 is 10 bit data, Meteosat-3 is 8 bit. The resolution and the bit depth of the sensors explains the difference in the y axes. Each pixel is 6.7 km for GOES-7 and 5km for Meteosat-3. On average, the GOES-7 raw counts varied from 100 to 500 (out of a possible 0 to 1023 range). For Meteosat-3 the counts were between 25 and 175 (cut of a possible 0 to 255 range

A look up table of M-3 counts to G-7 counts is generated from the EDFs. For raw count x from Meteosat-3, the corresponding cumulative percentage value from the Meteosat-3 EDF is matched to the GOES-7 EDF. Then the percentage value from the GOES-7 EDF is used to extract the adjusted raw count value x'.

Once the Meteosat-3 counts have been matched to GOES-7 counts, the original Meteosat-3 counts are correlated with GOES-7 radiances (via a linear or quadratic fit shown in Figure 2c). Then, GOES-7 radiances are converted to Meteosat-3 radiances (accounting for differences in their spectral response funtions). Figure 3 shows IRW results for two different approaches are used. One approach uses a simple quadratic fit from one Planck function to another (each Planck funtion has been adjusted for spectral band width as noted in Menzel et at., 1993); this is a viable approach only for very transparent spectral bands. A second approach uses a forward calculation for the given atmospheric state and the respective spectral response functions (FASCODE3P); this is the only approach applicable to the water vapor bands. Then the Meteosat-3 radiances that are calibrated with the GOES-7 blackbody are compared with the operationally calibrated radiances.

For the example shown in Figure 3, matching Meteosat-3 counts to GOES-7 radiances with a linear fit produced the best results. This is not always true for each of the individual cases that have been done. The FASCODE3P spectral adustment to the linear fit produced the best overall results. The mean temperature difference over the range of expected temperatures is 0.1 C, with a 0.5 C standard deviation. The quadratic spectral adjustment to a linear fit produced the most stable results with a standard deviation of .2 C, but had a mean temperature difference of 1.3 C. For the infrared window, using one of the above two methods, Meteosat-3 can be calibrated from GOES-7, to within 2 C of operational calibration.

For the EDF technique to be an alternative calibration method, it needs to be stable over a period of time. The study the stability of the EDF calibration over a 24 hour period, the calibration lookup table from the start was applied for the duration of the period (94355 12 UTC to 94356 12 UTC was chosen for the test). A lookup table of counts to temperatures was generated for 94355 12z; it selects the temperature closest to the Meteosat-3 operationally calibrated temperature out of the 4 possible temperatures from each EDF method. Figure 4a shows the agreement of the EDF calibration with the operational calibration over the range of possible temperatures. The temperature differences are almost all within 1 C. One day later, the result is almost the same; the 24 hour old EDF calibration is within 1.3 C of the new operational calibration (Figure 4b).

5. RECOMMENDATION

From these small examples, it is clear that the calibration of one sensor can be used to improve the calibration of another sensor or to provide a common reference for two other sensors. A geostationary satellite sensor can be used to calibrate one polar orbiting sensor with respect to another polar orbiting sensor; thus continuity in the calibration of the polar series of sensors can be achieved with the geosatationary sensors. And conversely, the geostationary sensors can be calibrated with respect to one another even if they have no overlap in time or space by using the polar orbiting sensors.

The international community of satellite operators should begin a study to intercalibrate their current sensors. There is also a need to determine fluctuations associated with the seasonal cycle for the spinning geostationary sensors, with the diurnal cycle for the three axis stable geostationary sensors, and with the day-night cycle for the polar orbiting sensors; each affects the temperature regime aboard the respective platform. For climate or trend analyses, all temporal transitions from one sensor to another (eg. G-6 to G-7) should be covered with an independent sensor (eg. N-9).

While much more work needs to be done to study the necessary sample sizes and the best intercalibration techniques, it appears that when individual sensors overlap in space and time their combined calibration has reduced calibration uncertainty than could be achieved with either sensor by itself.

6. REFERENCES

de Waard, J., W.P. Menzel, and J. Schmetz, 1992: Atlantic data coverage by Meteosat-3. Bull. Amer. Met. Soc., 73, 977-983.

Menzel, W.P., J. Schmetz, S. Nieman, L. van de Berg, V. Gaertner, and T.J. Schmit, 1993: Intercomparison of the Operational Calibration of GOES-7 and Meteosat 3/4. NOAA Technical Report NESDIS 73, 14 pages.

Menzel, W. P., S. Wanzong, S. Nieman, F. Wu, C. Velden, and J. Schmetz, 1994: Comparison od GOES and Meteosat Calibration and Products. Proceedings of the 10th Meteosat Scientific User's Conference, Cascais, Portugal, 5-9 Sep 1994, Eumetsat publication ISSN 1011-3932, 71-81.

Schmit, T.J. and L.D. Herman, 1992: Comparison of multi-spectral data: GOES-7 (VAS) to NOAA-11 (HIRS). Sixth Conference of Satellite Meteorology and Oceanography, Atlanta, GA.

Smith, W.L., H.M. Woolf, C.M. Hayden, D.Q. Wark and L.M. McMillin, 1979: The TIROS-N Operational Vertical Sounder, Bull. Amer. Meteor. Soc., 58, 1177-1187.

Weinreb, M.P., R. Xie, J.H. Lienesch, and D.S. Crosby, 1989: Destriping GOES images by matching empirical distribution functions. Remote Sens. Environ, 29, 185-195.

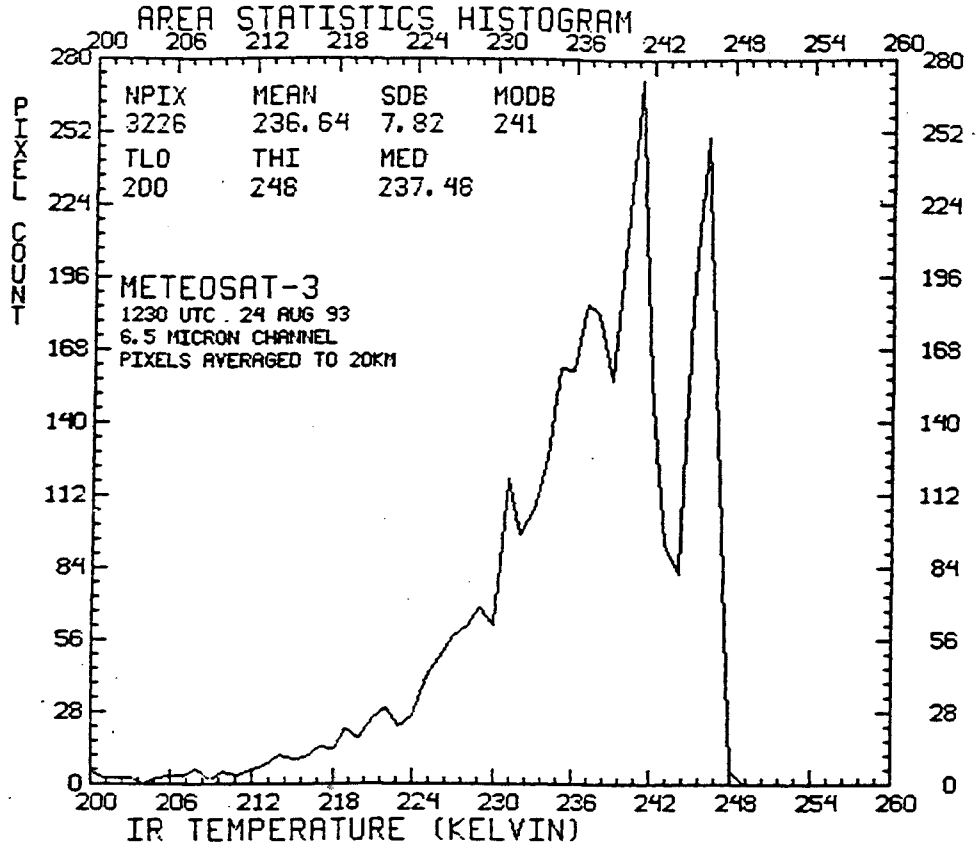

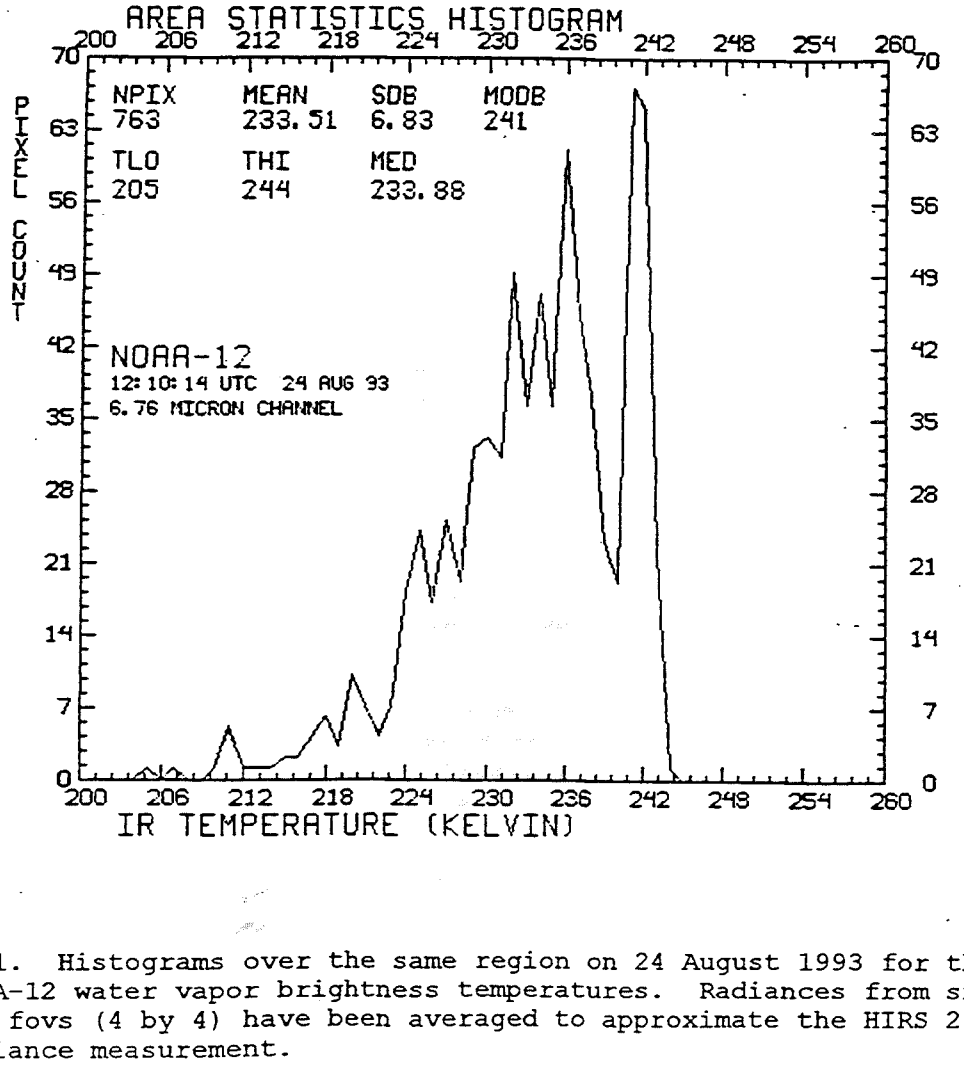

Figure 1. Histograms over the same region on 24 August 1993 for the M-3 and NOAA-12 water vapor brightness temperatures. Radiances from sixteen M-3 5km fovs (4 by 4) have been averaged to approximate the HIRS 20 km fov radiance measurement.

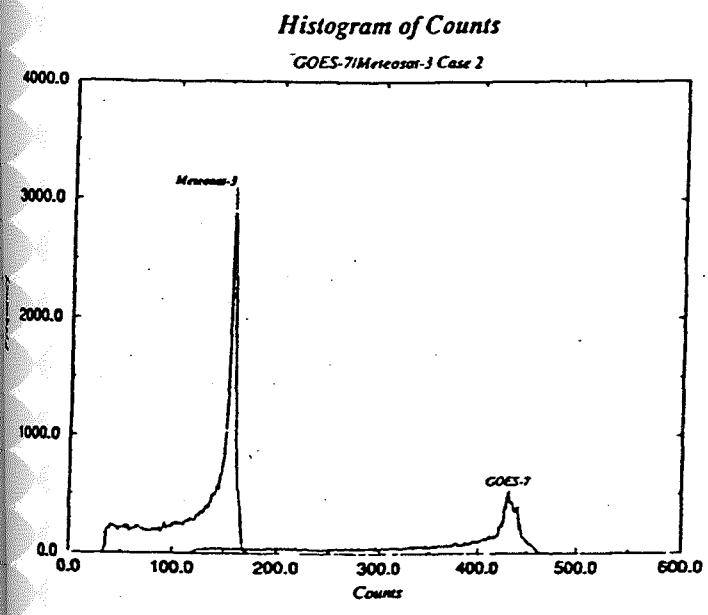

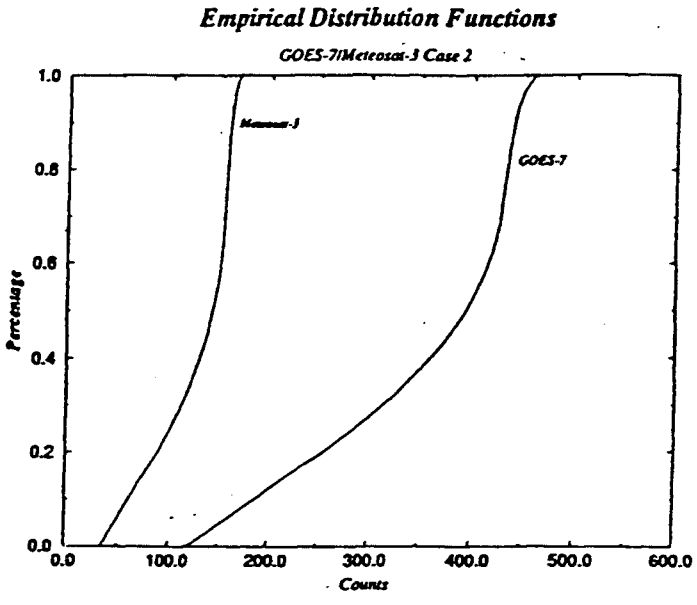

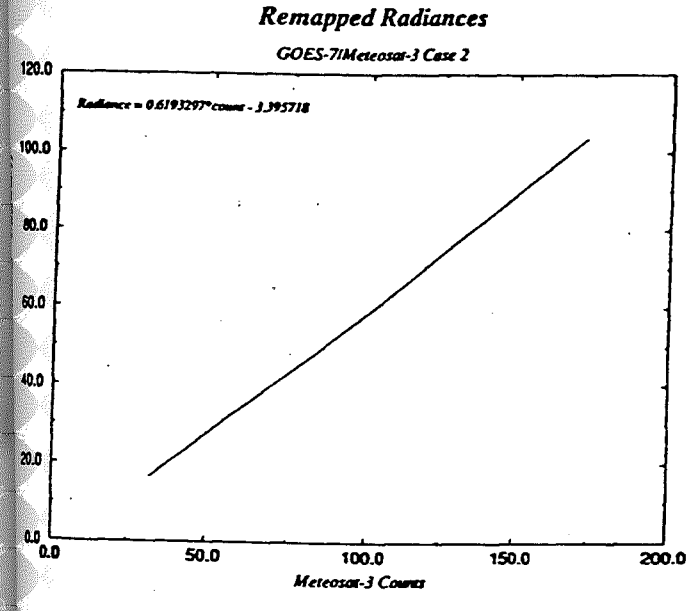

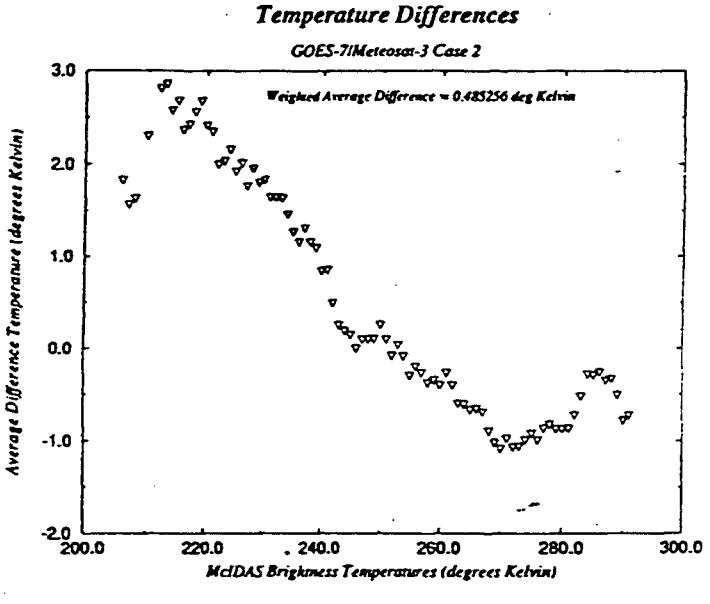

Figure 2. Calibration of M-3 using G-7 blackbody for IRW data on 31 August 1994: 2a shows the histogram of counts for the colocated scene (note that G-7 is 10-bit and M-3 is 8-bit); 2b plots the empirical distribution functions (EDF) for both sensors that establishes a one to one relationship between the two sensors; 2c shows the linear relationship of G-7 radiances to M-3 counts; and 2d shows the difference of recalibrated minus operational brightness temperatures over the range of observed temperatures.

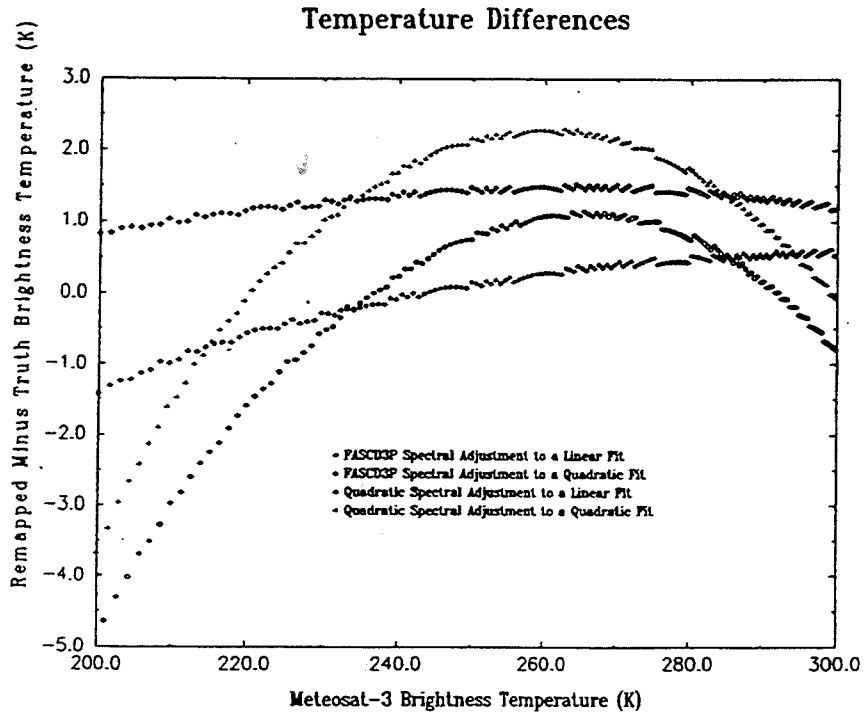

Figure 3. Comparison of M-3 operational calibration with respect to the calibration accomplished by matching the M-3 EDF to the G-7 EDF. Four different approaches are indicated.

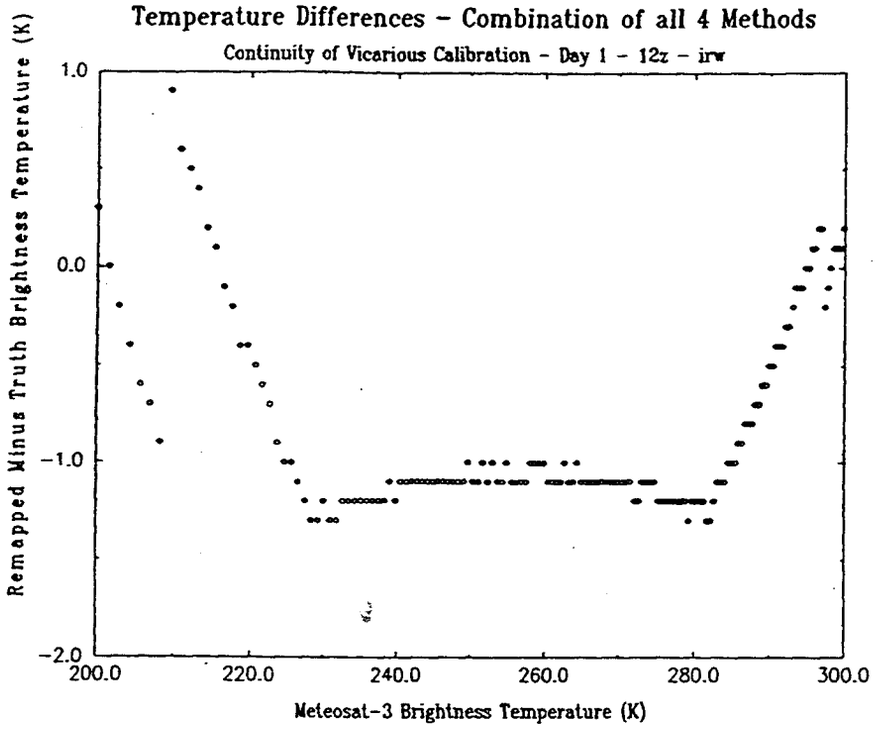

Figure 4a. EDF calibration compared to operational calibration at 94355 12 UTC.

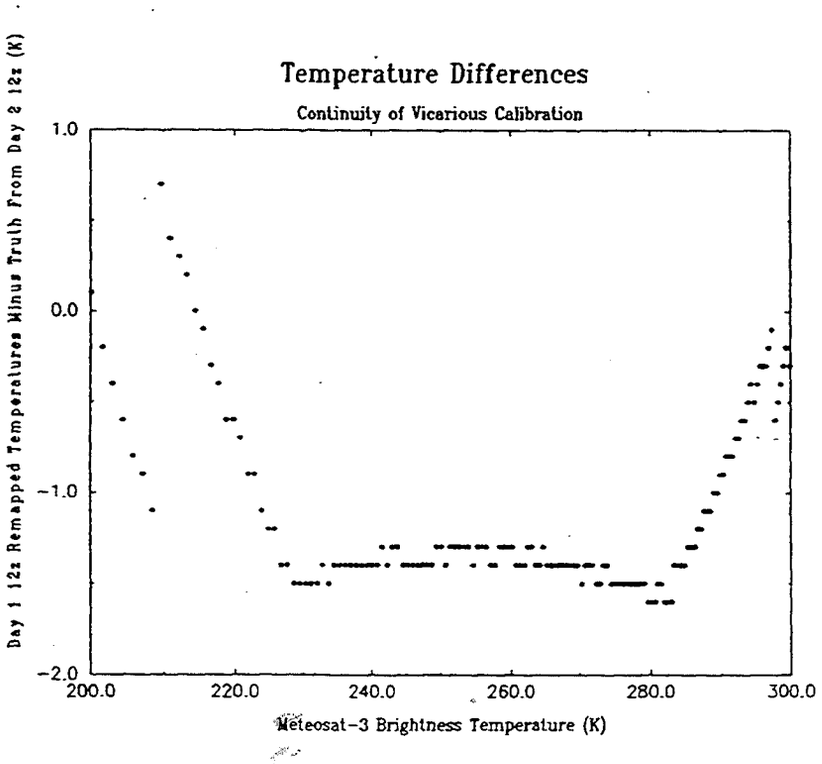

Figure 4b. One day old EDF calibration compared to current operational calibration 94356 12 UTC.

CGMS-XXIII WP-12
Prepared by Japan
Agenda Item: II/4

PRODUCTS UTILIZING DATA FROM NEW GMS-5 SENSORS:

I. SEA SURFACE TEMPERATURES FROM SPLIT WINDOW CHANNELS

II. UPPER TROPOSPHERIC AIR HUMIDITY AND PRECIPITABLE WATER AMOUNT

GMS-5 has additional observation sensors: thermal infrared split window sensors and water vapor sensor. Various products will be produced from the data of the additional sensors. Upper tropospheric air humidity will be newly made from a combination of the water vapor sensor data and the first sensor data of the split window. Precipitable water amount will be newly made from both the sensor data of the split window. Sea surface temperature will be calculated from both the sensor data of the split window.

Details are described in Attachment.

Derivation of Sea Surface Temperatures from Split Window Channels

1. Introduction

Sea Surface Temperatures (SSTs) are to be derived from the split window channels data using a MultiChannel SST (MCSST) retrieval algorithm beginning with the operation of GMS-5 in 1995. This algorithm was developed by National Oceanic and Atmospheric Administration (NOAA)/ National Environmental Satellite, Data and Information Service (NESDIS) in the 1980s and has been widely used for SST derivation using Advanced Very High Resolution Radiometer (AVHRR) data from the NOAA polar orbit satellite.

SSTs are derived every three hours, at 00, 03, 06, 09, 12, 15, 18 and 21UTC. SSTs are obtained in each area of 0.5 degrees latitude by 0.5 degrees longitude within the field from 50°N to 50°S and from 90°E to 170°W.

This paper describes a tentative procedure for deriving SSTs from split window channels at MSC.

2. Derivation procedure

The SST derivation procedure consists of the following steps:

Calculating surface temperature using the MCSST retrieval algorithm
Determining the representative SSTs using histogram analysis

(1) *Calculation by MCSST retrieval algorithm*

SSTs are derived using an MCSST retrieval algorithm which uses two simultaneous brightness temperatures in different spectral bands to correct the atmospheric attenuation of surface temperature. The thermal infrared (IR) channel of 10.5-12.5 μm equipped on GMS-4 and its predecessors does not, however, provide the information on atmospheric absorption which is needed for attenuation correction. The information must be provided by another source to estimate the amount of atmospheric absorption.

Two simultaneous brightness temperatures on the IR split window channels are different, because the brightness temperature depends on the absorption efficiency which varies according to the spectral band. Therefore, the information of atmospheric absorption is obtained indirectly from split window data and the accuracy of SST estimation from satellite data is improved.

The equation for MCSST retrieval algorithm is:

$$SST = a\,T_{11} + b\,(T_{11}-T_{12}) + c\,(T_{11}-T_{12})(\sec\theta-1) + d$$

where T_{11} is the brightness temperature in IR1, T_{12} is the brightness temperature in IR2, θ is satellite zenith angle, and a, b, c, and d are the coefficients of the linear regression. The second and third terms in the equation are for atmospheric attenuation correction. To deal with different absorption corresponding to the optical path length, the term of atmospheric attenuation based on satellite zenith angle is included.

The coefficients of the retrieval equation for GMS-5 have been tentatively calculated by model computation using LOWTRAN-7 radiation transfer code which calculates atmospheric transmittance and radiance for given atmospheric path. This model computation uses vertical profile data from objective analysis to obtain the following equation:

$$SST = 0.9807\,T_{11} + 4.0395\,(T_{11}-T_{12}) + 0.3806\,(T_{11}-T_{12})(\sec\theta-1) + 7.069$$

T_{11}, T_{12} (input) and SST (output) are expressed in degrees Kelvin.

The coefficients are adjusted comparing satellite observations with in-situ measurements at later stage.

IR data from split window channels are converted from digital count values to brightness temperature values by referring the calibration tables which are updated at every observation, in principle. The surface temperature data of full resolution (5 km at the sub-satellite point) are calculated from the brightness temperatures of IR data. In this step cloud screening is not performed on the assumption that all IR data is in cloud-free sea.

(2) *SST Determination*

The retrieval algorithm developed by NOAA/NESDIS for Global Operation Sea Surface Temperature Computation (GOSSTCOMP) is used for determination of SST. This algorithm is based on histogram tests.

The segments of SST with the regular intervals of 0.5 degree latitude by 0.5 degree longitude are classified as cloud-free segment or cloud-contaminated segment by referring the results of histogram tests. The only segment whose status is 'cloud free' and 'sea' is selected.

For a uniform-scene temperature field, the actual SST can be given by simply calculating the arithmetic mean or modal class of the histogram. However, most scenes have some cloud present and the cold side of histogram of these scenes is slightly contaminated by clouds. Calculations of mean from the contaminated histogram could be in error. Then calculations of mean are made from combinations of the classes constituting the warm side of the histogram. The mean is employed as the representative SST at each segment.

3. Statistic

It is widely accepted that approximately 40 to 50% of the earth on any given day is obscured by clouds. As far as SST is derived from single observation data, the probability of obtaining cloud-free scenes of sea surface is small. The SSTs data from observations made at different time are combined to increase the probability of obtaining the SST of a cloud-free scenes.

The geostationary satellite has an advantage that a given area is always observed with the same viewing geometry. Since satellites observe the earth continuously and frequently, the probability of obtaining cloud-free sea surface scenes is enhanced.

The daily mean SSTs in every area 0.5 degrees latitude by 0.5 degrees longitude are produced from combination of the SST data every three hours, at 00, 03, 06, 09, 12, 15, 18 and 21UTC.

Five-day mean SSTs or ten-day mean SSTs is produced from combination of the daily mean SST every five days or every ten days respectively. Monthly mean SSTs is produced every month.

4. References

Bates, J. J. and W. L. Smith, 1985: Sea surface temperature: observation from geostationary satellites. *Journal of Geophysical Research*, **90**, 11609-11618.

Brower, R. L., H. S. Gohrband, G. P. William, T. L. Signore and C. C. Walton, 1976: Satellite derived sea surface temperature from NOAA spacecraft. NOAA Technical Memorandum NESS **78**, 1-74.

McClain, E. P., G. P. William and C. C. Walton, 1985: Comparative performance of AVHRR-based multichannel sea surface temperature. *Journal of Geophysical Research* **90**, 11587-11601.

————, C. C. Walton, and L. L. Stowe, 1990: CLAVR cloud/clear algorithms and non-linear atmospheric correction for multi-channel sea surface temperatures. *Preprint volume of the fifth conference on satellite meteorology and oceanography*, 133-139.

Walton, C. C., 1978: The AVHRR/HIRS operational method for satellite based sea surface temperature determination. NOAA Technical Report NESDIS **28**, 1-58.

New products utilizing GMS-5 new sensors in Japan; Upper Tropospheric Air Humidity and Precipitable Water Amount

1. Introduction

Observations of behavior of water in the atmosphere are important to understand weather and climate. By conventional observations, we can get the distribution of water vapor only at limited number of points on the earth. The water vapor channel sensor on GMS-5 will visualize the distribution of water vapor in upper troposphere. On the other hand, split window channel sensors are sensitive to water vapor in lower troposphere. MSC has been developing two new products by GMS-5; Upper Tropospheric Air Humidity (UTH) and Precipitable Water Amount(PWA).

UTH is considered as a vertical mean humidity in upper troposphere. The European Space Agency (ESA) has already developed and disseminated UTH product retrieved from METEOSAT data (Schmetz and Turpeinen,1988), and UTH is used in objective analysis for the Numerical Weather Prediction (NWP). Recently, it is suggested that a monthly mean UTH is a suitable product for climate monitoring data (Schmetz and Leo van de Berg, 1993). Our UTH derivation program is being developed based upon ESA's algorithm stated above.

PWA is expected to provide complementary data of water vapor distribution in the areas with sparse sonde observations. PWA as well as UTH will be used for NWP. The retrieval of PWA product is based upon the technique which was developed by Chesters et al.(1983).

UTH and PWA will be disseminated four times a day (6 hourly) in the form of grid point data with 0.5 degree lat./lon. intervals. UTH and PWA are expected to increase accuracy of humidity analysis, especially under clear sky condition.

This paper describes theories, processing, and examples of these products.

2. Upper Tropospheric Air Humidity

2.1 *Theory*

Water vapor has strong absorption in 6.7 micro meter band, which GMS-5 water vapor sensor observes. The contribution from upper troposphere dominates the net up-welling radiation in this band. The level of the largest contribution is usually located in the layer between 600 hPa and 300 hPa. If profiles of temperature and humidity are known at a point under clear sky condition, intensity of radiance observed by GMS-5 will be estimated by numerical calculation according to the radiation transfer theory. Theoretical radiances for temperature profile and a set of fixed upper tropospheric humidity are employed to relate the observed radiance to a UTH value for a layer between 600hPa and 300hPa. The UTH value at the point is retrieved by checking that its theoretical radiance coincides with observed radiance. Because we are not yet able to calculate radiance correctly in case of high level cloudy atmosphere, UTH retrieval is restricted within the condition of clear or with only low level clouds.

2.2 *Processing*

Radiances observed by GMS–5 are converted to equivalent Temperatures of the Black–Body (TBB) in this processing. UTH is retrieved by interpolation using a table of water vapor channel TBB (WV–TBB). The WV–TBB table contains WV–TBBs of a set of fixed upper tropospheric (relative) humidity values, such as 1%, 10%, 20%, 30%, 50%, 70% and 100%. Each WV–TBB is calculated using the profile modified in humidities at upper troposphere from the original profile forecasted by NWP. WV–TBBs are converted from WV channel radiances calculated using the k–distribution method. The calculation of WV channel's radiances regards water vapor absorption only. UTH product is derived through the following steps.

Step 1. Generation of a WV–TBB table.
Step 2. Generation of a two–dimensional histogram of IR1 and WV channels.
Step 3. To read IR1–TBB and WV–TBB of pixels in a grid from the two–dimensional histograms.
Step 4. To average IR1–TBB and WV–TBB of pixels of which IR1–TBBs are warmer than threshold value determined by the discrimination process of clear and cloudy conditions (MSC, 1989).
Step 5. To derive the value of UTH by interpolation.
(Iterate from step 3 to step 5 until all grid's data are processed.)

2.3 *Example*

To demonstrate the algorithm, some examples are made using GOES VISSR Atmospheric Sounder (VAS) data. The MSC's discrimination process of clear sky (MSC, 1989) is not applicable to GOES VAS data at this time, because it requires surface condition and some experimental parameters on the diurnal and annual change obtained by statistics. In this study, a grid is discriminated to clear, or cloudy with only low level clouds, if it satisfies the condition; All of infrared channel TBBs in a grid are less than a threshold value, and standard deviation of IR TBBs in a grid is less than 3 K. The threshold value is the black body temperature of virtual cloud at 850hPa level with unity emissivity. Though the GOES VAS data is originally 12 bits data, it is degraded into 8 bits, about 0.5K temperature resolution, to emulate the resolution of GMS–5 in this study.

The result at 00 UTC on 16 October 1988 is shown in Fig.1a. Though UTH is retrieved on grids with quarter degree interval, the figure is drawn with smoothing by averaging in 2.5 degree square areas. The objective analysis of humidity at 400hPa level is shown in Fig.1b for comparison. In the south area of the United States, the retrieved UTH distribution corresponds to the analysis. Values of UTH has large gradients near the boundary between clear and cloudy region. It is thought to be the causes that cloudy pixels are not excluded completely.

3. Precipitable Water Amount

3.1 *Theory*

GMS–5 split window channel sensors has been designed to observe radiances from the earth in two bands of 10.5–11.5 micro meter for one sensor, IR1, and 11.5–12.5 micro meter for the other

sensor, IR2. Difference of observed radiances between IR1 and IR2 is mainly due to absorption by water vapor. A single layer model of the atmosphere is used to estimating PWA, and monochromatic approximation is applied to radiation transfer in the model. Up–welling radiances under clear sky condition is expressed by

$$I_{obs} = I_{suf} * \tau + I_{atm} * (1-\tau) \qquad (3.1).$$

τ is a transmittance from the surface of the earth to the top of the atmosphere. I_{obs} is a radiance observed by a satellite. I_{suf} is a radiance from the surface. I_{atm} is a radiance from the atmosphere. It is assumed that the emissivity of the surface is unity. Each of radiances is expressed using the Planck's function, B(T), and corresponding TBB;

$$I_{obs} = B(T_{obs}),\ I_{suf} = B(T_{suf}),\ \text{and}\ I_{atm} = B(T_{atm}).$$

By rewriting B(T) in the form of the Taylor's expansion around $T=T_{atm}$, and neglecting higher order terms, following equation is derived.

$$T_{obs} = T_{suf} * \tau + T_{atm} * (1-\tau) \qquad (3.2).$$

For GMS–5 split window channel data, we assume T_{suf} and T_{atm} are same for IR1 and IR2. $T_{IR1(2)}$ is a Black body equivalent temperature of IR1(2). $\tau_{1(2)}$ is a transmittance for IR1(2).

$$T_{IR1} = T_{suf} * \tau_1 + T_{atm} * (1-\tau_1) \qquad (3.3a)$$
$$T_{IR2} = T_{suf} * \tau_2 + T_{atm} * (1-\tau_2) \qquad (3.3b)$$

By eliminating T_{suf},

$$\tau_1/\tau_2 = (T_{IR1}-T_{atm})/(T_{IR2}-T_{atm}) \qquad (3.4)$$

is derived.

Transmittance τ is assumed to decrease exponentially with water vapor amount summing up through path of radiation from the surface to the sensor. Transmittance τ is expressed by

$$\tau = \exp[-a \sec(\theta)\ pwa] \qquad (3.5).$$

θ is a satellite zenith angle at the surface. a is a parameter that depends on sensor's filter function. pwa is precipitable water amount in unit of g/cm^2.
Applying this expression to GMS–5 IR1 and IR2 sensors derives

$$\tau_1/\tau_2 = \exp[-(a_1-a_2) \sec(\theta)\ pwa] \qquad (3.6).$$

To eliminate τ_1/τ_2 from equations, (3.4) and (3.6), pwa could be retrieved by following expression.

$$pwa = -\ln[(T_{IR1}-T_{atm})/(T_{IR2}-T_{atm})]/\sec(\theta)/(a_1-a_2) \qquad (3.7).$$

To retrieve the value of pwa, T_{atm} and a_1-a_2 are needed to determine. T_{atm} can be determined fr

rawin sonde data. But most of GMS–5 observation area, few sonde observations are available. MSC has been developing a method for estimating T_{atm} from NWP data. On the other hand, the term, a_1–a_2, can be determined by the regression analysis that uses rawin sonde data for objective variable, because the term, a_1–a_2, does not depend on time and location.

3.2 *Processing*

PWA on a grid is derived according to following steps.

Step 1. Generation of a two–dimensional histogram from data of split window channels, IR1 and IR2.

Step 2. Discrimination of grids under clear sky condition (MSC, 1989).

Step 3. Calculation of PWA according to equation (3.7).

3.3 *Example*

The algorithm is applied to the data of GOES VAS split window channels, namely channel 7 and 8.

Since the method of estimating T_{atm} is not established at this time, we use 700hPa level temperature provided from NWP as T_{atm}. The discrimination method of the clear grids is the same as referred to in section 2.3.

Three cases on 00 UTC 5 April, 00 UTC 15 September, and 00 UTC 16 October 1988, are processed. Using the sonde data, the result of the regression analysis is shown in Fig.2. The correlation factor is 0.73, and the root mean square of errors is 0.74 g/cm^2 for the 70 samples. This is worse than the result of Chesters et al. (1987), 0.57 g/cm^2. But their optimization of T_{atm} using sonde data was not applied in our process. The distribution of PWA resulted from the satellite estimation is shown in Fig.3a and of PWA estimated from the objectively analyzed profile is shown in Fig.3b. In Fig.3a, PWAs by sonde observations are also plotted. The objective analyzed PWA with 2.5 degree lat./lon. resolution cannot represent feature of PWA on small scale. The satellite retrieved PWA shows almost good representation in large scale.

References

Chesters, D.,L.W.Uccellini, and W.D.Robinson, 1983:Low–level watervapor fields from the VISSR Atmospheric Sounder(VAS) split window channels. J.Climate Appl. Meteor., 22. 725–743.

————————, W.D.Robinson, and L.W.Uccellini, 1987: Optimized retrievals of precipitable water from the VAS split window. J. Climate Appl. Meteor., 26, 1059–1066.

MSC, 1989:Retrieval of Clear Sky Radiance, The GMS Users' Guide (second edition), 56–61.

Schmetz, J., and O. M. Turpeinen, 1988: Estimation of the upper tropospheric relative humidity field from METEOSAT water vapor image data. J. Appl. Meteor., 27, 889–899.

————————, and Leo van de Berg, 1993: Upper tropospheric humidity observations from Meteosat and comparisons with ECMWF forecasts. Technical Proceedings of the seventh international TOVS study conference. 443–442.

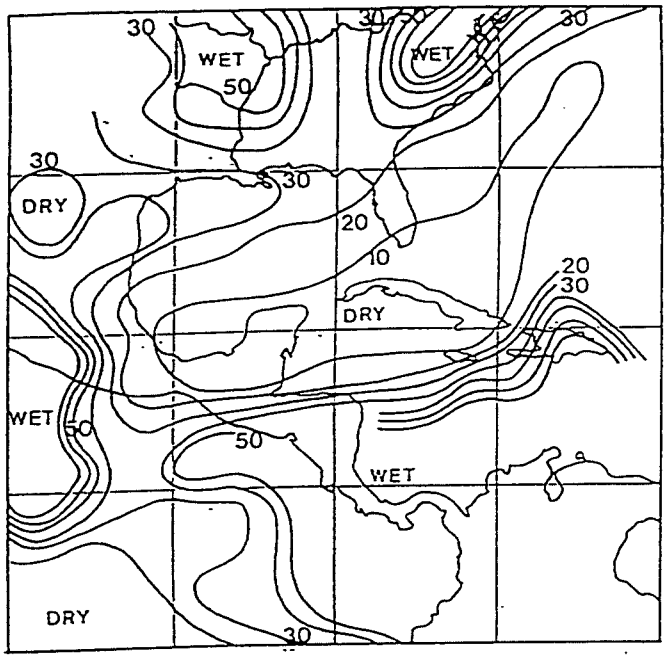

Fig.1a Satellite estimated UTH (percent)
for 00 UTC 16 October 1988

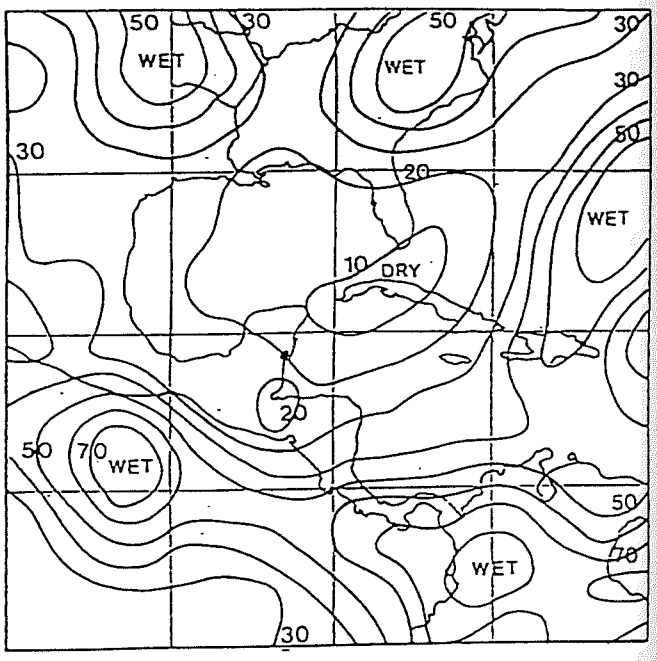

Fig.1b Objective analyzed UTH (percent)
for 00 UTC 16 October 1988

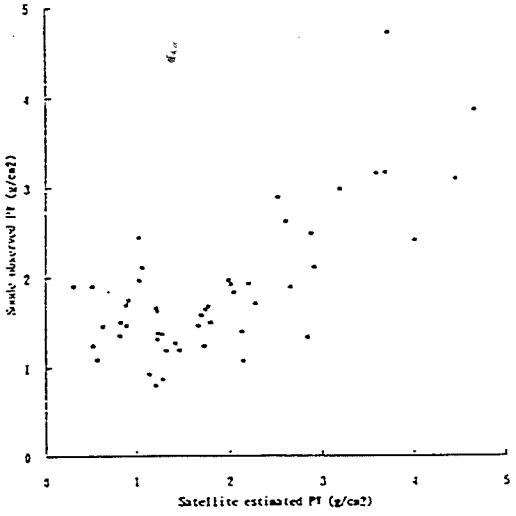

Fig.2 Satellite estimated precipitable water
versus sonde observed precipitable water

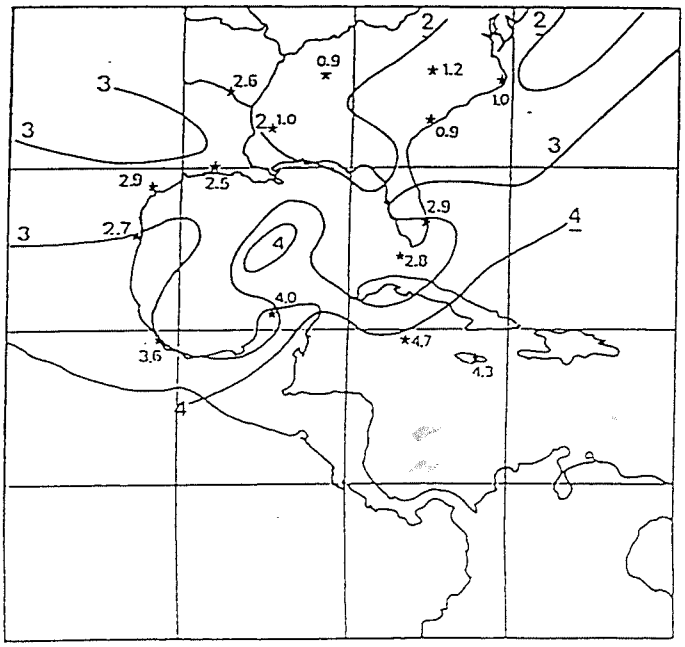

Fig.3a Satellite estimated precipitable water (g/cm2)
for 00 UTC 16 October 1988. Sonde observed
precipitable water are plotted on its location.

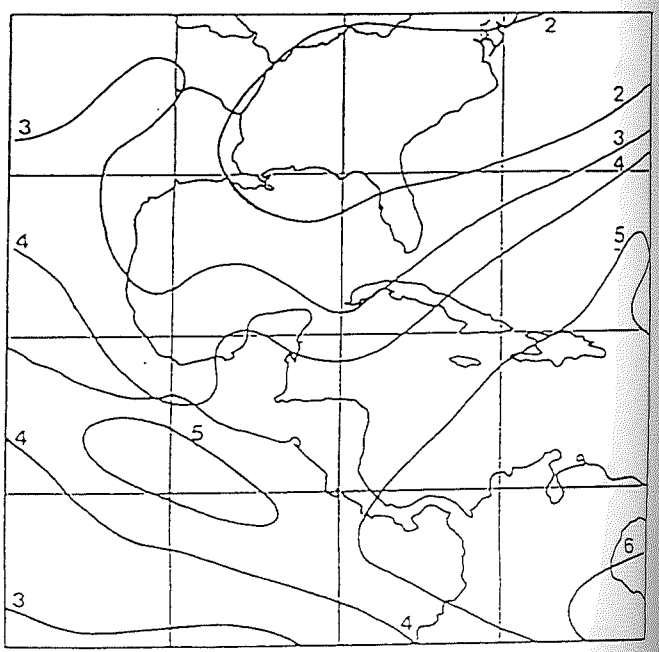

Fig.3b Objective analyzed precipitable water (g/cm2)
for 00 UTC 16 October 1988.

WIND VERIFICATION STATISTICS

1 INTRODUCTION

The paper provides a summary of METEOSAT cloud motion wind verification results from the operational wind extraction scheme for cloud motion winds and Water Vapour (WV) winds.

The assessment is based on monthly verification data of cloud motion winds as compared to collocated radiosonde wind measurements. It follows the procedure laid out in the Consolidated CGMS Report with the exception that the collocation criterion between satellite derived and radiosonde winds is still based on latitude-longitude boxes as specified in the original version of the Annex 9 of the Consolidated Report.

Date	Change
Nov 84	Major revision of the methods for automatic and manual quality control.
Mar 87	Radiance windowing for high level clouds
Sep 87	New WV channel calibration scheme.
Mar 89	Guided search for tracking (use of ECMWF first guess wind) for high level winds.
Mar 90	Spatial coherence information used as an additional criterion for tracer test and height assignment.
Feb 91	Automatic Quality Control using horizontal wind gradients.
Nov 91	Using VIS data at 7 bits resolution for histogram processing.
Dec 92	Image filtering using cold cloud radiance after semitransparency correction
Oct 93	Image rectification by cubic spline interpolation
Feb 94	Revised WV calibration scheme, and start of operational use of METEOSAT-5
Sep 94	Improved METEOSAT-5 real time rotating lens correction scheme
Nov 94	Improved IR calibration
Jan 95	Cloud base height assignment for low level clouds. ECMWF forecast 12 UTC more actual

Table 1: Summary of changes to the METEOSAT cloud motion wind extraction scheme since 1984.

An overview of changes of the operational METEOSAT cloud motion wind extraction scheme since 1984 is given in Table 1. Most of the changes were discussed in earlier papers, so that this paper focuses on the changes after October 1993.

There were frequent changes during the year of 1994 and another change in January 1995. This causes some difficulties to the validation method which relies on scatter diagrams of monthly averages of verification data. In order to avoid too many such diagrams with too few samples, data from September 1994 onwards are treated in this paper as one group.

2 METEOSAT HIGH LEVEL WINDS

Scatter diagrams of the periods starting with October 1993, of monthly averages of high level wind speed bias and RMS vector difference between METEOSAT derived and radiosonde winds are drawn in Figure 1. It shows that in general, monthly averages are well aligned along linear regression lines.

However, there are deviations from the regression line which are considered as indicators for anomalies and merit special attention.

Regarding the scatter diagrams from October 1993 to February 1995 in Figure 1, the following general observations can be made:

- there is considerable variance between the monthly values in each diagram

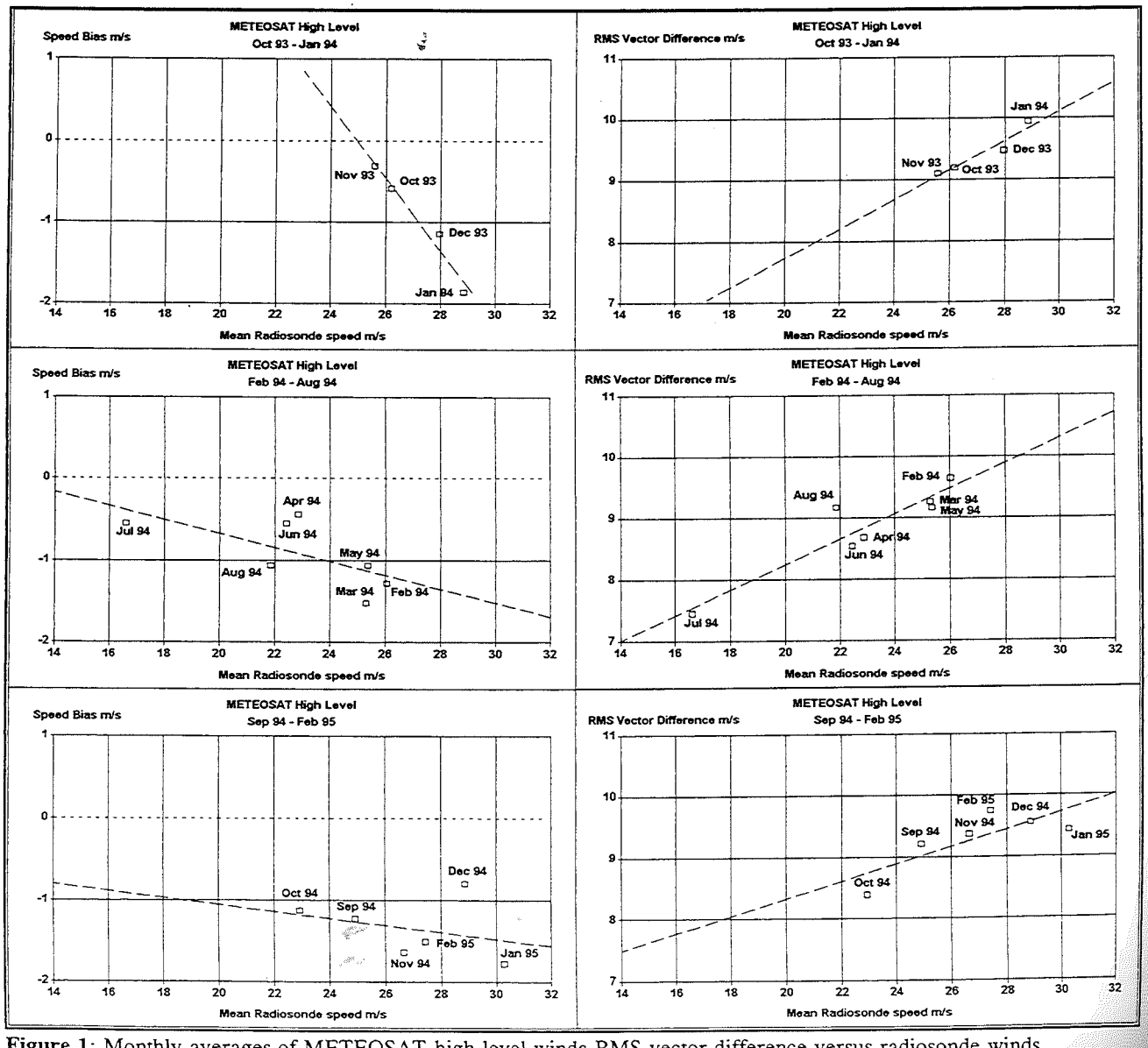

Figure 1: Monthly averages of METEOSAT high level winds RMS vector difference versus radiosonde winds.

- there is considerable variance between the slopes of the regression lines of the different diagrams

- This applies in particular to the diagrams of speed bias

- Speed bias values are between 0 and -2 m/s

This suggests that speed bias might have reached a steady state level with no obvious further improvements, as opposed to the past when great reductions could be achieved (see Figure 3).

The month of February 1994 shows a greater RMS vector difference than predicted by the regression line. This is explained as a negative effect caused by the transition from METEOSAT 4 to METEOSAT 5 in early February 1994. The effect can also be seen in the corresponding diagrams for medium level winds. Although METEOSAT 4 has been operational throughout the period, it is assumed that the effect was strongest immediately after the change, and it was reduced later during the year 1994 through further optimisation.

Image quality statistics of the MOP programme showed particularly bad performance during the months of July and August 1994. The effect can be seen in the middle right diagram of Figure 1 for the month of August. It cannot be seen so clearly for the month of July although we strongly suspect that July was equally affected but there are too few data in the period to provide better evidence. This assumption is somewhat supported by the corresponding diagrams for medium level winds in Figure 4 where the July value looks more anomalous than the one for August.

The effect of improved IR calibration after November 1994 cannot be verified. One would expect improved height assignment during periods of increased detector contamination during the winter. However, METEOSAT 5 has been launched in 1991 so that detector contamination has reached now a very low level.

Improved performance is expected from January 1995 onwards when more actual wind forecast for 12.00 UTC became available from ECMWF. This applies, in particular, to the tropics and maybe the southern hemisphere where the accuracy of wind forecast degrades more rapidly with time. Some improvement can actually be seen for January 1995 but not for February.

3 METEOSAT WATER VAPOUR WINDS

Water Vapour (WV) winds were produced regularly by ESOC since December 1992 and monthly performance statistics data are available since that date. These are based on collocated radiosonde data and therefore, directly comparable with IR cloud motion winds.

A first evaluation of WV winds was carried out by the European Centre for Medium Range Weather Forecast (ECMWF) by validation through its internal numerical analysis scheme. Following their positive assessment and following a modification of the SATOB code by WMO, WV winds were disseminated regularly via the GTS since 3rd November 1993 on a trial basis. After further evaluation, EUMETSAT declared these winds operational in early 1994. It should be noted that WV winds are produced without manual quality control, while all other cloud motion winds are quality controlled by human operators before transmission to GTS.

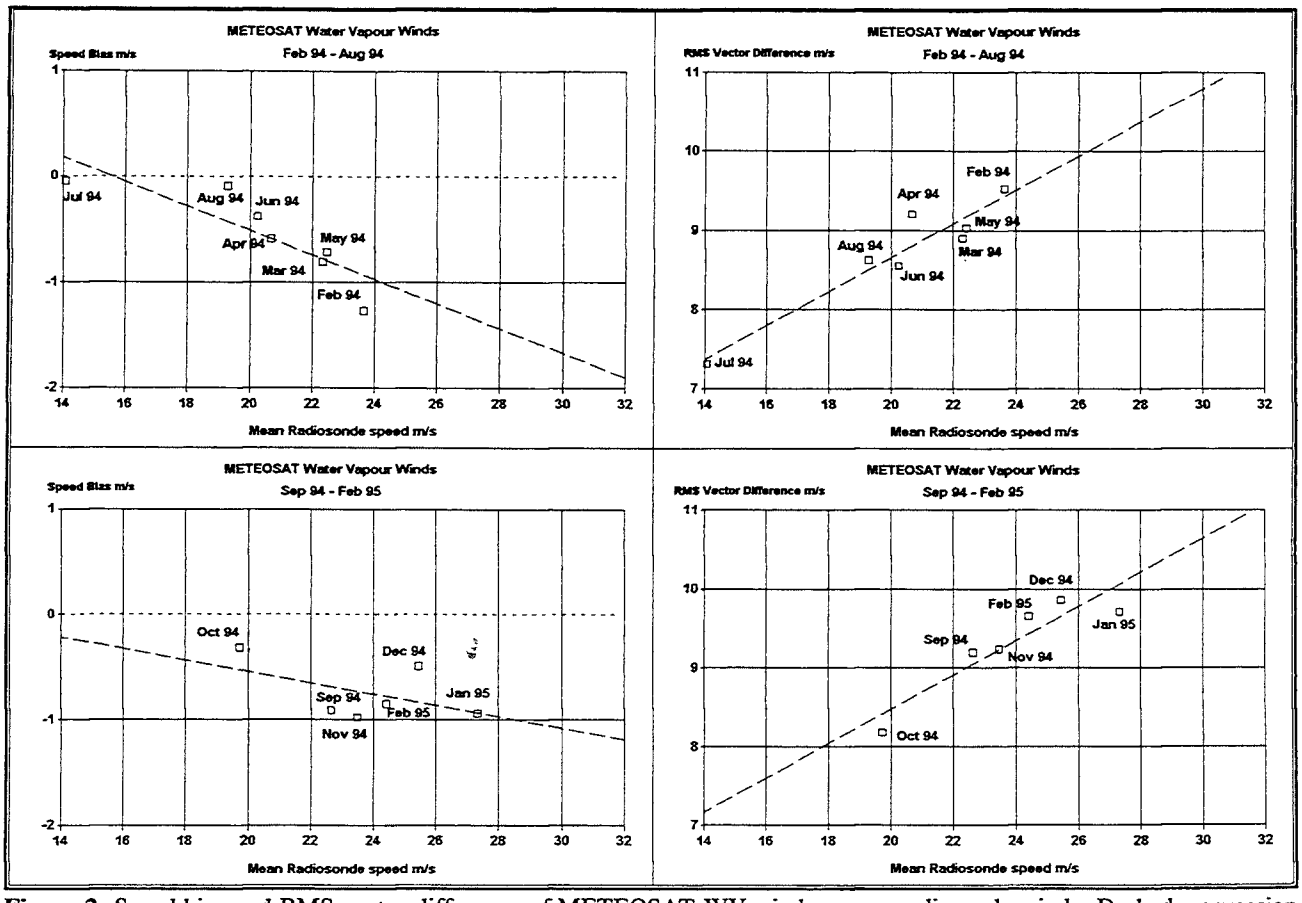

Figure 2: Speed bias and RMS vector difference of METEOSAT WV winds versus radiosonde winds. Dashed: regression lines.

A correlation of the speed bias with average wind speed is also found for the water vapour winds, with a similar slope of the regression line as for IR cloud motion winds. However, the average speed bias of WV winds is smaller than for IR cloud motion winds.

Verification with NWP data shows a different picture. Results supplied by ECMWF and UK Meteorological Office (not shown in this paper) indicate that there is a tendency towards zero or positive speed bias for most speed classes.

The bias/speed scatter diagrams in Figure 2 look very similar to those for the IR cloud motion winds in Figure 1. This applies to the variance of monthly values, their locations in the diagram relative to the regression line, and the slopes of the regression lines. Hence, the information from these diagrams is merely the same as for the IR cloud motion winds.

The effect of degraded image quality during the months of July and August 1994 is not evident from the scatter diagrams.

Scatter diagrams of RMS vector difference between WV and radiosonde winds in the right part of Figure 2 show that monthly averages are similarly well aligned along a linear regression line as for IR cloud motion winds.

Scatter diagrams since February 1994 look very similar to those for the IR cloud motion winds.

more difficult here to find and explain anomalies in Figure 2.

LONG TERM EVOLUTION OF HIGH LEVEL IR CLOUD MOTION AND WATER VAPOUR WINDS

lower part of Figure 3 shows the long term evolution of METEOSAT High Level IR Cloud ion Winds since 1984, and the effects of changes to the wind extraction scheme at the different ds. The units plotted in the diagrams are averages over periods, and the associated regression of monthly averages within each period.

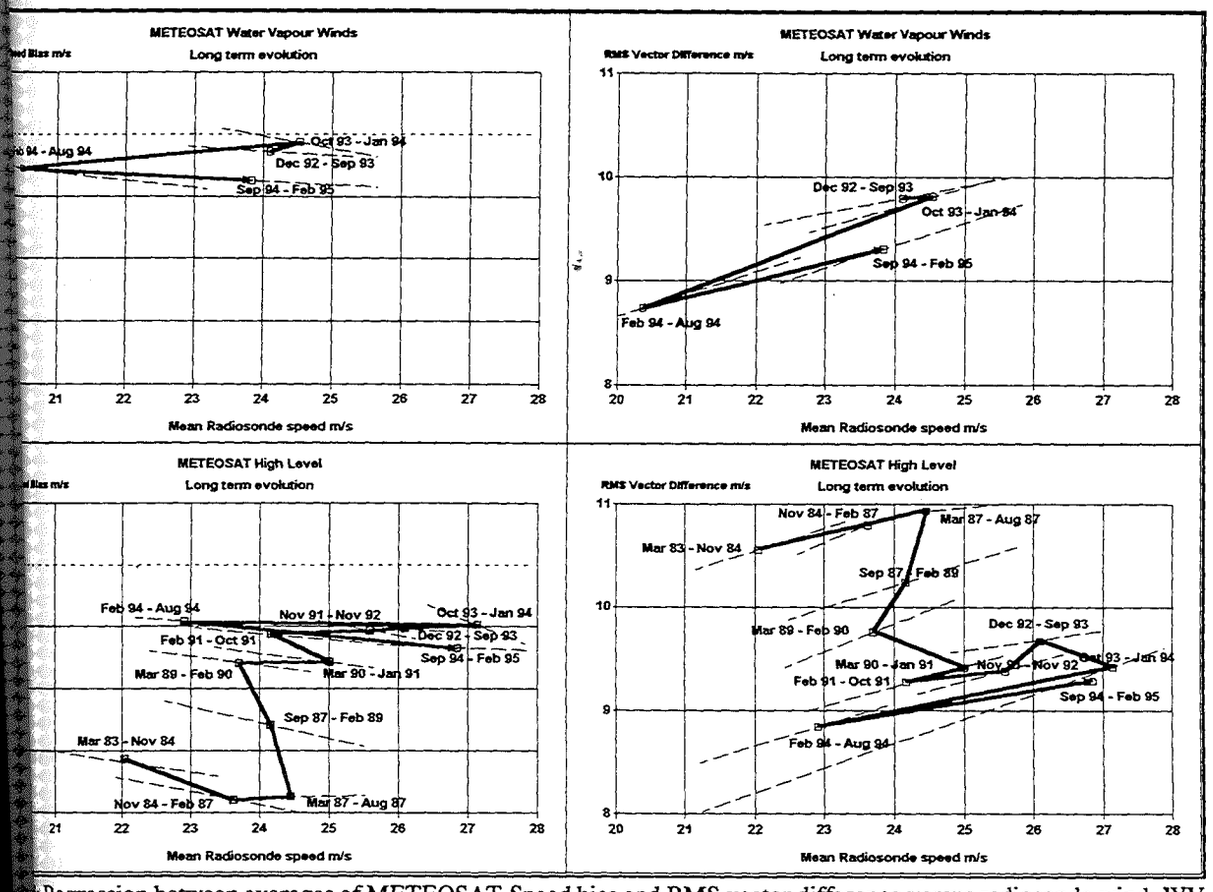

Regression between averages of METEOSAT Speed bias and RMS vector difference versus radiosonde wind, WV p) and High level winds (bottom). Dashed: regression lines throughout the periods.

tory is drawn in each diagram to show the evolution from the oldest to the most recent Trajectory sections parallel to regression lines indicate that performance changes are caused nal effects only. On the other hand, lateral separation between regression lines indicates erformance changes.

dent from Figure 3 there has been great reduction of speed bias and RMS vector difference motion winds since 1984. The improvement has been slower after 1991, and a saturation een in particular for the speed bias where it seems as if the long term goal of -1 m/s cannot oved further.

r conclusion can be drawn for the RMS vector difference except that further improvement

was possible even during the last months. However, there were also two periods when performance was degraded, e.g. those starting December 1992 and February 1994.

The summary diagrams of the WV winds in the upper part of Figure 3 show a similar evolution. Using the regression lines as a supporting tool, it is possible to estimate the performance difference between cloud motion winds and WV winds. Considering the period between September 1994-February 1995 and referring to a reference wind speed of 25 m/s, the RMS vector difference would be estimated at 9.6 m/s for WV winds which is larger than the 8.9 m/s estimated for IR cloud motion winds.

The result is opposite for the speed bias which is smaller for the WV winds than for IR cloud motion winds.

There is no degradation of WV wind RMS vector difference after February 1994, and just a little improvement after October 1993, both dates related to significant changes of geometric image quality. Hence, WV winds are less sensitive to image quality.

As a conclusion for the IR cloud motion winds, the most successful changes were the following:

Sep 87	New WV channel calibration scheme.
Mar 89	Use of ECMWF first guess wind for high level winds.
Mar 90	Spatial coherence information used for tracer test and height assignment.
Oct 93	Image rectification by cubic spline interpolation.

5 MEDIUM AND LOW LEVEL

Scatter diagrams in Figure 4 show that the regression between radiosonde wind speed and bias or RMS vector difference is also present for medium and low level winds. However, there is considerable variance between single monthly values so that the slopes of the different regression lines has to be taken with some care.

The effect of bad image quality during the months of July and August 1994 can be seen for the month of July but less clearly for August 1994. The conclusion is that the period from February to August 1994 is rather short, and more than half of the months are anomalous. This shows the limitations of the validation method used in this paper.

The improved correction scheme for the rotating lens effect introduced in September 1994 had a noticeable effect on the low level winds only, while medium level winds perform significantly worse than expected.

Low level winds for the two last months of the statistics, i.e. January and February 1995, look significantly better than the average expected from the regression line. This is most likely the effect from the modified height assignment of low level winds that was introduced in January 1995.

6 LONG TERM EVOLUTION OF MEDIUM AND LOW LEVEL WINDS

The overall performance evolution for medium and low level winds is shown in Figure 6.

There is a general reduction of speed bias since 1984. For low level winds, speed bias is within $\pm$ 1 m/s around zero which is difficult to improve further. For medium level winds, bias values are converging to -1 m/s with some outlier indicating anomalous months.

There has been a long term reduction of the RMS Vector Difference over the time since 1984. The most significant improvements for the medium level winds were observed after the following

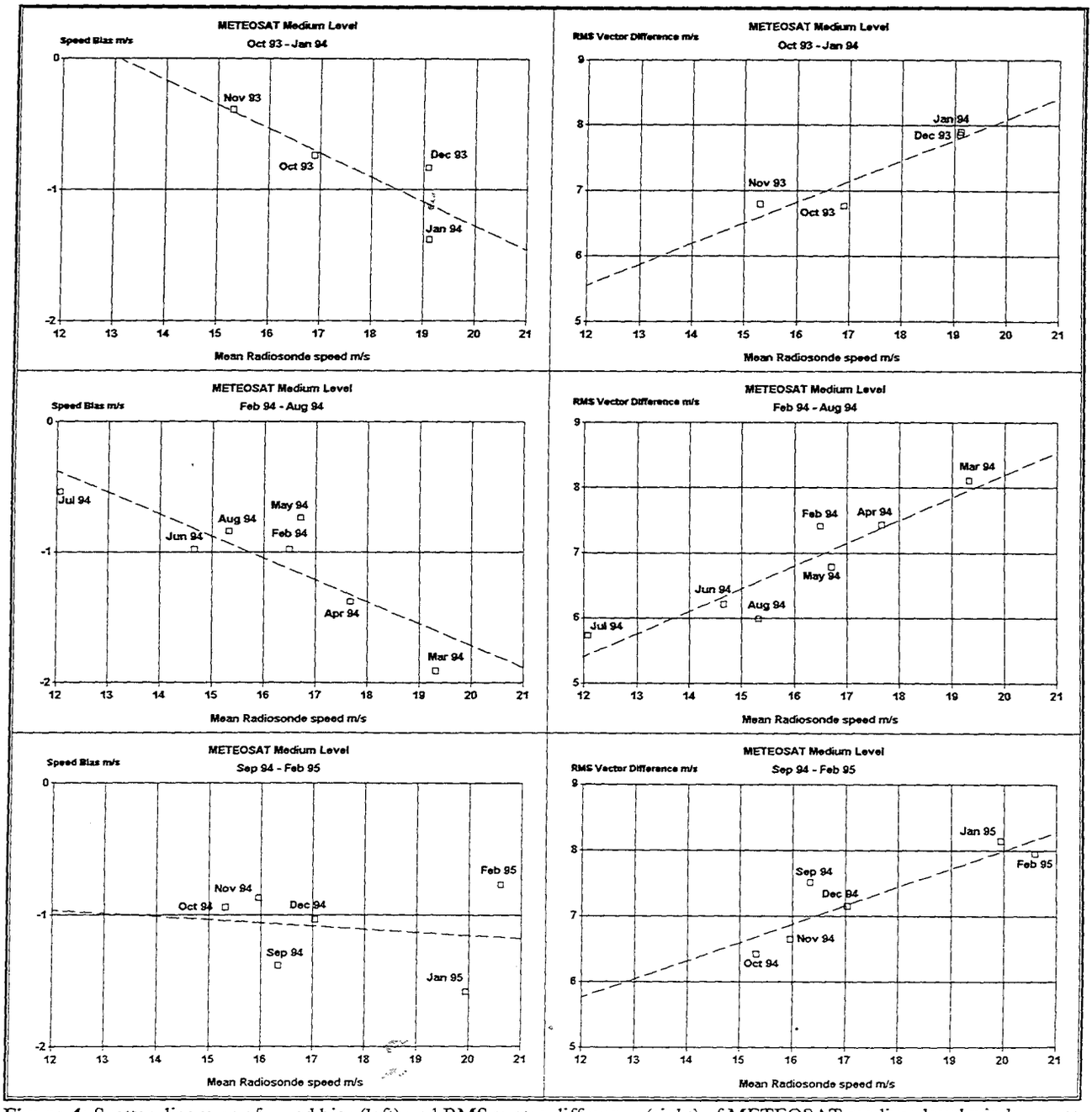

Figure 4: Scatter diagrams of speed bias (left) and RMS vector difference (right) of METEOSAT medium level winds versus radiosonde winds for different periods. Dashed: regression lines.

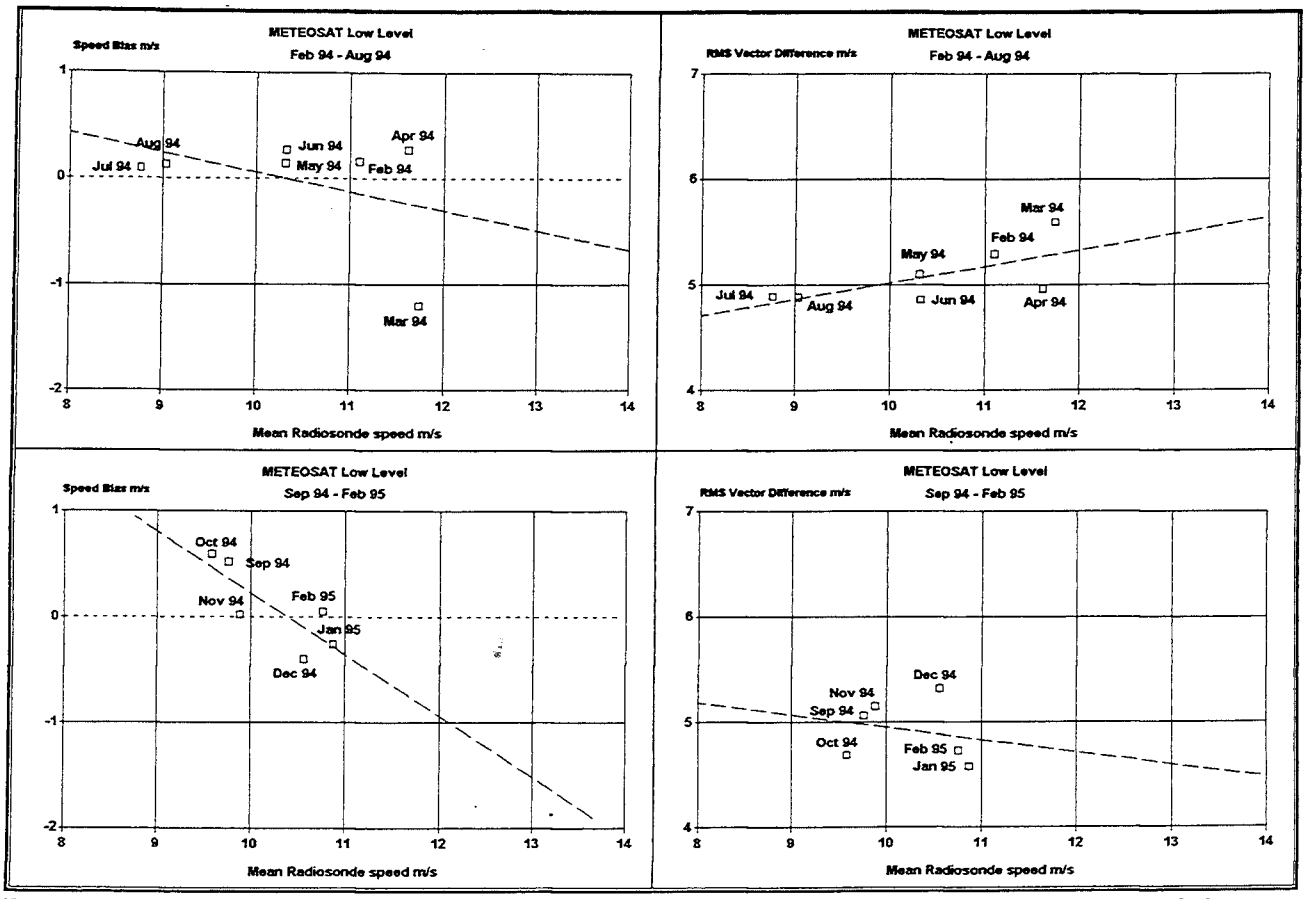

Figure 5: Scatter diagrams of speed bias (left) and RMS vector difference (right) of METEOSAT low level winds versus radiosonde winds for different periods. Dashed: regression lines.

changes:

Nov 84	Major revision of the methods for automatic and manual quality control.
Mar 87	Radiance windowing for high level clouds
Mar 89	Use of ECMWF first guess wind for high level winds.
Mar 90	Spatial coherence information used for tracer test and height assignment.
Oct 93	Image rectification by cubic spline interpolation

The corresponding success dates for the low level winds are:

Nov 84	Major revision of the methods for automatic and manual quality control.
Mar 87	Radiance windowing for high level clouds
Oct 93	Image rectification by cubic spline interpolation
Jan 95	Cloud base height assignment for low level clouds (based on only two months of data, so far)

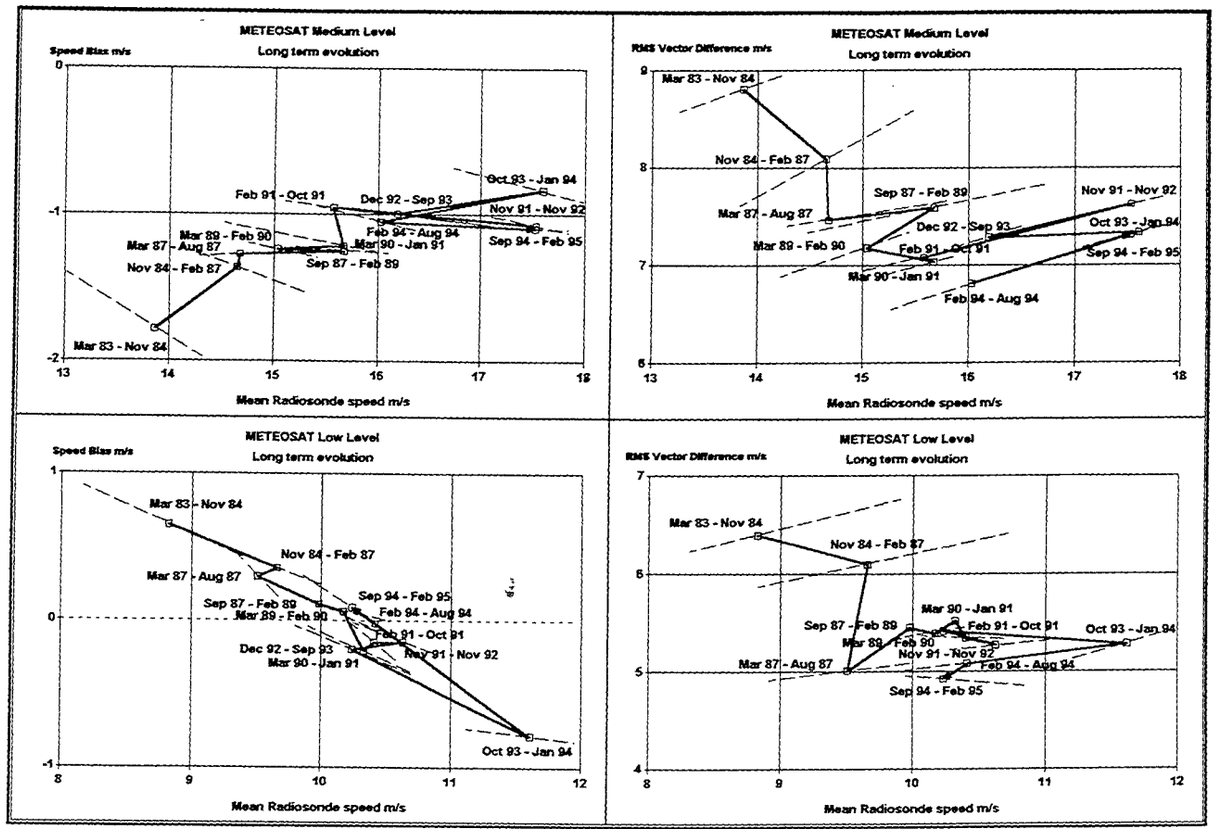

Figure 6: Long term evolution diagrams of medium and low level winds. Dashed: regression lines of the individual periods.

7 CONCLUSION

The new WV winds are of nearly comparable quality as the high level cloud motion winds with an RMS Vector Difference about 0.7 m/s greater than for high level cloud motion winds.

Improvement at medium and low level is also visible, the actual dates of the improvement being different from high level winds.

The introduction of the new rectification scheme had a noticeable positive impact on cloud motion winds at all three levels, but not on WV winds.

The transition from METEOSAT 4 to METEOSAT 5 in February 1994 had a negative effect on cloud motion wind quality but was partially corrected by a software improvement in September 1994.

The speed bias at all three levels has been reduced to a level which is very difficult to improve further.

There has been improvement of wind quality at all height levels until very recently, which justifies and encourages further effort.

CGMS-XXIII WP-13
Prepared by Japan
Agenda Item: IV/1

Current Status of GMS Wind Derivation

The monthly mean differences between Cloud Motion Winds (CMWs) and radiosonde winds were calculated in the same way as the International Comparison of the Satellite Winds. Vector and speed differences from April 1989 to February 1995 are shown in Figs. 1 and 2.

1. Low-level

The Root Mean Square (RMS) vector differences are smaller than 5.0 m/s since 1991. And the absolute values of the speed differences are smaller than 0.5 m/s since 1992 except for February and June 1994. These comparison results show that the quality of low-level CMWs has been good.

2. High-level

The Meteorological Satellite Center (MSC) had made efforts concentrated on the improvement of high-level CMWs from April 1990 to April 1993. The details were shown in wp-16, CGMS XXII.

The quality of high-level CMWs was improved in stages corresponding to the changes of the height assignment method and the employment of improved manual quality control software from April 1990 in spite of the increasing mean CMWs speed. The average values of RMS vector differences and absolute values of the speed differences after April 1994 are 8.2 m/s and 1.1 m/s respectively. High-level CMWs have been kept good in quality.

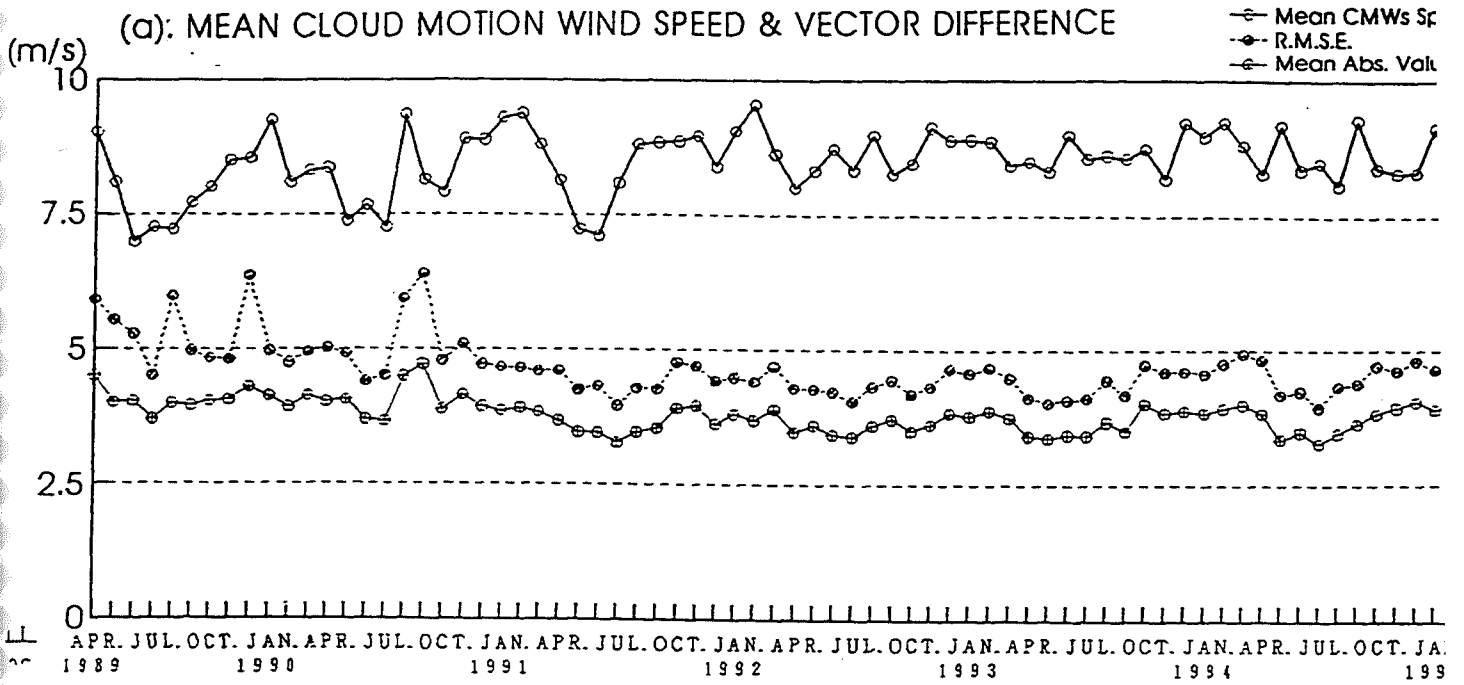

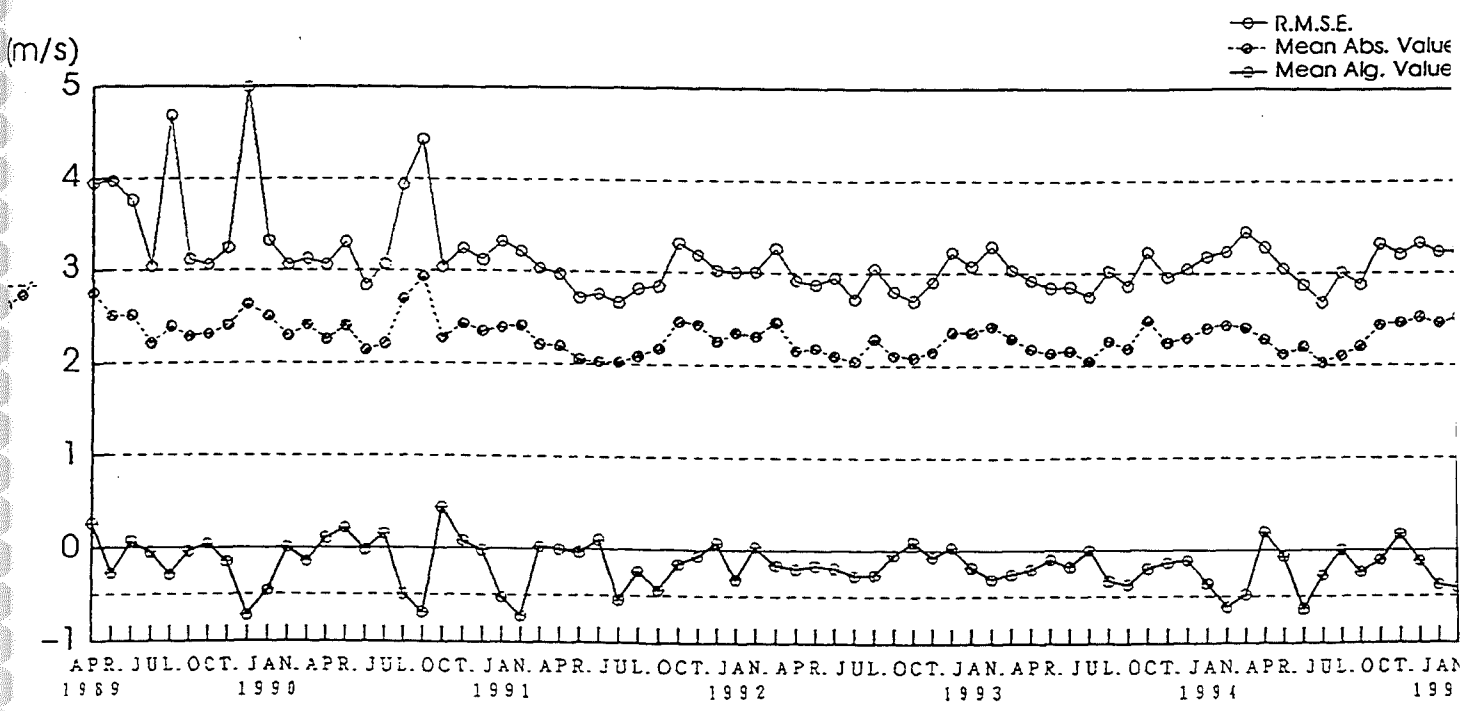

Fig.1 Monthly means of differences between low-level CMWs and radiosonde wind.
(a). mean CMWs speed & vector differences, (b). speed differences.

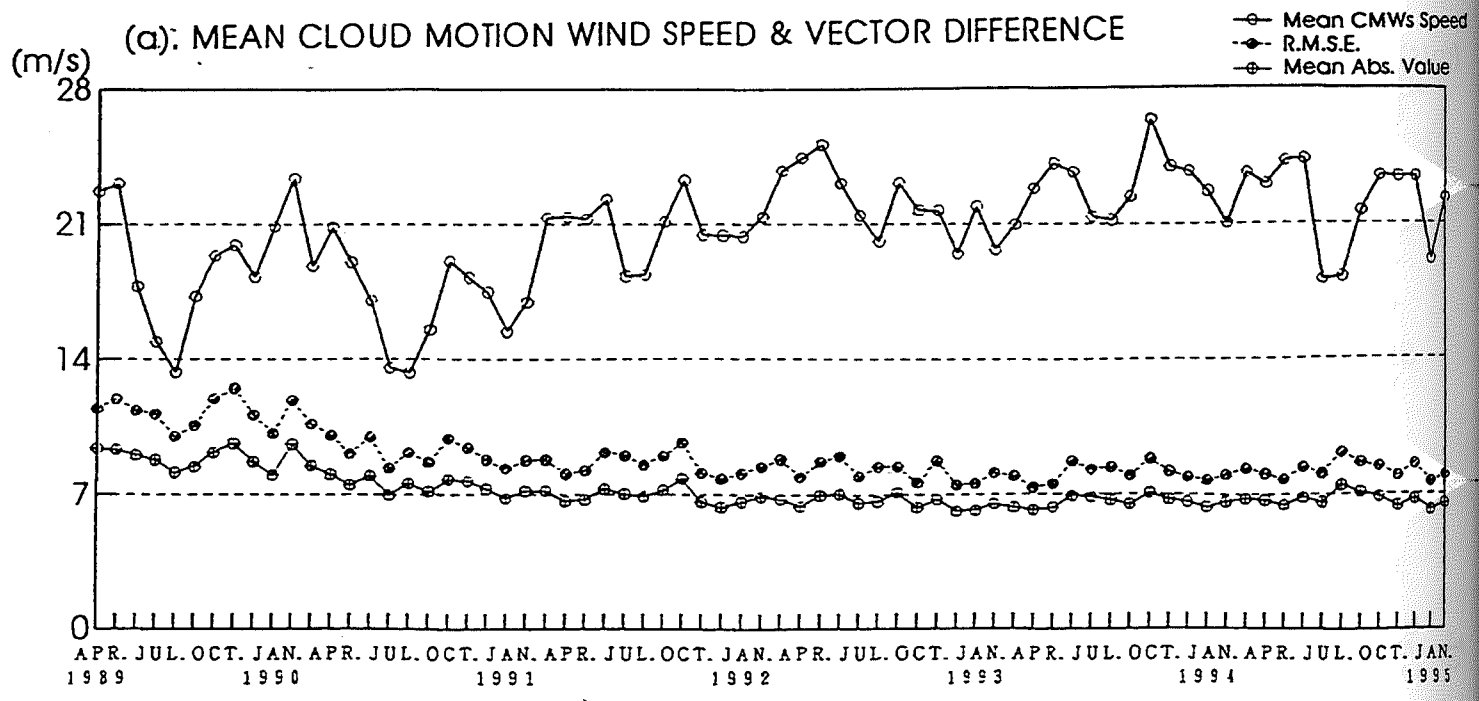

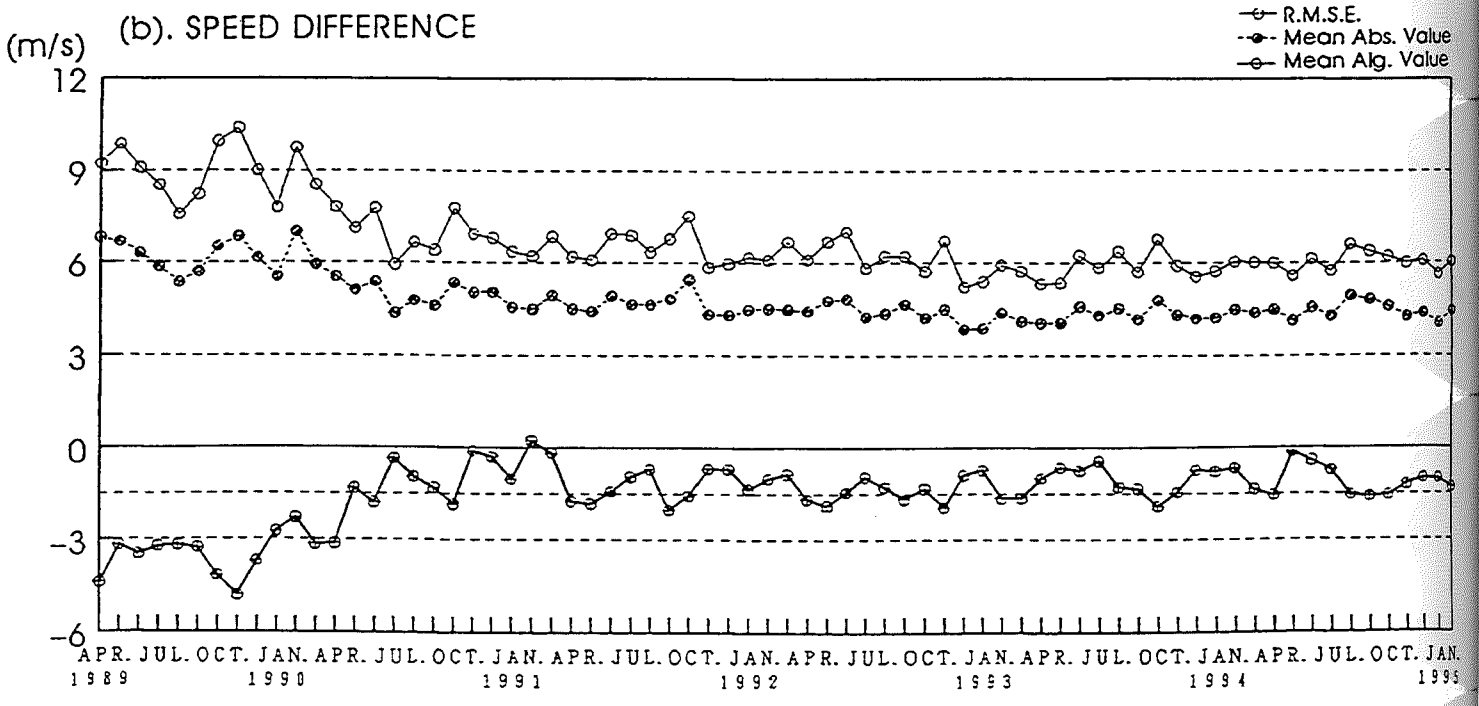

Fig.2 Same as Fig. 1, but for high-level CMWs

CGMS XXIII
USA WP-26
Agenda Item WG IV/1

DERIVATION OF GOES WIND VECTORS AND WIND PERFORMANCE STATISTICS

W. Paul Menzel

Advanced Satellite Products Project
Office of Research and Applications
National Environmental Satellite Data and Information Service
NOAA, Madison, Wisconsin

Steve Nieman

Cooperative Institute for Meteorological Satellite Studies
University of Wisconsin - Madison
Madison, Wisconsin

NESDIS operational winds are produced using an automated winds algorithm for mid and upper level winds (Merrill et al., 1991). This technique uses an objective pattern matching technique (Space Science and Engineering Center, 1985) in a sequence of three half hourly infrared window (IRW) images to estimate a velocity. Cloud heights are assigned to the higher of the CO_2/IRW ratio and the IRW estimates for GOES-7; for GOES-8 it is the higher of the H_2O/IRW intercept and the IRW estimates (Nieman et al., 1993). The preliminary height assignments are modified objectively as necessary after assimilation with other wind estimates (Hayden, 1993). As of late 1994, GOES wind speeds are also adjusted to reduce to slow bias; a percentage of the model guess speed is added to the GOES wind estimate (currently 7%).

With GOES-8 wind processing, tracer selection has been improved so that spatial coherence of the radiances within the selection box is used as a filter. Too much coherence eliminates a tracer from consideration; this filters out coastlines and leading edges of thunderstorm anvils. Too many radiance clusters also eliminates a tracer; this filters out mixed level scenes. The new tracer selection algorithm yields 50% more wind vectors.

For the GOES-7 wind fields, following objective quality control, manual quality control is performed at an interactive computer terminal modelled after the Man computer Interactive Data Access System (Suomi et al., 1983); wind fields are investigated for excessive acceleration in successive image pairs, horizontal and vertical consistency of neighboring vectors, and excessive deviations from the first guess and rawinsondes. Manual quality control is not performed on the GOES-8 wind fields. NESDIS intends to eliminate the manual quality control later in 1995.

The following chart indicates the quality of the GOES wind vectors as compared to wind measurements by radiosondes over the continental United States. All values shown are for objectively edited winds. The impact of manual quality control is not indicated; we find that manual editing usually has no impact on the satellite vector root mean square difference (srmse) with respect to radiosondes, but it does marginally reduce the slow bias (sbias) of the upper level vectors.

The GOES-7 cloud drift winds srmse has stabilized in the past year between 7.0 and 7.5 m/s; it does not vary with the seasonal mean wind speeds (roughly 25 m/s in the winter and 15 m/s in the summer plotted as rspd/10). The slow bias (sbias) of the GOES-7 winds has gradually been reduced over the past two years, with values less than 2 m/s for the past year. The GOES-7 srmse is typically within 0.5 m/s of the colocated NMC model 6-hour forecast guess root mean square error with respect to the radiosondes (grmse). GOES-8 cloud drift winds for 1995 show srmse between 6.5 and 7.0 m/s and sbias less than 1.0 m/s.

Several changes in the processing procedures are noted in the following table, as they affected the overall quality of the satellite derived cloud motion wind vectors.

Table. Recent Milestones in the Operational Winds Processing

April 1992	Autowinds operational at NESDIS
Winter 1992-93	00z objective editing not being done due to error
Winter 1993-94	First cold season without reduced wind quality
September 1994	G-7 winds moved from mainframe to RISC workstation; no degradation in quality
Oct-Nov 1994	G-8 winds production begins at CIMSS in reserach mode. Improved G-8 wind algorithm includes * H2O/IRW intercept height assignment * Slow bias adjustment * Improved tracer selection
December 1994	G-8 winds production moved to NESDIS. Slow bias adjustment included in G-7 operational winds

REFERENCES

Hayden, C. M., 1993: Recent research in the automated quality control of cloud motion vectors at CIMSS/NESDIS. Proceedings of the Second International Wind Workshop, Dec 13-15, Tokyo, Japan, EUMETSAT publication ISSN1023-0416, 219-226.

Merrill, R. T., W. P. Menzel, W. Baker, J. Lynch, and E. Legg, 1991: A report on the recent demonstration of NOAA's upgraded capability to derive satellite cloud motion winds. Bull. Amer. Meteor. Soc., 72, 372-376.

Nieman, S. A., J. Schmetz, and W. P. Menzel, 1993: A Comparison of Several Techniques to Assign Heights to Cloud Tracers. Jour. Appl. Meteor., 32, 1559-1568.

Space Science and Engineering Center, 1985: Cloud drift winds. McIDAS Applications Guide, 11.1-11.25. A Space Science and Engineering Center Manual.

Suomi, V. E., R. Fox, S. S. Limaye, and W. L. Smith, 1983: McIDAS III: A modern interactive data access and analysis system. J. Clim. Appl. Meteor., 22, 714-724.

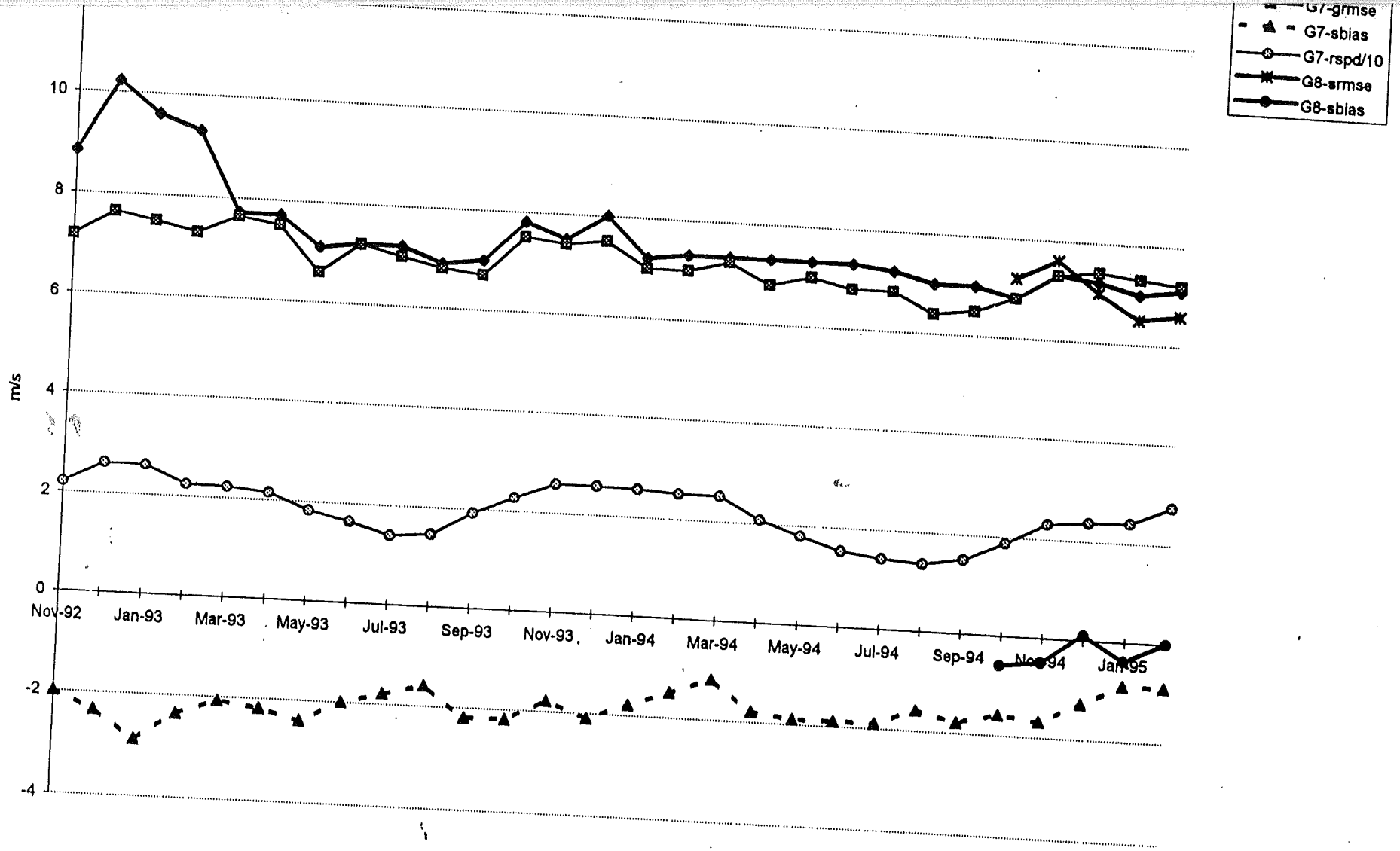
G7-grmse
G7-sbias
G7-rspd/10
G8-srmse
G8-sbias
m/s
10
8
6
4
2
0
-2
-4
Nov-92
Jan-93
Mar-93
May-93
Jul-93
Sep-93
Nov-93
Jan-94
Mar-94
May-94
Jul-94
Sep-94
Jan-95

PRESENT STATUS OF WATER VAPOUR WIND EXTRACTION AT ESOC

Abstract

The first wind vector fields derived automatically from consecutive water vapour images were produced at the European Space Operations Centre (ESOC) already in 1990. Intensive development work related to the different aspects of the derivation technique lead to a pre-operational scheme, which produced water vapour wind vector (WVWV) fields twice per day already in 1992. During 1992 further refinements in the areas of height assignment and automatic quality control further improved the quality and the product derivation moved after extensive validation into an operational phase in November 1993 with four vector fields per day. This paper gives a brief overview of the present quality of the WVWVs and the major improvements which have led to the present status. Furthermore some results from a new automatic quality control prototype are presented.

1 Introduction

The depiction of upper tropospheric flow with the aid of Cloud Motion Winds (CMWs) derived from consecutive infrared (IR: 10.5 -12.5 μm) has been successful over a decade. The use of water vapour (WV: 5.7-7.1 μm) images for winds derivation has equally been recognized as a possible source for the derivation of wind fields, but the use of the WV wind vectors (WVWVs) as single level measurements has remained problematic. At the European Space Operations Centre (ESOC) WVWVs have been produced regularly since 1992 and operationally four times per day since November 1993. The major breakthrough to this achievement was the introduction of a new height assignment method and an enhanced quality control.

2 Height assignment of WVWVs

During the development phase (Laurent, 1990) the possibility to assign a representative height according to the WV weighting function was extensively studied, but a stable height assignment method was not found. It was therefore decided to derive a simple height assignment based on the 25% coldest water vapour pixels. This method provides a rough height estimation in all atmospheric conditions, but it was found that the quality was on the average inferior to the CMWs. During the tuning phase in 1992 (Holmlund, 1993) a new height assignment scheme for areas where medium or high clouds are present was developed. In high cloud areas the IR Equivalent Black Body Temperature (EBBT) of the coldest cloud is used for the height assignment. In areas where only medium level clouds are identified, the EBBT derived from the WV pixels colder than the cloud mean value is utilised. The new improved height assignment schemes were validated with statistics derived from collocated radiosonde measurements. It was shown that in high cloud areas the RMS speed difference improved by 0.5 m/s and speed bias with 1.4 m/s. In the medium cloud areas the speed bias remained almost the same, but the vector difference RMS still improved by 0.3 m/s.

3 Automatic quality control of WVWVs

The CMWs are at present surpassed to an automatic quality control (AQC) and a manual quality control (MQC). Of 2-2500 derived vectors roughly half are subjected to MQC. Winds rejected by symmetry check (a comparison of the two vectors derived from a sequence of three images) are removed completely and winds marked suspect by a forecast check are scrutinised by experienced shift meteorologists. As the WVWVs are potentially produced in 3500 segments it is not feasible to perform a MQC. Therefore also the use of forecast for AQC is doubtful as there is an increased risk that a tight forecast check would actually remove winds important to the forecast. The sole use of the symmetry check is also not sufficient to remove all obviously bad vectors. In order to produce a more internally consistent wind field a local consistency check was developed. This check compares each wind vector to its neighbouring vectors and it is only accepted if one of the surrounding vectors is very similar in speed, direction and height. The symmetry check improved the vector difference RMS with roughly 1 m/s and the speed bias 0.5 m/s in high cloud areas. In the medium cloud areas the improvements were clearly smaller (0.2 - 0.3 m/s) and the overall quality in the medium cloud areas remained worse than in the high cloud areas. Therefore it was decided to disseminate only winds derived in high cloud areas.

4 Present quality of the WVWVs

The modifications described in sections 2 and 3 improved the quality of the WVWVs to an operational level. Figure 1 presents the WVWV-radiosonde speed bias and vector RMS statistics for collocated radiosondes. The same statistics for CMWs are simultaneously shown.

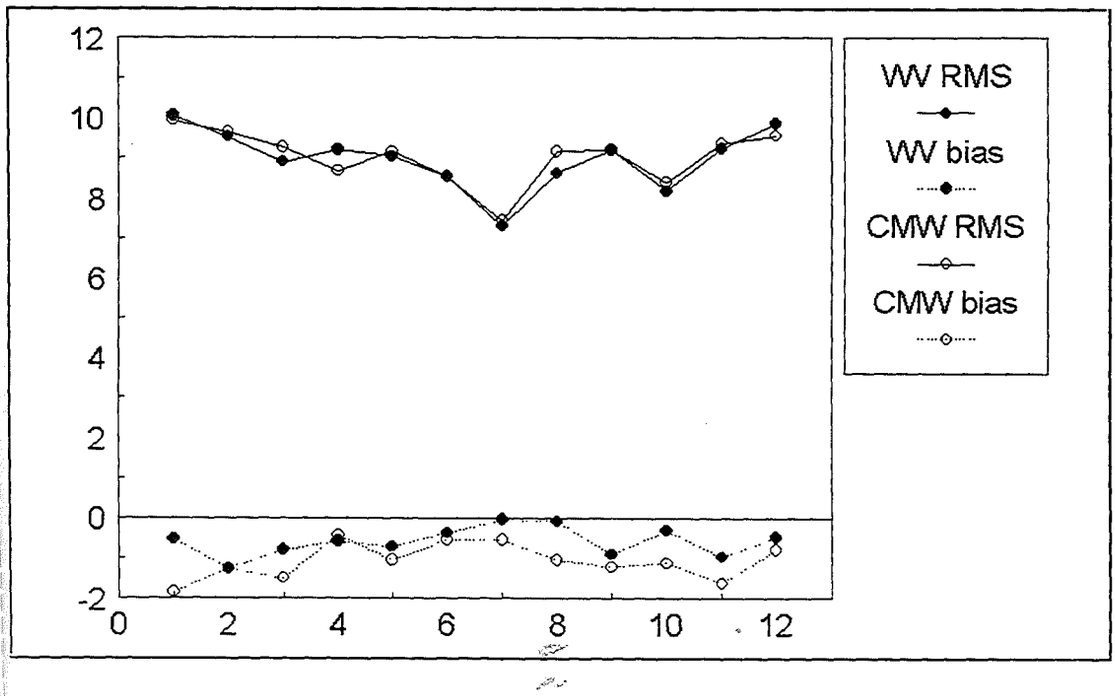

Figure 1. WVWV-radiosonde and CMW-radiosonde statistics for 1994.

The WVWVs and the CMWs are according to Figure 1 of an comparable quality. It should however be noted that the mean wind speed tends to be lower for the WVWVs than for the CMWs. This would indicate that the CMWs are still superior to the WVWVs. Table 1 presents the statistics for March 1995 for collocated CMW-WVWV-radiosonde measurements.

	Number of collocations	Speed bias (m/s)	Vector diff. RMS (m/s)	Mean R/S speed (m/s)
CMW	797	-1.5	8.5	26.0
WVWV	797	-1.3	8.4	26.1

Table 1. Collocated CMW-WVWV-radiosonde statistics.

These statistics are derived only using measurements from segments where both the IR and the WVWVs were successful. It is obvious that collocated winds are of equal quality implicitly indicating that outside the overlap area the WVWVs are slower and hence maybe not as good than the rest. The difference in overlap could be a result of different quality control, but it is also possible that the IR image filtering is not successful in certain situations. This could be an indication that when image filtering is difficult, also height assignment is less reliable.

5 Quality indicators for WVWVs

The present operational AQC for the WVWVs is only accepting vectors which pass all tests. Furthermore each test is a binary function only returning the value good or bad. During the tuning of the WVWV extraction scheme it was noted that several tests seemed to be capable of assigning different levels of reliability to the individual vectors. During the prototype development of a Transputer Augmented Workstation (TAW) (Holmlund, 1994) a sophisticated AQC tool was implemented. The tool consists of 15 normalised tests which can be combined to give an overall quality mark to every vector. During a two week validation campaign in August and September 1994, hourly wind fields were disseminated to ECMWF (European Centre for Medium range Weather Forecasts) for validation. Table 2 shows the relationship between the quality as specified by the TAW AQC and vector RMS and speed bias as derived against comparisons against the ECMWF analysis.

Table 2 clearly indicates that the AQC tool is capable of sorting the WVWVs into 5-6 useful quality classes. In comparing the results with the operational WVWVs the lower mean wind speed of the TAW good quality WVWVs should be noted. This is a result of the fact that the TAW statistics includes significantly more slow winds, especially winds slower than 5 m/s. The high mean speed of the two very low quality classes are results of a large number of spurious vectors, which can be visually verified to be completely wrong.

TAW quality mark	Number of cases	Speed correl.	Speed bias (m/s)	Vector RMS diff (m/s)	Mean vel. (m/s)
0.0..0.1	49799	-0.07	33.8	55.6	45.5
0.1..0.2	65064	0.03	14.7	36.9	27.1
0.2..0.3	81652	0.21	4.4	23.2	16.9
0.3..0.4	89090	0.40	0.9	17.3	14.1
0.4..0.5	106283	0.56	-0.2	14.0	13.5
0.5..0.6	111970	0.68	-0.8	11.8	13.4
0.6..0.7	134638	0.77	-0.8	9.8	13.4
0.7..0.8	131798	0.82	-1.0	8.9	13.4
0.8..0.9	81955	0.88	-0.6	7.8	16.6
0.9..1.0	26128	0.93	0.2	6.0	15.8

Table 2 Speed bias and vector difference RMS between ECMWF analysis and TAW WVWVs for different quality classes as specified by the TAW AQC.

Conclusion

he operational WVWVs are of a comparable quality to the CMWs. The WVWVs provide otentially an easy solution to image filtering and a better horizontal coverage. It has also een shown that it is possible to assign a quality mark to each of the derived vectors and that is mark is a true indication of the representativeness of the WVWV as a single level wind easurement. The dissemination of these quality marks together with the derived vector is ghly desirable and would improve the utilisation of this valuable data.

References

lmlund, K., 1993: Operational Water Vapour Wind Vectors from Meteosat Imagery data. ond International Wind Workshop, Tokyo, 13-15 December 1993. EUM P 14, ISSN 3-0416, Eumetsat.

lmlund, K., 1994: Half Hourly Wind Data from Satellite Derived Water Vapour asurements. COSPAR 30th Scientific Assembly, Hamburg 1994.

rent, H., 1990: Feasibility Study on Water Vapour Wind Extraction Techniques. oratoire de Meteorologie Dynamique du CNRS, Ecole Polytechnique, Palaiseau, France.

CLOUD MOTION WINDS FROM VISIBLE METEOSAT IMAGES

Since June 1994 cloud-motion winds from Meteosat full resolution visible images (VIS-CMWs) have been derived on a daily basis at 11 UTC at the European Space Operations Centre (ESOC). The derivation technique for the VIS-CMWs is conceptually similar to the IR-CMW retrieval method as described in Schmetz et al. (1993) However, it should be noted that the height assignment of the VIS-CMWs relies on the cloud brightness temperature obtained in the infrared channel of Meteosat and that the derivation of VIS-CMWs is currently restricted to marine regions where no high- or medium-level clouds are present.

Figure 1 provides an example of the VIS-CMW product as obtained with one production run for 1100 UTC 2 July 1994. A total of 3488 low-level VIS-CMWs was produced. This particular example shows that the derived VIS-CMWs clearly depict the low-level flow over the marine stratocumulus regions down to mesoscale wind features.

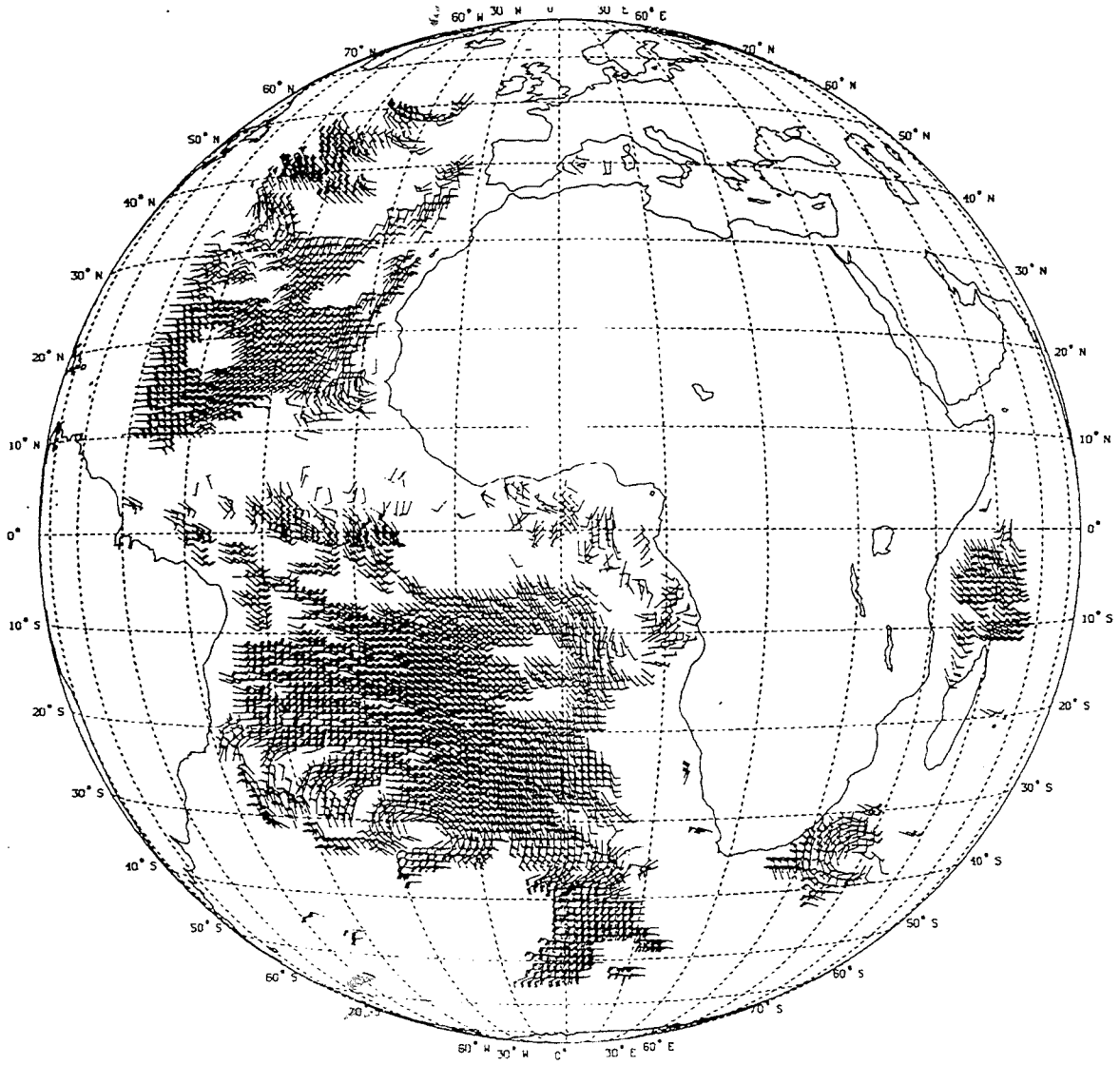

Fig. 1. Cloud-motion winds from Meteosat visible images (VIS) for 1100 UTC 2 July 1994.

The monthly mean speed bias and rms vector difference between disseminated low-level (<700 hPa) VIS-CMWs and IR-CMWs and the ECMWF forecast winds for the period of July 1994 through January 1995 is shown in Fig. 2. The monthly mean rms vector difference is about 4,5 ms^{-1} for the VIS-CMWs and about 3 ms^{-1} for the IR-CMWs, while the monthly mean speed bias is about 1,2 ms^{-1} for the VIS-CMWs and about 0,9 ms^{-1} for the IR-CMWs.

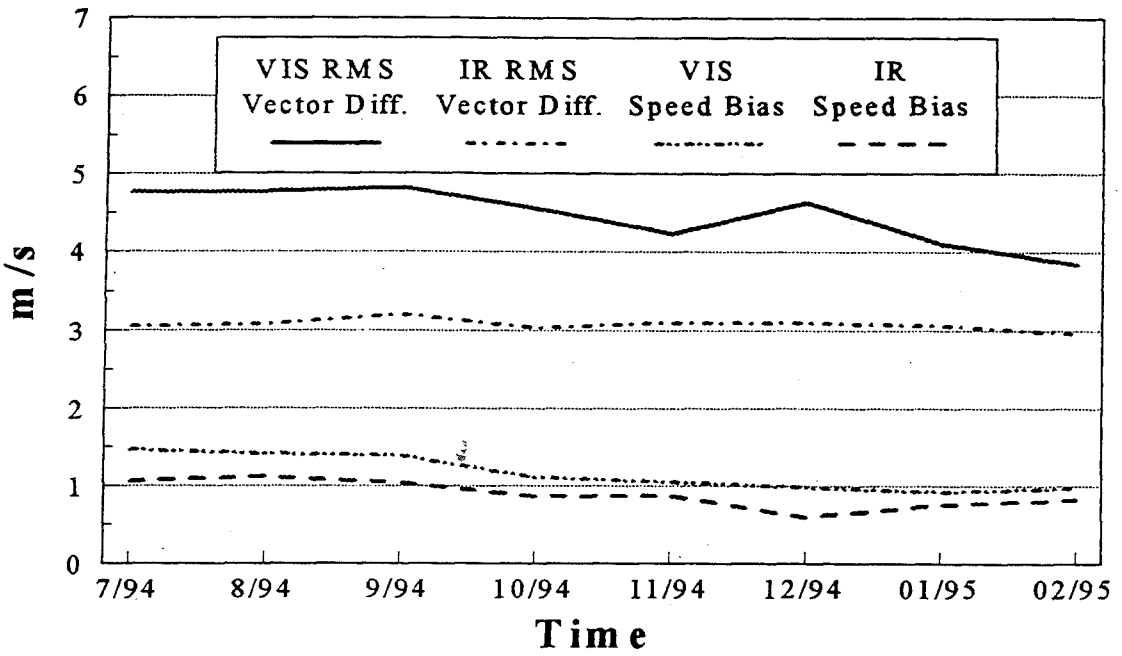

Fig. 2. Monthly mean speed bias and rms vector difference between disseminated low-level (<700 hPa) VIS-CMWs and IR-CMWs and the ECMWF forecast winds for July 1994 through January 1995.

The higher monthly mean rms vector difference and monthly mean speed bias between the VIS-CMWs and the ECMWF forecast winds as compared to the corresponding values for the IR-CMWs are due to two different reasons: i.) The automatic quality control of the IR-CMWs consists already of a rough check against the ECMWF forecast winds, whereas the final quality control of the VIS-CMWs consists of a local consistency check only. ii) The cloud motion winds derived from full resolution visible images may resolve low-level wind field features better than the ECMWF forecast model.

As a conclusion one can state that the VIS-CMWs show a good potential in resolving mesoscale wind features since the spatial resolution of the VIS channel is better than in the IR and WV channel. An important perspective of the VIS-CMWs would be the supply of low-level wind information over the subtropical North Atlantic which could help the early analysis of tropical storm formation (Reed et al., 1986).

Reed, R.J., A. Hollingsworth, W.A. Heckley and F. Delsol, 1986: An evaluation of the performance of the ECMWF operational forecasting system in analysing and forecasting tropical easterly wave disturbances. Part 1: Synoptic investigations. ECMWF Tech. Rep. 58.

Schmetz, J., K. Holmlund, J. Hoffmann, B. Strauss, B. Mason, V. Gärtner, A. Koch and Leo van de Berg, 1993: Operational Cloud-Motion Winds from METEOSAT Infrared Images. *J. Appl. Meteorology*, **32**, 1206-1225.

CGMS-XXIII WP-14
Agenda Item : IV/3
Prepared by Japan

Derivation of Cloud Motion and Water Vapor Motion Winds

1. Introduction

The Meteorological Satellite Center (MSC) of the Japan Meteorological Agency (JMA) has produced cloud motion wind (CMW) since 1978 using visible (VIS) and infrared (IR) channels. GMS series satellites preceding the GMS-4 have only one IR channel and it is therefore difficult to determine the cloud top height of semi-transparent cirrus accurately. Therefore, intensive efforts have been made to improve to certain extent the height assignment to the extracted high-level CMW (Uchida 1991 ; Takata 1993).

The GMS-5 is equipped with water vapor (WV) channel which improves the height assignment and target selection for high-level CMW extraction and also makes it possible to calculate water vapor motion wind (WVMW).

This paper describes CMW and WVMW extraction methods for GMS-5 which has been developed using METEOSAT data.

2. Cloud motion wind extraction

A flow chart of the MSC Cloud Wind Estimation System (CWES) is shown in Fig. 1. CMWs are obtained four times a day, at 00, 06, 12, and 18 UTC using three consecutive images at 30-minute intervals by CWES. There are two ways for target cloud selection and tracking process : manual and automatic. In automatic process, the IR brightness temperature is used for selecting the suitable target cloud to be tracked. Tracking is conducted by a pattern matching technique. In manual process, an operator selects and tracks suitable targets using animation on a display. Two types of CMWs are obtained by the CWES; one is cumulus level or low-level CMW which is derived through the automatic process, and the other is cirrus level or high-level CMW which is derived through a combination of automatic and man-machine interactive processes.

Processes in Fig. 1 are shown in the following subsections.

2.1 Automatic target cloud selection (L_1 and H_1 in Fig. 1)

Automatic target cloud selection is an objective procedure. First, we prepare grid points at intervals of 1° longitude and latitude over the 90°E-171°W and 50°N-49°S domain. We then consider a small area for each grid point whose center coincides with the grid point (hereafter target area). A certain number of pixels is included in the area. A corresponding IR brightness temperature is assigned to each pixel. A histogram of the IR brightness temperatures is made for

the area. The features of the histogram are analyzed to obtain parameters concerning the cloud amount, the cloud-top height, and the thickness of the cloud. We estimate the altitude of cloud (low- or high-level) and determine whether the area has enough cloud so that the grid point can be sent to the next procedure, tracking, by comparing these parameters with threshold values.

For the high-level target selection, a cumulonimbus check is further performed using IR and WV data. Since the cumulonimbus is not good tracer for high-level wind extraction, the area containing cumulonimbus is excluded in this procedure. Using only IR data, it is difficult to distinguish cumulonimbus from thick multi-layered cloud. However, the cumulonimbus is identified by the difference between IR and WV brightness temperatures (Tokuno, 1994).

2.2 Tracking (Matching) (L_2 and H_2 in Fig. 1)

The target area in the middle image of the three sequential images is tracked on previous and subsequent images, 30 minutes before and after the middle image, using cross-correlation. Two successive displacement vectors are calculated from the target in consequence. If the magnitude of the difference between the two successive vectors does not exceed the threshold value, the latter vector is adopted as the resultant wind.

2.3 CMW height assignment

(1) Low-level (L_2 in Fig. 1)

It is widely accepted that the velocity of low-level cloud agrees with that of the environmental wind at the altitude of the cloud base. In the MSC, we made some statistical investigation (Hamada, 1982a and 1982b) and compared the low-level CMW with the velocity observed by a radiosonde, which revealed that the velocity of the low-level CMW well represents the atmospheric wind at the altitude of 850 hPa. Therefore, we assign 850 hPa to each low-level CMW.

(2) High-level (H_2 in Fig. 1)

Since target areas for the high-level wind extraction often contain semi-transparent cirrus and there is no theoretical basis for correlating the emissivity of the semi-transparent cirrus by its temperature, it is difficult to estimate the exact cloud top temperature of the semi-transparent cirrus from IR data. We therefore have used a height assignment table determined by a statistical method until GMS-4. The heights of high-level CMWs have been checked intensively and reassigned if necessary in subsequent man-machine interactive procedure.

After the initiation of GMS-5 operation, the cloud top height of semi-transparent cirrus will be estimated using an IR and WV intercept technique following the theory described by Bowen and Saunders (1984). It is expected that this technique would improve the accuracy of height assignment of high-level CMW and reduce a load of man-machine interactive procedure.

2.4 Objective Quality Control (Q_1 in Fig. 1)

Three types of quality control are provided in the CWES, (a) horizontal consistency

Proceedings of Second International Wind Workshop, Tokyo, 13–15 Dec. 1993. Published by EUMETSAT, 6100 Darmstadt, Germany, EUM P14, p.77–84.

Laurent, H., 1991: Wind extraction from multiple METEOSAT channels. Proceedings of Workshop on Wind Extraction from Operational Meteorological Satellite Data, Washington D.C., 17–19 Sept. 1991. Published by EUMETSAT, 6100 Darmstadt, Germany, EUM P10, p.71–76.

————, 1993: Wind extraction from METEOSAT water vapor channel image data. J. Appl. Meteor., 32, p.1124–1133.

Szantai, A., and M. Desbis, 1991: Wind extraction and validation from the water vapor channel of METEOSAT during The International Cirrus Experiment. Proceedings of Workshop on Wind Extraction from Operational Meteorological Satellite Data, Washington D.C., 17–19 Sept. 1991. Published by EUMETSAT, 6100 Darmstadt, Germany, EUM P10, p.63–69.

Takata, S., 1993: Current status of GMS wind and operational low–level wind derivation in a typhoon vicinity from short–time interval images. Proceedings of Second International Wind Workshop, Tokyo, 13–15 Dec. 1993. Published by EUMETSAT, 6100 Darmstadt, Germany, EUM P14, p.29–36.

Tokuno, M., 1994: Classification of cloud types based on data of multiple satellite sensors. Adv. Space Res., Vol. 14, No. 3, p.(3)199–(3)206.

Uchida, H., 1991: Height assignment of GMS high–level cloud motion wind. Proceedings of Workshop on Wind Extraction from Operational Meteorological Satellite Data, Washington D.C., 17–19 Sept. 1991. Published by EUMETSAT, 6100 Darmstadt, Germany, EUM P10, p.27–32.

check, (b) vertical shear check, and (c) comparison with Numerical Weather Prediction (NWP) wind. Through these procedures, unreliable wind data are automatically flagged and then assessed in the process of man–machine interactive quality control.

2.5 Man–machine interactive process (H_3 and Q_2 in Fig. 1)

This process is performed using the graphic display and TV display of the image processing console. The TV screen displays animation of time–sequential images in which the resultant CMWs are superimposed with colors given according to height (high or low). The operator examines the resultant CMWs, comparing them with the movement of the target cloud in the animation. On a graphic display, the vector arrows of the CMWs are shown in the same color for the following purposes;

(1) In addition to winds calculated automatically, CMWs are derived in data sparse areas by man–machine interactive processing.
(2) Quality check including reassignment of wind height is performed.

The CMWs considered reliable through this process are coded into WMO SATOB format and sent to the JMA Automated Data Editing and Switching System (ADESS) and transmitted thence to users worldwide via Global Telecommunication System (GTS).

3. Water vapor motion wind extraction

WVMW extraction will be performed automatically four times a day, at 00, 06, 12, and 18 UTC. The WVMW extraction scheme is basically the same as that of CMW using three successive WV images at 30–minute intervals. Manual quality check will not be done on the WVMWs, whereas, CMW data are checked by the manual quality control process as stated above.

3.1 Target selection

Target areas, prepared in the same manner as for CMW, are selected using the middle image of three successive WV images. If the lowest WV brightness temperature in the target area is colder than the threshold temperature, it is selected as a target. Because the feature of WV image is smooth and vague, strict quality assessment of the WV data in the target area is not done by histogram analysis, but is conducted in CMW extraction.

3.2 Tracking

The tracking procedure is the same as that for CMW extraction.

3.3 Height assignment

The tracked targets for WVMW are clouds at mid– and/or high–levels and water vapor structures. The observed WV radiances come from the clouds and the atmosphere above the

background.

Previous studies on WVMW extraction from METEOSAT WV images employed the height determined from the WV brightness temperature for the height assignment. Namely, Szantai et al. (1991) and Laurent (1991 and 1993) used the lowest and the lowest 20% of the temperature in the target area(32 lines x 32 pixels).

In a semi-operational WVMW extraction system at the European Space Operations Center, the lowest 25% of the WV brightness temperature in the same-sized target is adopted. Holmulund (1993) performed the statistical comparison between WVMWs and collocated radiosonde winds using several height assignment methods and revealed that (a) the difference in the two winds is smaller in areas where high-level clouds are present than in areas where no high-level clouds are present and (b) the smallest difference is achieved with the height assignment method using cloud top height involved semi-transparency correction.

The two height assignment methods were tested at the MSC using preliminary WVMW extracted from METEOSAT data. In one method, the height determined from the WV brightness temperature in the target area is assigned to WVMW. In the other, the height determined by the same method stated before for the WVMW calculated from the target area containing thick clouds or water vapor structures and the cloud top height estimated from IR and WV intercept technique as described in Section 2.3 is assigned to the WVMWs calculated from the target area containing semi-transparent clouds. The result indicates that the height assignment method by the WV brightness temperature and cloud top height was found to be more efficient in height assignment (Uchida, 1993), which agrees with the research by Holmulund. On the basis of this investigation, the latter height assignment method is adopted.

3.4 Objective Quality Control

A quality check of WVMW is performed only automatically. The homogeneity of speed, direction, and height is checked and, if the WVMW is determined to be unreliable, the wind is rejected automatically. WVMWs passed through this process are coded into SATOB format for transmission to users.

We intend to begin transmission after the adjustment of threshold values used in WVMW extraction and the evaluation of data quality.

References

Bowen, R., and R. Saunders, 1984: The semitranspancy correction as applied operationally to METEOSAT infrared data. : A remote sensing problem. ESA Journal, 8, p.125-131.

Hamada, T., 1982a: New procedure of height assignment to GMS satellite winds. Meteorological Satellite Center Technical Note, No. 5, p.91-95.

Hamada, T., 1982b: Representative heights of GMS satellite winds. Meteorological Satellite Center Technical Note, No. 6, p.35-47.

Holmlund, K., 1993: Operational water vapor wind vectors from METEOSAT imagery data.

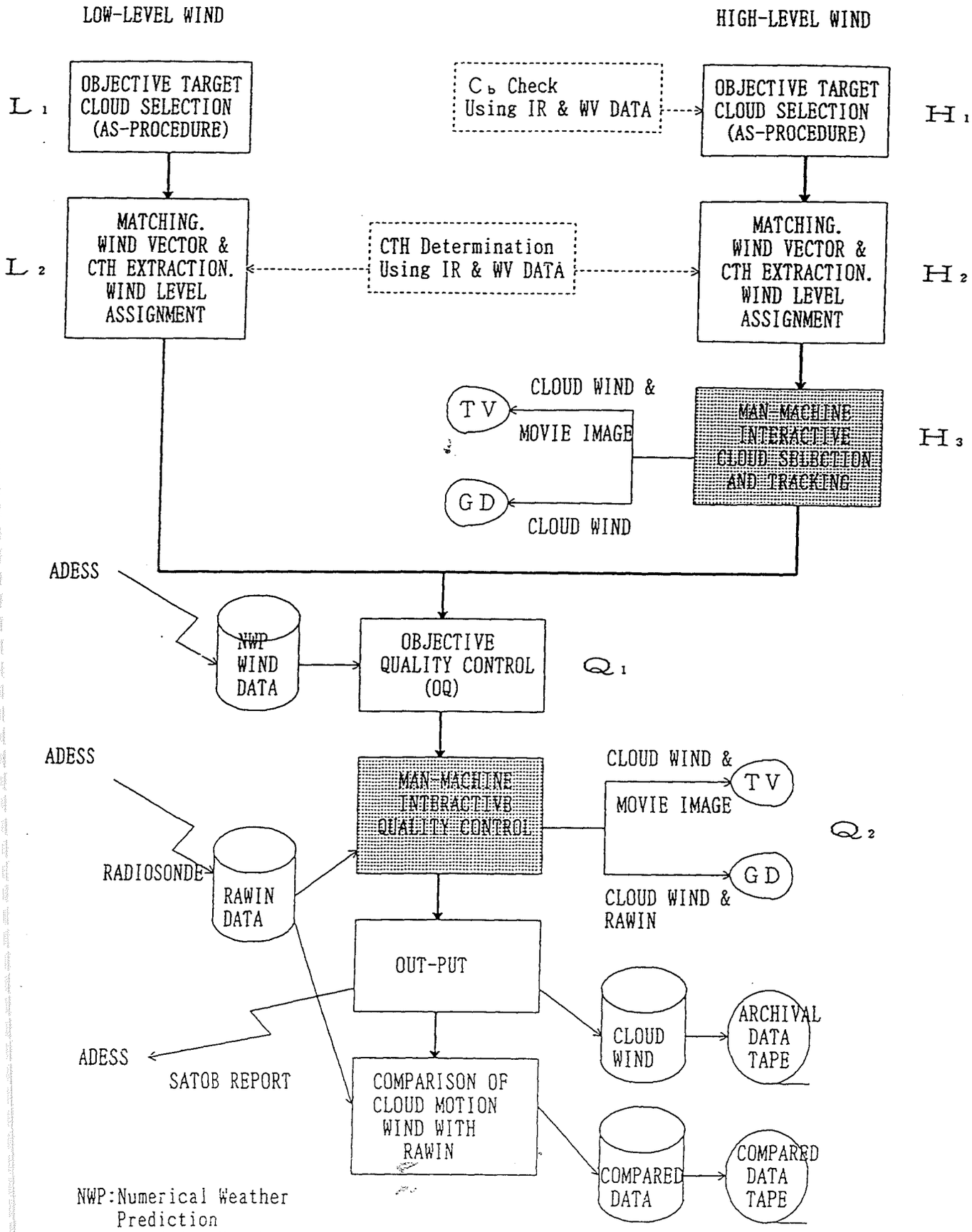

NWP:Numerical Weather Prediction
CTH:Cloud Top Height
ADESS:Automated Data Editing and Switching System

Fig. 1. Flow chart of the Cloud Wind Estimation System (CWES).

Appendix B:

GENERAL CGMS INFORMATION

CHARTER FOR

THE COORDINATION GROUP FOR METEOROLOGICAL SATELLITES (CGMS)

PREAMBLE

RECALLING that the Coordination on Geostationary Meteorological Satellites (CGMS) has met annually as an informal body since September 1972 when representatives of the United States (National Oceanic and Atmospheric Administration), the European Space Research Organisation (now the European Space Agency), and Japan (Japan Meteorological Agency) met to consider common interests relating to the design, operation and use of these agencies' planned meteorological satellites,

RECALLING that the Union of Soviet Socialist Republics (State Committee for Hydrometeorology), India (India Meteorological Department) and the People's Republic of China (State Meteorological Administration) initiated development of geostationary satellites and joined CGMS in 1973, 1978, and 1986 respectively,

RECOGNIZING that the World Meteorological Organization (WMO) as a representative of the meteorological satellite data user community has participated in CGMS since 1974,

NOTING that the European Organisation for the Exploitation of Meteorological Satellites (EUMETSAT) has, with effect from January 1987, taken over responsibility from ESA for the METEOSAT satellite system and the current Secretariat of CGMS,

CONSIDERING that CGMS has served as an effective forum through which independent agency plans have been informally harmonized to meet common mission objectives and produce certain compatible data products from geostationary meteorological satellites for users around the world,

RECALLING that the USA, the USSR, and the PRC have launched polar-orbiting meteorological satellites, that Europe has initiated plans to launch an operational polar-orbiting mission and that the polar and geostationary meteorological satellite systems together form a basic element of the space based portion of the WMO Global Observing System,

BEING AWARE of the concern expressed by the WMO Executive Council Panel of Experts over the lack of guaranteed continuity in the polar orbit and its recommendation that there should be greater cooperation between operational meteorological satellite operators worldwide, so that a more effective utilisation of these operational systems, through the coordination and standardisation of many services provided, can be assured,

RECOGNIZING the importance of operational meteorological satellites for monitoring and detection of climate change,

AND **RECOGNIZING** the need to update the purpose and objectives of CGMS,

AGREE

I. To change the name of CGMS to the Coordination Group for Meteorological Satellites

II. To adopt a Charter, establishing Terms of Reference for CGMS, as follows:

OBJECTIVES

a) CGMS provides a forum for the exchange of technical information on geostationary and polar orbiting meteorological satellite systems, such as reporting on current meteorological satellite status and future plans, telecommunications matters, operations, intercalibration of sensors, processing algorithms, products and their validation, data transmission formats and future data transmission standards.

b) CGMS harmonises to the extent possible meteorological satellite mission parameters such as orbits, sensors, data formats and downlink frequencies.

c) CGMS encourages complementarity, compatibility and possible mutual back-up in the event of system failure through cooperative mission planning, compatible meteorological data products and services and the coordination of space and data related activities, thus complementing the work of other international satellite coordinating mechanisms.

MEMBERSHIP

d) CGMS Membership is open to all operators of meteorological satellites, to prospective operators having a clear commitment to develop and operate such satellites, and to the WMO, because of its unique role as representative of the world meteorological data user community.

e) The status of observer will be open to representatives of international organisations or groups who have declared an intent, supported by detailed system definition studies, to establish a meteorological satellite observing system. Once formal approval of the system is declared, membership of CGMS can be requested by the observer.

Within two years of becoming an observer, observers will report on progress being made towards the feasibility of securing national approval of a system. At that time CGMS Members may review the continued participation by each Observer.

f) The current Membership of CGMS is listed in an annex to this charter.

g) The addition of new Members and Observers will be by consensus of existing CGMS Members.

ORGANISATION

h) CGMS will meet in plenary session annually. Ad hoc Working Groups to consider specific issues in detail might be convened at the request of any Member provided that written notification is received and approved by the Membership at least 1 month in advance and all Members agree. Such Working Groups will report to the next meeting of CGMS.

i) One Member, on a voluntary basis, will serve as the Secretariat of CGMS.

j) Provisional meeting venues, dates and draft agenda for plenary meetingswill be distributed by the Secretariat 6 months in advance of the meeting, for approval by the Members. An agreed Agenda will be circulated to each Member 3 months in advance of the meeting.

k) Plenary Meetings of CGMS will be Chaired by each of the Members in turn, the Chairman being proposed by the host country or organisation.

l) The Host of any CGMS meeting, assisted by the Secretariat, will be responsible for logistical support required by the meeting. Minutes will be prepared by the Secretariat, which will also serve as the repository ofCGMS records. The Secretariat will also track action items adopted at meetings and provide CGMS Members with a status report on these and any other outstanding actions, four months prior to a meeting and again at the meeting itself.

PROCEDURE

m) The approval of recommendations, findings, plans, reports, minutes of meetings, the establishment of Working Groups will require the consensus of Members. Observers may participate fully in CGMS discussions and have their views included in reports, minutes etc., however, the approval of an observer will not be required to establish consensus.

n) Recommendations, findings, plans and reports will be non-binding on Members or Observers.

o) Once consensus has been reached amongst Members on recommendations, findings, plans and reports, minutes of meetings or other such information from CGMS, or its Working Groups, this information may be made publicly available.

p) Areas of cooperation identified by CGMS will be the subject of agreement between the relevant Members.

COORDINATION

q) The work of CGMS will be coordinated, as appropriate, with the World Meteorological Organisation and its relevant bodies, and with other international satellite coordination mechanisms, in particular the Committee on Earth Obser-

vation Satellites (CEOS) and the Earth Observation International Coordination Working Group (EO-ICWG) and the Space Frequency Coordination Group (SFCG).

Organisations wishing to receive information or advice from the CGMS should contact the Secretariat; which will pass the request on to all Members and coordinate an appropriate response, including documentation or representation by the relevant CGMS Members.

AMENDMENT

r) These Terms of Reference may be amended or modified by consensus of the Members. Proposals for amendments should be in the hands of the Members at least one month prior to a plenary meeting of CGMS.

EFFECTIVE DATE AND DURATION

s) These Terms of Reference will become effective upon adoption by consensus of all CGMS Members and will remain in effect unless or until terminated by the consensus of CGMS Members.

MEMBERSHIP OF CGMS

The current Membership of CGMS is :

EUMETSAT	-	Joined 1987. Currently CGMS Secretariat
India Meteorological Department	-	Joined 1979.
Japan Meteorological Agency	-	Founder Member, 1972
State Meteorological Administration of the PRC	-	Joined 1989
NOAA/NESDIS	-	Founder Member, 1972
Hydromet Service of the Russian Federation	-	Joined 1973
WMO	-	Joined 1973

(The table of Members shows the lead Agency in each case. Delegates are often supported by other Agencies, for example, ESA (with EUMETSAT) and NASDA (with Japan)

ADDRESSES FOR PROCURING ARCHIVE DATA

EUMETSAT (from 1 December 1995)

The Meteosat Data Archive Manager
EUMETSAT
Am Kavalleriesand 31,
64295 Darmstadt
Germany

INDIA

India Meteorological Department
Attention: Director (Satellite Service)
Lodi Road
New Delhi
110003 India

JAPAN

International Meteorological Planning Division
Japan Weather Association
2-9-2, Kanda Nishiki-cho
Chiyoda-ku
Tokyo 100
Japan

PRC

Mr. Xu Jianmin
Director, Satellite Meteorology Center
China Meteorological Administration
46 Baishiqiaolu
Beijing, 100081
People's Republic of China

RUSSIA

Dr. A. Uspensky
NPO Planeta
B. Predtechenskii Per. 7
123242 Moscow
Russia

USA

Satellite Data Services Division (E/CC6)
Room 100, World Weather Building
NOAA/NESDIS
Washington DC 20233
U.S.A.

CONTACT LIST FOR OPERATIONAL ENGINEERING MATTERS

EUMETSAT

Dr. G. Szejwach
EUMETSAT
Am Kavalleriesand 31,
64295 Darmstadt, Germany
Telex: 4197335 emet d
Telephone: +49 6151 807-7

INDIA

Dr. R. R. Kelkar
Directorate of Satellite Meteorology
India Meteorological Department
Lodi Road
New Delhi 110003, India
Telex: 3166412
Telephone: +91 11611710

JAPAN

Mr. K. Ide
Earth Observation Satellite Department
NASDA
Hamamatsu-cho Central Bldg. 10F
1-29-6 Hamamatsu-cho, Minato-ku
Tokyo 105, Japan
Telephone: +813 5401 8651

Mr. K. Kimura
Head/System Engineering Division
Meteorological Satellite Center
3-235 Nakakiyoto, Kiyose
Tokyo 204 , Japan
Telex: 2222163 METTOK J
Telephone: +81 424 93 1111

PRC

Mr. Xu Jianmin
Director
Satellite Meteorology Center
China Meteorology Administration
46 Baishiqiaolu
Beijing, 100081
People's Republic of China
Telex: 22094
Telephone: +86-10-8332277 , Ext. 2367

RUSSIAN FEDERATION

Mr. V. Kharitonov
Russian Federal Service
for Hydrometeorology and Environmental Monitoring
Novovagan' kovsky Street 12
123242 Moscow
Russia
Telex: 411117 RUMS RF
Telephone: +7 095 252 07 08
Fax: +7 095 252 11 58
Internet: vkh@hymet.msk.ru

USA

Mr. G. Davis
Director, Office of Satellite Operations
NOAA/NESDIS, (E/S01)
Room 0226, Mail Stop B
Washington DC 20233, USA
NASCOM: GTOS
Telex: RCA 248376
Telephone: +1 301 457 5130
Internet: gdavis@nesdis.noaa.gov

ADDRESS LIST FOR THE DISTRIBUTION OF CGMS DOCUMENTS

ESA
Dr. D. Andrews
Head of Earth Observation missions
ESA/ESOC
Robert-Bosch-Str. 5
64293 Darmstadt, Germany
Tel: +49 6151 90 2502
Fax: +49 6151 90 30 82

EUMETSAT
Mr. G. C. Bridge
Meteosat Operations Manager
EUMETSAT
Am Kavalleriesand 31,
64295 Darmstadt, Germany
Tel: +49 6151 807-7
Fax: +49 6151 807-555
Tx: 4197335 emet d

EUMETSAT
Mr. J. Lafeuille
International Affairs Officer
EUMETSAT
Am Kavalleriesand 31,
64295 Darmstadt, Germany
Tel: +49 6151 807-7
Fax: +49 6151 807-555
Tx: 4197335 emet d

EUMETSAT
Dr. T. Mohr
Director
EUMETSAT
Am Kavalleriesand 31,
64295 Darmstadt, Germany
Tel: +49 6151 807-7
Fax: +49 6151 807-555
Tx: 4197335 emet d

EUMETSAT
Dr. J. Schmetz
Head of Meteorological Division
EUMETSAT
Am Kavalleriesand 31,
64295 Darmstadt, Germany
Tel: +49 6151 807-7
Fax: +49 6151 807-555
Tx: 4197335 emet d

EUMETSAT
Dr. G. Szejwach
Head of Technical Department
EUMETSAT
Am Kavalleriesand 31,
64295 Darmstadt, Germany
Tel: +49 6151 807-7
Fax: +49 6151 807-555
Tx: 4197335 emet d

EUMETSAT
Mr. R. Wolf
Head/Ground Segment Support Division
EUMETSAT
Am Kavalleriesand 31,
64295 Darmstadt, Germany
Tel: +49 6151 807-7
Fax: +49 6151 807-555
Tx: 4197335 emet d

INDIA
Dr. R. R. Kelkar
Deputy Director General of Meteorology
India Meteorology Department
Lodi Road
10003 New Delhi, India
Tel: +91 11 611 710
Fax: +91 11 69 9216
Tx: 3166494

JAPAN
Dr. T. Hiraki
Head, Office of Met. Sat. Planning
Administration Department
Japan Meteorological Agency
1-3-4, Otemachi, Chiyoda-ku
Tokyo 100, Japan
Tel: +81 3 32 01 86 77
Fax: +81 3 32 11 20 32
Tx: 2222163
E-mail:cgms-jma@hq.kishou.go.jp

JAPAN
Mr. S. Yamada
Director
Earth Observation Satellite Department
NASDA
Hamamatsu-cho Central Bldg. 10F
1-29-6 Hamamatsu-cho, Minato-ku
Tokyo 105, Japan
Tel: +813 5401 8651

JAPAN
Dr. I. Kubota
Director-General
Meteorological Satellite Center
3-235 Nakakiyoto
Kiyose-shi
Tokyo 204, Japan
Tel: +81 424 93 1111

PRC
Mr. H. Hanwen
Senior Engineer
Shanghai Institute of Satellite Engineering
251 Hua-Yin Road
200240 Shanghai
People's Republic of China
Tel: +86 21 43 01 091 ext. 30
Fax: +86 21 43 00 410

PRC
Mr. Xu Jianmin
Director
Satellite Meteorology Center
China Meteorology Administration
46 Baishiqialou
100081 Beijing
People's Republic of China
Tel: +86 10 83 32 277 ext. 23
Fax: +86 10 83 21 135
Tx: 22094

PRC
Mr. Xu Jianping
Satellite Meteorological Center
China Meteorology Administration
46 Baishiqialou
100081 Beijing
People's Republic of China
Tel: +86 10 83 32 277 ext. 2437
Fax: +86 10 83 21 135
Tx: 22094

RUSSIAN FEDERATION
Dr. A. V. Karpov
Chief/International Coop. Dept.
Russian Federal Service for
Hydrometeorology and
Environmental Monitoring
Novovagan'kovsky Street, 12
123242 Moscow, RUSSIA
Tel: +7 095 252 3873
Fax: +7 095 252 11 58
Tx: 411117 RUMS RF

RUSSIAN FEDERATION
Mr. V. F. Kharitonov
Russian Federal Service for
Hydrometeorology &
Environmental Monitoring
Novovagan'kovsky Street, 12
123242 Moscow, RUSSIA
Tel: +7 095 252 07 08
Fax: +7 095 252 11 58
Tx: 411117 RUMS RF

RUSSIAN FEDERATION
Dr. A. Uspensky
NPO Planeta
7, B. Predtechenskii Per.
Moscow, 123242
RUSSIA
Tel: +7 095 252 37 17
Fax: +7 095 200 42 10
Tx: 411117 RUMS RF

USA
Mr. W. J. Hussey
Director, Office of Systems Development
NOAA/NESDIS
Room 3301C, FB4 (E/OSD)
Suitland
Washington DC 20233, USA
Tel: +1 301 457 5277
Fax: +1 301 420 0932
E-mail: wjhussey@rdc.noaa.gov

USA
Mr. C. P. Staton
Deputy Chief/Inf. Processing Div.
NOAA/NESDIS E/SP1
Room 0301, FB4
Suitland
MD 20233, USA
Tel: +1 301 457 5165
Fax: +1 301 457 5199
E-mail: cstaton@nesdis.noaa.gov

USA
Ms. V. Fratta
International Relations Specialist
NOAA/NESDIS
Room 0110, FB4, Suitland (E/IA1)
Washington DC, 20233, USA
Tel: +1 301 457 5214763 45 86
Fax: +1 301 736 58 28
Tx: 7407641
E-mail: vfratta@nesdis.noaa.gov

USA
Dr. P. Menzel
Advanced Satellite Processing Project
NOAA/NESDIS
1225 West Dayton St.
Madison, WI 53706, USA
Tel: +1 608 264 5325
Fax: +1 608 262 5974
E-mail: paulm@ssec.wisc.edu

USA
Ms. Maria Weaks
Acting Chief, Data Collection and
Direct Broadcast Branch
NOAA/NESDIS/SSD/DCDB
World Weather Building - E/SP21
Room 806
5200 Auth Road
Camp Springs, Maryland 20233, USA
Tel: +1 301 763 8062
Fax: +1 301 763 8449
Tx: 7400359

USA
Mr. F. S. Zbar
Chief/System Requirements Branch
Chair/CBS WG on Observation
NOAA/National Weather Service
Office of Meteorology/13118
1325 East-West Highway
Silver Springs, Maryland 20910, USA
Tel: +1 301 713 1867
Fax: +1 301 589 1321

WMO
Dr. D. Hinsman
Senior Scientific Officer
WMO
Case Postale 2300
1211 Geneva 20, Switzerland
Tel: +41 22 730 8285
Fax: +41 22 734 0357
Tx: 045414199

WMO/CBS WG-SAT
Dr. P. Ryder
Deputy Chief Executive (DCE)
Meteorological Office
London Road
Bracknell
Berkshire, RG12 2SZ, United Kingdom
Tel: +44 344 85 46 08
Fax: +44 344 85 49 48
Tx: 051 849801

E-MAIL LIST SERVERS

CGMS was informed by WMO that the following list servers have been installed as follows:

CONTACT POINTS FOR CGMS PLENARY:

cgmsplen@www.wmo.ch

dexter@www.wmo.ch
hinsman@www.wmo.ch
landis@www.wmo.ch
schiessl@www.wmo.ch
vfratta@nesdis.noaa.gov
tstryker@nesdis.noaa.gov
szejwach@eumetsat.de
wolf@eumetsat.de
vkh@hymet.msk.ru
uspensky@planeta.msk.su
cgms_jma@hq.kishou.go.jp
fzbar@smtpgate.ssmc.noaa.gov
jreyre@meto.govt.uk

CONTACT POINTS FOR CGMS FREQUENCY MATTERS:

cgmsfreq@www.wmo.ch

rbarth@noaa.gov
guettlich@eumetsat.de
hinsman@www.wmo.ch
schlapia@noaa.gov
vfratta@nesdis.noaa.gov
szejwach@eumetsat.de
wolf@eumetsat.de
vkh@hymet.msk.ru
dmcginnis@rdc.noaa.gov

CONTACT POINTS FOR CGMS WIND MATTERS:

cgmswind@www.wmo.ch

imk122@ucla.hdi.kfk.d400.de
graeme.kelly@ecmwf.co.uk
jhalle@cmc.aes.doe.ca
hinsman@www.wmo.ch
kholmlun@esoc.bitnet
jlm@bom.gov.au
rwlunnon@email.meto.govt.uk
paulm@ssec.wisc.edu
purdom@terra.cira.colostate.edu
qwu@gih.grace.cri.nz
ccheasman@meto.govt.uk
schmetz@eumetsat.de
bernard.strauss@ecmwf.co.uk
vfratta@nesdis.noaa.gov
szantai@lmdx07.polytechnique.fr
/g=SED/s=MSC/o=MSC/admd=ati/c=jp/@sprint.com
chrisv@ssec.wisc.edu
woick@eumetsat.de
szejwach@eumetsat.de
uspensky@planeta.msk.su

LIST OF ABBREVIATIONS AND ACRONYMS

ACARS	Automated Communications Addressing and Reporting System
ACC	ASAP Coordinating Committee
ACMAD	African Centre for the Applications of Meteorology to Development
AMS	American Meteorological Society
AMSU	Advanced Microwave Sounding Unit
APT	Automatic Picture Transmission
ARGOS	Data Collection and Location System
ASAP	Automated Shipboard Aerological Programme
ASCII	American Standard Code for Information Interchange
ASDAR	Aircraft to Satellite Data Relay
ATOVS	Advanced TOVS
AVHRR	Advanced Very High Resolution Radiometer
BBC	Black Body Calibration (METEOSAT)
BUFR	Binary Universal Form for data Representation
CAL	Computer Aided Learning
CBS	Commission for Basic Systems (WMO)
CCIR	Consultative Committee on International Radio
CCSDS	Consultative Committee on Space Data Systems
CD	Compact Disk
CEOS	Committee on Earth Observations Satellites
CEPT	Conference Européenne des Postes et Télécommunications
CGMS	Coordination Group for Meteorological Satellites
CHRPT	Chinese HRPT (FY-1C and D)
CIIS	Common Instrument Interface Studies
CLS	Collecte Localisation Satellites (Toulouse)
CMS	Centre de Meteorologie Spatiale (Meteo France, Lannion)
CMV	Cloud Motion Vector
CMW	Cloud Motion Wind
COSPAR	Committee on Space Research
DAPS	DCS Automated Processing System (USA)
DBS	Direct Broadcast Service
DCP	Data Collection Platform
DCS	Data Collection System
DIF	Directory Interchange Format
DMSP	Defense Meteorological Satellite Program
DOMSAT	Domestic telecommunications relay Satellite (USA)
DPT	Delayed Picture Transmission
DRS	DCP Retransmission System (Meteosat)
DRT	Data Relay Transponder (INSAT)
DUS	Data Utilisation Station (USA) (Japan)
EBB	Electronic Bulletin Board
EC	Executive Council (WMO)
ECMWF	European Centre for Medium range Weather Forecasts

EES	Earth Exploration Satellite
ENVISAT	ESA future polar satellite for environment monitoring
EO	Earth Observation
EO-ICWG	EO-International Coordination Working Group (Space Station)
EOS	Earth Observation System
EPS	EUMETSAT Polar System
ERBE	Earth Radiation Budget Experiment
ESA	European Space Agency
ESOC	European Space Operations Centre (ESA)
EUMETSAT	European Meteorological Satellite Organisation
FAA	Federal Aviation Authority (USA)
FAX	Facsimile
FSS	Fixed Satellite Services (Telecom)
FXTS	Facsimile Transmission System (USA)
FY-1	Polar Orbiting Meteorological Satellite (PRC)
FY-2	Future Geostationary Meteorological Satellite (PRC)
GAC	Global Area Coverage (AVHRR)
GCOS	Global Climate Observing System
GEOSAR	Geostationary Earth Orbit Search And Rescue
GIMTACS	GOES I-M Telemetry and Command System
GMR	GOES-Meteosat Relay
GMS	Geostationary Meteorological Satellite (Japan)
GOES	Geostationary Operational Environmental Satellite (USA)
GOMS	Geostationary Operational Meteorological Satellite (Russ. Fed.)
GOS	Global Observing System
GPCP	Global Precipitation Climatology Project
GSLMP	Global Sea Level Monitoring Programme
GTS	Global Telecommunications System
GVAR	GOES Variable (data format) (USA)
HIRS	High Resolution Infra-red Sounder
HR	High Resolution
HRPT	High Resolution Picture Transmission
IASI	Infrared Atmospheric Sounding Interferometer (EPS, EUMETSAT)
IDCP	International DCP
IDCS	International Data Collection System
IDN	International Directory Network (CEOS)
IFRB	International Frequency Registration Board
IJPS	Initial Joint Polar System (USA-EUMETSAT)
INSAT	Indian geostationary satellite
IPOMS	International Polar Orbiting Meteorological Satellite Group
IR	Infrared
ISCCP	International Satellite Cloud Climatology project
ITT	Invitation to Tender
ITU	International Telecommunications Union
ITWG	International TOVS Working Group

JMA	Japanese Meteorological Agency
JPS	Joint Polar System (USA-EUMETSAT)
LR	Low Resolution
LRIT	Low Rate Information Transmission
LRPT	Low Rate Picture Transmission
LST	Local Solar Time
MARF	Meteorological Archive and Retrieval Facility (EUMETSAT)
MDD	Meteorological Data Distribution (Meteosat)
MDUS	Medium-scale Data Utilization Station (for GMS S-VISSR)
METOP	Future European meteorological polar orbiting satellite
METEOR	Polar orbiting meteorological satellite (Russian Fed.)
METEOSAT	Geostationary meteorological satellite (EUMETSAT)
MHS	Microwave Humidity Sounder (EPS)
MOP	Meteosat Operational Programme
MPEF	Meteorological Product Extraction Facility (EUMETSAT)
MSC	Meteorological Satellite Centre (Japan)
MSG	Meteosat Second Generation
MSS	Mobile Satellite Services (Telecom)
MSU	Microwave Sounding Unit
MTP	Meteosat Transition Programme
MTS	Microwave Temperature Sounder (EPS)
MTSAT	Multi-functional Transport Satellite (Japan)
MVIS	Multi-channel VIS and IR Radiometer (FY-1C and D of PRC)
NASA	National Aeronautics and Space Agency
NASDA	Japanese National Space Agency
NEDT	Noise Equivalent Delta Temperature
NESDIS	National Environmental Satellite Data and Information Service
NGDC	National Geophysical Data Centre (USA)
NMC	National Meteorological Centre
NOAA	National Oceanographic and Atmospheric Administration (USA)
NOAAPORT	Meteorological Information Satellite Broadcast System (USA)
NOS	National Ocean Service (USA)
NPOESS	National Polar Orbiting Environmental Satellite System (USA)
NTIA	National Telecommunications and Information Agency (USA)
NWP	Numerical Weather Prediction
NWS	National Weather Service (USA)
OCAP	Operational Consortium of ASDAR Participants
OWSE-AF	Operational WWW Systems Evaluation for Africa
PC	Personal Computer
POES	Polar-orbiting Operational Environmental Satellite (USA)
PRC	Peoples Republic of China
PTT	Post Telegraph and Telecommunications authority
RDCP	Regional DCP (Japan)
RESURS	Environmental remote-sensing satellite (Russian Fed.)

RMS	Root Mean Square
RMTC	Regional Meteorological Training Centre (WMO)
RSMC	Regional Specialised Meteorological Centre (WMO)
SAA	Satellite Active Archive (USA)
SAF	Satellite Applications Facility (EUMETSAT)
S&R	Search and Rescue mission
SARSAT	Search And Rescue, Satellite Aided Tracking
SATOB	WMO code for Satellite Observation
SBUV	Solar Backscattered Ultra-Violet (ozone)
SEAS	Shipboard Environmental (data) Acquisition System
SEM	Space Environment Monitor
SEVIRI	Spinning Enhanced Visible and Infra-Red Imager (MSG)
S-FAX	S-band facsimile broadcast of FY-2 (PRC)
SFCG	Space Frequency Coordination Group
SMA	State Meteorological Administration (PRC)
SSM/I	Special Sensor Microwave Imager (DMSP, USA)
SSP	Sub Satellite Point
SST	Sea Surface Temperature
SSU	Stratospheric Sounding Unit
S-VISSR	Stretched VISSR
SWI	Soil Wetness Index
TOMS	Total Ozone Mapping Spectrometer
TOVS	TIROS Operational Vertical Sounder
UHF	Ultra High Frequency
UK	United Kingdom
UN	United Nations
USA	United States of America
UTC	Universal Time Coordinated
UTH	Upper Tropospheric Humidity
VAS	VISSR Atmospheric Sounder
VHF	Very High Frequency
VIRSR	Visible and Infra-Red Scanning Radiometer (EPS)
VIS	Visible channel
VLSI	Very Large Scale Integrated circuit
WRC	World Radio Conference
WCRP	World Climate Research Programme
WEFAX	Weather facsimile
WG	Working Group
WMO	World Meteorological Organization
WP	Working Paper
WV	Water Vapour
WWW	World Weather Watch
X-ADC	Extended Atlantic Data Coverage